UNIVERSITÄT LEIPZIG

REPORT

Institute für Physik
The Physics Institutes

2007


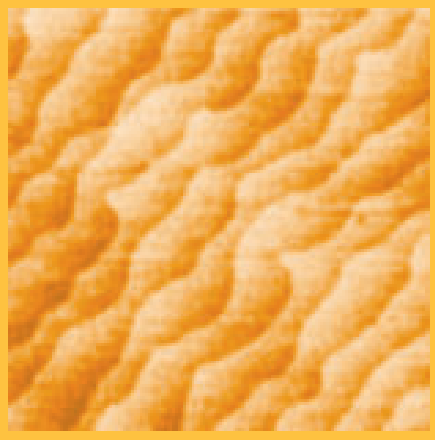
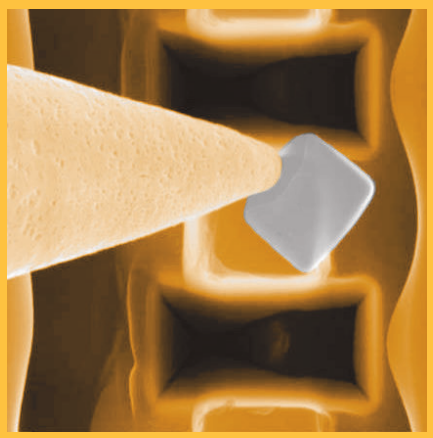
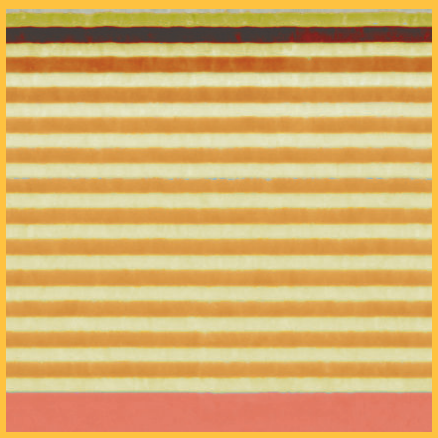

The Physics Institutes of Universität Leipzig, Report 2007
M. Grundmann (Ed.)

ISBN 978-3-934178-94-6

Technical Editor: Gregor Zimmermann

Printed in Germany by
MERKUR Druck und Kopierzentrum GmbH, Leipzig

online available at
http://www.uni-leipzig.de/~exph2/report_2007.pdf

Front cover
Upper left: array of ZnO nanowires (diameter about 100 nm) with MgZnO/ZnO quantum dots at their tips grown with pulsed laser deposition (SEM image).
Upper right: surface of MgZnO/ZnO/MgZnO quantum well with terraces and monoatomic steps grown homoepitaxially on ZnO substrate in step-flow growth mode using pulsed laser deposition (AFM image, $2 \times 2\ \mu m^2$).
Lower right: dielectric Bragg mirror (quarter wave stack) for the UV from 12.5 pairs of ZrO_2 (*bright stripes*, thickness 42 nm) and Al_2O_3 (*dark*) layers on sapphire (*red*) with 99.8 % reflectance at 3.31 eV (SEM image of FIB-prepared cross section).
Lower left: graphite flake (*grey*) prepared with a micromanipulator (SEM image).

Back covers
Recent book publication.

Institut für Experimentelle Physik I
Institut für Experimentelle Physik II
Institut für Theoretische Physik

Fakultät für
Physik und Geowissenschaften

Universität Leipzig

Institute for Experimental Physics I
Institute for Experimental Physics II
Institute for Theoretical Physics

Faculty of Physics and Geosciences

Universität Leipzig

Report 2007

Addresses

Institute for Experimental Physics I

Linnéstraße 5
D-04103 Leipzig, Germany
Phone: +49 341 97-32551
Fax: +49 341 97-32599
WWW: http://www.uni-leipzig.de/~gasse/nysid_a/inst/exp_1.htm
Mailing address: Postfach 100 920, D-04009 Leipzig, Germany

Institute for Experimental Physics II

Linnéstraße 5
D-04103 Leipzig, Germany
Phone: +49 341 97-32650
Fax: +49 341 97-32668
WWW: http://www.uni-leipzig.de/~exph2
Mailing address: Postfach 100 920, D-04009 Leipzig, Germany

Institute for Theoretical Physics

Vor dem Hospitaltore 1
D-04103 Leipzig, Germany
Phone: +49 341 97-32420
Fax: +49 341 97-32548
WWW: http://www.physik.uni-leipzig.de
Mailing address: Postfach 100 920, D-04009 Leipzig, Germany

Preface

The year 2007 has been rich with events in our Physics Institutes, both scientific and social. We thank Professor Dr. Dieter Freude for many years of teaching and fruitful research at our faculty, in particular in the field of the application of nuclear magnetic resonance to zeolite science and technology. Also Professor Dr. Bernd Rheinländer retired in 2007. We are especially grateful to him for insightful teaching, managing the colloquia and the setup of the ellipsometry laboratory. We wish both colleagues well in their retirement. Petrik Galvosas has been now formally appointed as junior professor. Ulrich Keyser received an Emmy-Noether grant from Deutsche Forschungsgemeinschaft.

In the short notes of this booklet we have compiled the most interesting results of our research, often performed in cooperation within and among the Physics Institutes and with many colleagues in Leipzig, nationally and worldwide. This work is made possible by the generous support from various funding agencies. We are glad that we were particularly successful in attracting funding for cooperative projects last year. Foremost we could establish the Leipzig Graduate School of Natural Sciences – Building with Molecules and Nano-objects (BuildMoNa) within the Federal German Excellence Initiative. This project is in close and interdisciplinary cooperation with Chemistry and Biosciences of the Universität Leipzig, Max-Planck-Institute for Mathematics in the Sciences (MPI-MiS) and Leibniz-Institute for Surface Modification (IOM). About one hundred doctoral candidates will learn and perform research in the school, many of them receiving grants.

In the newly established research unit FOR 845 "Self-organized nanostructures by low-energy ion-beam erosion" the nanoscopic pattern formation at surfaces is investigated together with colleagues from Dresden, Köln and Münster. The "Sächsische Forschergruppe" FOR 877 "From Local Constraints to Macroscopic Transport" unites our work on diffusion on the nanoscale with work of colleagues from other Saxonian universities, the TU Chemnitz and TU Dresden. The cooperative research project (Sonderforschungsbereich) SFB 762 "Functionality of Oxide Interfaces" has been positively evaluated in 2007 and has started work effective 1/1/2008. It is a joint initiative with MLU Halle-Wittenberg, MPI for Microstructure Physics in Halle and Magdeburg University. Experimental physics from Leipzig is represented in six of the projects studying novel oxide multi-ferroic heterostructures with interface-driven properties. The DFG-Research group FOR 723 "Functional Renormalization Group for Correlated Systems", Coordinator: Prof. Dr. M. Salmhofer, started its work in spring 2007.

Please enjoy browsing through our report. Maybe you feel stimulated to intensify the contact with us – Science in and the City of Leipzig are always worth a visit!

Leipzig,
May 2008

M. Grundmann
F. Kremer
G. Rudolph
Directors

Contents

1

Structure and Staff of the Institutes

1.1 Institute for Experimental Physics I

1.1.1 Office of the Director

Prof. Dr. Friedrich Kremer (director)
Prof. Dr. Jörg Kärger (vice director)

1.1.2 Molecular Nano-Photonics, Molekulare Nanophotonik [MON]

Prof. Dr. Frank Cichos

Secretary
Christine Adolph

Technical staff
Dipl.-Phys. Uwe Weber

Academic staff
Thomas Riedel

PhD candidates
Dipl.-Phys. Nicole Amecke
Dipl.-Phys. Romy Radünz
Dipl.-Phys. Rebecca Wagner

Students
Miriam Wähnert
Sven Zimmermann
Martin Pumpa
Markus Selmke
Carl Meusinger
Rüdiger Kürsten
Eugen Ehrenpreis

Momchil Ivanov
Angel Topalov

1.1.3 Molecular Physics, Molekülphysik [MOP]

Prof. Dr. Friedrich Kremer

Secretary

Karin Girke
Ines Grünwald

Technical staff

Dipl.-Ing. Jörg Reinmuth
Dipl.-Phys. Wiktor Skokow

Academic staff

Dr. Ulrich Keyser
Dr. Gustavo Dominguez
Dr. Periklis Papadopoulos
Dr. Mathias Salomo
Dr. Anatoli Serghei

PhD candidates

Dipl.-Phys. Christof Gutsche
Ciprian Ghiorghita Iacob, M.Sc.
Julius Tsuwi Kazungu, M.Sc.
Dipl.-Phys. Kati Kegler
Joshua Rume Sangoro, M.Sc.
Ilya Semenov, M.Sc.
Lorenz Steinbock, M.Sc.
Dipl.-Phys. Gunter Stober
Michael Tammer, M.Sc.

Students

Hergen Brutzer
Benjamin Gollnick
Oliver Otto
Jan H. Peters
Jan Sölter
Carolin Wagner
Immanuel Weidner

1.1.4 Physics of Interfaces, Grenzflächenphysik [GFP]

Prof. Dr. Jörg Kärger

Secretary

Katrin Kunze

Technical staff

Dipl.-Phys. Cordula Bärbel Krause
Dipl.-Ing. Bernd Knorr
Lutz Moschkowitz
Dagmar Prager
Stefan Schlayer

Academic staff

Prof. Dr. Dieter Freude
Dr. Karen Friedemann
Dr. Petrik Galvosas
PD Dr. Farida Grinberg
Dr. habil. Grit Kalies
Dr. Margarita Krutyeva
Prof. (i.R.) Dr. Dr. h.c. Harry Pfeifer
Dr. Andreas Schüring
Dr. habil. Frank Stallmach
Dr. Rustem Valiullin

PhD candidates

Dipl.-Phys. Christian Chmelik
Dipl.-Phys. Muslim Dvoyashkin
Dipl.-Phys. Moisés Fernadez
Dipl.-Phys. Wadinga Fomba
Dipl.-Chem. Filipe Furtado
Dipl.-Phys. Lars Heinke
Dipl.-Phys. Aleksey Khokhlov
Dipl.-Phys. Sergej Naumov
Dipl.-Phys. Ekaterina Romanova
Dipl.-Phys. Oraphan Saengsawang
Dipl.-Phys. Denis Schneider
Dipl.-Geophys. Wiete Schönfelder
Dipl.-Ing. Despina Tzoulaki
Dipl.-Phys. Konstantin Ulrich
Dipl.-Phys. Markus Wehring

Students

Florian Hibbe
Carsten Horch
Tomas Binder
Marcel Gratz
Mario Grossmann
Jakob Mauritz

1.1.5 Soft Matter Physics, Physik der weichen Materie [PWM]

Prof. Dr. Josef A. Käs

Secretary

Claudia Honisch
Christine Kreft (Vertretung)

Technical staff

Dipl.-Ing. Undine Dietrich
Dipl.-Phys. Bernd Kohlstrunk
Ing. Elke Westphal

Academic staff

Dr. Carsten Selle

PhD candidates

Dipl.-Phys. Timo Betz
Dipl.-Phys. Claudia Brunner
Susanne Ebert, M.Sc.
Allen Ehrlicher, M.Sc.
Kristian Franze, M.Sc.
Anatol Fritzsch, M.Sc.
Brian Gentry, M.Sc.
Dipl.-Phys. Jens Gerdelmann
Dipl.-Phys. Michael Gögler
Dipl.-Phys. Florian Huber
Dipl.-Phys. Tobias Kießling
Daniel Koch, M.Sc.
Dipl.-Phys. Mireille Martin
Dipl.-Phys. Karla Müller
Dipl.-Phys. Florian Rückerl
David Smith, M.Sc.
Dipl.-Phys. Dan Strehle
Björn Stuhrmann, M.Sc.
Carsten Stüber, M.Sc.
Dipl.-Phys. Franziska Wetzel
Dipl.-Phys. Lydia Woiterski

Students

José Alvarado
Thomas Fuhs
Marc Großerüschkamp
Markus Gyger
Lukas Hilde
Kenechukwu David Nnetu

Melanie Knorr
Philipp Rauch
Maren Romeyke
Matthias Steinbeck
Johannes Stelzer
Markus Streicher

1.2 Institute for Experimental Physics II

1.2.1 Office of the Director

Prof. Dr. Marius Grundmann (director)
Prof. Dr. Tilman Butz (vice director)

1.2.2 Magnetic Resonance of Complex Quantum Solids, Magnetische Resonanz Komplexer Quantenfestkörper [MQF]

Prof. Dr. Jürgen Haase

Secretary

Teresa Nitsch

Technical staff

Ursula Heinich
Dipl.-Ing. Joachim Hoentsch
Dipl.-Phys. Gert Klotzsche
Dipl.-Ing. Heinz-Jürgen Rauchfuß

Academic staff

Dr. Marko Bertmer
Prof. Dr. Rolf-Michael Böttcher
apl. Prof. Dr. Andreas Pöppl
Dr. Damian Rybicki

PhD candidates

Dipl.-Phys. Özlen Ferruh Erdem
Dipl.-Chem. Anke Matthes
Dipl.-Phys. Vijayasarathi Nagarajan
Dipl.-Phys. Pavel Sedykh

Students

Susanne Richter

1.2.3 Nuclear Solid State Physics, Nukleare Festkörperphysik [NFP]

Prof. Dr. Tilman Butz

Secretary

Teresa Nitsch

Technical staff

Dipl.-Ing. Bernd Krause
Carsten Pahnke
PTA Raimund Wipper †

Academic staff

Dr. Yuriy Manzhur
Dr. Tilo Reinert
Dr. Jürgen Vogt
Dr. Daniel Spemann

PhD candidates

Dipl.-Biol. Anja Fiedler
Dipl.-Phys. Steffen Jankuhn
Dipl.-Phys. (Med.-Phys.) Torsten Koal
Dipl.-Phys. Christoph Meinecke
Dipl.-Phys. Frank Menzel
Charlotta Nilsson, M.Sc.
Dipl.-Phys. Martin Rothermel

Students

Tobias Andrea
Nirav Barapatre
Roman Follert
Frank Heymann
Marcus Hohlweg
Daniela Kolbe
Stefan Noak
Peter Steinbach
Draco Szathmáry

1.2.4 Semiconductor Physics, Halbleiterphysik [HLP]

Prof. Dr. Marius Grundmann

Secretary

Anja Heck

SANDiE Network Office

Dr. Alexander Weber (Network Officer)
Birgit Wendisch (Secretary)

Technical staff

Dipl.-Phys. Gabriele Benndorf
Dipl.-Ing. Gisela Biehne
Dipl.-Ing. Holger Hochmuth
Dipl.-Phys. Jörg Lenzner
Gabriele Ramm
Roswitha Riedel

Academic staff

Dr. Bingqiang Cao
Dr. Nilotpal Ghosh
Dr. Michael Lorenz
PD Dr. Rainer Pickenhain
Prof. Dr. Bernd Rheinländer
Dr. Heidemarie Schmidt
Dr. Rüdiger Schmidt-Grund
Dr. Alexander Weber
Dr. Qingyu Xu

PhD candidates

Dipl.-Phys. Matthias Brandt
Dipl.-Phys. Christian Czekalla
Dipl.-Phys. Heiko Frenzel
Dipl.-Phys. Daniel Fritsch
Dipl.-Phys. Karsten Goede
Dipl.-Phys. Lars Hartmann
Susanne Heitsch, M.Sc.
Dipl.-Ing. Stefan Jaensch
Dipl.-Phys. Alexander Müller
Dipl.-Phys. Andreas Rahm
Dipl.-Phys. Matthias Schmidt
Dipl.-Phys. Jan Sellmann
Dipl.-Phys. Chris Sturm
Mariana Ungureanu, M.Sc.
Dipl.-Phys. Holger von Wenckstern
Dipl.-Phys. Gregor Zimmermann

Students

Ronny Bakowskie
Martin Ellguth
Christoph Henkel
Helena Hilmer
Alexander Lajn
Martin Lange
Dominik Lausch
Thomas Lüder

Robin Weirauch
Jan Zippel

1.2.5 Solid State Optics and Acoustics, Festkörperoptik und -akustik [FKO]

Prof. Dr. Wolfgang Grill

1.2.6 Superconductivity and Magnetism, Supraleitung und Magnetismus [SUM]

Prof. Dr. Pablo Esquinazi

Technical staff

Dr. Winfried Böhlmann
Klaus Grünwald
Dipl.-Krist. Annette Setzer
Monika Steinhardt

Academic staff

Dr. José Luis Barzola Quiquia
Dr. YuanFu Chen
Dr. Roland Höhne
Dr. Detlef Spoddig
Dr. Jin-lei Yao
PD Dr. Michael Ziese

PhD candidates

Dipl.-Phys. Kristian Schindler

Students

Ingo Hilschenz
Holger Motzkau
Peter Rödiger
Thomas Scheller
Yashwant Verma

1.3 Institute for Theoretical Physics

1.3.1 Office of the Director

Prof. Dr. Gerd Rudolph (director)
Prof. Dr. Klaus Kroy (vice director)

Secretary
Susan Hussack
Gabriele Menge
Lea Voigt

1.3.2 Computational Quantum Field Theory, Computerorientierte Quantenfeldtheorie [CQT]

Prof. Dr. Wolfhard Janke

Academic staff
Dr. Michael Bachmann
Dr. Elmar Bittner
Dr. Viktoria Blavatska
Dr. habil. Martin Hasenbusch
Dr. Bartłomiej Wacław

PhD candidates
Dipl.-Phys. Andreas Nußbaumer
Dipl.-Phys. Stefan Schnabel
Dipl.-Phys. Thomas Vogel
Sandro Wenzel, M.Sc.
Dipl-Phys. Rainer Bischof

Students
Mathias Aust
Frank Beyer
Niklas Fricke
Monika Möddel
Hannes Nagel
Micha Wiedenmann

1.3.3 Molecular Dynamics / Computer Simulation, Moleküldynamik / Computersimulation [MDC]

PD Dr. H.L. Vörtler (Speaker)
PD Dr. S. Fritzsche

Academic staff
Prof. Dr. R. Haberlandt (retired)
Dr. A. Schüring

PhD candidates
O. Saengsawang, M.Sc.
S. Thompho, M.Sc.
R. Chanajaree, M.Sc.
K. Seeharmart, M.Sc.

Students

C. Sripong-Ngam

1.3.4 Quantum Field Theory and Gravity, Quantenfeldtheorie und Gravitation [QFG]

Prof. Dr. Gerd Rudolph (Speaker)
Prof. Dr. Rainer Verch

Academic staff

PD Dr. Michael Bordag
Dr. Pjotr Marecki
Dr. Vladimir Nikolaev
Dr. Matthias Schmidt

Retired

Prof. em. Bodo Geyer
Prof. em. Armin Uhlmann

PhD candidates

Dipl.-Phys. Marcus Borris
Dipl.-Phys. Alexander Hertsch
Dipl.-Phys. Jan Schlemmer

Students

Jörn Boehnke
Andreas Degner
Rainer Mühlhoff
Christoph Solveen
Konrad Zimmermann

1.3.5 Statistical Physics, Statistische Physik [STP]

Prof. Dr. Manfred Salmhofer

Academic staff

Dr. Oliver Lauscher

PhD candidates

Dipl-Phys. Christoph Husemann
Dipl-Phys. Kay–Uwe Giering

Students

Giulio Schober

1.3.6 Theory of Condensed Matter, Festkörpertheorie [TKM]

Prof. Dr. Ulrich Behn (Speaker)
Prof. Dr. Klaus Kroy

Prof. Dr. Dieter Ihle (retired)
Prof. Dr. Adolf Kühnel (retired)

Academic staff

Dr. Abigail Klopper (long term guest scientist)
Dr. Pablo Fernandez (long term guest scientist)

PhD candidates

Dipl.-Phys. Jens Glaser
Dipl.-Phys. Iren Juhász Junger
Dipl.-Phys. Micaela Krieger-Hauwede
Dipl.-Phys. Daniel Rings
Dipl.-Phys. Holger Schmidtchen

Students

Philipp Altrock
Stefan Grosser
Fridolin Groß
Susanne Gütter
Marcel Hennes
Christian Hubert
Melanie Knorr
Andrea Kramer
Sebastian Schöbl
Sebastian Sturm
Mario Thüne
Lucas Wetzel

1.3.7 Theory of Elementary Particles, Theorie der Elementarteilchen [TET]

Prof. Dr. Klaus Sibold

Academic staff

PD Dr. Roland Kirschner
PD Dr. Holger Perlt
PD Dr. Arwed Schiller

I

Institute for Experimental Physics I

2

Molecular Nano-Photonics

2.1 Introduction

The challenge of experimental physics on the nanoscale is to access local phenomena, that occur for example at interfaces, at specific molecular sites or at certain places within nano-structured materials. These local phenomena may control molecular dynamics, drive self-organization, cause charge separation or alter light propagation. Their importance extends to almost every field involved in future nanotechnology. The research of the molecular nano-photonics group thus aims at the development and application of optical techniques to access nanoscale (dynamical) processes in various fields such as chemical physics, biology or semiconductor physics. The understanding of these dynamical processes shall ultimately lead to a control over single molecules and other nano-objects by applying heat, flow, shear forces, electric fields or current.

The main experimental tool within our research is optical single molecule detection by ultra-sensitive microscopic techniques including time-resolved confocal microscopy, wide-field fluorescence or photothermal microscopy. Single molecules or semiconductor quantum dots provide the ideal local probes to access nanoscale physical properties inside materials while keeping the information on the heterogeneity of the system. Using these techniques recent projects focused on

- Photothermal detection of single gold nanoparticles,
- Local thermal measurements with single gold nanoparticles,
- Nanometric distance measurements with single gold nanoparticle pairs,
- Fluorescence correlation spectroscopy on single semiconductor quantum dots,
- Photophysics of single silicon nanoparticles,
- Defocused imaging of single emitters in photonic crystals,
- Single molecule diffusion in ultrathin confined liquid films.

During the year 2007 the Molecular Nanophotonics Group has setup most of their experimental equipment. The current experimental facilities include

- confocal sample scanning optical microscope for fluorescence correlation spectroscopy and time-resolved detection,
- sample scanning photothermal microscope coupled with a fluorescence wide field and optical confocal microscope,

- fluorescence wide field microscope for high speed single molecule detection,
- single molecule wide field fluorescence microscope for defocused imaging and orientational mapping of single molecules.

The group has contributed in 2007 significant work to establish the DFG research unit 877 "From Local Constraints to Macroscopic Transport".

Frank Cichos

2.2 Photothermal Detection of Single Gold Nanoparticles

R. Radünz, M. Wähnert, F. Cichos

Single molecule detection is meanwhile a widely used technique to study dynamical processes in complex materials, especially in biophysics. It is, however, always restricted to fluorescent probes such as organic dye molecules or quantum dots. Within this project, we analyze the capabilities of photothermal microscopy for the detection of single non-fluorescent nano-objects such as gold nanoparticles or quantum dots. The detection is based on the absorption of light not on the fluorescence and therefore free of processes as for instance photo-blinking. We have set up a photothermal optical microscope with heterodyne optical detection within the last year. The microscope is based on a standard sample scanning confocal microscope. Two lasers are coupled collinearly into the microscope. The first, an intensity modulated laser (typically 532 nm) is used to heat nano-objects optically via its absorption. The heat released by the object creates a temperature field and therefore a refractive index gradient around it. This refractive index gradient scatters the light of a second laser at a different wavelength (typically around 800 nm). The scattered light is due to the intensity modulation of the heating laser also modulated and can therefore be analyzed with a lock-in system. This current setup images with typical scanning times of 1 ms per pixel and is capable of detecting

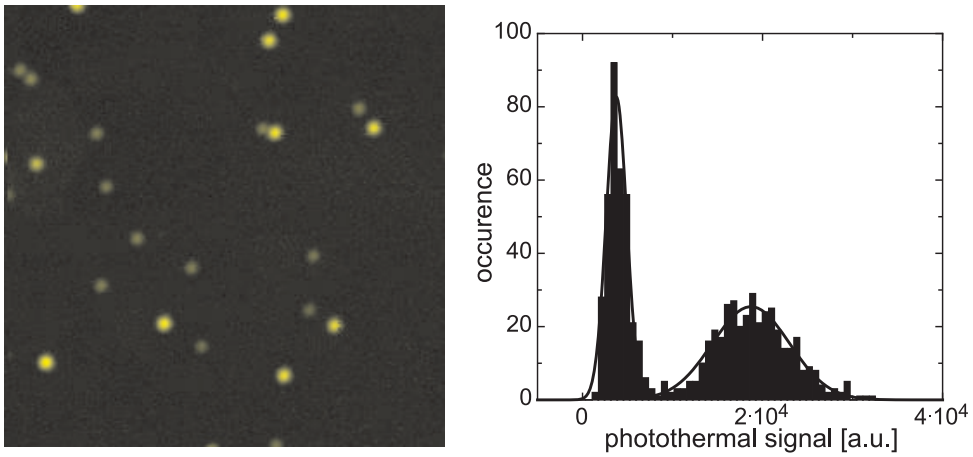

Figure 2.1: *Left*: Scanning photothermal microscopy image of single gold nanoparticles of 20 nm and 40 nm diameter in a 20 μm × 20 μm region. *Right*: Intensity histogram of the *left image* to demonstrate that single gold particles of the same size deliver the same signal strength. Different sized particles can be seperated by their signal strength.

gold nano-particles down to 10 nm diameter (absorption cross section 5×10^{-13} cm^2), see Fig. 2.1. The setup further allows to carry out photothermal correlation spectroscopy, which detects the diffusional dynamics of gold nanoparticles in solution. This technique first developed in our group is equivalent to fluorescence correlation spectroscopy and demonstrates that fast photothermal fluctuations can be recorded.

2.3 Local Thermal Measurements with Single Gold Nanoparticles

R. Radünz, F. Cichos

The photothermal detection technique shortly described in Sect. 2.2 is based on the release of heat from e.g. gold nanoparticles. Thus single gold nanoparticles can also be intentionally used as nano heat sources, which opens new possibilities for the study of thermal properties of materials. When particles become as small as 10 nm or even smaller, heat transfer from the nanoparticle to the local environment will be largely determined by the interface of the particle with the surrounding. Details of heat transfer such as the interfacial heat transfer resistance will become dominating. However, these variables are still not well understood especially their connection to molecular scale

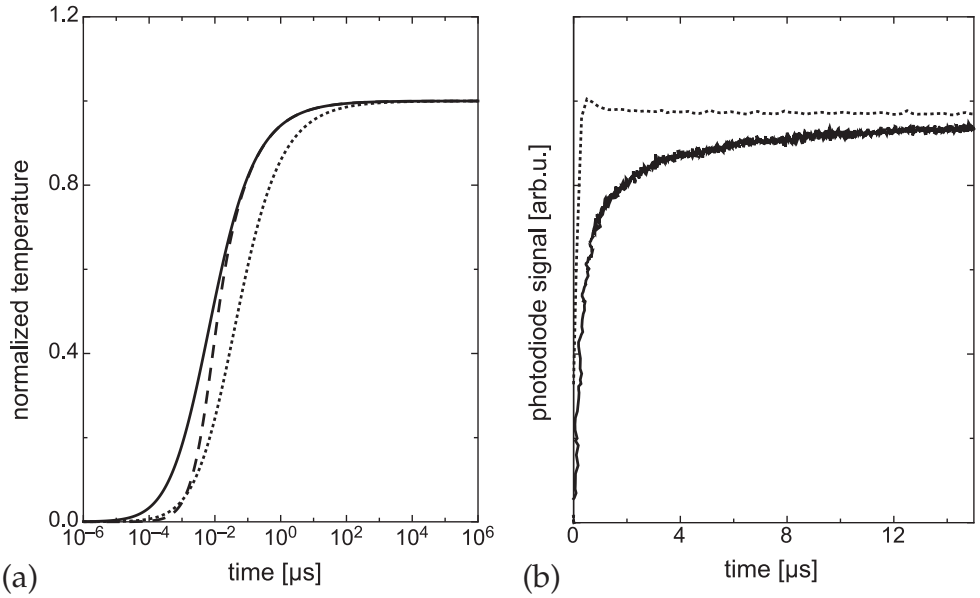

Figure 2.2: (**a**) Calculated time resolved temperature in a medium directly at the surface of an 80 nm gold nanoparticle after a constant heating of the particle has been switched on. The *solid line* shows the time dependent temperature in water, the *dotted line* the temperature for a medium with 6 times smaller thermal conductivity than water. In both cases, the thermal boundary resistance between nanoparticle and medium is zero. The *dashed line* shows the response for the same heat conductivity as for the solid line only with a thermal boundary resistance. It can be clearly seen that either the thermal conductivity as well as the thermal boundary resistance (for gold/water interface) can be resolved. (**b**) Measured time resolved photothermal signal for an 80 nm gold particle in PDMS at room temperature compared to the system response measured with the modulated heating laser beam (*dotted line*).

processes is missing. Nevertheless, heat transfer is vibrational coupling of entities and therefore connected to molecular interactions. Thus nanoscale heat transfer studies should reveal insights into vibrational molecular coupling at interfaces.

During the last year, we have started to employ photothermal detection on single gold nanoparticles as a tool to measure heat transfer on the nanoscale. To do so, a single gold nano-particle is heated with a laser at the plasmon resonance. The heat release is probed with a non-resonant laser corresponding to Sect. 2.2 and recorded with a fast photodiode and an AD converter. This detection scheme allows a time triggered photothermal signal detection with at least nanosecond time resolution. Figure 2.2b shows the photothermal signal rise over time in comparison with the system response measured for a single 80 nm gold nanoparticle in polydimethylsiloxane (PDMS). The delayed photothermal signal rise can be described by material parameters of the PDMS, but requires an interfacial heat transfer resistance. Figure 2.2a demonstrates the influence of thermal conductivity and interfacial heat transfer resistance on the time resolved photothermal signal as simulated in numerical calculations. Thus both theory and experimental results provide a first proof of concept. Currently these experiments are extended to different materials and further used to induce local phase transitions on length scales of a few nanometers.

2.4 Nanometric Distance Measurements with Single Gold Nanoparticle Pairs

R. Radünz, M. Wähnert, F. Cichos

The number of optical techniques capable of measuring distances and distance fluctuations on the nanoscale is limited to charge and electron transfer processes. The upper limit of distances being measured with these methods is currently 10 nm and no other method is available, which fills the gap between 10 nm and 1 μm (corresponding to optical resolution). This project develops a technique based on pairs of gold nanoparticles for this intermediate distance range. Gold particles are strongly interacting with light due to a collective excitation of free electrons in the nanoparticle. These plasmon can be resonantly excited with visible light. The electric field associated with the plasmon resonance couples between closely spaced nanoparticles and forms a new resonance. Absorption and extinction spectra of these particles have been calculated by a T-matrix method.

The absorption cross section in Fig. 2.3a clearly shows this additional absorption feature due to the coupling of plasmon resonances in a nanoparticle dimer. The strength of this absorption feature is distance dependent. This has been calculated for the wavelength of maximum change between the two spectra in Fig. 2.3a. The red curve in Fig. 2.3b demonstrates that this distance dependence is much weaker than for Förster type energy transfer and thus indeed allows distance measurements on a wider range of up to 60 nm. This distance dependence can now be measured in different ways. To allow for a distance measurement with very small nanoparticles of 10 nm diameter or even smaller, we have evaluated the capabilities of photothermal detection (see Sect. 2.2). It turns out, that the weak distance dependence of the plasmon coupling in the absorption cross section is favorable of measuring directly distance fluctuations

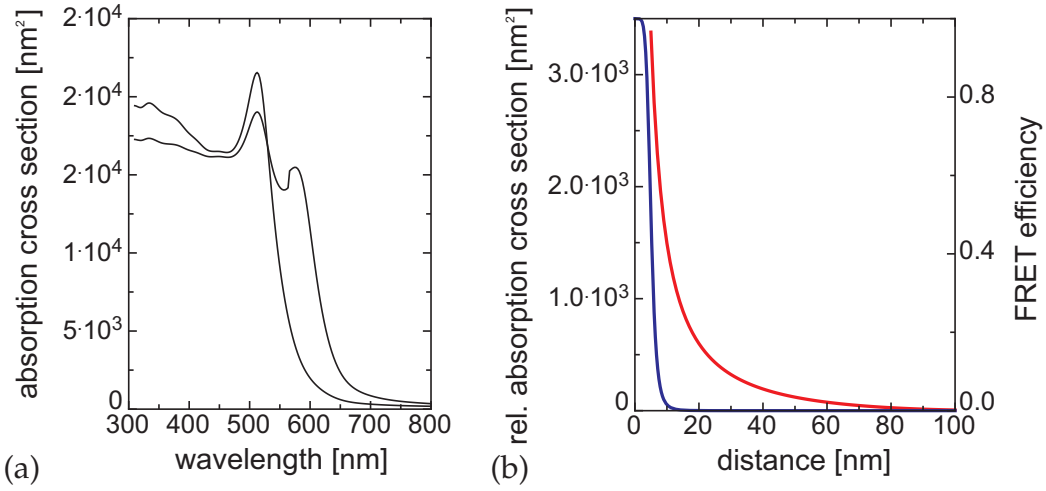

Figure 2.3: (**a**) Simulated absorption cross section of a gold nanoparticle dimer (80 nm) at random orientations and an inter-particle distance of 5 nm and 200 nm (surface-to-surface distance). The peak in the spectrum at 200 nm distance corresponds to the plasmon resonance of the gold nanoparticles. The spectrum at 5 nm distance clearly reveals two plasmon modes due to a coupling of the electric field of both metal particles. This coupling strength is distance dependent and provides the basis of plasmon based distance measurements. (**b**) Distance dependence of the absorption cross section of a randomly oriented gold nanoparticle dimer at a wavelength of 594 nm. The coupling between both nanoparticles decreases in strength with the distance. The decay is however much slower than for Förster type energy transfer (FRET) and therefore provides sensitivity for much larger distance fluctuations than FRET.

with a photothermal correlation technique as developed by the group. The group made first step to establish a simple system consisting out of DNA bound gold nanoparticles to determine the photothermal signal of gold nanoparticle dimers. This system will be further used to measure distance fluctuations.

2.5 Fluorescence Correlation Spectroscopy on Single Semiconductor Quantum Dots

N. Amecke, F. Cichos

Semiconductor nanocrystals and dye molecules show an intermittent emission on timescales ranging from microseconds up to several hundred seconds. Such extremely long periods without any emission are still a mystery. They are thought to be related to photoinduced charging processes. A charge, presumably an electron is ejected from the excited state of an emitter by a tunneling process to the surrounding environment, which is often an amorphous, disordered polymer or glass. Tunneling to distant states ($\sim 1-2$ nm distance) provides the required timescale for this intermittency. The nature of the accepting state in the polymer has been related to a self-trapping of charges due to intra- and intermolecular relaxation processes. Our studies in this direction are aimed to take control of the blinking processes. We therefore develop a fluorescence correlation based method to study emission intermittency of quantum dots in an electrochemical cell. The electrochemical cell shall allow a controlled removal or addition of electrons to

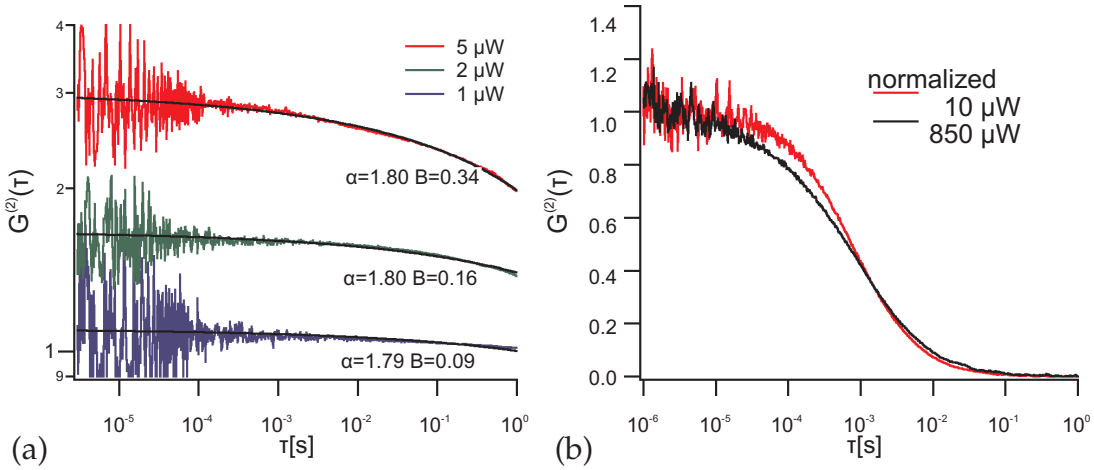

Figure 2.4: (**a**) Fluorescence intensity autocorrelation functions of single CdSe/ZnS quantum dots at different excitation powers. The curves reveal a power law for the probability distribution of emitting and non-emitting periods, which is independent of the excitation power. (**b**) Fluorescence intensity autocorrelation function of CdSe/ZnS quantum dots in solution at different excitation power. The curves reveal a standt correlation function for a diffusion process in solution, which is at high excitation power modified due to the emission intermittency of the quantum dots.

the quantum dot. The fluorescence based detection with picosecond timeresolution will correlate the photophysics with the charge state of the quantum dots. First fluorescence correlation experiments on single CdSe/ZnS core/shell quantum dots immobilized in polymer films and dissolved in water have been carried out (Fig. 2.4).

The correlation functions obtained for single CdSe/ZnS quantum dots show the typical power law behavior in the correlation function, which means that the emission intermittency is not determined by an exponential distribution of bright and dark periods but by a power law distribution with a extremely wide distribution of lifetimes (Fig. 2.4a). The correlation functions in solution (Fig. 2.4b) also display signs of this blinking at high excitation powers. This is visible as a deviation of the fluorescence correlation curve from the usual form of the correlation function as determined by diffusion. Currently an electrochemical cell for single molecule detection is developed, which allows to measure the influence of applied voltages and currents to the blinking by optical means. This method shall be extended from a fluorescence correlation spectroscopy experiment on quantum dots in solution to a more general method which allows an optically detected cyclic voltammetry on single molecules and quantum dots.

2.6 Photophysics of Single Silicon Nanoparticles

F. Cichos, C. von Borczyskowski*

*Institut für Physik, Technische Universität Chemnitz

Silicon is as a bulk material a poor emitter due to its indirect band gap. When confining electron hole pairs in a small nanocrystallite of silicon, the indirect character is, however, lifted and silicon can efficiently emit light. The details of the emission process are

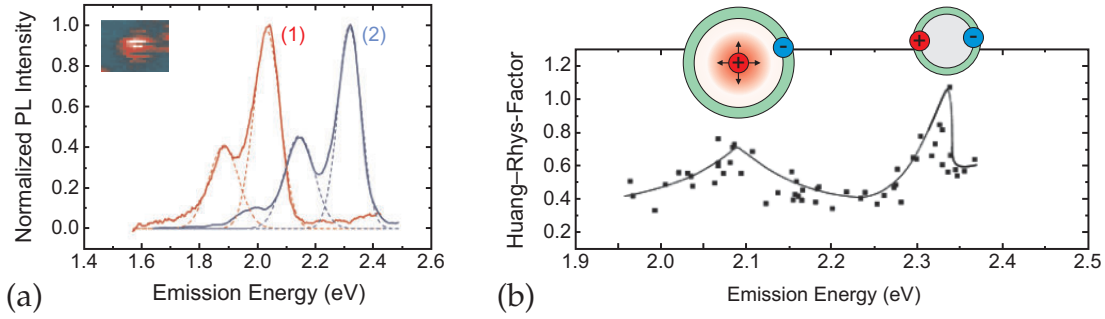

Figure 2.5: (**a**) Emission spectra of single silicon quantum dots of different size at room temperature (*inset*: confocal image of a single silicon nanocrystal). The spectra reveal a vibrational progression at 160 cm^{-1}, which corresponds to a O−Si−O vibration. (**b**) Calculated Huang–Rhys factor, which expresses the strength of the vibrational coupling. The two maxima in the Huang–Rhys factor represent the localization of electron and hole at the Si−SiO_2 interface of the silicon quantum dot.

nevertheless still not very clear especially the role of the interface to silicon dioxide. We have studied the emission of single silicon nanocrystals prepared by different techniques, such as gas phase pyrolysis and wet chemical procedures. Emission spectra and intensity time-traces we recorded. The results demonstrate, that small silicon nanocrystals (< 3 nm diameter) exhibit a strong vibrational progression in their emission spectra at room temperature, a fact that is not visible in ensemble spectroscopy. The vibrational modes have been identified as O−Si−O vibrations (Fig. 2.5a). The strength of the vibrational coupling was evaluated by the Huang–Rhys factor as a function of the emission energy of the quantum dots. This reveals two distinct maxima in the vibrational coupling, which we interpreted in terms of a charge carrier localization at the Si – SiO_2 interface (Fig. 2.5b). The first maximum at about 2.1 eV corresponds to the localization of the electron. The second maximum at about 2.3 eV corresponds to the localization of the hole. This is therefore for the first time direct evidence, that the emission of small silicon quantum dots is strongly related to a radiative recombination of excitons at the silicon dioxide interface [1].

[1] J. Martin et al.: Nano Lett. **8**, 656 (2008)

2.7 Defocused Imaging of Single Emitters in Photonic Crystals

R. Wagner, S. Zimmermann, F. Cichos

Photonic crystals provide a powerful way to manipulate light on a basis, which is very similar to that of semiconductors. Photonic crystals structure can be controlled in every detail in contrast to semiconductors. Compared to homogeneous dielectric materials, the optical properties of photonic crystals are now, however, local properties, which is of special importance for applications, where light sources shall be integrated in photonic crystals. This spatial change of optical properties is difficult to explore in three dimensional systems. We have therefore developed a method, which is based

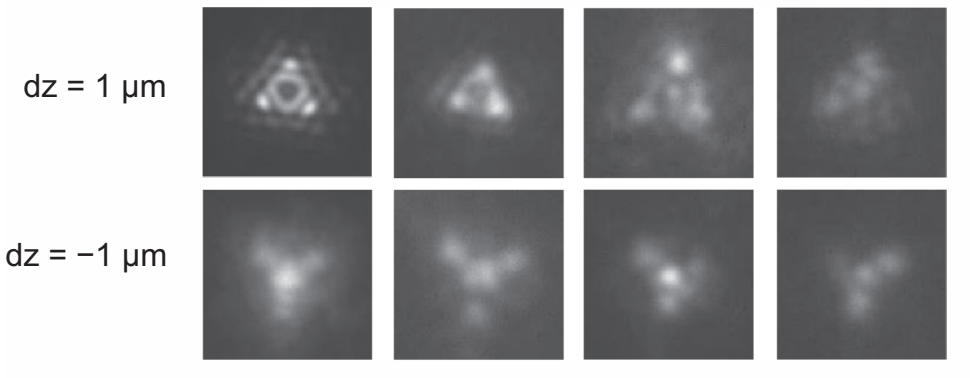

Figure 2.6: Defocused images of a single dye doped polystrene bead in a colloidal photonic crystal. All beads have a diameter of 460 nm. The defocusing diffraction pattern clearly reveals the symmetry of the photonic crystal and provides information on the local light propagation inside the crystal.

on the imaging of single emitters inside a photonic crystal [1]. The method employs a defocusing of single emitters (e.g. quantum dots), in which a diffraction pattern of the emitting object appears. This diffraction pattern contains information on the anisotropic light propagation in material.

This type of study has revealed the anisotropic light propagation in colloidal photonic crystals from a single image of a quantum dot and is now further applied wavelength selective studies in colloidal photonic crystals. We have therefore incorporated single fluorescent beads into photonic crystals. The defocused imaging of these systems reveal a new diffraction pattern, which is related to the symmetry of the crystal structure (see Fig. 2.6). This pattern is further wavelength dependent, which allows to probe the band structure and light propagation inside photonic crystals locally as a function of wavelength.

[1] M. Barth et al.: Phys. Rev. Lett. **96**, 243 902 (2006)

2.8 Single Molecule Diffusion in Ultrathin Confined Liquid Films

M. Pumpa, F. Cichos

The experiments of this project are aimed at the direct manipulation of molecular mobility due to local chemical modifications of a solid surface. Chemical modifications alter locally the hydrodynamic boundary conditions which also effect the viscous drag experienced by any tracer molecule or particle at the solid surface. To proof this effect, we have applied micro-contact printing to prepare alternating stripes of hydrophilic and hydrophobic regions on a glass substrate. This glass slide is used together with a hydrophilic one to confine a liquid containing dye labeled polystyrene beads (100-nm diameter) down to a film thickness of 150 nm in a home built surface forces apparatus. This surface forces apparatus is coupled to a wide field single molecule microscope.

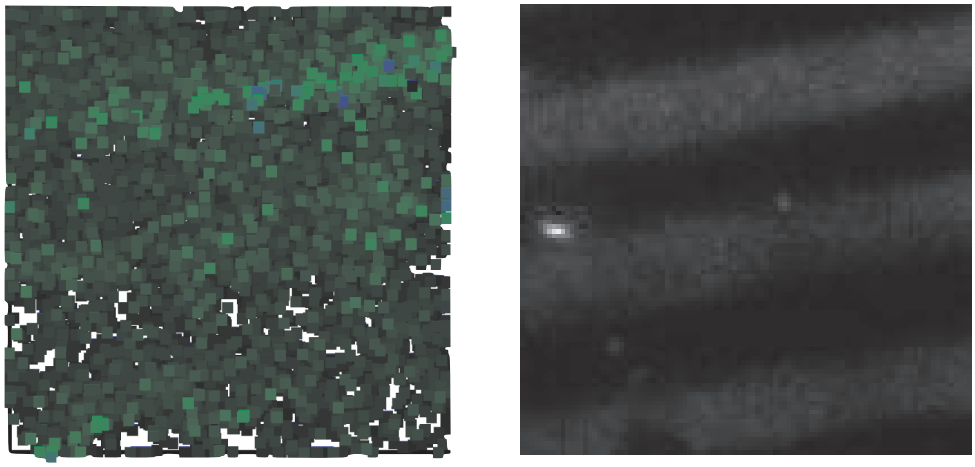

Figure 2.7: *Left*: Measured local square displacement of single polystyrene beads (100 nm) in a liquid film confined between two chemically structured glass slides (150 nm film thickness, 2 μm hydrophobic/hydrophilic stripes). The light areas indicate regions of higher bead mobility. This higher bead mobility is found in hydrophobically modified surface regions. *Right*: Structure of the chemically modified glass slide. The lighter regions indicate hydrophobic surface areas, the darker ones, hydrophilic surface areas. The hydrophobic areas appear brighter due to a selective attachement of dye molecules to the surface.

Trajectories of single polystyrene beads were recorded and analyzed in terms of their local square displacement. This local square displacement records the square displacement of a bead between two subsequent exposures as a function of the particle position in the image. Our results reveal that the mobility (square displacement) of the bead is modulated spatially by the chemical structure of the functionalized glass slide (see Fig. 2.7). There is a direct match of the high mobility regions with the hydrophobic regions on the glass slide. The local hydrophobicity therefore modifies the hydrodynamic boundary conditions for liquid flow and also diffusion, which finally leads to a higher mobility of the bead in the interface region. This higher mobility is therefore a direct consequence of liquid slip on the hydrophobic surface and demonstrates that hydrodynamic boundary conditions can be artificially modulated on a nanoscale to adjust interfacial mobilities. The variety of chemical structuring possibilities can therefore open a wide range of possibilities to manipulate liquids on a nanoscale. This is one of the major topics within this project for future studies.

2.9 Funding

Light Emission of Single Emitters in 3-dimensional Photonic Crystals
F. Cichos
CI 33/5-1

Ortsaufgelöste Detektion von Struktur und Dynamik in nematischen Phasen biaxialer Moleküle
F. Cichos
CI 33/6-1

FG 877: Constrained Single Molecule Dynamics in Glassy Polymer Systems
F. Cichos
CI 33/7-1

2.10 Organizational Duties

F. Cichos

- Vorsitzender Eignungsfeststellungskommission Fakultät für Physik und Geowissenschaften
- Co-Speaker DFG Research Unit 877 "From Local Constrainst to Macroscopic Transport"
- Referee: Phys. Rev. B, Nature, Chem. Phys. Lett., Appl. Phys. Lett., ACS Petroleum Research Fund

2.11 External Cooperations

Academic

- Technische Universität Chemnitz, Germany
  Prof. Dr. C. von Borczyskowski
- Universität Mainz, Germany
  Prof. Dr. T. Basché

2.12 Publications

Journals

C. von Borczyskowski, F. Cichos, J. Martin, J. Schuster, A. Issac, J. Brabandt: *Common luminescence intensity fluctuations of single particle and single molecules in non-conducing matrices*, Eur. Phys. J. **144**, 13 (2007)

F. Cichos, C. von Borczyskowski, M. Orrit: *Power-Law Intermittency of Single Emitters*, Curr. Opin. Colloid Interface Sci. **12**, 272 (2007)

M.M.I. El-Sayed, T. Blaudeck, F. Cichos, S. Spange: *Synthesis, Solvatochromism, and Photophysical Properties of the Polymer-Tetherable 3-[4-Di(2-hydroxyethyl)amino]-7-phenyl-1-(2-furyl)-2-propene-1-one*, J. Photochem. Photobiol. A **185**, 44 (2007)

E.I. Zenkevich, T. Blaudeck, A.M. Shulga, F. Cichos, C. von Borczyskowski: *Identification and Assignment of (Porphyrin/CdSe Nanocrystal) Heteronanoassemblies*, J. Lumin. **122**, 784 (2007)

2.13 Graduations

Doctorate

- Thomas Blaudeck
  Self-Assembly of Functionalized Porphyrin Molecules on Semiconductor Nanocrystal Surfaces
  September 2007 (TU Chemnitz)

Diploma

- Romy Radünz
  Photothermische Detektion einzelner Quantenobjekte
  February 2007 (TU Chemnitz)
- Nicole Amecke
  Investigations to the Fluorescence of Single CdSe/ZnS-Nanocrystals Under One- and Two-Photon-Excitation at Low Temperatures
  May 2007 (TU Chemnitz)

3

Molecular Physics

3.1 Introduction

Πάυτα ῥεῖ – everything is in flow. This famous statement of Heraklit holds for the situation of our group in 2007 especially well: In October 2006 Ulrich Keyser joined the group, in Januar 2007 he received an Emmy-Noether award and an offer for a lecturer position at the University of Cambridge in October 2007. Furthermore Anatoli Serghei was asked if he would be interested in a Post. Doc. position at the University of Massachusetts in Amherst, the center of polymer research in the USA. So both will leave the group in 2008.

The activities in our *classical* fields of expertise Broadband Dielectric Spectroscopy, experiments with Optical Tweezers and 2D-Fourier-Transform Infrared Spectroscopy developed nicely. A variety of important publications appeared in leading journals and the funding situation – mainly through the Deutsche Forschungsgemeinschaft (German Science Foundation) – substantially improved. This is a solid basis for the future prospects.

Friedrich Kremer

3.2 Molecular Dynamics of Isolated Polymer Chains

A. Serghei, F. Kremer

A recent experimental development [1] is employed to measure the molecular dynamics of isolated polymer chains (Fig. 3.1). Three different preparative approaches are followed: (i) spin-coating of strongly diluted polymer solutions, leading to samples which exhibit nearly isolated polymer chains adsorbed on a solid substrate (Fig. 3.1a); (ii) chemical grafting of polymer chains using a low grafting density to ensure isolated polymer chains; (iii) "physical" grafting by adsorption of strongly asymmetric diblock copolymers (from a diluted solution), with phase separation and large differences in the glass transition temperature between the two blocks, and additionally with the property that one component shows a good wetting of the supporting substrate while the second one exhibits dewetting.

[1] A. Serghei, F. Kremer: Rev. Sci. Instrum. **79**, 026 101 (2008)

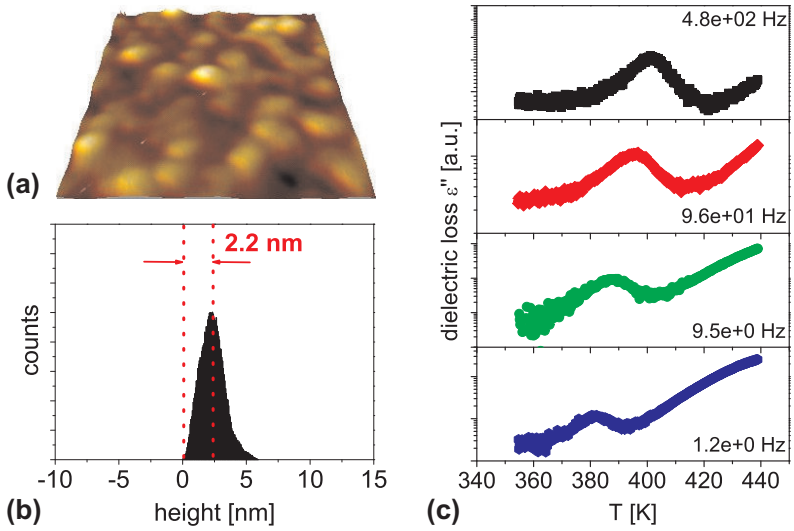

Figure 3.1: (**a**) AFM image (300 nm × 300 nm) showing individual polymer chains (poly-2-vinylpyridine) adsorbed on the surface of a silicon wafer; (**b**) the corresponding heights histogram; (**c**) dielectric loss vs. temperature at different frequencies showing the dynamic glass transition of the sample in (**a**).

3.3 Interfacial Dynamics of Polymers in Interaction with Solid Substrates

A. Serghei, F. Kremer

The aim of the present project is to investigate the dynamics of polymers in the immediate vicinity of solid interfaces. For this purpose, Broadband Dielectric Spectroscopy (BDS) is employed to measure in a wide frequency and temperature range molecular fluctuations of polymer segments taking place in a (nanometric) proximity to a solid substrate. As probes, ultra-thin polymer films are used. A recently developed experimental approach (Fig. 3.2a,b) has been optimized and employed to render to BDS (traditionally a bulk technique) the character of an interfacial method. A systematic

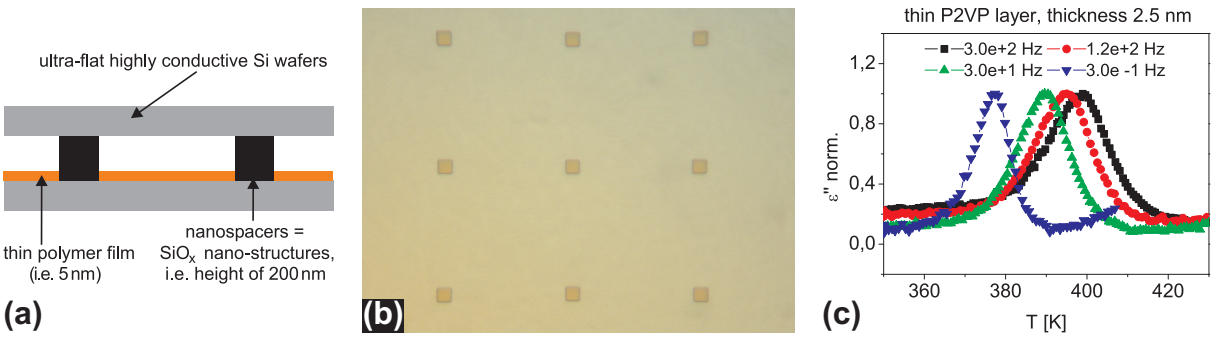

Figure 3.2: (**a**) Schematic representation of the experimental approach; (**b**) matrix of silica nanostructures (5 μm × 5 μm × 200 μm) acting as spacers; (**c**) dielectric loss vs. temperature at different frequencies, as indicated, showing the dynamic glass transition of a thin P2VP layer deposited on a silicon wafer and having a thickness of 2.5 nm.

adjustment of the interfacial interactions is furthermore allowed by a controlled deposition on the surface of the electrodes of various (metallic but as well organic) layers prior to the preparation of thin polymer films [1].

[1] A. Serghei, F. Kremer: Rev. Sci. Instrum. **79**, 026 101 (2008)

3.4 A Minimal Model for the Electrode Polarization

A. Serghei, J. Rume, F. Kremer

Electrode polarization is a phenomenon manifested when the diffusion of charge carriers is (partially) blocked due to the presence of interfaces. It causes pronounced changes of the dielectric function and hence of the complex conductivity. These changes show a peculiar dependence on the length of the sample cell and on the material of the electrodes. The current project aims to develop a minimal model for electrode polarization, i.e. based on a minimal set of assumptions. It can be shown that, assuming a thin interfacial layer (~ 1 nm thickness) having a much lower dielectric loss than in the bulk ($\varepsilon''_{\text{interface}} \ll \varepsilon''_{\text{bulk}}$), leads to dielectric spectra (Fig: 3.3) which exhibit – on a qualitative as well as quantitative level – all experimental features of the electrode polarization:

1. the characteristic spectral dependence of the dielectric response;
2. the experimental observation that the electrode polarization shifts to higher frequencies with increasing temperature;
3. the scaling in respect to the temperature variation;
4. the dependence on the length of the sample cell, i.e. the electrode polarization shifts to higher frequencies when decreasing the sample length;

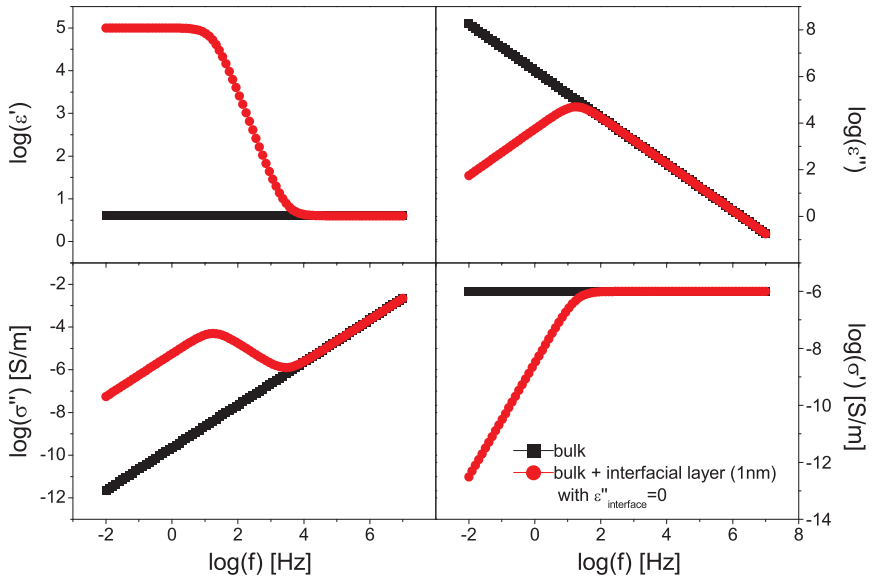

Figure 3.3: Complex dielectric function and complex conductivity of a usual ionic conductor in the bulk (black squares) and calculated under the assumption of interfacial layers (1 nm thickness) with negligible dielectric losses (red circles).

5. the experimental observation that the dielectric response does not scale in respect to the variation of the sample length;
6. the dependence on the material of the electrodes, by allowing different thicknesses of the interfacial layer;
7. the experimental observation that the dielectric response does not scale in respect to the variation of the electrodes material;

3.5 Charge Transport and Mass Transport in Ionic Conductors

J. Rume, A. Serghei, F. Kremer

The mechanism of charge transport in the imidazolium based ionic liquid 1,3-dimethylimidazolium dimethylphosphate is analyzed by combining Broadband Dielectric Spectroscopy (BDS) and Pulsed Field Gradient Nuclear Magnetic Resonance (PFG NMR), see Fig: 3.4. The dielectric spectra are dominated – on the low-frequency side – by electrode polarization effects while, for higher frequencies, charge transport in a disordered matrix is the underlying physical mechanism. Using the Einstein and Einstein–Smoluchowski equation enables one to determine – in excellent agreement with direct measurements by PFG NMR – the diffusion coefficient of the charge carriers. By that, it becomes possible to extract from the dielectric spectra separately the number density and the mobilities of the charge carriers and the type of their thermal activation. It is shown that the observed Vogel–Fulcher–Tamman dependence of the DC conductivity can be traced back to a similar temperature dependence of the mobility while for the number density an Arrhenius-type thermal activation is found.

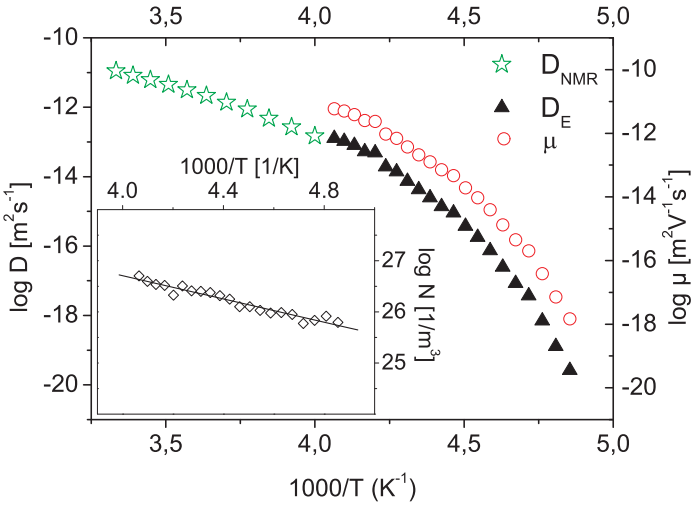

Figure 3.4: Diffusion coefficient determined by the Einstein–Smolokowski equation (using ω_e as hopping rate and $\lambda = 0.2\,\text{nm}$ as hopping length) compared with the diffusion coefficient measured by PFG NMR. Additionally, the mobility of the charge carriers is determined. *Inset*: effective number of charge carriers as a function of inverse temperature.

Extrapolating the latter to room temperature indicates that nearly all charge carriers are participating to the conduction process [1].

[1] J. Rume et al.: *Charge transport and mass transport in imidazolium based ionic liquids*, Phys. Rev. E (2008), accepted

3.6 Correlation Between Rotational and Translational Diffusion under Conditions of Geometrical Confinement

C. Iacob, A. Serghei, F. Kremer

The molecular dynamics, as reflected on the microscopic scale by rotational and translation diffusion, exhibits deviations from its bulk behaviour when organic materials are investigated under geometrical confinement [1–4] (Fig. 3.5). Although both these components of diffusion are manifestations of the same phenomenon – molecular structural fluctuations – no systematic investigations exist concerning the correlations between

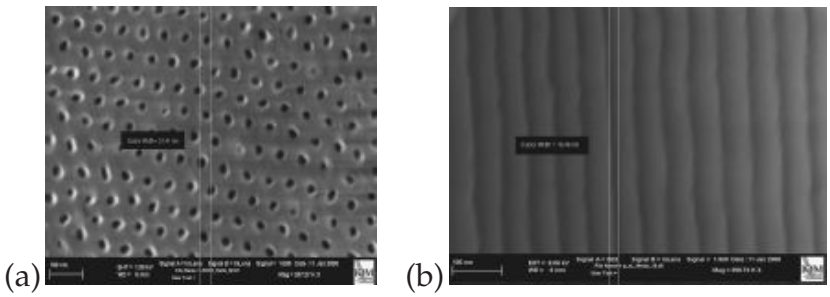

Figure 3.5: a) SEM images of the porous alumina Al_2O_3 host membranes (top view, pore size 30 nm); (**b**) the corresponding cross section.

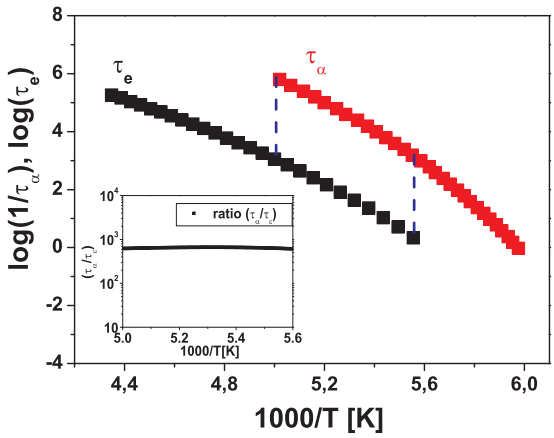

Figure 3.6: Correlation between the translational and the rotation diffusion for 1-butylimidazole: τ_e represents the hopping time of the charge carriers, as defined by the Dyre theory, while τ_α is the fluctuation time related to the dynamic glass transition. *Inset*: The ratio between τ_e and τ_α

the translational and rotational diffusion under conditions of 2D geometrical confinement (Fig. 3.6). The goal of the present project is to investigate these correlations (in the bulk but as well in confinement), in dependence on the molecular structure.

[1] V. Lehmann et al.: Mat. Sci. Eng. B **69-70**, 11 (2000)
[2] M. Arndt et al.: Phys. Rev. E **54**, 5377 (1996)
[3] P. Kumar, P. Huber: J. Nanomater. **2007**, 89 718 (2007), doi:10.1155/2007/89718
[4] F. Ronkel, J.W. Schultze: J. Porous Mater. **7**, 11 (2000)

3.7 Polyelectrolyte-Compression Forces Between Spherical DNA Brushes

K. Kegler, F. Kremer

Optical tweezers are employed to measure the forces of interaction within a single pair of DNA-grafted colloids in dependence of the molecular weight of the DNA-chains (250 basepairs (bp), 500 bp, 750 bp, 1000 bp; Fig. 3.7a), and the concentration and valence (mono-, di-, trivalent) of the surrounding ionic medium (Fig. 3.7b). The resulting forces are short-range and set in as the surface-to-surface distance between the colloidal cores reaches the value of the brush height . The measured force–distance relation is analyzed by means of a theoretical treatment that quantitatively describes the effects of compression of the chains on the surface of the opposite-lying colloid. Quantitative agreement with the experiment is obtained for all parameter combinations [1, 2].

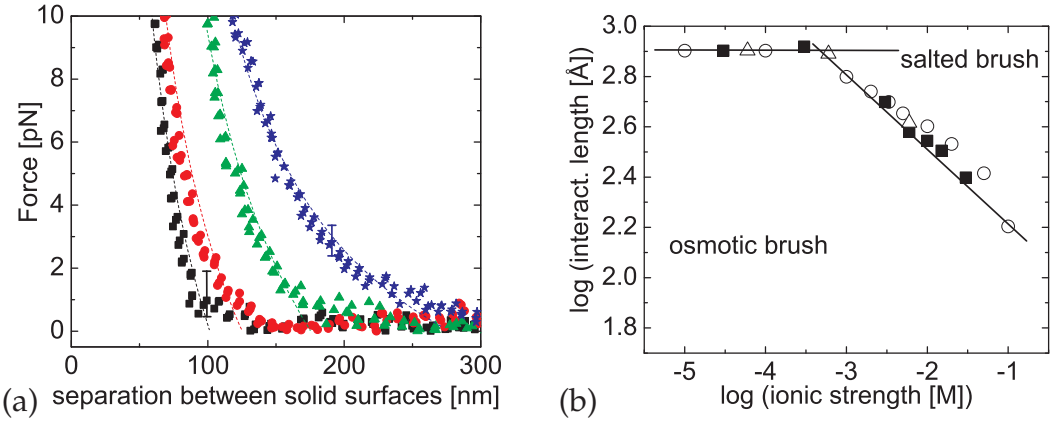

Figure 3.7: (**a**) $F(D)$ curves between DNA-grafted colloids in buffered solution (10 mM $C_4H_{11}NO_3$, pH = 8.5) for a constant grafting density and various bp-number (250 bp (*square*), 500 bp (*circle*), 750 bp (*triangle up*) and 1000 bp (*star*)). (**b**) Double-logarithmic plot of the interaction length for a force $F = 2$ pN versus the ionic strength of the added salt. Here, the molecular weight of the grafted DNA is $N = 1000$. Different types of symbols correspond to different salt valencies (NaCl – *circle*, $CaCl_2$ – *square*, $LaCl_3$ – *triangle*). The *line* of slope -1/3 indicates theoretical scaling law predictions for comparison.

[1] K. Kegler et al.: Phys. Rev. Lett. **98**, 058 304 (2007)
[2] K. Kegler et al.: Phys. Rev. Lett. **100**, 118 302 (2008)

3.8 Drag-Induced Forces on Colloids in Polymer Solutions of Varying Concentration

C. Gutsche, F. Kremer

We present a first direct experimental observation of jamming-induced drag-enhancement on colloids pulled through a solution of λ-DNA (used here as a monodisperse model polymer) with an optical tweezers [1]. The experiments show a drag force which is larger than expected from the Stokes formula and the independently measured vis-

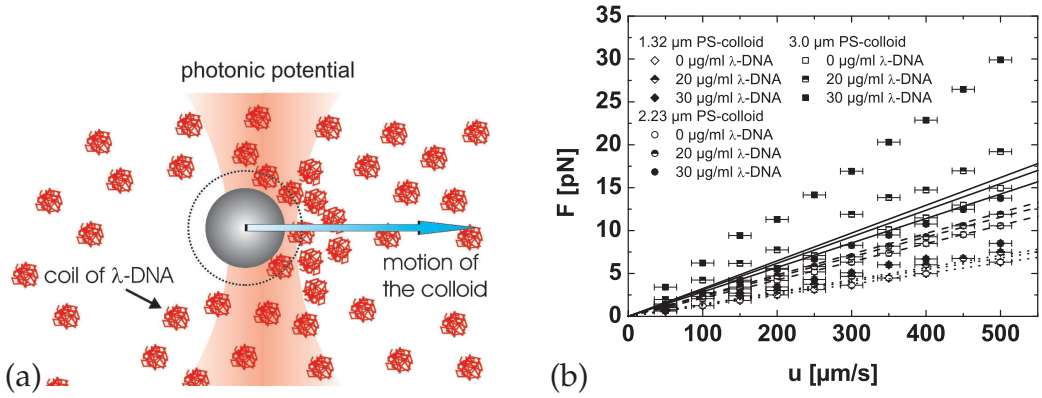

Figure 3.8: (**a**) Illustration of the experimental set up. The colloid (*grey*) surrounded by coils of DNA (*red*) is held in an optical trap (*magenta*). (**b**) Drag force F on colloids in λ-DNA as a function of the pulling speed u. Also shown is the Stokes force on the colloids (*solid line*) as expected for the viscosities measured for the given DNA concentration in a viscosimeter.

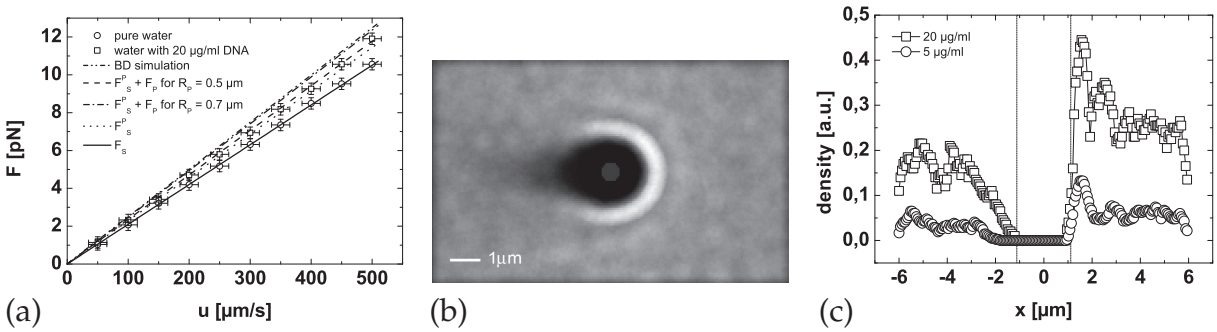

Figure 3.9: (**a**) Drag force F on a colloid of radius 1.12 µm measured in pure water and in a DNA solution as a function of the velocity u. The data is compared to the Stokes friction (F_S) in pure water (*full line*) and in the DNA solution F_S^P (*dotted line*) calculated from the measured viscosity, as well as to F_S^P plus the contribution F^P from the DNA jam in front of the colloid for $R_P = 0.5$ µm (*dashed line*) and for $R_P = 0.7$ µm (*dashed-doted line*). Also shown is a fit to BD simulation results between 0 µm and 50 µm (*dashdot-dotted line*). (**b**) Polymer density around the colloid at a concentration of 20 µg/ml and $u = 50$ µm/s. *Lighter colors* denote higher polymer densities. (**c**) Normalized average polymer density on a line through the colloid center in the direction of motion for concentrations of 5 µg/ml (*open circles*) and 20 µg/ml (*open squares*) and velocity $u = 50$ µm/s. Polymers accumulate in front of the colloid and the concentration in the back is reduced due to the finite Peclet number of the polymers. Lines connecting data points are guides to the eye. Also visible are density oscillations in front of the colloid, which are characteristic for hard sphere systems. The vertical lines indicate the size of the colloid (±1.12 µm).

cosity of the DNA solution. We attribute this to the accumulation of DNA in front of the colloid and the reduced DNA density behind the colloid. This hypothesis is corroborated by a simple drift-diffusion model for the DNA molecules, which reproduces the experimental data surprisingly well, as well as by corresponding Brownian dynamics simulations. The experiments (Fig. 3.8) show that the drag force on colloids pulled through a solution of λ-DNA with an optical tweezers cannot be explained by the Stokes force for the solution viscosity. This drag force is much larger than that predicted by Stokes' law and increases approximately linear with the drag velocity and non-linearly with the DNA-concentration.

First theoretical approaches to this problem as well as the Brownian dynamics simulations are in good agreement with the experiments and represent a first quantitative modelling of the microrheology of a complex fluid (Fig. 3.9).

[1] C. Gutsche et al.: *Colloids dragged through a polymer solution: experiment, theory and simulation*, submitted to J. Chem. Phys. (2007), arXiv:0709.4142

3.9 In-Situ Analysis of the Forces of Interaction in Polyelectrolyte Brushes

G. Dominguez, F. Kremer

The forces of interaction between colloids being grafted with poly acrylicacid (PAA) brushes are measured by means of optical tweezers. Parameters to be varied are the ionic strength, the valence of the conterions and the pH of the surrounding medium.

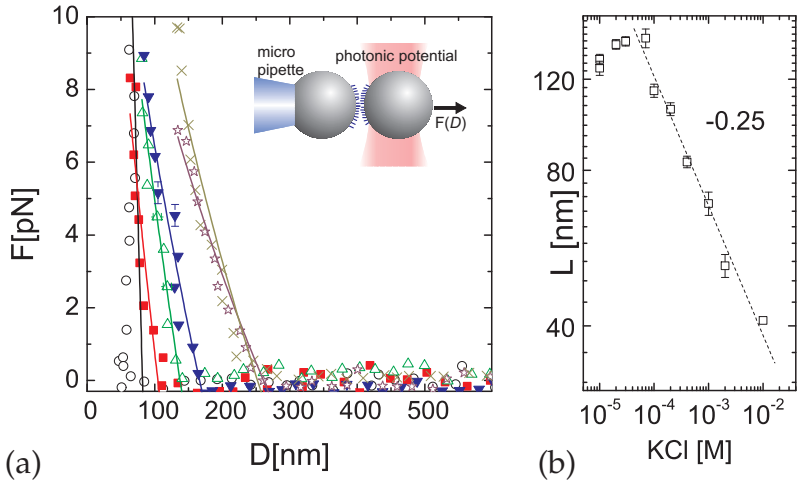

Figure 3.10: (**a**) Force (F) vs. separation (D) between the solid surfaces of two PAA-grafted particles under conditions of varying ionic strength of the surrounding medium at pH 7. *Open circles*, *full squares*, *open triangles*, *full triangles*, *open stars* and *crosses* represent [KCl] in molar units for 10^{-2}, 2×10^{-3}, 10^{-3}, 4×10^{-4}, 10^{-5}, and 10^{-5} (measured at the end of the experimental run to show the reversibility of the process), respectively. Error bars are indicated. The *dashed lines* represent fits according to a model by Jusufi et al. [1]. *Inset*: Scheme of the experimental set-up. (**b**) Brush height (L) vs. salt concentration as determined from the Jusufi model; the *dashed lines* indicates the power law dependence with the exponent −1/4.

The observed force distance dependence (Fig. 3.10) enables one to trace – within a *single* pair of PAA-grafted colloids – the swelling of the polymer brush with decreasing KCl concentration. The data are well described by a recently published theory [1] of the effective interaction between spherical polyelectrolyte brushes. According to this the dominant term in the interaction arises from the entropic contribution of the counterions inside the brush. This enables one to determine the brush height in dependence of the salt concentration. An exponent of −1/4 is found which ranges between the value being predicted for planar (−1/3) and spherical brushes (−1/6).

[1] A. Jusufi et al.: Colloid Polym. Sci. **282**, 910 (2004)

3.10 Optical Tweezers to Study Single Receptor/Ligand-Interactions

M. Salomo, K. Kegler, M. Struhalla, J. Reinmuth, W. Skokow, F. Kremer

Receptor/Ligand-interactions are crucial for a manifold of biological processes like the transport of substances within cells or the exchange with their environment. They also have central impact on signal transduction by initializing signal cascades. Most studies have been performed with the reactants in solution. This does not reflect the general conditions that are relevant in vivo. Optical tweezers are ideally suited to study the interaction of single receptor-ligand bonds. We developed an assay using optical tweezers to investigate the interactions between Protein A from Staphylococcus aureus and Immunoglobulin G from rabbit serum (RIgG) (Fig. 3.11). We demonstrate that the rupture forces depend on the loading rate (Fig. 3.12a) and sodium chloride concentration (Fig. 3.12b). The measured loading rate effect is well known in the literature and the data we obtained were found to be in good agreement with an already published theoretical model. The dependence of the rupture forces on the salt concentration demonstrates the influence of hydrophobic interactions on the bond strength. Our experimental setup can

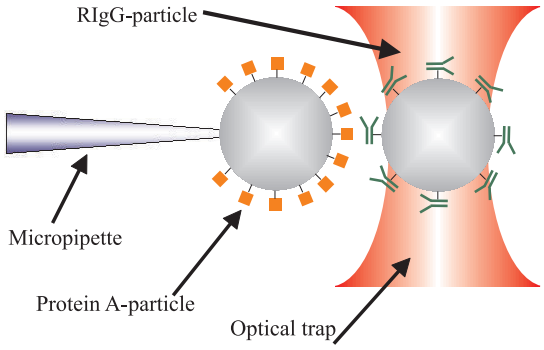

Figure 3.11: Experimental setup. One particle with protein A on its surface is fixed at a micropipette by suction. The other one carrying Immunoglobulin G is held in the optical trap. In the course of the measurement the particles are brought together in order to establish a single bond between Protein A and RIgG. By pulling the colloids apart the junction breaks and the resulting rupture forces can be measured directly.

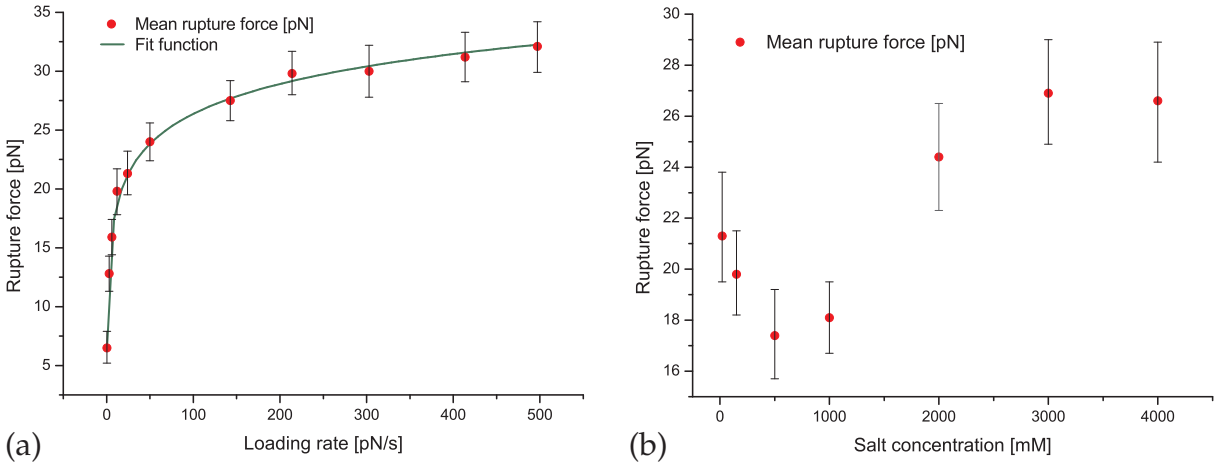

Figure 3.12: (**a**) Loading rate dependence. With increasing loading rates the rupture force rises and levels of above 150 pN/s. (**b**) Salt dependence. Electrostatic forces decrease with higher salt concentrations while hydrophobic interactions increase.

probe the interaction between a single receptor and its specific ligand under changing conditions and hence offers manifold applications in single molecule biotechnology.

[1] M. Salomo et al.: *Optical tweezers to study single protein A/Immunglobulin G interaction at varying conditions*, Eur. Biophys. J. (2008), accepted

3.11 DNA Condensation under the Action of the Protein TmHU as Studied on a Single Molecule Level

C. Wagner, M. Salomo, U.F. Keyser, K. Kegler, C. Gutsche, F. Kremer

Optical Tweezers enable one to analyse the binding of the histone-like Protein TmHU (from Thermotoga maritima) to DNA on a single molecule level [1, 2]. Like the eucariotic histone proteins, TmHU acts on the DNA by condensating it. Therefore we give special emphasis to the question if there exist similar levels of organization. As a further refinement, our set-up is now accomplished with a fast feed-back loop which allows to carry out the experiment under conditions of a constant and adjustable force. By that it should be possible to unravel the energetics and dynamics of the TmHU/DNA-interaction in detail. In the experiment, the DNA molecule is established between two microparticles, the force acting on the DNA is set to the designated value and the TmHU-solution is flushed into the cell. The condensation of the DNA leads to a decrease in the separation of the particles that we can observe with nanometer resolution. By reducing the protein concentration stepwise from 250 µg/ml down to 20 µg/ml we found that the condensation proceeds with a lower rate and with step-like interruptions (Fig. 3.13a). As characteristic for cooperative binding, this rate depends on the concentration in a sigmoidal manner (Fig. 3.13b) [1–3]. The fact that the condensation is much more efficient than one could explain just by an elementary protein binding as well as the observed retardations (Fig. 3.13a) suggest that higher levels of organization exist.

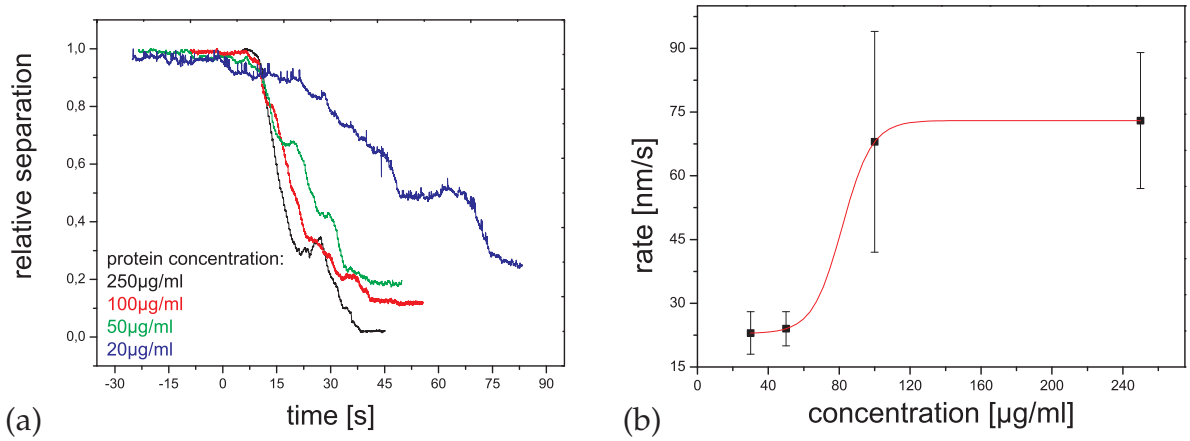

Figure 3.13: (**a**) Temporal evolution of the relative length of a single DNA-chain in media of varying TmHU concentration as indicated. The force was kept constant at a level of 2 pN. Especially for low concentrations sequences of progress and arrest are observed reflecting the action of the protein. (**b**) Sigmoidal dependency of the absolute velocity on the concentration.

[1] M. Salomo et al.: Microsc. Res. Techniq. **70**, 938 (2007)
[2] M. Salomo et al.: Mol. Biol. **359**, 769 (2006)
[3] D. Esser et al.: Mol. Biol. **291**, 1135 (1999)

3.12 Dynamics of DNA under Tension and in Confinement

I. Semenov, U.F. Keyser, M. Salomo, F. Kremer

While the structural properties of the DNA are well explored, much less is known concerning its dynamics as a single polymer chain and under conditions of geometrical confinement. Extended theoretical studies were carried out to explore the sub-diffusive internal macroscopic dynamics and to study how it is affected by external constraints, constrictions and confinements [1–3]. Optical Tweezers offer [4, 5] the unique possibility to carry out dedicated experiments with respect to this; in detail it is planned to determine the relaxation of single DNA-chain which is hold under tension between two colloids with one located in an optical trap (Fig. 3.14a). The DNA is labeled by a quantum dot and cut by adding restriction enzymes to the surrounding medium. The relaxation of the molecule is observed by monitoring the position of the fluorescently excited quantum dot. Further experiments of highest interest are similar studies in the presence of a polymer gel (Fig. 3.14b).

It is expected that these studies will deliver detailed novel insights into the dynamics of DNA under conditions of confinement with varying character.

[1] O. Hallachek et al.: Phys. Rev. E **75**, 031 905 (2007)
[2] O. Hallachek et al.: Phys. Rev. E **75**, 031 906 (2007)
[3] O. Hallachek et al.: Phys. Rev. E **70**, 031 802 (2004)
[4] M. Salomo et al.: Colloid Polym. Sci. **284**, 1325 (2006)
[5] U. Keyser et al.: Nature Phys. **2**, 473 (2006)

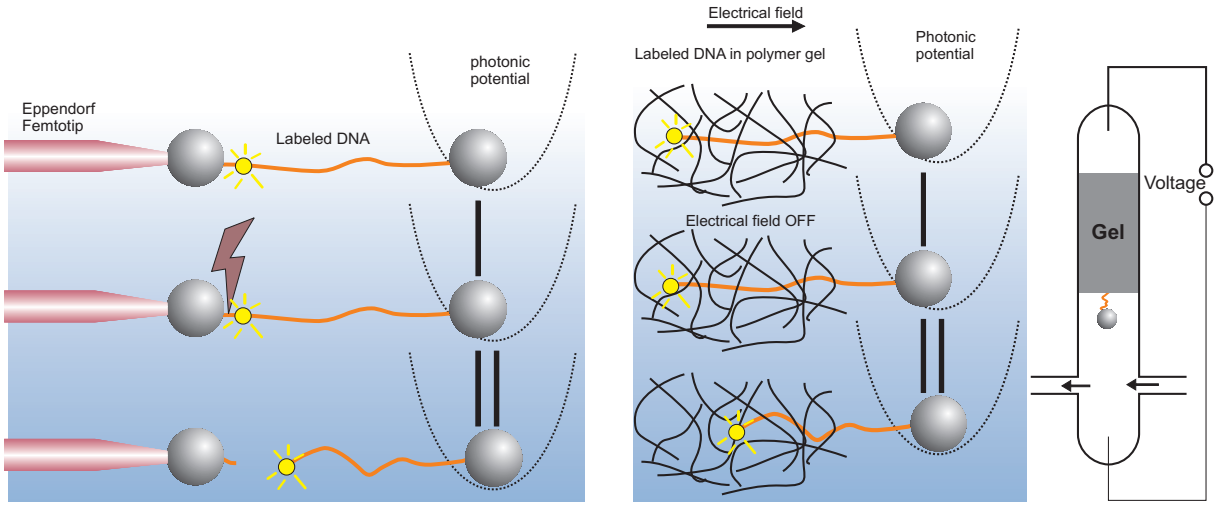

Figure 3.14: (**a**) Relaxation of a single DNA-chain kept under a defined tension by use of OT. (**b**) Relaxation of a single DNA-chain kept under a defined tension by use of an external electric field and in the presence of a polymer-gel.

3.13 Study of Protein–DNA Interaction with Atomic Force Microscopy

H. Brutzer, M. Salomo, U.F. Keyser, F. Kremer

Atomic force microscopy (AFM) was used to investigate single macromolecules, in particular DNA, proteins and protein–DNA complexes. DNA contour and persistence length were studied yielding results comparable to literature values. The volume of

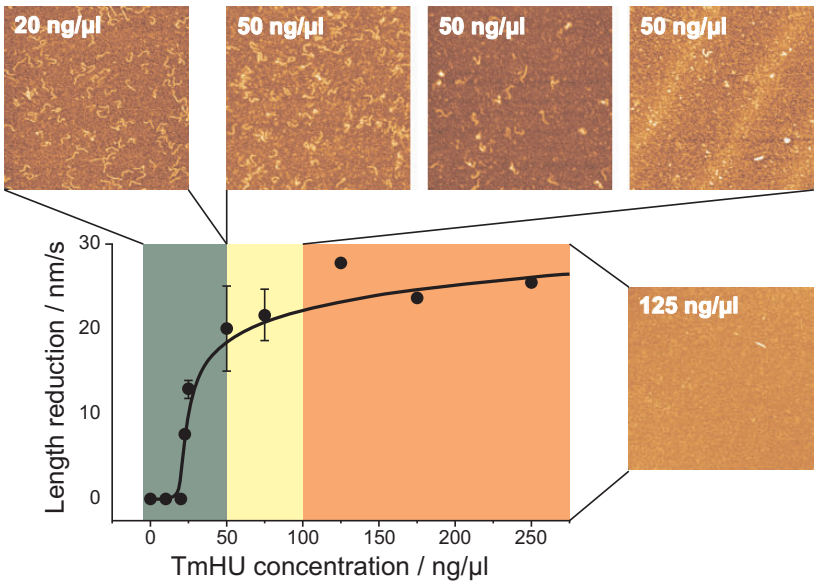

Figure 3.15: Results based on AFM measurements compared with data achieved using optical tweezers (taken from [1] and modifed). TmHU compacts the DNA above a concentration of 50 ng/l.

histone-like HU protein dimers from Thermotoga maritima (TmHU) could be determined in good agreement with results calculated from their molecular weight. Furthermore, the concentration dependence of binding for TmHU dimers to DNA was examined (Fig. 3.15). For the end-to-end distance of the DNA strands a concentration-dependence is found with a threshold-limit below which hardly any influence of the concentration is observable. Above that, no DNA molecules can be deposited onto the surface, which suggests the formation of large clusters consisting of TmHU-DNA complexes. By analysing the coverage of TmHU molecules on the DNA strand a simple model of one relatively short binding site per protein becomes highly unlikely. Instead, evidence is found that multiple binding sites for each protein contribute to the creation of globular structures, possibly due to a secondary organizational level of the TmHU-DNA complex.

[1] M. Salomo et al.: Microsc. Res. Techniq. **70**, 938 (2007)

3.14 Optical Tweezers for Single-Colloid-Electrophoresis

O. Otto, C. Gutsche, U.F. Keyser, F. Kremer

Properties of colloidal dispersions have been studied intensively for decades. A fundamental understanding is of great importance in many fields of work, e.g. to analyze complex transport mechanisms in living organisms or to examine rheological phenomena of condensed matter. Colloidal dispersions find wide spread industrial applications as coatings, aerosol, ceramics and drugs. Crucial for their properties are the size and charge of the colloids, both can be varied over a broad range and thus the intercolloidal interactions can be adjusted. This makes colloidal dispersions an excellent model system to investigate fundamental issues in condensed matter physics. We developed an optical tweezers setup to study the electrophoretic motion of colloids in an external electric field. The setup is based on standard components for illumination and video

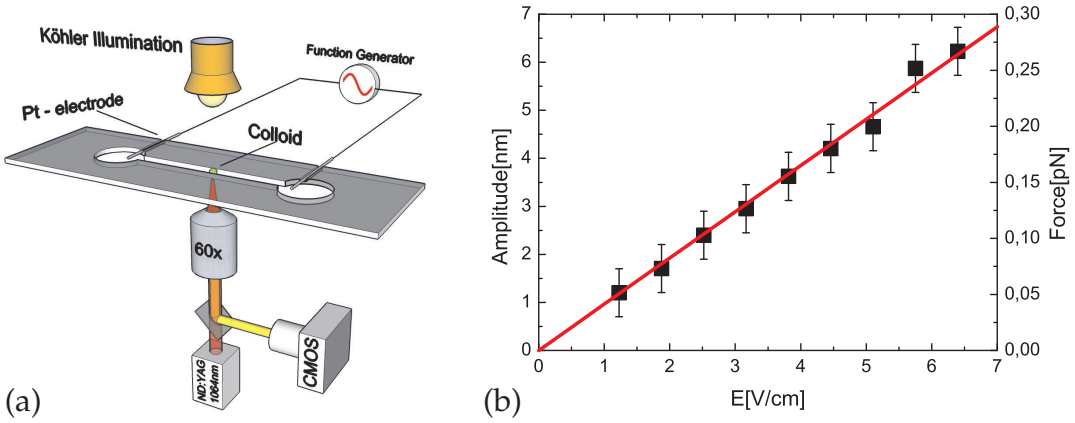

Figure 3.16: (**a**) Schematic of the Optical Tweezers setup with custom made fluidic cell. A single colloid is held in the optical trap and its movement due to an external electrical field recorded by video detection. (**b**) Amplitude and force as a function of electric field for a single 2.23 μm colloid in aqueous solution. Amplitudes as low as 1 nm and forces of 50 fN are detected.

detection (Fig. 3.16a). Our video-based optical tracking of the colloid motion has a time resolution of 0.2 ms resulting in a bandwidth of 2.5 kHz. This enables one to calibrate the optical tweezers by Brownian motion without applying a quadrant photo detector. We demonstrate that our system has a spatial resolution of 0.5 nm and a force sensitivity of 20 fN using a Fourier algorithm to detect periodic oscillations of the trapped colloid caused by an external AC-field (Fig. 3.16b). The electrophoretic mobility and Zeta-potential of a single colloid can be extracted in aqueous solution avoiding screening effects common for usual bulk measurements.

[1] O. Otto et al.: Rev. Sci. Instrum. **79**, 023 710 (2008)

3.15 Structural Levels of Organisation in Spider Silk as Unraveled by Combined Mechanical and Time-Resolved Polarized FTIR Studies

P. Papadopoulos, J. Sölter, I. Weidner, F. Kremer

The understanding of the mechanical properties of the various types of spider silk requires a combination of techniques which can trace the effects of external fields on the microscopic level (Fig. 3.17). FTIR is particularly suitable, because it can distinguish between different aminoacid groups as well as different secondary structures.

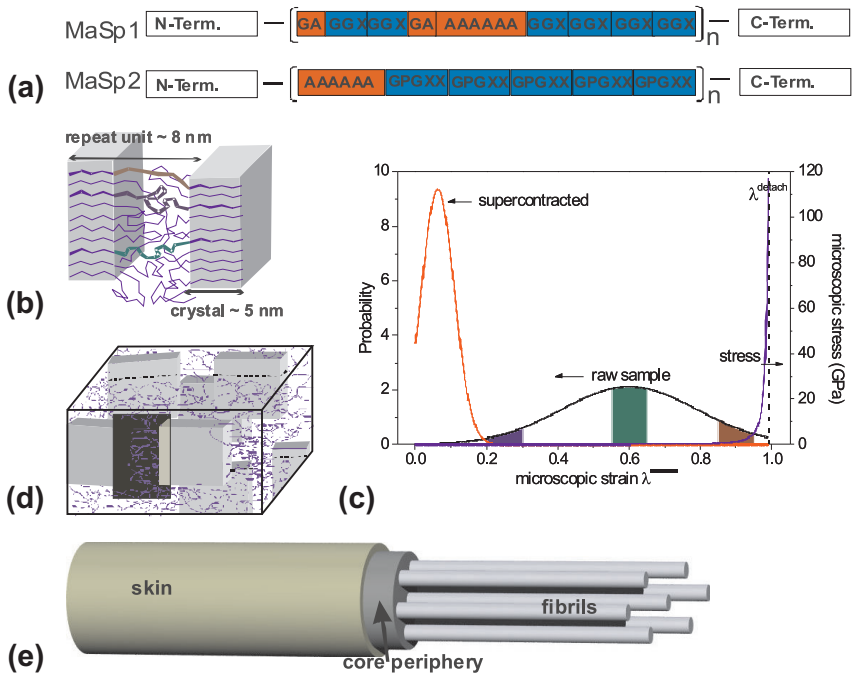

Figure 3.17: Proposed structural levels of organization in spider silk. The alanine-rich protein parts (**a**) form highly oriented crystals (**b**) which are interconnected by amorphous worm-like chains with a Gaussian pre-strain distribution (**c**). The so assembled β-sheeted blocks (**d**) form a core of fibrils inside the silk fiber (**e**). The skin balances the internal pre-strain.

The simultaneous stress-strain measurements unravel the microscopic response under equilibrium and non-equilibrium conditions. In the case of major ampullate silk, crystalline and amorphous regions are affected in different ways by external strain. The alanine-rich crystals remain always almost perfectly aligned parallel to the fiber axis, whereas the glycine-rich amorphous chains exhibit a very low order parameter. An important effect is the frequency shift of vibrations corresponding to crystalline structures, which depends on stress rather than strain and can be used as a microscopic probe of the force [1]. The linear thresholdless response implies that crystals are interconnected by pre-strained chains. This pre-stress is counterbalanced by the fiber skin and is released upon hydration. A model assuming a gaussian distribution of pre-strain and a worm-like behavior of the amorphous chains can reproduce the mechanical properties of both native and supercontracted silk [2]. This model applies also to minor ampullate silk, which has different properties, even though its chemical structure is not very different. The difference can be explained by a lower degree of pre-strain.

[1] P. Papadopoulos et al.: Eur. Phys. J. E **24**, 193 (2007)
[2] P. Papadopoulos et al.: *Hierarchies in the structural organization of spider silk – a quantitative model*, submitted to Phys. Rev. Lett. (2008)

3.16 Noise in Solid-State Nanopores

U.F. Keyser

We study ionic current fluctuations in solid-state nanopores over a wide frequency range and present a complete description of the noise characteristics (Fig. 3.18). At low frequencies ($f < 100\,\mathrm{Hz}$) $1/f$-type of noise is observed. Analysis of this low-frequency noise at different salt concentrations shows that the noise power remarkably

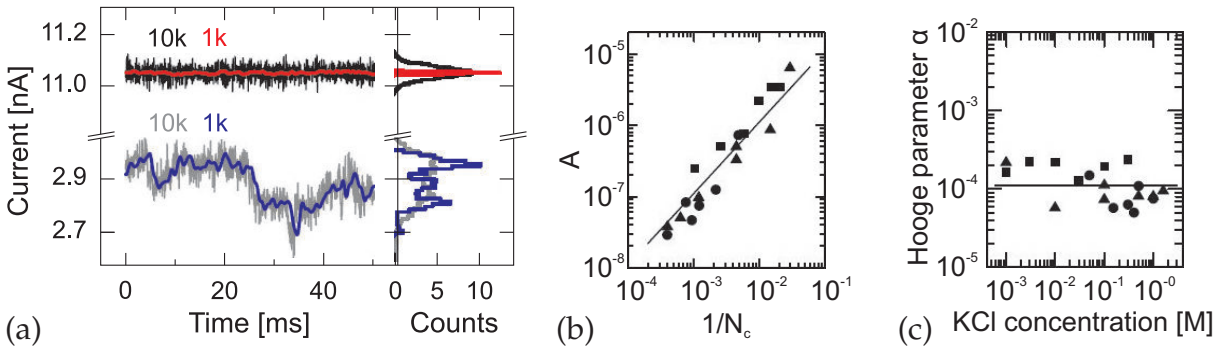

Figure 3.18: (**a**) Current recordings and histograms of two nanopores (at 100 mV) with substantially different resistance values, illustrating clear differences in current noise. The nanopores diameters are 20.8 nm (*bottom traces*) and 22.0 nm (*top traces*). The current was filtered at 10 and 1 kHz, as indicated. (**b**) Noise power as a function of the calculated inverse number of charge carriers in the nanopore. (**c**) The value of the Hooge parameter over the salt concentration. The Hooge parameter is constant and results from the product of the noise power and the number of charge carriers.

scales linearly with the inverse number of charge carriers, in agreement with Hooge's relation. We find a Hooge parameter of $(1.1 \pm 0.1) \times 10^{-4}$. In the high-frequency regime ($f > 1$ kHz), the increase in current power spectral density with frequency is modelled through a calculation of the Johnson noise. Finally, we use these results to compute the signal-to-noise ratio for DNA translocation for different salt concentrations and nanopore diameters, yielding the parameters for optimal detection efficiency.

[1] R.M.M. Smeets et al.: Proc. Nat. Acad. Sci. USA **105**, 417 (2008)

3.17 Modelling Colloidal Transport Through Capillaries

G. Stober, L. Steinbock, B. Gollnick, U.F. Keyser

The charge and diameter of colloidal particles determine their interaction in aqueous solutions. Measuring the surface charge remains a challenge despite the numerous existing approaches. Here we investigate the possibility to determine the diameter and surface charge of colloids passing a small capillary leading to a brief obstruction of an ionic current (Fig. 3.19). We developed a simple model founded on simple geometrical considerations to understand this process. The ionic conductance in such a system is given by the cross section of the capillary tip. A colloid passing through the tip reduces this cross section and replaces the charges of the ionic solvent in his volume by his own. Using this idea in a computer simulation using Newtons equation of motion for the colloid and a rotational geometry for the capillary, the time dependency of signal could be investigated. Adding some realistic features like an uncertainity in the size of the colloids, a Hagen Poiseuille velocity profile in the capillary and the possibility to manipulate the charges of the colloid, allows simulation of the expected current

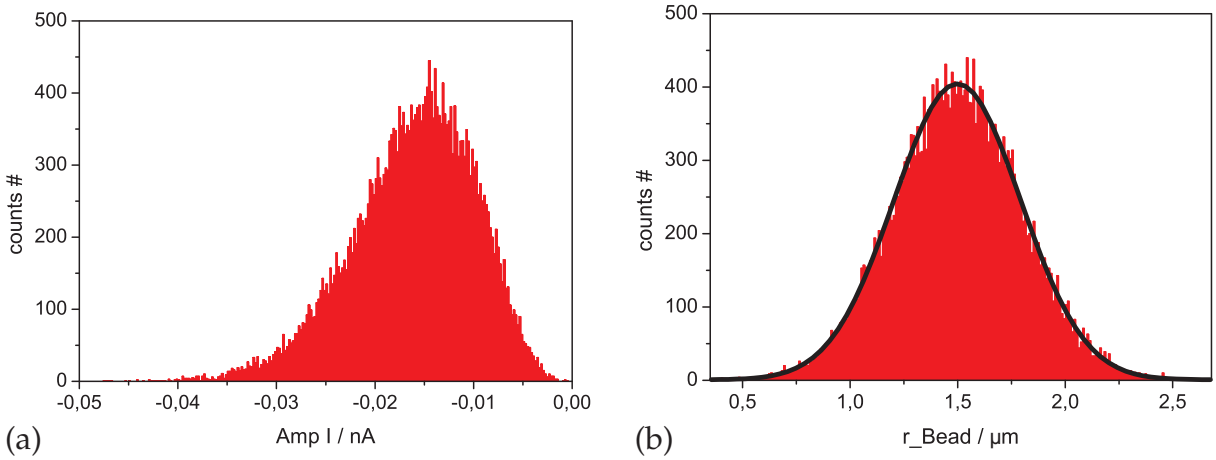

Figure 3.19: The histograms were calculated for a 3 µm colloid in a 48 µm capillary. The monovalent salt concentration was $c = 10^{-2}$ mol at a voltage of 100 mV. (**a**) In this simulation a Gaussian size distribution was used with an RMS of 20 %. The Gaussian distribution was generated with Marsaglia Pseudo random numbers. (**b**) The simulated size distribution is clearly Gaussian. Obviously the asymmetry is a real effect due to the dependency of the signal from the cross section and so a further moment enters in the distribution in the amplitudes.

amplitude. The model together with the simulation enables one to perform several millions of experiments in a few hours for several sets of parameters (ionic strength of the solvent, colloid sizes and capillary geometries). With the simulations we are able to assess the influence of the surface charge and colloid size on the expected distribution of blockage current.

[1] U.F. Keyser et al.: Rev. Sci. Instr. **77**, 105 105 (2006)
[2] C. Gutsche et al.: Phys. Rev. E **76**, 031 403 (2007)
[3] O. Otto et al.: Rev. Sci. Instrum. **79**, 023 710 (2008)

3.18 Transport of Colloids Through Glass Capillaries

L. Steinbock, G. Stober, B. Gollnick, U.F. Keyser

Nanopores promise a new avenue in DNA sequencing. By restricting the polymer inside the pore, translocating the nucleotides one by one by electrophoresis DNA sequencing could be done at a much faster speed, without the high costs involved in chemicals, proteins necessary in current techniques. We started to study translocation of colloids through micrometer sized pores, while measuring the ionic current. Once source for these pores are borosilicate capillaries, which are drawn with a pipette puller to pores of several micrometer to sub-micrometer diameters (Fig. 3.20a). The second source is a focused ion beam (FIB), which allows the fabrication of holes into silicon chips from micrometer to nanometer size (Fig. 3.20b). While measuring the ion current flowing through the pore the translocating DNA-colloids will disturb the ion signal. This will enable us to estimate the charge of the colloids and the number of attached polymers like e.g. DNA strands. Further, we will combine the ionic current measurements with an optical trap to manipulate colloids in the capillaries. In the future we aim to decrease the pore size to below 10 nm to detect specific DNA sequences, which are complementary to distinct segments on the DNA. These will be detected, by measuring the ionic current.

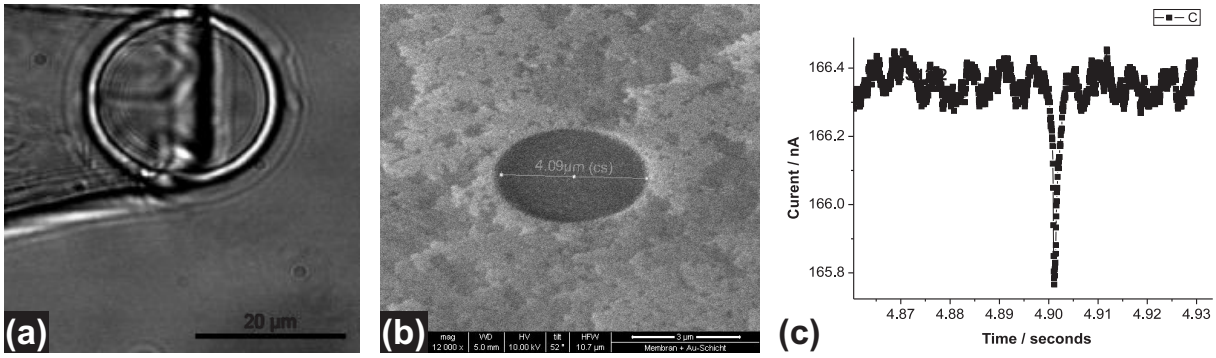

Figure 3.20: (**a**) Image of a borosilicate glass capillary, which is blocked by colloid. (**b**) Image of a 4-µm pore within in a gold coated Si_3N_4 membrane etched by a focused ion beam (FIB). (**c**) Ionic current measurement through a glass capillary. The peak is caused by the translocation of a colloid, which results in a decreased current.

[1] U.F. Keyser et al.: Rev. Sci. Instr. **77**, 105 105 (2006)

3.19 Localized Heating Effects in Optical Tweezers Investigated Using Ionic Currents Through Nanopores

J.H. Peters, U.F. Keyser

Optical tweezers are a powerful and widely used experimental tool in biological physics including single molecule investigations. The strongly focused laser-beam in such a setup can reach power densities in the order of 10^8 W/cm^2 that cause significant heating exceeding 10 K per Watt of incident laser power for a 1064-nm-Laser (Fig. 3.21) [1, 2]. As the reaction constants of biomolecules are temperature dependent, heating effects should be considered in biophysical experiments. The ionic current through a nanopore depends on the local temperature in a well-defined manner and hence can be used for temperature measurements with high spatial resolution [1]. We compare experiments using nanopores with numerical finite element calculations and investigate the dependence of heating effects on parameters like geometry and thermal conductivity of water and nanopore material. We were able to confirm earlier findings as the logarithmic dependence of the maximal temperature on the size of the system [2] and also gain a more detailed insight into the temperature distribution found in optical tweezers.

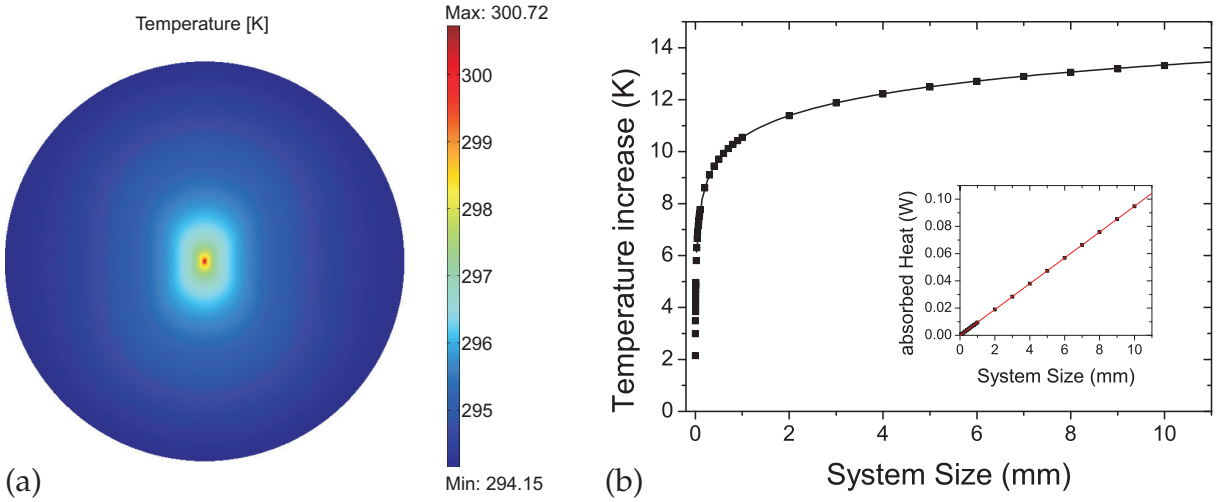

Figure 3.21: (**a**)Temperature-distribution generated by a focussed (gaussian) Laser-beam in a sphere of water (r = 50 µm). The distribution has been calculated numerically from the heat equation using the finite-element method (FEM). (**b**) Dependence of the temperature in the focus and of the absorbed heat *inset* on the system size calculated by FEM. The temperature was fitted (*line*) with a model based on the analytic solution given in [2].

[1] U.F. Keyser et al.: Nano Lett. **5**, 2253 (2005)
[2] E. Peterman et al.: Biophys. J. **84**, 1308 (2003)

3.20 Funding

Einzelmolekülanalyse: Optische Pinzetten zum Studium der Wechselwirkung von einzelnen Rezeptor/Ligand-Komplexen

Prof. Dr. F. Kremer
SMWK-Projekt 4-7531.50-02-0361-06/1 (2006-2007)

DFG-Teilprojekt im Rahmen des Schwerpunktprogramms "Nano- und Mikrofluidik: Von der molekularen Bewegung zur kontinuierlichen Strömung" SPP 1164
Prof. Dr. F. Kremer
DFG-Schwerpunktprogramm 1164, KR 1138/14-2 (2006-2008)

DFG-Projekt "Confinement effects on the molecular dynamics of polymers with special architectures"
Prof. Dr. F. Kremer, Dr. A. Serghei
KR 1138/17-1 (2006-2008)

DFG-Projekt "Physicochemical characterisation of ionic liquids-mediated peptide acylation reactions"
Prof. Dr. F. Kremer
KR 1138/18-1 (2006-2008)

DFG-Projekt "In-situ Untersuchung der Wechselwirkungskräfte an Polyelektrolytbürsten"
Prof. Dr. F. Kremer
KR 1138/20-1 (2006-2008)

FOR877, DFG-Projekt: "From local constraints to macroscopic transport: Dynamics of DNA under tension and confinement"
Prof. Dr. F. Kremer, Dr. U.F. Keyser
KR 1138/21-1 (2007-2010)

Emmy Noether-Programm der Deutschen Forschungsgemeinschaft "Nanopores for biological and soft-matter physics"
Dr. U.F. Keyser
KE 1452/1-1 (2007-2012)

Prof. Dr. F. Kremer is Principal Investigator and Lecturer in the International Research Training Group "Diffusion in Porous Materials" headed by Prof. Dr. J. Kärger and Prof. Dr. F. Kapteijn

Prof. Dr. F. Kremer is Principal Investigator in the "Leipzig School of Natural Sciences - Building with Molecules and Nano-Objects" in the framework of a Graduate School funded by the "Federal Excellence Initiative". Several Ph.D. projects are supported by that.

3.21 Organizational Duties

F. Kremer
- Director of the Institute of Experimental Physics I
- Project Reviewer: Deutsche Forschungsgemeinschaft (DFG)
- Editor: J. Colloid Polymer Sci.

- Member of Editorial Board: Macromol. Rapid Comm., Macromol. Chem. Phys., Polym. Adv. Technol.

3.22 External Cooperations

Academic

- Max-Planck-Institute for Microstructure, Halle, Germany
  M. Alexe, F. Bordusa
- Delft University of Technology, The Netherlands
  C. Dekker
- Leibniz-Institut für Oberflächenmodifizierung, Leipzig, Germany
  D. Hirsch
- University of California, Santa Barbara, USA
  Y. W. Kim
- Universität Konstanz, Germany
  M. Krüger
- Universität Düsseldorf, Germany
  C.N. Likos
- Lund University, Sweden
  P. Linse
- Technische Universität München, Germany
  V. Lobaskin, R. Netz
- Technische Universität Dresden, Germany
  M. Mertig
- Universität Stuttgart, Germany
  J. Harting, M. Rauscher
- Institute of Entomology, Ceske Budejovice, Czech Republic
  A. Sponner
- Leibniz-Institut für Polymerforschung, Dresden, Germany
  A. Drechsler, M. Stamm, A. Synytska, P. Uhlmann
- Brown University, Providence, USA
  D. Stein
- University of Oxford, UK
  F. Vollrath
- Universität Bayreuth, Germany
  W. Zimmermann

Industry

- Novocontrol, Hundsangen, Germany
- Comtech GmbH, München, Germany
- Freudenberg Dichtungs- und Schwingungstechnik KG, Weinheim, Germany
- Kempchen Dichtungstechnik GmbH, Leuna, Germany
- inotec FEG mbH, Markkleeberg, Germany
- MicroFAB, Bremen, Germany

3.23 Publications

Journals

C. Gutsche, U.F. Keyser, K. Kegler, F. Kremer, P. Linse: *Forces between single pairs of charged colloids in aqueous salt solutions*, Phys. Rev. E **76**, 031 403 (2007)

D. Jehnichen, D. Pospiech, L. Häußler, P. Friedel, S.S. Funari, J. Tsuwi, F. Kremer: *Microphase separation in semifluorinated polyesters*, Z. Kristallogr. Suppl. **26**, 605 (2007)

K. Kegler, M. Konieczny, G. Dominguez-Espinosa, C. Gutsche, M. Salomo, F. Kremer, C.N. Likos: *Polyelectrolyte-Compression Forces between Spherical DNA Brushes*, Phys. Rev. Lett. **100**, 118 302 (2008)

K. Kegler, M. Salomo, F. Kremer: *Forces of Interaction between DNA-Grafted Colloids: An Optical Tweezer Measurement*, Phys. Rev. Lett. **98**, 058 304 (2007)

M. Massalska-Arodz, J. Krawczyk, B. Procyk, F. Kremer: *Dielectric relaxation studies of 4–(2-hexyloxyethoxy)4´–cyanobiphenyl (6O2OCB) enclosed in SiO2 nanopores*, Phase Transit. **80**, 687 (2007)

O. Otto, C. Gutsche, F. Kremer, U.F. Keyser: *Optical tweezers with 2.5 kHz bandwidth video detection for single-colloid-electrophoresis*, Rev. Sci. Instrum. **79**, 023 710 (2008)

P. Papadopoulos, J. Sölter, F. Kremer: *Structure-property relationships in major ampullate spider silk as deduced from polarized FTIR spectroscopy*, Eur. Phys. J. E **24**, 193 (2007)

M. Salomo, U. Keyser, K. Kegler, M. Struhalla, C. Immich, U. Hahn, F. Kremer: *Kinetics of TmHU binding to DNA as observed by optical tweezers*, Microsc. Res. Techniq. **70**, 938 (2007)

A. Serghei, L. Hartmann, F. Kremer: *Molecular dynamics in thin films of isotactic poly(methylmethacrylate) – revisited*, J. Non-Cryst. Solids **353**, 4330 (2007)

J. Tsuwi, D. Pospiech, D. Jehnichen, L. Häußler, F. Kremer: *Molecular dynamics in semifluorinated-side-chain polysulfone studied by broadband dielectric spectroscopy*, J. Appl. Polym. Sci. **105**, 201 (2007)

in press

A. Serghei, F. Kremer: *Broadband dielectric studies on the interfacial dynamics enabled by use of nano-structured electrodes*, Rev. Sci. Instrum. (2007)

A. Serghei, F. Kremer: *Metastable states of arrested glassy dynamics, possibly mimicking confinement effects in thin polymer films*, Macromol. Chem. Phys. (2007)

3.24 Graduations

Doctorate

- Mathias Salomo
  Optische Pinzetten zum Studium der Wechselwirkungen zwischen histonähnlichen Proteinen und einzelnen DNA-Molekülen
  April 2007

Diploma

- Jan Sölter
  FTIR-Untersuchungen zu Struktur-Eigenschaftsbeziehungen von Spinnenleitfadenseide
  June 2007

3.25 Guests

- Malgorzata Jasuirkowska
  H. Niewodniczański Instute of Nuclear Physics, Polish Academy of Science, Kraków, Poland
  March – May 2007
- cand. phys. Mario E. del Pozo
  Departamento de Quimica Fisica I, Facultad de Ciencias Quimicas, Universidad Comlutentense de Madrid, Spain
  September – December 2007
- Prof. Dr. Gamal Turkey
  Microwave Physics and Dielectrics Department, National Research Center, Cairo, Egypt
  April – September 2007

4

Physics of Interfaces

4.1 Introduction

Research on molecular dynamics in complex systems, in particular the study of mass transfer and of phase transitions under geometric confinement, and the methodical development of the related techniques of diffusion measurement, including pulsed field gradient nuclear magnetic resonance, interference microscopy and IR microimaging, remained in the centre of our scientific activities. Particular highlights were the successful defence of our application for extension of our work within the International Research Group "Diffusion in Zeolites" with our partners in France, Great Britain and the USA, jointly sponsored by DFG, CNRS, EPSRC and NSF, and the establishment of the first "Saxon" Research Unit (FOR 877), "From Local Constraints to Macroscopic Transport", in which researchers in our Institutes of Experimental Physics I and Theoretical Physics are going to cooperate with colleagues from the Universities of Technology in Chemnitz and Dresden. Finally, we took the award of our Dutch colleague Rajamani Krishna as a DFG Mercator Professor at our University as a very special recognition of the success of our research and teaching activities within the Dutch-German International Research Training Group "Diffusion in Porous Materials", as the third research network presently chaired by our group.

The second event in the Diffusion-Fundamentals Conference series, jointly organized in August 2007 with Stefano Brandani from Edinburgh and Roberto Volpe from l'Aquila, the conference location, repeated the success of the first meeting in Leipzig. The worldwide community is looking forward to Diffusion Fundamentals III in October 2009 in Athens. It will again be organized with participation from Leipzig and has all potentials for becoming one of the highlights among the scientific events celebrating the great anniversary of Leipzig University. Jointly with the conference series, the Diffusion-Fundamentals Online Journal (www.diffusion-online.org, now already with 7 volumes completed) and the associated Diffusion-Fundamentals homepage (www.diffusion-fundamentals.org) have become valuable and broadly accepted tools of communication within the community. A general introduction (in both English and German languages) into this type of research, which strives to address a broad audience, may be found in the book edition "Leipzig, Einstein, Diffusion" by the Leipzig Universitätsverlag, jointly with some reminiscences on Leipzig's history and arts and on the physics in Leipzig quite in general.

Personnel fluctuations in 2007 were of particular relevance. Dieter Freude's retirement gives us the deplorable occasion to thank him for his most success- and fruitful work as a university professor and researcher of high international reputation, expressed, e.g., by the Breck-Award of the International Zeolite Association in 1986 for his pioneering work in the application of solid-state NMR to zeolite science and technology. We are happy that eventually, after recent legislation, Petrik Galvosas has now also formally been appointed a Juniorprofessor. Owing to his most recent achievements in the methodology of NMR diffusiometriy, we notably intensified our collaboration with researchers in the Leipzig Max Planck Institute of Human Cognitive and Brain Science (MPI CBS) and in the Institute for Medical Physics and Biophysics of our university. Moreover, our group has found important reinforcement in the field of adsorption by Grit Kalies who joined us with a Heisenberg stipend.

Jörg Kärger

4.2 Memory Effects in Confined Fluids

S. Naumov, R. Valiullin, J. Kärger

Fluid dynamics in disordered materials where anomalous patterns in molecular propagation are generated by various mechanisms is a subject of continuous interest with diverse applications [1]. In particular, it has recently been suggested [2] that slow density relaxation due to an activated fluid rearrangement in random mesopores partially saturated by fluids may provide a new avenue for understanding of the adsorption hysteresis phenomenon. As an important premise, this approach elaborates on a complex free-energy landscape with large number of metastable states reflecting different fluid configurations in disordered matrices. Being resulted from mean-field density functional theory, this has not yet found experimental verification.

Here, by measuring molecular diffusion in the hysteresis region of adsorption using pulsed filed gradient NMR technique (Fig. 4.1), we provide direct experimental

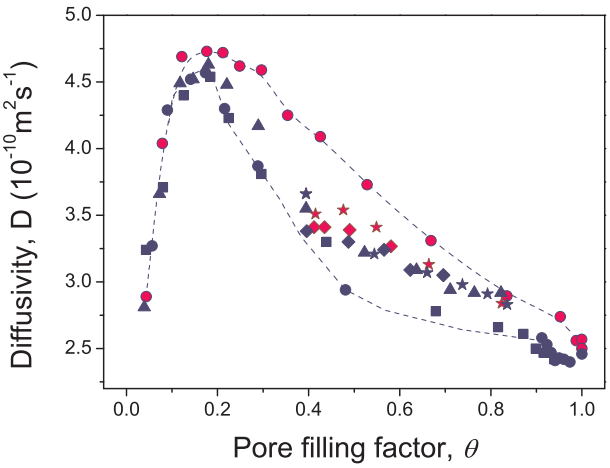

Figure 4.1: Diffusivities of cyclohexane in random mesoporous Vycor glass at different pore loadings. Different data on diffusivities corresponding to one and the same loading were obtained by changing the history how a particular state in the pores was attained.

evidence of a history-dependent character of a fluid distribution in random pores. In particular, we have profited from the abilities of NMR technique to simultaneously probe the amount adsorbed and the molecular self-diffusivities [3]. By performing adsorption scanning experiments, i.e. series of incomplete adsorption/desortion cycles, we have been able, in addition to the adsorption scanning curves, to compile those for the diffusivities. In this way, different diffusion scanning curves lying within the main diffusion hysteresis loop have been obtained. In our opinion, the existence of such diffusion scanning behavior has to be associated with different, history-dependent geometry of the capillary-condensed phase in the pores. In turn, this may be considered as a probe of a change of the free-energy landscape with varying external conditions and may have implications for a deeper understanding of random-field systems.

[1] J.P. Bouchaud, A. Georges: Phys. Rep. **195**, 127 (1990)
[2] H.J. Woo, P.A. Monson: Phys. Rev. E **67**, 041 207 (2003)
[3] S. Naumov et al.: Eur. Phys. J. Special Topics **141**, 107 (2007)

4.3 Diffusion of Adsorbates in Agglomerated MCM-41 Material

M. Dvoyashkin, R. Valiullin, J. Kärger

The diffusion process of organic molecules in an agglomerated MCM-41 material having complex meso- and macroporous architecture has been probed using the pulsed field gradient NMR method [1]. The measurements have been performed under variation of the external gas pressures, in immediate contact with the porous material.

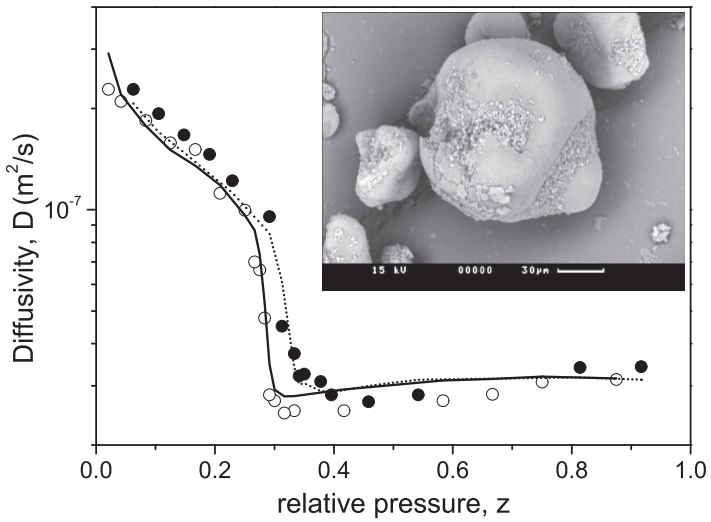

Figure 4.2: The effective self-diffusion coefficients for cyclohexane in MCM-41 agglomerates as a function of the relative vapor pressure measured on the adsorption (*filled symbols*) and the desorption (*open symbols*) branches. The *inset* shows electron scanning micrographs of a typical MCM-41 cluster of the investigated MCM-41 material.

On the time scale of the experiments from a few up to a few hundred milliseconds, the diffusion process is found to be strongly influenced by an exchange between different regions of porosity, including "fast" exchange between the individual mesoporous MCM-41 crystallites and the gaseous phase in the intergrain space, and "intermediate" exchange between the molecular ensembles in the different macroscopic particles, composed of the grains [2]. With pressure variation, the measured effective diffusivities, as the characteristic parameter of overall molecular transport, are found to exhibit three regimes with notably different pressure dependencies (Fig. 4.2). The experimental results reveal that the occurrence of these regimes is the consequence of three different regions in the sorption isotherms resulting from the MCM-41 crystallites. The high values of the diffusivities result from molecular displacements in the macropores, primarily in the interparticle void space. Importantly, the contribution of such high diffusion rates to the overall transport is simply controlled by the equilibrium conditions between meso- and macropores via the gas pressure and may provide therefore a flexible tool for varying the transport rates.

[1] R. Valiullin et al.: J. Chem. Phys. **126**, 054 705 (2007)
[2] J. Kärger et al.: Adv. Magn. Reson. **12**, 2 (1988)

4.4 Melting and Freezing of Fluids in Structured Mesopores

A. Khokhlov, R. Valiullin, J. Kärger

Freezing and melting behavior of nitrobenzene in mesoporous silicon with different pore size and with different porous structure have been studied using ^{1}H NMR cryoporometry [1]. Due to a huge difference in the NMR transverse relaxation times in solid and liquid phases, this method allows to monitor relative fractions of these phases as a function of temperature [2]. With the bulk phase surrounding the porous monoliths, in the materials with uniform channel-like pores distinct pore-size-dependent freezing and melting transitions have been measured. The obtained shift of both transitions as compared to the bulk substance is a typical feature of phase transitions under confinement. These data were further used for the analysis of the fluid behavior in samples with modulated porous structure, namely linear pores with alternating sections having different pore diameters. We have, in particular, considered two materials consisting of channel sections, which were separated by almost identical channel "necks" but notably differed in the respective channel diameters. In the smaller channel segments,

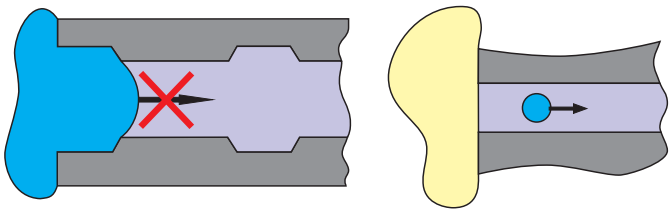

Figure 4.3: Schematics of pore blocking (*left*) and homogeneous nucleation (*right*) in pores.

the observed shift in the freezing temperature provides direct evidence of the relevance of a pore blocking mechanism [3], i.e. of the retardation in the propagation of a solid front by the channel necks (Fig. 4.3). In the channel segments with larger diameter, on the other hand, freezing is found to be initiated by homogeneous nucleation.

[1] A. Khokhlov et al.: New J. Phys. **9**, 272 (2007)
[2] J.H. Strange et al.: Phys. Rev. Lett. **71**, 3589 (1993)
[3] G. Mason: Proc. R. Soc. Lon. A **415**, 453 (1988)

4.5 Effects of Self-Assembly on Molecular Diffusion of Poly(Ethylene Oxide)–Poly(Propylene Oxide)–Poly(Ethylene Oxide) in Water

K. Ulrich, J. Kärger, F. Grinberg

Self-assembling systems find widespread applications in drug delivery, gene therapy, nanotechnology and in molecular engineering. They usually tend to arrange themselves in hierarchical levels revealing structures on the mesoscopic length scale. Complex self-organization is in turn accompanied by multiple molecular dynamical processes that tend to range over many time decades [1, 2]. Symmetric triblock copolymers (BCP) based on poly(ethylene oxide) (PEO) and poly(propylene oxide) (PPO) have proven to be especially useful due to their reach lyotropic and thermotropic properties. Owing to the amphiphilic character of molecules, these BCPs exhibit remarkable variety of super-molecular structures in water [3]. Molecular dynamical properties and their relationship with the microstructure of BCPs is an area of intensive research [4]. However, structure properties of the BCPs systems are much better understood than their dynamics. This is because super-molecular formations give rise to very slow dynamical processes not easily accessible by conventional methods.

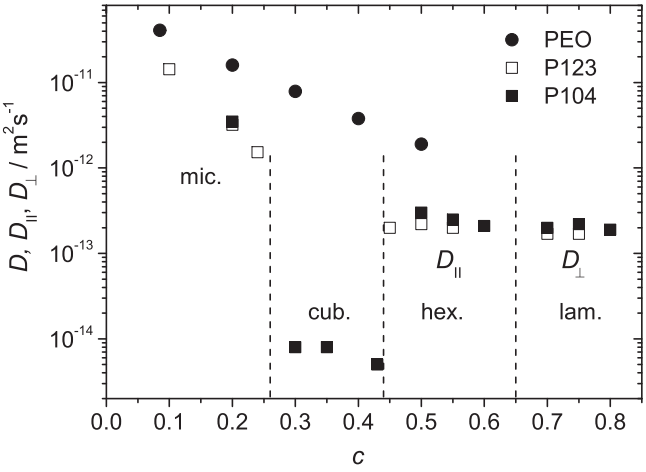

Figure 4.4: The diffusion coefficients of triblock copolymer molecules (Pluronic P123, Pluronic P104) and the homopolymer PEO in water as a function of polymer concentration in the broad range from 0.1 to 0.8 at T = 23 °C.

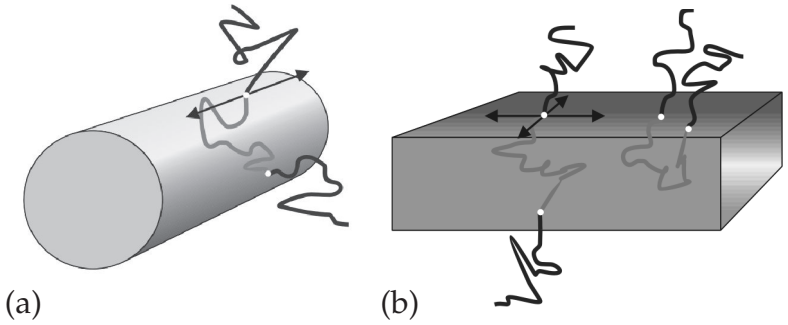

Figure 4.5: Schematic presentation of possible diffusion displacements of the triblock copolymer chains in rod-like cylindrical (**a**) and lamellar (**b**) substructures. The *arrows* indicate the directions of unrestricted interface diffusion.

In this work, molecular self-diffusion of PEO-PPO-PEO molecules in water was studied with the help of Pulsed Field Gradient (PFG) NMR in the broad range of polymer weight fractions from 0.09 to 0.8. These BCPs in water exhibit rich super-molecular structures owing to their amphiphilic nature. In particular, they form micelles and three liquid crystalline mesophases: cubic, hexagonal, and lamellar. All four structure formations were studied with the same block copolymer and at the same temperature. Self-assembly was shown to produce dramatic effects on molecular self-diffusion (Fig. 4.4).

Strong jump-like changes were observed when phase transitions between the different structure formations occurred. This is in contrast to the behavior of homopolymers like PEO which exhibit smooth decrease of the diffusivities with increasing concentration. Diffusion in the micellar phase was found to be normal (Gaussian) and isotropic. In the cubic crystal phase, diffusion appeared to be dramatically retarded. Diffusion in the hexagonal phase was demonstrated to be quasi one-dimensional in the direction parallel to the long axis of the ordered molecular rods (Fig. 4.5a). In the lamellar phase diffusion was essentially two-dimensional, in the plane of the lamellar structures (Fig. 4.5b). The observed anisotropy of diffusion was shown to be the effect of specific molecular ordering on the mesoscopic length scale.

[1] F. Grinberg et al.: in *NMR of Orientationally Ordered Liquids*, ed. by E. Burnell, C. de Lange (Kluwer, Dordrecht 2003)
[2] F. Grinberg: Magn. Reson. Imag. **25**, 485 (2007)
[3] G. Wanka et al.: Macromolecules **27**, 4145 (1994)
[4] P. Alexandridis: Langmuir **12**, 2690 (1996)

4.6 Exploring the Influence of the Surface Resistance of Nanoporous Particles on Molecular Transport

M. Krutyeva, J. Kärger

Transport of sorbate molecules through nanoporous materials consisting of individual crystallites plays an important role in industrial processes such as mass separation and catalysis. A detailed knowledge of molecular diffusion properties, in particular

the permeability of crystallite's surface, in such materials is therefore a necessary prerequisite of their efficient use [1]. We demonstrate the potentials of PFG NMR in studying the surface permeability of nanoporous crystallites in a broad range of length scales. A new method to determine the surface permeability of nanoporous particles was proposed [2]. It is based on the comparison of experimental data on tracer exchange and intracrystalline molecular mean square displacements as obtained by the PFG NMR tracer desorption technique with the corresponding solutions of the diffusion equation via dynamical Monte Carlo simulations. The surface permeability of zeolite crystals of type NaCaA for small alkane molecules (methane and ethane) was estimated by using this method, analysing NMR tracer desorption measurements. For the two NaCaA specimens investigated, already in the as-synthesized zeolite crystals notable surface resistances have been observed. Surface permeabilities have been studied in dependence on temperature, sorbate and crystal size [3].

Generally, the industrially produced nanoporous materials are much smaller in size (about a few micrometers). During accessible observation times almost all molecules of the sorbate overcome distances larger than the size of the crystallites. Often, the determination of the surface resistance turns out to be difficult to perform, since the industrially produced specimens are characterised by a large crystalline size distribution. Moreover, the shape much more complicated than generally found with laboratory synthesized crystallites provides additional problems. Therefore, the NMR tracer desorption technique can not be applied for that small industrial samples. As a first step to respond to this problem, we performed dynamic Monte Carlo simulations of the diffusion in a bed of nanoporous particles.

In complete agreement with the well established formalism of PFG NMR diffusion studies with zeolites [1], three diffusion regimes can be clearly distinguished (Fig. 4.6).

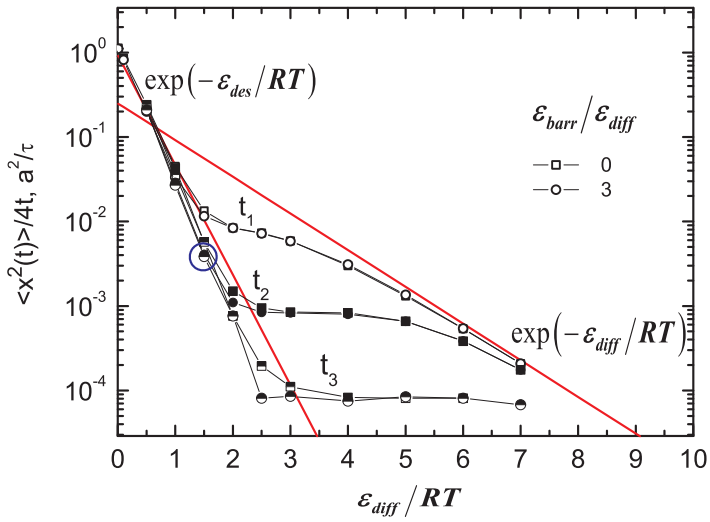

Figure 4.6: Dependence of the apparent diffusivity, calculated from the mean squared displacement, as a function of the temperature. *Open*, *full* and *half-full points* correspond to different observation times $t_1 < t_2 < t_3$ ($t_1 = 10^5$, $t_2 = 10^6$, $t_3 = 10^7$ Monte Carlo steps), respectively. The simulations have been performed with $\varepsilon_{\mathrm{des}} = 3\varepsilon_{\mathrm{diff}}$ and for $\varepsilon_{\mathrm{barr}} = 0$ (*squares*) and $\varepsilon_{\mathrm{barr}} = \varepsilon_{\mathrm{des}} = 3\varepsilon_{\mathrm{diff}}$ (*circles*). The *large circle* highlights the data point at $\varepsilon_{\mathrm{diff}}/k_{\mathrm{B}}T = 1.5$ which refers to the presentation in Fig. 4.7.

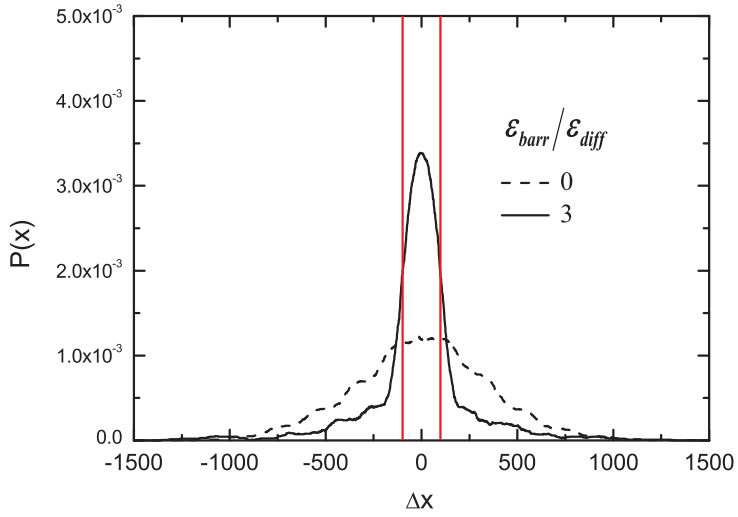

Figure 4.7: Probability distribution of the molecular desplacements (the "propagator" [5]) for the molecules moving through the 2D model system with and without surface barriers for $\varepsilon_{\mathrm{diff}}/RT = 1.5$, $\varepsilon_{\mathrm{des}} = 3\varepsilon_{\mathrm{diff}}$ and 10^7 Monte Carlo steps (*large circle* in Fig. 4.6). The extension La = 100 of a crystallite (edge length) is indicated by the *two vertical lines*.

The regime of intracrystalline diffusion at the lower temperatures is merely controlled by the activation energy of diffusion $\varepsilon_{\mathrm{diff}}$.

In the regime of restricted diffusion, at higher temperatures, the mean square displacement approaches the particle size. At higher temperatures, the displacements substantially exceed the particle dimensions establishing the regime of long-range diffusion. The slope of this part of the plot arises from the temperature dependence the equilibrium distribution of the diffusing molecules, which is directly related to the desorption energy $\varepsilon_{\mathrm{des}}$. As to be required [4], diffusivities in the plateau are inversely proportional to the observation time. While in the limiting cases of both intracrystalline diffusion and long-range diffusion there is essentially no difference between the diffusivities determined with and without an additional surface barrier $\varepsilon_{\mathrm{bar}}$, this difference becomes significant in the transient range from restricted to long-range diffusion. The difference becomes particularly obvious in the so-called propagator presentation shown in Fig. 4.7, i.e. in a plot of the probability distribution for molecular displacements during the PFG NMR experiment.

Since the propagator is nothing else than the Fourier transform of the PFG NMR spin echo attenuation [5], the simulation results shown in Fig. 4.7 may open up a new way for the experimental determination of surface barriers by means of PFG NMR. The corresponding combined experimental and theoretical work is still in progress.

[1] J. Kärger, D.M. Ruthven: *Diffusion in Zeolites* (Wiley, New York 1992)
[2] M. Krutyeva et al.: J. Magn. Res. **185**, 300 (2007)
[3] M. Krutyeva et al.: Micropor. Mesopor. Mater. **104**, 89 (2007)
[4] J. Kärger et al.: Inter. Sci. **84**, 240 (1981)
[5] J. Kärger, W. Heink: J. Magn. Res. **51**, 1 (1983)

4.7 Two-Dimensional NMR Relaxometry Study of Pore Space Characteristics of Carbonate Rocks from a Permian Aquifer

W. Schönfelder, F. Stallmach, H.-R. Gläser*, I. Mitreiter*

*UFZ Helmholtz Centre for Environmental Research, Leipzig

Storage capacity and transport of reservoir fluids through subsurface rock formation are important properties, which characterize aquifer systems as well as hydrocarbon reservoir formations. The corresponding pore space properties can be investigated in laboratory NMR studies. ^{1}H 2D NMR relaxometry and PFG NMR diffusometry was, e.g., applied on limestones and dolostones from a Permian aquifer in Central Germany. Information concerning pore size distribution and water diffusion were in accord for different samples of each type of rock, but differed fundamentally between limestones and dolostones.

The results of the 2D relaxometry measurements revealed a ratio of surface relaxation times T_1^s/T_2^s of about 2 for the limestones and about 4.5 for the dolostones, mirroring the different content of Fe and Mn in the pore walls. In consideration of thin section interpretation, the corresponding fraction in the T_1-T_2 relaxation time distributions was attributed to interparticle porosity. Porosity of large vugs is clearly displayed by $T_1 \approx T_2 > 1$ s in the dolostones only. A third fraction of the total water-saturated pore space in the dolostones, which is clearly displayed in the 2D relaxation time distributions at the shortest relaxation times and a high T_1^s/T_2^s ratio, is attributed to intrafossil porosity. The porosity classification, basing on non-destructive NMR experiments, is verified by mercury intrusion porosimetry and thin section interpretation (Fig. 4.8).

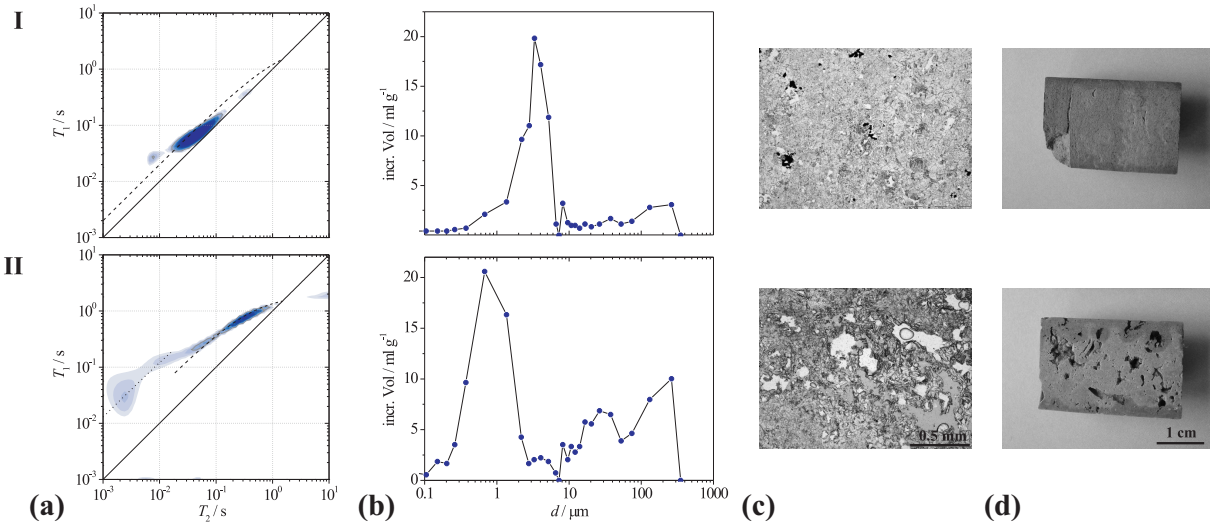

Figure 4.8: Limestone (*I*) and dolostone (*II*): (**a**) $T_1 - T_2$ relaxation time distribution, (**b**) pore throat size distribution obtained from mercury intrusion experiment, (**c**) photomicrograph of thin slice and (**d**) photograph of the sample.

4.8 NMR Relaxometry Study on Internal Curing of Portland Cements by Lightweight Aggregates

K. Friedemann, W. Schönfelder, F. Stallmach, J. Kärger

The water dynamics in hydrating ordinary Portland cement of initial w/c-ratio of 0.25 with internal curing by water-saturated expanded glass aggregates were investigated by non-destructive low-field NMR relaxometry. Because of the different relaxation rates the physically bound water in hydrating cement and the water stored in the aggregates yield separate peaks in the T_2 relaxation time distributions. By systematic analyses of the positions and intensities of these peaks, the hydration progress can be followed. The migration of water from the water-saturated glass aggregates into the hydrating cement mainly occurs during the accelerated (II) and decelerated (III) periods of cement hydration. In case of addition of superplasticizer (sp) the transition is delayed by the retarding influence of sp on the hydration process. It occurs during the delayed starting accelerated (II, sp) and decelerated (III, sp) periods (Fig. 4.9).

From experiments with addition of an excess of water-saturated aggregates to the hydrating cement, we estimate a water requirement of about (33 ± 2) g of water per kilogram dry cement for internal curing of the investigated Portland cement limes of initial w/c-ratio of 0.25. The results are discussed in detail in [1].

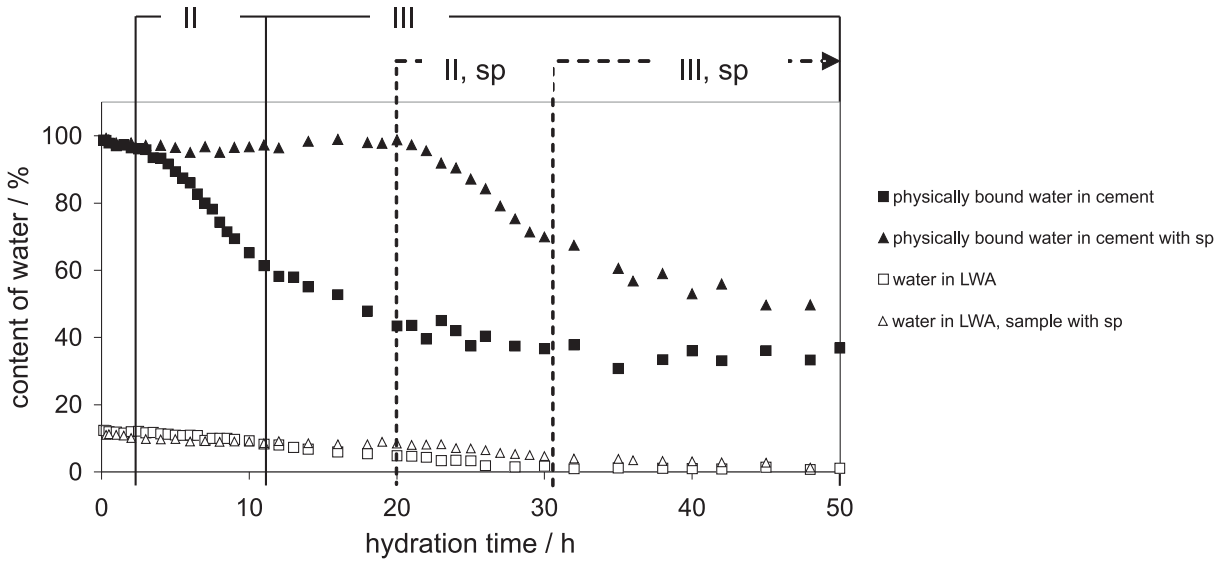

Figure 4.9: Time dependence of physically bound water in the cement phase (*full symbols*) and of the curing water in the expanded glass aggregates (*empty symbols*). Data are shown for sample without and with superplasticizer (sp). 100 % refers to the amount of water necessary to achieve the initial w/c ratio of 0.25.

[1] K. Friedemann et al.: Mater. Struct. (2008), doi:10.1617/s11527-008-9355-0

4.9 Self-Diffusion and Adsorption of Hydrocarbons in Cu-BTC

M. Wehring, F. Stallmach, J. Gascon*, F. Kapteijn*

*DelftChemTech Reactor & Catalysis Engineering, Delft University of Technology, The Netherlands

The adsorption and self-diffusion of propane and propylene in the metal-organic framework compound copper(II) benzene-1,3,5-tricarboxylate, $(Cu_3(BTC)_2(H_2O)_3$: short Cu-BTC [1]) were investigated experimentally. Single-component adsorption isotherms were measured over a temperature range of 318 K to 383 K. The adsorption isotherms were analysed using a one-site Langmuir adsorption model, which yielded heats of adsorption of 31.3 kJ/mol for propane and 42.9 kJ/mol for propylene showing that propylene is stronger adsorbed in Cu-BTC than propane. The self-diffusion of propane and propylene adsorbed in Cu-BTC was measured using proton (^{1}H) pulsed field gradient (PFG) NMR [2] – an experimental technique, which recently proved to be applicable for self-diffusion studies in MOF-5 [3]. However, in Cu-BTC the NMR relaxation times of adsorbed species are rather short, which is caused by magnetic interaction of the nuclear spins with the electron spin of the copper and complicates NMR diffusion studies [2]. The NMR measurements were carried out in a temperature range from 298 K to 470 K, yielding activation energies of the self-diffusion of 7.9 kJ/mol for propane and 16 kJ/mol for propylene, respectively. These values are significantly smaller than the corresponding heats of adsorption (see above), which indicates that the observed diffusion process is not influenced by diffusion of the C_3 hydrocarbons between neighbouring Cu-BTC crystals. At room temperature, the self-diffusion coefficients amount to about 5.1×10^{-10} m^{2}s^{-1} for propane and 1.2×10^{-10} m^{2}s^{-1} for propylene, respectively [4].

[1] S.S.-Y. Chui et al.: Science **283**, 1148 (1999)
[2] F. Stallmach, P. Galvosas: Ann. Rep. NMR Spectr. **61**, 52 (2007)
[3] F. Stallmach et al.: Angew. Chem. Int. Ed. **45**, 2123 (2006)
[4] M. Wehring et al.: Poster, 19. Deutsche Zeolith-Tagung, Leipzig (2007)

4.10 The Striking Influence of the Amount of Silica on the Diffusion Properties of SAPO STA-7 Samples Investigated by Interference Microscopy

D. Tzoulaki, M. Castro*, P.A. Wright*, J. Kärger

*School of Chemistry, University of St. Andrews, Scotland

Interference microscopy has been applied and successfully pointed out the impact of the amount of silica on the diffusion properties of two samples of SAPO STA-7. The intracrystalline concentration profiles, obtained by this experimental technique, revealed outstanding differences regarding both the diffusion of methanol inside the crystals and the strength of surface barriers. The first sample of SAPO STA-7 containing

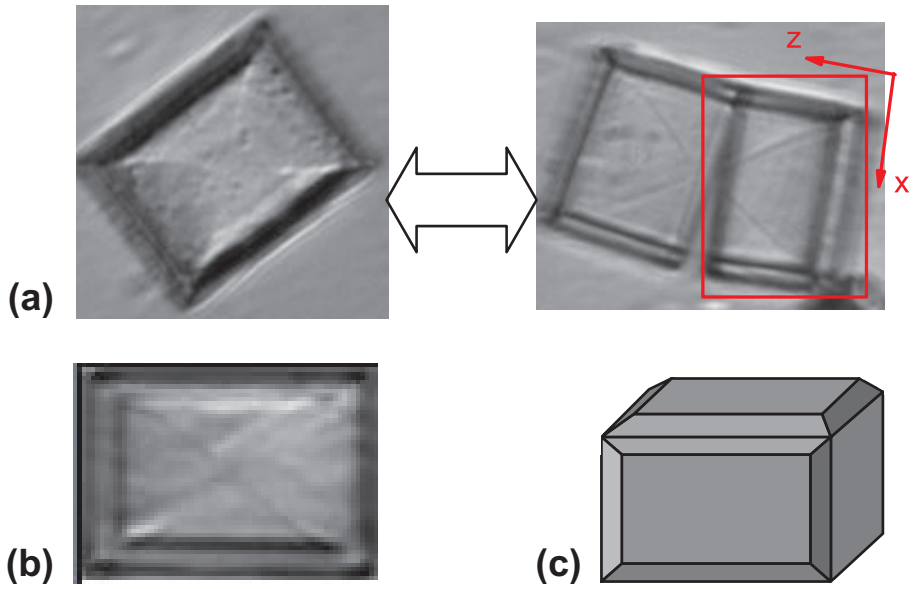

Figure 4.10: (**a**) a SAPO STA-7 30 % Si crystal after calcination (*left*) and after activation (*right*); (**b**) a SAPO STA-7 10 % Si crystal after in-situ calcination; (**c**) a schematical representation of SAPO STA-7 crystals.

30 % Si was received already calcined (at 550 ℃ in O_2 atmosphere) from the University of St. Andrews (Fig. 4.10a left) and its crystals were broken into two parts after heating at 200 ℃ for 10 h under vacuum, namely during the activation procedure (Fig. 4.10a right). On the other hand, the second sample with only 10 % Si was calcined in-situ at the University of Leipzig just prior to the diffusion experiments and proved to be more stable (Fig. 4.10b).

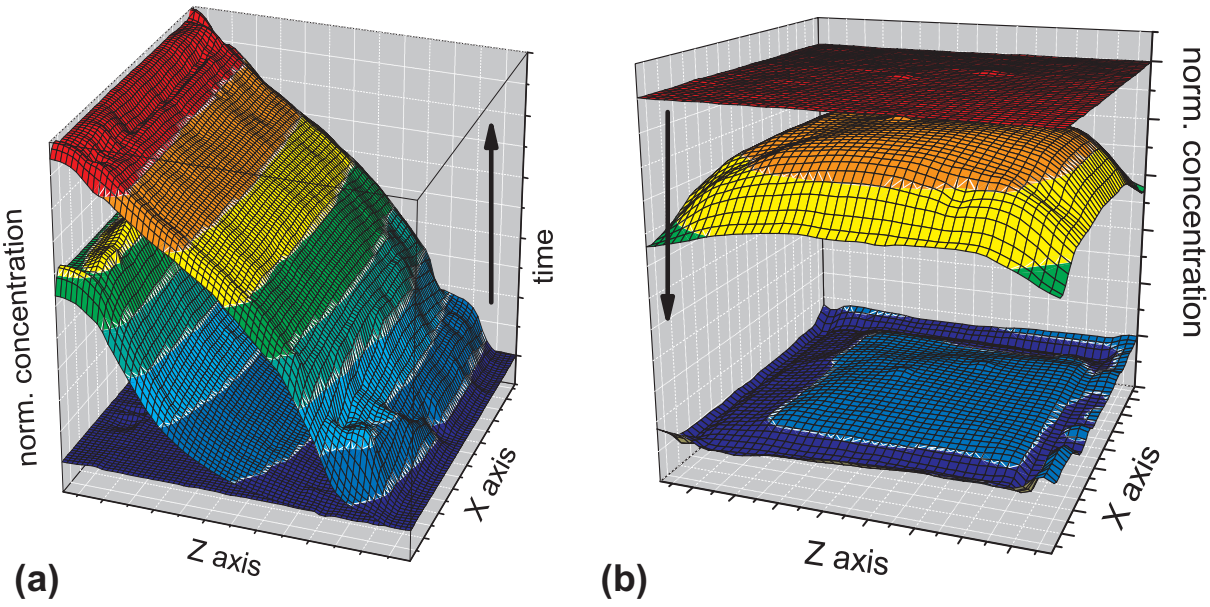

Figure 4.11: Evolution of concentration profiles during (**a**) adsorption in the case of SAPO STA-7 30 % Si crystal and (**b**) during desorption in the case of SAPO STA-7 10 % Si crystal.

The sorption experiments under given pressure steps were performed with a selected crystal from each sample at room temperature (25 °C). Figure 4.11a refers to the sample with 30 % Si and illustrates the evolution of intracrystalline methanol-concentration profiles. The profound slope of the profiles reveals a slow diffusivity within the crystal, and the values of concentration at both edges along the z-axis demonstrate, on one hand, very high surface barriers and, on the other hand, uptake through the surface where the crystal is broken (big values of z). On the contrary, in case of the SAPO crystal with 10 % Si (Fig. 4.11b) the molecules of methanol do not have to overcome such strong surface barriers. Both types of crystals, though, posses activated sites, which strongly attract methanol molecules. In this work it is shown that investigations of different generations of SAPO STA-7 crystals, by means of interference microscopy, will essentially contribute to the study of influence of silica on the properties of those crystals.

4.11 Inflection in the Loading Dependence of the Maxwell–Stefan Diffusivity of Iso-Butane in MFI Zeolites

C. Chmelik, L. Heinke, J. Kärger, W. Schmidt*, D.B. Shah†, J.M. van Baten‡, R. Krishna‡

*Max-Planck-Institut für Kohlenforschung, Mülheim a.d. Ruhr
†Department of Chemical & Biomedical Engineering, Cleveland State University, USA
‡Van 't Hoff Institute for Molecular Sciences, University of Amsterdam, The Netherlands

Configurational-Bias Monte Carlo simulations of the adsorption isotherm for iso-butane (iC4) in MFI zeolite show a strong inflection at a loading $\Theta = 4$ molecules per unit cell (Fig. 4.12a). The consequence of the isotherm inflection on the loading

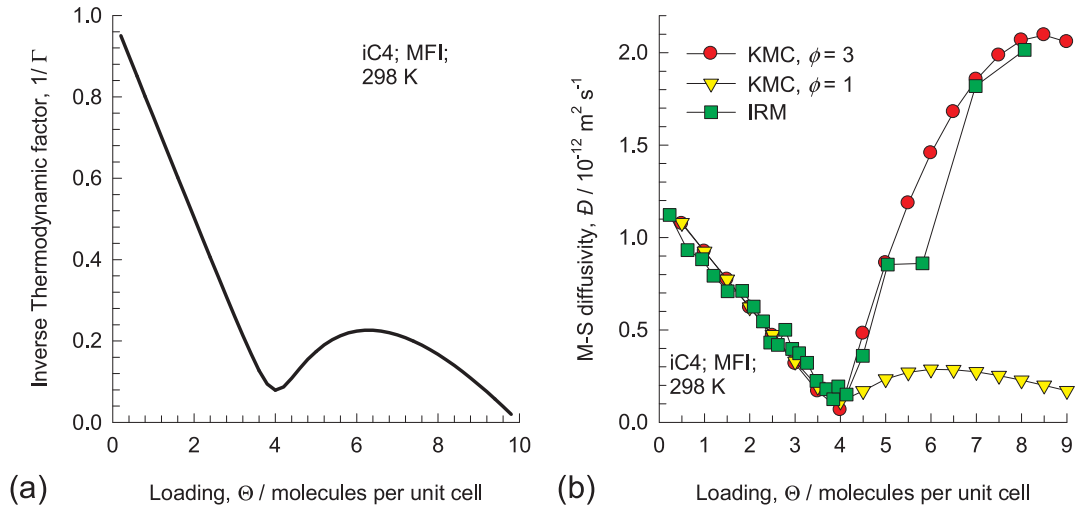

Figure 4.12: (**a**) The inverse thermodynamic correction factor, $1/\Gamma$, as a function of the loading of iC4 in MFI. (**b**) Comparison of $Đ$ obtained from IRM experiments with KMC simulations with repulsion factors $\phi = 0$ and $\phi = 3$.

dependence of the Maxwell-Stefan diffusivity, $Đ$, was investigated using Infra-red microscopy for a range of loadings $0 < \Theta < 8.4$ [1]. The experimental data show that $Đ$ decreases nearly linearly as Θ is increased to 4; further increase in Θ results in a sharp increase in $Đ$ with a cusp at $\Theta = 4$ (Fig. 4.12b). Here, for the first time, such strong inflection behaviour for diffusivities in zeolites could be measured experimentally. Kinetic Monte Carlo simulations are used to rationalize the experimental observations [1]. The simulations indicate that significant inter-molecular repulsions are present for $\Theta > 4$. The experimental data are quantitatively matched by KMC simulations provided intermolecular repulsions are taken into consideration (Fig. 4.12b).

This work is of considerable practical significance, not only for iC4 diffusion. On the basis of the experimental data presented here, we may expect a similar strong inflection behaviour in $Đ$ vs. Θ also for other branched alkanes, and aromatics (e.g. benzene, ethylbenzene). For example, this inflection behaviour has a strong influence on permeation fluxes across an MFI membrane.

[1] C. Chmelik et al.: *Inflection in the Loading Dependence of the Maxwell-Stefan Diffusivity of Iso-Butane in MFI Zeolite*, Chem. Phys. Lett., submitted

4.12 Assessing Transport Diffusion in Nanoporous Materials from Transient Concentration Profiles

L. Heinke, J. Kärger

The use of interference microscopy has enabled the direct observation of transient concentration profiles generated by intracrystalline transport diffusion in nanoporous materials. The thus accessible intracrystalline concentration profiles contain a wealth of information which can not be deduced by any macroscopic method. We illustrate different ways for determining the concentration-dependent diffusivity [1–5]. The exchange dynamics at the interfaces of the nanoporous materials are also discussed [6]. It is shown that the sticking probability, which gives the probability that a gas molecule

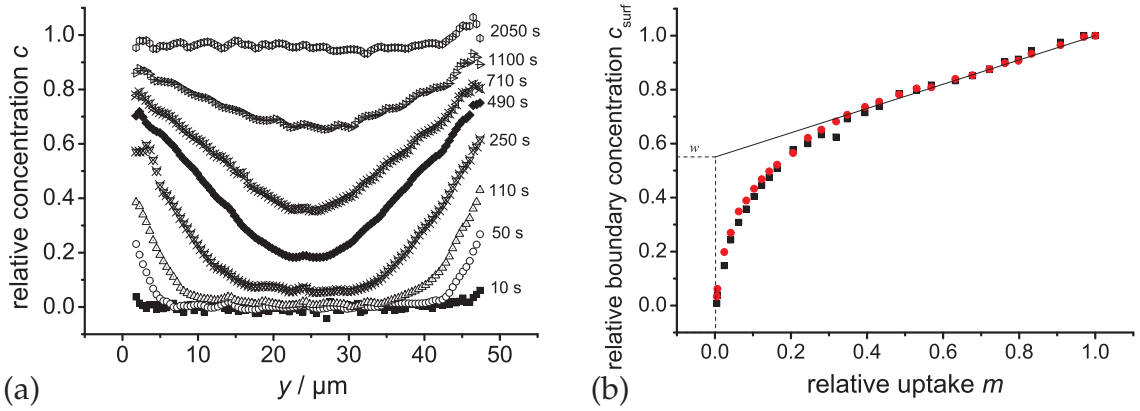

Figure 4.13: (**a**) Concentration profiles of methanol in ferrierite measured by interference microscopy. (**b**) Plotting the boundary concentration versus the overall uptake yields the factor by which the uptake process is retarded because of the surface barrier.

hitting the surface continues its trajectory into the crystal, can vary over many orders of magnitude. Furthermore, we present a simple way which enables the estimation of the influence of the surface barrier to the overall uptake process by plotting the boundary concentration versus the overall uptake (Fig. 4.13a) [7, 8].

[1] P. Kortunov et al.: J. Am. Chem. Soc. **129**, 8041 (2007)
[2] L. Heinke: Diff. Fundam. **4**, 9.1 (2007)
[3] J. Kärger et al.: Stud. Surf. Sci. Catal. **170**, 739 (2007)
[4] L. Heinke et al.: Chem. Eng. Technol. **30**, 995 (2007)
[5] P. Kortunov et al.: Chem. Mater. **19**, 3917 (2007)
[6] L. Heinke et al.: Phys. Rev. Lett. **99**, 228 301 (2007)
[7] L. Heinke: Diff. Fundam. **4**, 12.1 (2007)
[8] L. Heinke et al.: Adsorption **13**, 215 (2007)

4.13 Revealing Complex Formation in Acetone–*n*-Alkane Mixtures by MAS PFG NMR Diffusion Measurement in Nanoporous Hosts

M. Fernandez, A. Pampel*, R. Takahashi†, S. Sato‡, D. Freude, J. Kärger

*Max-Planck-Institute for Human Cognitive and Brain Sciences, Leipzig
†Graduate School of Science and Engineering, Ehime University, Matsuyama, Japan
‡Department of Applied Chemistry & Biotechnology, Chiba University, Chiba, Japan

The application of solid-state MAS NMR in combination with pulsed field gradients opens new possibilities for measuring multi-component diffusion in nanoporous materials. These options are related to an enhancement of the sensitivity with respect to smaller molecular displacements, and to an increased spectral resolution, which allows selective diffusion measurements from different components [1, 2]. Magic-angle spinning pulsed field gradient nuclear magnetic resonance (MAS PFG NMR) was applied for selective self-diffusion measurements of acetone–*n*-alkane (C6 up to C9) mixtures in mesoporous silica gel [3], see Fig. 4.14.

Two specimens of silica gel with mean pore sizes of about 4 and 10 nm are considered. In the smaller pores, the *n*-alkane diffusivities are by about one and the acetone diffusivities by about two orders of magnitude smaller than in the larger pores. In addition, the acetone diffusivities in the narrow-pore specimen exhibit a pronounced oscillation with increasing chain length of the solvent *n*-alkanes: the diffusivities of acetone dissolved in odd-carbon number *n*-alkanes exceed those of acetone dissolved in even-carbon number *n*-alkanes by about 50 %. These findings reproduce the tendencies observed in previous macroscopic release studies from Takahashi et al. [4] and suggest the formation of acetone–*n*-alkane complexes in the narrow-pore silica gel. Diluted solutions of acetone in *n*-alkanes as a guest liquid in nanoporous silica gel host systems has been found to dramatically change their internal transport dynamics on reducing the pore size from about 10 to 4 nm. As the most important result of our studies, the magnitude of the acetone diffusivities nicely reproduces the oscillation with increasing

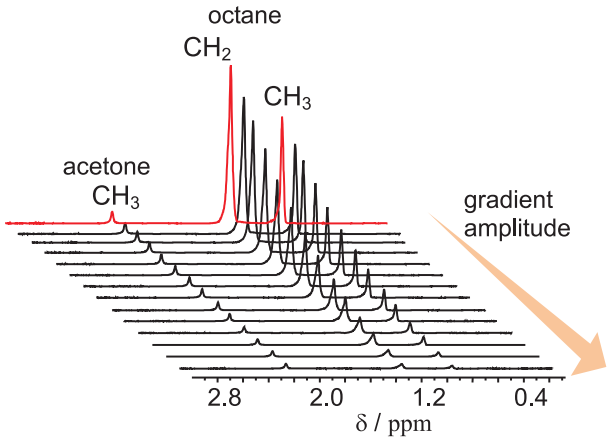

Figure 4.14: Stack plot of the ^{1}H MAS PFG NMR spectra at 10 kHz of the 1:10 acetone–*n*-octane mixture absorbed in specimen N_m with increasing pulsed gradient amplitude for an observation time Δ = 600 ms.

chain lengths, as reported in the previous macroscopic release studies by Takahashi et al. [4]. They claimed that the acetone and *n*-alkane diffusivities are the same. In the light of the present MAS PFG NMR studies which yield notably larger *n*-alkane diffusivities, this assumption has to be abandoned. Most importantly, there is also no perceptible indication of an oscillation in the magnitudes of the *n*-alkane diffusivities with increasing chain length. Figure 4.15 illustrates, that the oscillation of the acetone diffusivities with increasing solvent chain length consistently appeared in all our measurements, which we performed by varying the observation time from 600 ms up to 1200 ms.

This oscillation of the acetone diffusivities with increasing solvent chain length vanishes when the mixture is confined in the 10 nm pores. Jonkheijm et al. [5] found, by probing the solvent-assisted nucleation pathway in chemical self-assembly, an oscillatory dependence of the aggregation number on whether the solvent contains an odd or even number of carbon atoms. Assuming the formation of acetone–*n*-alkane complexes in the narrow-pore silica gel specimen, all major experimental findings may be rationalized by a simple microdynamic model.

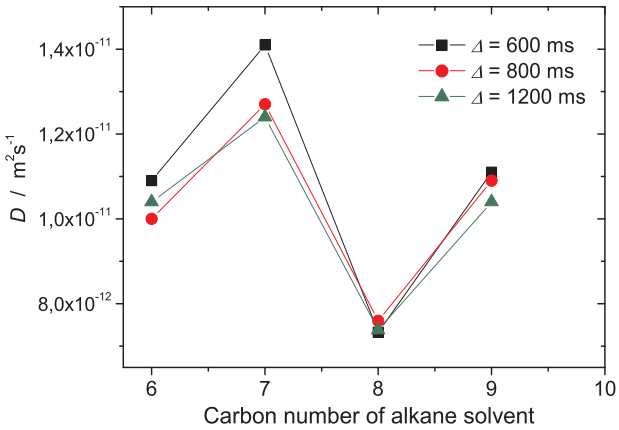

Figure 4.15: Diffusivity of acetone dissolved in an *n*-alkane solvent in the narrow-pore silica gel N_m for observation times of Δ = 600 ms, 800 ms and 1200 ms, as a function of the *n*-alkane chain length.

[1] A. Pampel et al.: Chem. Phys. Lett. **407**, 53 (2005)
[2] M. Fernandez et al.: Micropor. Mesopor. Mater. **105**, 124 (2007)
[3] M. Fernandez et al.: *Revealing Complex Formation in Acetone – n-Alkane Mixtures by MAS PFG NMR Diffusion Measurement in Nanoporous Hosts*, Phys. Chem. Chem. Phys., submitted (2008)
[4] R. Takahashi et al.: Phys. Chem. Chem. Phys. **5**, 2476 (2003)
[5] P. Jonkheijm et al.: Science **313**, 80 (2006)

4.14 Diffusion Studies in Liquid Crystals by MAS PFG NMR

E. Romanova, F. Grinberg, A. Pampel*, J. Kärger, D. Freude

*Max Planck Institute for Human Cognitive and Brain Sciences, Leipzig

The pulsed-field gradient nuclear magnetic resonance (PFG NMR) technique is the most direct and non-invasive method of measuring self-diffusion coefficients. This method

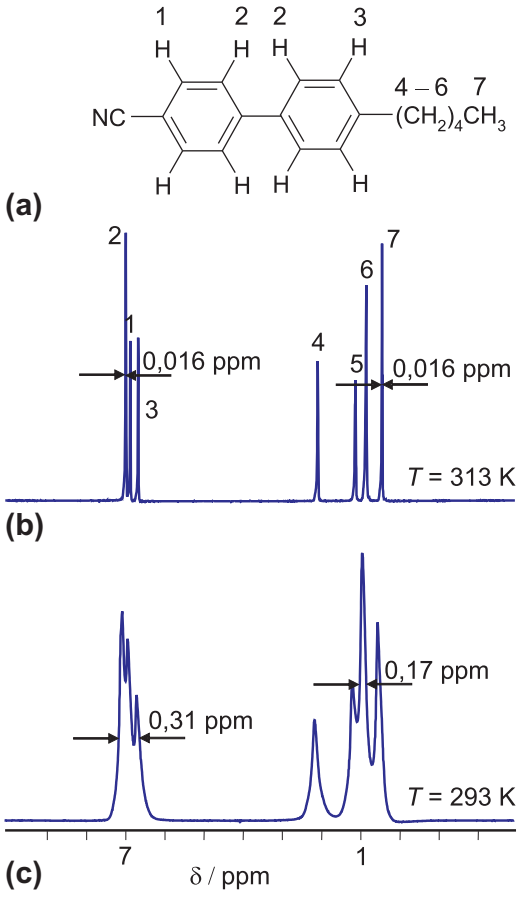

Figure 4.16: (**a**) The chemical structure of 5CB. ^{1}H MAS NMR spectra of 5CB confined in Bioran glasses with pore diameter 200 nm above (**b**) and below (**c**) the isotropization temperature T_c = 308.5 K.

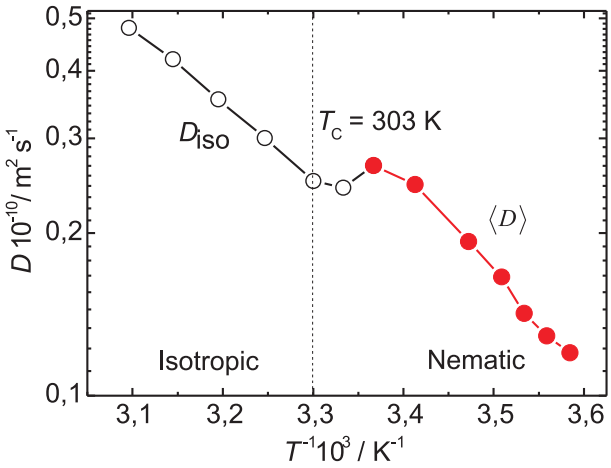

Figure 4.17: The temperature dependence of the diffusion coefficient D of 5CB confined in Bioran glasses. The *dashed line* indicates the isotropization temperature in bulk.

is routinely applied to isotropic liquids [1, 2] and molecules in confined geometries [3]. However, in liquid crystals dipole-dipole interactions are not completely averaged out by molecular motions. As a result, conventional NMR peaks are very broad, and the free induction signals decay is fast. This limits the time available for the application of gradient pulses [4] and makes impossible measuring diffusion in liquid crystals without special line-narrowing techniques.

Such problems could be overcome by combining magic-angle spinning (MAS) with pulsed field gradient to MAS PFG NMR [5, 6]. MAS implies the orientation of the spinning axes with respect to the external magnetic field at the angle of $\Theta_m = 54.7°$. In comparison with other techniques [7, 8] this type of measurements has considerable advantages. First, the increased resolution in the ppm scale permits one to observe separately each individual group with identical electronic surroundings (Fig. 4.16). Second, the longer transverse relaxation time upon MAS allows for sufficient time for the application of pulsed magnetic field gradients.

Dynanic properties of confined nematic liquid crystal 5CB has been studied by several techniques including the Dipolar Correlation Effect [9] and Field Cycling Relaxometry [10, 11]. However, no diffusion measurements were performed so far. In this work we apply for the first time the MAS PFG NMR technique [5, 6] to nematic liquid crystal 5CB confined in Bioran glasses (Fig. 4.17), in order to get a deeper insight to the aspects of anisotropic molecular interactions and the effects of confinements on dynamic properties of mesophases.

[1] E.O. Stejskal, J.E. Tanner: J. Chem. Phys. **42**, 288 (1965)
[2] W.S. Price: Concept. Magnet. Res. **9**, 299 (1997)
[3] J. Kärger, D.M. Ruthven: *Diffusion in Zeolites and Other Microporous Solids* (Wiley, New York 1992)
[4] G.J. Kruger: Phys. Rep. **82**, 229 (1982)
[5] A. Pampel et al.: Chem. Phys. Lett. **407**, 53 (2005)
[6] A. Pampel et al.: Micropor. Mesopor. Mater. **90**, 271 (2006)
[7] S.V. Dvinskikh et al.: J. Magn. Reson. **153**, 83 (2001)
[8] S.V. Dvinskikh et al.: Phys. Rev. E **65**, 050 702 (2002)

[9] F. Grinberg et al.: J. Chem. Phys. **105**, 9657 (1996)
[10] F. Grinberg: Magn. Reson. Imag. **25**, 485 (2007)
[11] F. Grinberg: in *Diffusion Fundamentals II*, ed. by S. Brandani et al. (Leipziger Universitätsverlag, Leipzig 2007)

4.15 Methodical Aspects of 2D NMR Spectroscopy under Conditions of Ultra-High Pulsed Field Gradients

M. Gratz, C. Horch, S. Schlayer, P. Galvosas

Multidimensional NMR correlation experiments based on an inverse Laplace transformation (see e.g. [1]) have been established as a powerful tool for the investigation of material structure and properties within the last few years. We successfully combined these recent methods with ultra-high pulsed magnetic field gradients of up to 35 T/m [2], which allows us to correlate molecular displacements in the order of 100 nm with NMR parameters, such as relaxation time T_2.

Basic concepts for the handling of ultra-high pulsed field gradients were adapted accordingly. This concerns in particular the introduction of a read gradient at suitable positions of the pulse sequences as well as the development of a script, automating the steps taken during the experiment. The software interface, controlling the NMR experiment, ensures the detection of mismatched pulsed field gradients and their subsequent correction as proposed in [2].

However, an additional requirement of experiments involving the inverse Laplace transformation for data processing, is to attenuate the NMR signal down to a signal-to-noise ratio of about one. This demand tends to let the aforementioned detection of gradient mismatches fail for evanescent signals. We overcame this challenge by the introduction of a termination condition, which was based on the NMR signal decaying below a distinct signal-to-noise ratio and/or the attempt to correct for a pulsed field gradient mismatch beyond measure.

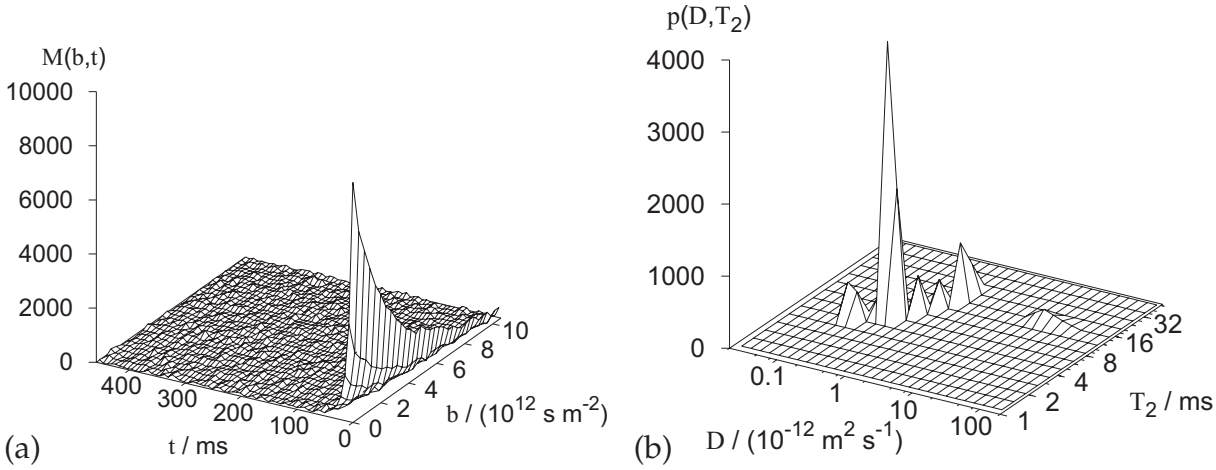

Figure 4.18: Diffusion-relaxation correlation experiment with lubricating oil at $T = 340$ K: (**a**) NMR signal map; (**b**) Inverse Laplace transformation of (**a**).

First experiments were successfully applied to several lubrication oil samples with distributions of diffusion coefficients and NMR relaxation times (Fig. 4.18). Please note the small diffusivities and short T_2 which indeed require short and ultra-high pulsed field gradients.

[1] M.D. Hurlimann, L. Venkataramanan: J. Magn. Reson. **157**, 31 (2002)
[2] P. Galvosas et al.: J. Magn. Reson. **151**, 260 (2001)

4.16 Investigation of Exchange in W/O/W Emulsions using Ultra-High Pulsed Field Gradients

M. Gratz, P. Galvosas

Water–oil–water (W/O/W) emulsions consist of three different phases with distinct diffusional characteristics. Small droplets of water are dispersed in bigger droplets of oil, which again are embedded in a water phase. Water molecules are able to move through the oil membrane from the inner to the outer phase and vice-versa, resulting in a change of their dynamic state.

This exchange behaviour was directly observed for the first time using the diffusion-diffusion exchange spectroscopy (DESXY) as suggested in [1], combined with methods for the application of ultra-high pulsed field gradients as introduced in [2]. The DEXSY pulse sequence traces the molecular displacements in two subsequent intervals, separated by a mixing time τ_m. After the data processing with the inverse Laplace transformation several peaks may appear in a two-dimensional map, characterizing the motional behavior of molecules in different sites of the sample. For a moisturizer, at a mixing time of 10 ms, most of the signal is to be found in the diagonal peaks, representing molecules with unchanged diffusion coefficient during τ_m (see Fig. 4.19).

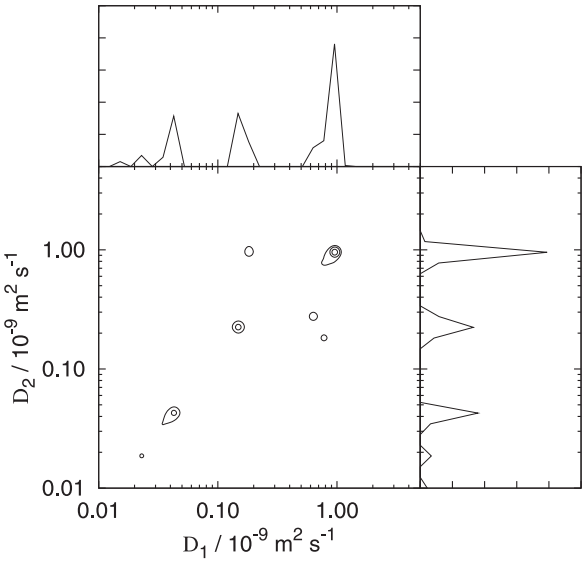

Figure 4.19: Laplace transformed NMR signal map of moisturizer with a mixing time τ_m = 10 ms and its projections showing the three components.

On the contrary, the off-diagonal peaks, which only exist for the two phases with the highest diffusion coefficients of water, represent molecules changing their diffusional properties, thus revealing exchange between the different water sites of the sample. The slowest phase, which is assigned to the only existing oil phase in the sample shows, as expected, no such behavior.

[1] P.T. Callaghan et al.: Magn. Reson. Imag. **21**, 243 (2003)
[2] P. Galvosas et al.: J. Magn. Reson. **151**, 260 (2001)

4.17 Development and Use of a New Probe for PFG-NMR Measurements in Sub-Micrometer Domains

M. Grossmann, S. Schlayer, P. Galvosas

NMR with pulsed magnetic field gradients (PFG-NMR) is a powerful method for the observation of molecular diffusion. Depending on the design of the NMR system, displacements of down to some ten nanometers have been detected so far [1]. Nevertheless, those measurements still remain a challenge in cases, where short observation times and/or short gradient pulses are required. We therefore set out to develop a new design for a gradient system suitable for the application of pulsed magnetic field gradients even higher than those as reported in [1], thus enabling the study of samples with a shorter relaxation time T_2.

In a first step, one-dimensional numerical solutions of the Biot–Savart law (based on a software written by the author M.G.) were determined, which allowed a rough estimate of the optimal gradient coil geometry (radius, number of turns, position of coils along the z-axis) and the maximum value of the magnetic field gradient. Based on these results two gradient coil configurations were selected, a down-scaled version of

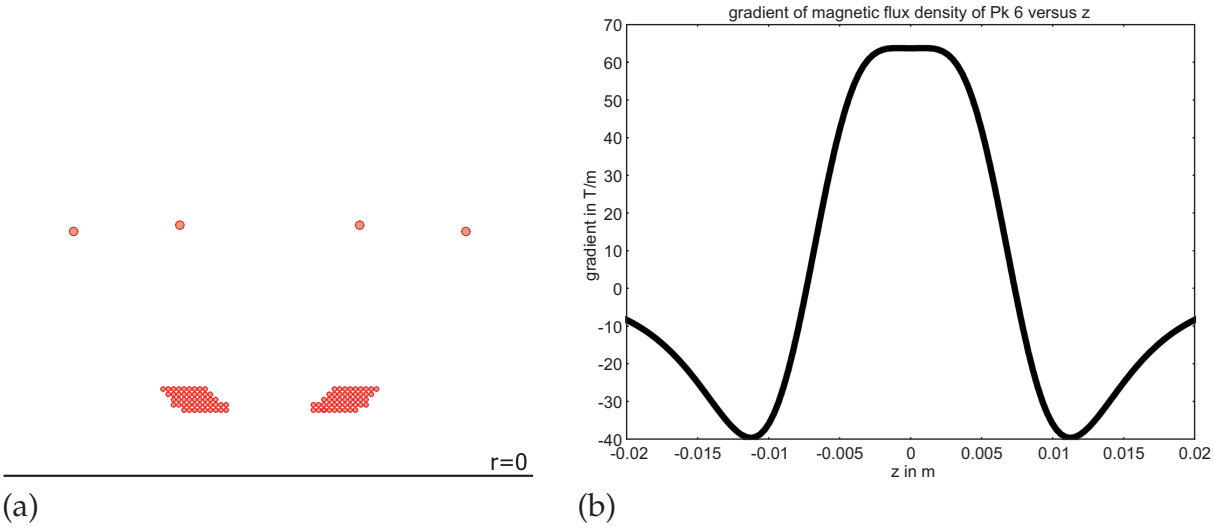

(a) (b)

Figure 4.20: Arrangement of the developed gradient system and shielding coil (**a**) and the achieved gradient along the z-axis as determined with COMSOL (**b**).

an existing probe (Pk4) and a newly designed probe with a rhombic cross section (see at the bottom of Fig. 4.20a).

In a second step we used a COMSOL model in which shielding coils were added (see at the top of Fig. 4.20a). Furthermore, solenoids were approximated by tori, thus reducing the model to two dimensions using the rotational symmetry along the *z*-axis. As a result of the numerical calculations the values for the magnetic field gradient, the magnetic field of the shielded area, the inductivity and ohmic resistance were determined. Finally, the gradient system was built and tested, confirming the properties, such as a maximum gradient of 58 T/m, as predicted by the COMSOL model. Further effort is required in the future for the decoupling of the gradient and the rf-system as well as for the stabilizing of the corresponding gradient current source.

[1] P. Galvosas et al.: J. Magn. Reson. **151**, 260 (2001)

4.18 Funding

Alkan- und Alken-Aktivierung in der heterogenen Säurekatalyse. In situ-C-13 und H-1 MAS NMR-Untersuchungen der Kinetik des Isotopen- Scramblings (C-13, H-2) im Reaktionsverlauf
Prof. Dr. D. Freude
DFG-Projekt FR 902 / 15-2

Combined NMR Studies of Diffusion and Reaction
Prof. Dr. D. Freude
im DFG-Projekt GRK 1056/1, International Research Training Group "Diffusion in Porous Materials"

Anwendungen der Doppelrotations- und Multiquanten-Messtechnik für Hochfeld-NMR-Untersuchungen an O-17-Kernen in porösen Festkörpern
Prof. Dr. D. Freude, Dr. H. Ernst
DFG-Projekt FR 902/16-2

Computersimulation und analytische Untersuchungen zum Einfluss der Kristallgrenze auf den Austausch von Gastmolekülen zwischen Zeolith-Nanokristallen und der Umgebung
Dr. S. Fritzsche, Prof. Dr. S. Vasenkov
DFG-Projekt FR 1486/2-1, SPP 1155 "Molekulare Modellierung und Simulation in der Verfahrenstechnik"

Studying Zeolitic Diffusion by Interference and IR Microscopy
Prof. Dr. J. Kärger
DFG-Projekt KA 953/18-3, International Research Group "Diffusion in Zeolites"

Bestimmung mikroskopischer Kenngrößen der Molekültranslation in Schüttungen nanoporöser Partikel mittels PFG NMR und Monte-Carlo-Simulation
Prof. Dr. J. Kärger
DFG-Projekt KA 953/19-1

Confinement Effects on Diffusion and Reaction in Zeolites, Studied by Dynamic MC Simulations, PFG NMR and Interference/IR Microscopy
Prof. Dr. J. Kärger
im DFG-Projekt GRK 1056/1, International Research Training Group "Diffusion in Porous Materials"

In situ study and development of processes involving nanoporous solids
Prof. Dr. J. Kärger
EU-Projekt NMP3-CT-2004-500895

PFG NMR studies of zeolitic diffusion
Prof. P. Galvosas, Prof. Dr. J. Kärger
DGF-Projekt GA 1291/1-2

PFG NMR investigations on formulated catalysts; Bestimmung von Diffusionskoeffizienten an Katalysatoren
Prof. Dr. J. Kärger, Dr. F. Stallmach
BASF AG

Fourier-Transform-PFG-NMR mit starken Feldgradientenimpulsen zur selektiven Selbstdiffusionsmessung
Prof. Dr. J. Kärger, Dr. F. Stallmach
DFG-Projekt KA 953/16-1

Innovative Zugabestoffe für die Innere Nachbehandlung von Hochleistungsbeton unter Berücksichtigung der räumlichen und zeitlichen Wasserbilanz
Prof. Dr. J. Kärger, Dr. F. Stallmach
DFG-Projekt KA 953/22-1

Intelligent design of nanoporous sorbents
Prof. Dr. J. Kärger, D. Tzoulaki
EU-Projekt CT-2004-005503

Fluid Transport in Porous Rocks and Sediments from Near-Surface Aquifers Studied by NMR and MRI
Dr. F. Stallmach
within DFG-Projekt GRK 1056/1, International Research Training Group "Diffusion in Porous Materials"

NMR and MRI studies of aquifer rocks; NMR- and MRI-Untersuchungen an Aquifergesteinen
Dr. F. Stallmach, Prof. Dr. J. Kärger
UFZ Halle/Leipzig GmbH

Messung intrakristalliner Diffusions-Reaktions-Profile in Zeolithen mittels IR-Imaging
Prof. Dr. J. Kärger
DFG-Projekt KA 953/21-1

Messung von Pasenübergangen in mesoskopisch beschränkten Systemen: kombinierter Einsatz von NMR und Molekulardynamik

Prof. Dr. J. Kärger, Dr. R. Valiullin
DFG-Projekt KA 953/20-1

Untersuchung der Diffusion in heterogenen Systemen mit PFG-MAS-NMR-Spektroskopie
Dr. A. Pampel, Prof. Dr. J. Kärger
DFG-Projekt PA 907/3-1

PFG NMR Untersuchung der Transporteigenschaften von Fluiden in Mesoporen in der Nähe des kritischen Punktes
Prof. J. Kärger, Dr. R. Valiullin
DFG-Projekt KA 953/25-1

P8 Particle Dynamics in Nano-Structured Channels
Prof. J. Kärger, Dr. R. Valiullin, Prof. Janke
DFG-Projekt KA 953/27-1

ZP Zentralprojekt gemeinsam beantragter Mittel für die Forschergruppe
Prof. J. Kärger
DFG-Projekt KA 953/28-1

Network of Excellence: Inside Pores
Prof. J. Kärger, Dr. F. Grinberg
EU-Projekt 23120 562

Mercator-Professur
Prof. Dr. R. Krishna
Le 758/25-1

4.19 Organizational Duties

D. Freude

- Director of the Magnetic Resonance Centre (MRZ) of Leipzig University
- Membership in Editorial Boards: Solid State NMR; Diff. Fundam. (Online Journal)
- Referee: Chem. Phys. Lett., J. Chem. Phys., J. Phys. Chem., J. Magn. Res., Solid State NMR

P. Galvosas

- Referee: Meas. Sci. Technol., Magn. Reson. Imaging, J. Magn. Reson., Concept. Magn. Reson.
- Faculty board member
- member of the advisory board of study affairs (Studienkommission)
- Member of the Board of Examiners (Prüfungskommission)
- General advisor for physic study affairs (Studienfachberater für Physik)
- Deputy institutional ERASMUS coordinator

F. Grinberg

- Membership in "AMPERE Division of Spatially Resolved Magnetic Resonance" Polish German Radiospectroscopy Group (PGRG)

- Membership in Editorial Boards: Diff. Fundam. (Online Journal, Editor)

J. Kärger

- Membership in the Programme Committee "Magnetic Resonance in Porous Media" (Bologna 2006, Boston 2008), "Fundamentals of Adsorption" (Giardini Naxos, Sicily, Italy 2007), International Zeolite Conference (Peking 2007), in the permanent DECHEMA committees Zeolites and Adsorption and in the Board of Directors of the Magnetic Resonance Centre (MRZ) of Leipzig University
- Membership in Editorial Boards: Micropor. Mesopor. Mater. (European Editor); Diff. Fundam. (Online Journal, Editor); Adsorption
- Referee: Phys. Rev., Phys. Rev. Lett., Europhys. Lett., J. Chem. Phys., J. Phys. Chem., Langmuir, Micropor. Mesopor. Mat., PCCP, J. Magn. Res., Nature, Angew. Chemie
- Project Reviewer: Deutsche Forschungsgemeinschaft, National Science Foundation (USA)

F. Stallmach

- Referee: Micropor. Mesopor. Mat., Angew. Chem., Membr. Sci., Am. Ceram. Soc.
- Project Reviewer: Deutsche Forschungsgemeinschaft

R. Valiullin

- Membership in Scientific Advisory Committee "Bologna MRPM Conference (Ampere Event)"
- Referee: J. Phys. Chem., J. Am. Chem. Soc., Adsorption, Micropor. Mesopor. Mat.

4.20 External Cooperations

Academic

- Academy of Sciences of the Czech Republic, J. Heyrovsky Institute of Physical Chemistry, Prague, Czech Republic
  Dr. Kocirik, Dr. Zikanova
- Delft University, DelftChemTech, Delft, The Netherlands
  Prof. Kapteijn
- Institut de Recherches sur la Catalyse, CNRS, Villeurbanne, France
  Dr. Jobic
- GeoForschungsZentrum Potsdam (GFZ), Potsdam, Germany
  A. Förster
- Helmholtz Zentrum für Umweltforschung UFZ Halle-Leipzig GmbH, Leipzig, Germany
  Prof. Kopinke, H.-R. Gläser, I. Mitreiter, S. Oswald
- Institut Francais du Petrole, Malmaison, France
  Dr. Methivier
- Max-Planck-Institut für Kohlenforschung, Mülheim, Germany
  Dr. Schmidt, Prof. Schüth

- Max-Planck-Institut für Metallforschung, Stuttgart, Germany
  Dr. Majer
- Russian Acadademy of Sciences, Boreskov Institute of Catalysis, Siberian Branch, Novosibirsk, Russia
  Dr. Stepanov
- TU München, Lehrstuhl Technische Chemie 2, Germany
  Prof. Lercher
- University Medical Center Hamburg-Eppendorf, Hamburg, Germany
  Dr. M. Koch
- Università di Sassari, Dipartimento Chimica, Sassari, Italy
  Prof. Demontis, Prof. Suffritti
- Universiät Eindhoven, Schuit Institute, Eindhoven, The Netherlands
  Prof. van Santen
- Universität Erlangen Nürnberg, Deptartment for Chemical Engineering, Erlangen, Germany
  Prof. Emig, Prof. Schwieger
- Universität Hannover, Institute of Physical Chemistry, Hannover, Germany
  Prof. Caro, Prof. Heitjans
- Universität Leipzig, Institut für Analytische Chemie, Leipzig, Germany
  Prof. Berger
- Universität Leipzig, Institut für Technische Chemie, Leipzig, Germany
  Prof. Einicke, Prof. Papp, Prof. Gläser
- Universität Leipzig, Institut für Anorganische Chemie, Leipzig, Germany
  Prof. Krautscheid
- Universität Leipzig, Institut für Medizinische Physik und Biophysik, Leipzig, Germany
  Prof. Arnold, Prof. Gründer
- Universität Regensburg, Inst. Biophysik & Physikalische Biochemie, Regensburg, Germany
  Prof. Brunner
- Universität Stuttgart, Institut für Technische Chemie, Stuttgart, Germany
  Prof. Hunger, Prof. Weitkamp
- University Athens, Deptartment for Chemical Engineering, Athens, Greece
  Prof. Theodorou
- University of Amsterdam, The Netherlands
  Prof. Krishna
- University of Maine, Deptartment for Chemical Engineering, Orono, USA
  Prof. Ruthven
- Cleveland University, USA
  Prof. Shah

- University College London, UK
  Prof. Brandani
- Westfälische Wilhelms-Universität Münster, Institut für Physikalische Chemie, Germany
  Prof. Schönhoff
- Victoria University of Wellington, MacDiarmid Institute for Advanced Materials and Nanotechnology, School of Chemical and Physical Sciences, New Zealand
  Prof. Callaghan

Industry

- Air Prod & Chem Inc., Allentown, USA
  Dr. Coe, Dr. Zielinski
- BASF, Ludwigshafen, Germany
  Dr. Müller, Dr. Nestle, Dr. Rittig
- Cepsa, Madrid, Spain
  Dr. Perez
- Grace, Worms, Germany
  Dr. McElhiney
- Resonance Instruments Ltd., Witney, UK
  J. McKendry
- SINTEF, Oslo, Norway
  Prof. Stöcker
- Südchemie, Berlin, Germany
  Dr. Tissler, Dr. Tufar, Dr. Lutz
- StatoilHydro, Stavanger, Norway
  C. v. d. Zwaag
- HeidelbergCement, Baustoffe für Geotechnik GmbH & Co. KG, Ennigerloh, Germany
  A. Märten, J. Dietrich

4.21 Publications

Journals

P.T. Callaghan, C.H. Arns, P. Galvosas, M.W. Hunter, Y. Qiao, K.E. Washburn: *Recent Fourier and Laplace Perspectives for Multidimensional NMR in Porous Media*, Magn. Reson. Imag. **25**, 441 (2007)

C. Chmelik, L. Heinke, A. Varma, D.B. Shah, J. Kärger, J.M. van Baten, R. Krishna: *Loading Dependence of Diffusion in Zeolites: Combined Benefits of Microscopic Measuring Techniques and Theoretical Approaches*, Diff. Fundam. **6**, 59.1 (2007)

C. Chmelik, A. Varna, L. Heinke, D.B. Shah, J. Kärger, F. Kremer, U. Wilczok, W. Schmidt: *Effect of Surface Modification on Uptake Rates of Isobutane in MFI Crystals: An Infrared Microscopy Study*, Chem. Mater. **19**, 6012 (2007)

M. Dvoyashkin, R. Valiullin, J. Kärger: *Supercritical Fluids in Mesopores - New Insight Using NMR*, Adsorption **13**, 197 (2007)

M. Dvoyashkin, R. Valiullin, J. Kärger: *Temperature Effects on Phase Equilibrium and Diffusion in Mesopores*, Phys. Rev. E **75**, 041 202 (2007)

M. Dvoyashkin, R. Valiullin, J. Kärger, W.-D. Einicke, R. Gläser: *Direct Assessment of Transport Properties of Supercritical Fluids Confined to Nanopores*, J. Am. Chem. Soc. **129**, 10344 (2007)

M. Fernandez, J. Kärger, D. Freude, A. Pampel, J.M. van Baten, R. Krishna: *Mixture Diffusion in Zeolites Studied by MAS PFG NMR and Molecular Simulation*, Micropor. Mesopor. Mater. **105**, 124 (2007)

P. Galvosas, Y. Qiao, M. Schönhoff, P.T. Callaghan: *On the Use of 2D Correlation and Exchange NMR Spectroscopy in Organic Porous Materials*, Magn. Reson. Imag. **25**, 497 (2007)

F. Grinberg: *Surface Effects in Liquid Crystals Constrained in Nano-Scaled Pores Investigated by Field-Cycling NMR Relaxometry and Monte Carlo Simulations*, Magn. Reson. Imag. **25**, 485 (2007)

L. Heinke: *Application of Boltzmann's Integration Method under non-ideal Conditions*, Diff. Fundam. **4**, 9.1 (2007)

L. Heinke: *Significance of Concentration-Dependent Intracrystalline Diffusion and Surface Permeation for Overall Mass Transfer*, Diff. Fundam. **4**, 12.1 (2007)

L. Heinke, C. Chmelik, P. Kortunov, D.B. Shah, S. Brandani, D.M. Ruthven, J. Kärger: *Analysis of Thermal Effects in Infrared and Interference Microscopy: n-Butane-5A and Methanol-Ferrierite Systems*, Micropor. Mesopor. Mater. **104**, 18 (2007)

L. Heinke, C. Chmelik, P. Kortunov, S. Vasenkov, D.M. Ruthven, D.B. Shah, J. Kärger: *Application of Interference Microscopy and IR-Microscopy for Characterizing and Investigating the Mass Transport in Nanoporous Materials*, Chem. Eng. Technol. **30**, 995 (2007)

L. Heinke, P. Kortunov, D. Tzoulaki, M.J. Castro, P.A. Wright, J. Kärger: *Three-dimensional Diffusion in Nanoporous Host-Guest Materials Monitored by Interference Microscopy*, Eur. Phys. Lett. **81**, 26 002 (2008)

L. Heinke, P. Kortunov, D. Tzoulaki, J. Kärger: *Exchange Dynamics at the Interface of Nanoporous Materials with their Surroundings*, Phys. Rev. Lett. **99**, 228 301 (2007)

L. Heinke, P. Kortunov, D. Tzoulaki, J. Kärger: *The Options of Interference Microscopy to Explore the Significance of Intracrystalline Diffusion and Surface Permeation for Overall Mass Transfer on Nanoporous Materials*, Adsorption **13**, 215 (2007)

J. Kärger, L. Heinke, P. Kortunov, S. Vasenkov: *Looking into the Crystallites: Diffusion Studies by Interference Microscopy*, Stud. Surf. Sci. Catal. **170**, 739 (2007)

A. Khokhlov, R. Valiullin, J. Kärger, F. Steinbach, A. Feldhoff: *Freezing and Melting Transitions of Liquids in Mesopores with Ink-Bottle Geometry*, New J. Phys. **9**, 272 (2007)

P. Kortunov, L. Heinke, M. Arnold, Y. Nedellec, D.J. Jones, J. Caro, J. Kärger: *Intracrystalline Diffusivities and Surface Permeabilities Deduced from Transient Concentration Profiles: Methanol in MOF Manganese Formate*, J. Am. Chem. Soc. **129**, 8041 (2007)

P. Kortunov, L. Heinke, J. Kärger: *Assessing Guest Diffusion in Nanoporous Materials by Boltzmann's Integration Method*, Chem. Mater. **19**, 3917 (2007)

M. Krutyeva, S. Vasenkov, J. Kärger: *Exploring the Influence of the Surface Resistance of Nanoporous Particles on Molecular Transport*, Diff. Fundam. **5**, 8.1 (2007)

M. Krutyeva, S. Vasenkov, X. Yang, J. Caro, J. Kärger: *Surface Barriers on Nanoporous Particles: a New Method of their Quantitation by PFG NMR*, Micropor. Mesopor. Mater. **104**, 89 (2007)

M. Krutyeva, X. Yang, S. Vasenkov, J. Kärger: *Exploring the Surface Permeability of Nanoporous Particles by Pulsed Field Gradient NMR*, J. Magn. Reson. **185**, 300 (2007)

S. Naumov, R. Valiullin, P. Galvosas, J. Kärger, P.A. Monson: *Diffusion Hysteresis in Mesoporous Materials*, Eur. Phys. J. Special Topics **141**, 107 (2007)

N. Nestle, A. Gädke, K. Friedemann, F. Stallmach, P. Galvosas: *NMR Diffusometry on Cementitious Materials: Expanding the Hydration Time Window by Static Field Gradient NMR in Ultrastrong Gradients*, Magn. Reson. Imag. **25**, 575 (2007)

N. Nestle, P. Galvosas, J. Kärger: *Liquid-Phase Self-Diffusion in Hydrating Cement Pastes – Results from NMR Studies and Perspectives for further Research*, Cem. Concr. Res. **37**, 398 (2007)

W. Schönfelder, J. Dietrich, A. Märten, K. Kopinga, F. Stallmach: *NMR Studies of Pore Formation and Water Diffusion in Self-Hardening Cut-Off Wall Materials*, Cem. Concr. Res. **37**, 902 (2007)

W. Schoenfelder, J. Dietrich, A. Märten, K. Kopinga, F. Stallmach: *Studying Diffusive Water Transport in Bentonite Cement Mixtures of Very Low Hydraulic Conductivity*, Magn. Reson. Imag. **25**, 582 (2007)

F. Stallmach, P. Galvosas: *Spin Echo NMR Diffusion Studies*, Ann. Rep. NMR Spectrosc. **61**, 55 (2007)

F. Stallmach, W. Schönfelder: *Mehrdimensionale NMR-Methoden zur Untersuchung gesteins-physikalischer und geotechnischer Parameter*, Mitteilungen der Deutschen Geophysikalischen Gesellschaft e.V., Sonderband I/2007, 3 (2007)

D. Tzoulaki, U. Wilczok, W. Schmidt, J. Kärger: *Formulation of Surface Barriers on Silicalite-1 Crystal Fragments by Residual Water as probed with Isobutane by Interference Microscopy*, Micropor. Mesopor. Mater. **110**, 72 (2008)

K. Ulrich, M. Sanders, S. Vasenkov: *Probing Lateral Diffusion in Lipid Membranes on Nanoscale by PFG NMR with High Gradient Strength*, Magnet. Reson. Imag. **25**, 493 (2007)

R. Valiullin, M. Dvoyashkin: *Diffusion Processes in Mesoporous Adsorbents Probed by NMR*, Adsorption **13**, 239 (2007)

R. Valiullin, M. Dvoyashkin, P. Kortunov, C. Krause, J. Kärger: *Diffusion of Guest Molecules in MCM-41 Agglomerates*, J. Chem. Phys. **126**, 054705 (2007)

R. Valiullin, S. Naumov, P. Galvosas, J. Kärger, P.A. Monson: *Dynamical Aspects of the Adsorption Hysteresis Phenomenon*, Magn. Reson. Imag. **25**, 481 (2007)

Books

F. Grinberg: *Reorientations Mediated by Translational Displacements in Confined Liquid Crystals Studied by Field Cycling NMR Relaxometry and Monte Carlo Simulations*, in *Diffision Fundamentals II*, ed. by S. Brandani, C. Chmelik, J. Kärger, R. Volpe (Leipziger Universitätsverlag, Leipzig 2007) p 336

E. Romanova, C. Krause, A. Stepanov, J.M. van Baten, R. Krishna, J. Kärger, D. Freude: ^{1}H *NMR Signal Broadening in Spectra of MFI Type Zeolites*, in *Diffusion Fundamentals II*, ed. by S. Brandani, C. Chmelik, J. Kärger, R. Volpe (Leipziger Universitätsverlag, Leipzig 2007) p 310

S. Brandani, C. Chmelik, J. Kärger, R. Volpe (Eds.): *Diffusion Fundamentals II* (Leipziger Universitätsverlag, Leipzig 2007)

J. Kärger: *Leipzig, Einstein, Diffusion* (Leipziger Universitätsverlag, Leipzig 2007)

in press

K. Friedemann, W. Schönfelder, F. Stallmach, J. Kärger: *NMR Relaxometry During Internal Curing of Portland Cements by Lightweight Aggregates*, Mater. Struct.

D. Tzoulaki, L. Heinke, U. Wilczok, W. Schmidt, J. Kärger: *Exploring Crystal Morphology of Nanoporous Hosts from Transient Guest profiles*, Angew. Chemie

Talks

S. Brandani, J. Caro, H. Jobic, J. Kärger, C. Krause, A. Möller, D. Ruthven, D. Shah, W. Schmidt, R. Staudt, X. Yang: *Recent Developments in the Measurement of Diffusion in Zeolites*, 9th Conf. Fundam. Adsorpt., Giardini Naxos, Italy, May 2007

M. Fernandes: *Diffusion of Acetone-Alkane Mixtures in Mesoporous Materials Studied by MAS PFG NMR*, 6th Workshop of the IRTG "Diffusion in Porous Materials", Leipzig, March 2007

P. Galvosas, M. Gratz, Y. Qiao, M. Schönhoff, P.T. Callaghan: *Experimental Aspects of NMR Diffusion Exchange and Diffusion-Relaxation Correlation Spectroscopy*, ICMRM 9, Aachen, September 2007

F. Grinberg: *Diffusion: Fundamentals and Applications in Biosciences*, 2nd Int. Summer School in Biomedical Engineering "Diffusion weighted Magnetic Resonance Imaging: Principles and Applications", Naumburg-Schönburg, August 2007

F. Grinberg: *Nuclear Magnetic Resonance. Basic Principles and Applications*, 2nd Int. INSIDE-PORES Workshop, Thessaloniki, Greece, February 2007

J. Kärger: *Diffusion and Evolution*, Univ. Leipzig, within the Colloquium dedicated to the retirement of Prof. K. Arnold, Leipzig, November 2007

J. Kärger: *Diffusion in nanoporösen Systemen*, Univ. Duisburg-Essen, within the Colloquium dedicated to the retirement of Prof. W. Veeman, November 2007

J. Kärger: *PFG NMR as a Tool for Diffusion Measurement on the Microscopic Scale*, RaiseBio Summerschool, UFZ Leipzig, September 2007

J. Kärger, C. Chmelik, F. Stallmach, D. Tzoulaki, M. Wehring: *Zur Moleküldiffusion in MOFs*, Colloquium of the ProcessNet-Fachausschuss Adsorption, Frankfurt, November 2007

J. Kärger, P. Galvosas, F. Stallmach, R. Valiullin, C. Krause: *Diffusometrie in Porösen Materialien*, Informationsveranstaltung des Zentrums für Magnetische Resonanz der Universität Leipzig, Leipzig, September 2007

J. Kärger, P. Galvosas, R. Valiullin, F. Stallmach, S. Vasenkov, C. Krause: *Fundamentals of Diffusion Processes*, 2nd Int. INSIDE-PORES Workshop, Thessaloniki, February 2007

J. Kärger, P. Kortunov: *Interference and IR Microscopy*, George-Kokotailo Award Lecture, 19th German Zeolite Conference, Leipzig, March 2007

J. Kärger, P. Kortunov: *The Facets of Molecular Transport in Nanoporous Materials Revealed by Interference Microscopy*, 9th Conf. Fundam. Adsorpt., Giardini Naxos, Italy, May 2007

J. Kärger, R. Valiullin: *Experimental Studies of Anomalous Diffusion in Nanoporous Materials*, 392nd Heraeus Seminar, Ilmenau, September 2007

S. Naumov: *Adsorption Hysteresis in Mesoporous Materials*, 6th International Research Training Group Diffusion in Porous Materials, Leipzig, March 2007

S. Naumov: *Adsorption Hysteresis in Mesoporous Materials*, AMPERE NMR Summer School, Bukowina Tatrzanska, Poland, June 2007

S. Naumov: *Diffusion Scanning Hysteresis Loops in Nanopores*, 9th Conf. Fundam. Adsorpt., Giardini Naxos, Italy, May 2007

M. Krutyeva, S. Vasenkov, J. Kärger: *Exploring the Surface Permeability of Nanoporous Particles by Pulsed Field Gradient NMR*, AMPERE NMR Summer School, Bukowina Tatrzanska, Poland, June 2007

K. Ulrich: *Influence of the Morphology on Self-Diffusion of Ordered Triblock Copolymers in Water Solutions*, 3rd INSIDE-PORES Workshop, Alicante, Spain, September 2007

R. Valiullin: *Diffusion Processes in Mesoporous Adsorbents Probed by NMR*, 9th Conf. Fundam. Adsorpt., Giardini Nexos, Italy, May 2007

R. Valiullin: *Dynamics of Guest Molecules in Mesoporous Hosts*, DECHEMA Fachtagung AEM 2007, Asselheim, Germany, March 2007

R. Valiullin: *Fluid Distribution in Mesoporous Materials*, 9th International "Heidelberg" Conference on Magnetic Resonance Microscopy, Aachen, Germany, September 2007

R. Valiullin: *Phase Transitions of Fluids in Mesopores Assessed by NMR*, DPG Spring Meeting, Regensburg, Germany, March 2007

Posters

C. Chmelik, L. Heinke, A. Varma, D.B. Shah, J. Kärger, R. Krishna: *Loading Dependence of Diffusion in Zeolites: Combined Benefits of Microscopic Measuring Techniques and Theoretical Approaches*, Diffusion Fundamentals II, L'Aquila, Italy, August 2007

C. Chmelik, D.B. Shah, L. Heinke, J. Kärger, U. Wilczok, W. Schmidt: *Effect of Surface Modification on Molecular Uptake Rates of Isobutane in MFI Crystals: An IR Microscopy Study*, 9th Int. Conf. Fundam. Adsorpt., Giardini Naxos, Italy, May 2007

C. Chmelik, D.B. Shah, L. Heinke, J. Kärger, U. Wilczok, W. Schmidt: *Manipulating Molecular Uptake Rates of MFI Crystals by Surface Modification: An IR Microscopy Study Systems*, 19. Deutsche Zeolithtagung, Leipzig, March 2007

R.P. Choudhury, P. Galvosas, M. Schönhoff: *Molecular Weight Dependence of PEO Permeation Through the Walls of Hollow Polyelectrolyte Capsules*, 71th Annual Meeting of DPG, Regensburg, March 2007

M. Dvoyashkin, A. Khokhlov, R. Valiullin, J. Kärger: *Molecular Dynamics on Surfaces - NMR Survey*, 1st Flash Conference ERA-Chemistry, Autrans, France, March 2007

M. Fernandez, A. Pampel, J. Kärger, D. Freude, J.M. van Baten, R. Krishna: *Mixture Diffusion in Zeolites Studied by MAS PFG NMR*, 19. Deutsche Zeolith-Tagung, Leipzig, March 2007

M. Fernandez, A. Pampel, J. Kärger, D. Freude, J.M. van Baten, R. Krishna: *Mixture Diffusion in Silicalite-1 Studied by MAS PFG NMR*, Diffusion Fundamentals II, L'Aquila, Italy, August 2007

M. Gratz, P. Galvosas: *Methodical Aspects of 2D NMR Correlation Spectroscopy under Conditions of Ultra-High Pulsed Field Gradients*, Diffusion Fundamentals II, L'Aquila, Italy, August 2007

L. Heinke, P. Kortunov, D. Tzoulaki, J. Kärger: *The Options of Interference Microscopy to Explore the Significance of Intracrystalline Diffusion and Surface Permeation for Overall Mass Transfer on Nanoporous Materials*, Diffusion Fundamentals II, L'Aquila, Italy, August 2007

L. Heinke, D.B. Shah, C. Chmelik, J. Kärger, P. Kortunov, S. Brandani, D.M. Ruthven: *Analysis of Thermal Effects in Infra-Red and Interference Microscopy: n-Butane-5A and Methanol-Ferrierite Systems*, 19. Deutsche Zeolithtagung, Leipzig, March 2007

M. Krutyeva, F. Furtado, F. Grinberg, A. Silvestre-Albero, F. Rodríguez-Reinoso, S. Vasenkov, J. Kärger: *Molecular Transport in Systems of Nanoporous Particles as Studied with Help of the Pulsed Field Gradient NMR*, 3rd INSIDE-PORES Workshop, Alicante, Spain, September 2007

M. Krutyeva, F. Grinberg, I. Berndt, W. Richtering, S. Stapf: *Phase Transitions in Thermosensitive Microgels Investigated by Proton NMR Spectroscopy, Diffusometry and Relaxometry*, AMPERE NMR Summer School, Bukowina Tatrzaska, Poland, June 2007

M. Krutyeva, J. Kärger, S. Vasenkov: *Exploring the Influence of Surface Resistance of Nanoporous Particles on the Molecular Transport by PFG NMR*, Diffusion Fundamentals II, L'Aquila, Italy, August 2007

M. Krutyeva, J. Kärger, S. Vasenkov, X. Yang, J. Caro: *Exploring the Surface Permeability of Zeolite Crystals by PFG NMR and Computer Simulations*, 19th Deutsche Zeolithtagung, Leipzig, March 2007

E. Romanova, C. Krause, A. Stepanova, J.M. van Baten, R. Krishna, J. Kärger, D. Freude: ^{1}H *NMR Line Broadening in MFI Type Zeolites*, 19. Deutsche Zeolith-Tagung, Leipzig, March 2007

E. Romanova, C. Krause, A. Stepanov, J.M. van Baten, R. Krishna, J. Kärger, D. Freude: ^{1}H *NMR Signal Broadening in Spectra of MFI Type Zeolites*, Diffusion Fundamentals II, L'Aquila, Italy, August 2007

W. Schönfelder, I. Mitreiter, H.-R. Gläser, F. Stallmach: *Charakterisierung der Porenraumstruktur von Karbonatgesteinen mit NMR* 67. Jahrestagung der Deutschen Geophysikalischen Gesellschaft (BP45), Aachen, March 2007

D. Tzoulaki, M.J. Castro, J. Kärger, P.A. Wright: *Interference Microscopy Highlights Properties and Peculiarities of SAPO STA-7 Crystals*, 15th International Zeolite Conference, Beijing, China, August 2007

D. Tzoulaki, M.J. Castro, P.A. Wright, J. Kärger: *Interference Microscopy Highlights Properties and Peculiarities of SAPO STA-7 Crystals*, Diffusion Fundamentals II, L'Aquila, Italy, August 2007

D. Tzoulaki, J. Kärger, W. Schmidt: *Investigation of Uptake Processes in Silicalite-1 and its Fragments by means of Interference Microscopy*, 2nd Int. INSIDE-PORES Workshop, Thessaloniki, Greece, February 2007

D. Tzoulaki, J. Kärger, W. Schmidt: *Investigation of Uptake Processes in Silicalite-1 and its Fragments by means of Interference Microscopy*, 19. Deutsche Zeolithtagung, Leipzig, March 2007

K. Ulrich: *Influence of the Morphology on Self-Diffusion of Ordered Triblock Copolymers in Water Solutions*, 3rd INSIDE-PORES Workshop, Alicante, Spain, September 2007

K. Ulrich: *Study of Molecular Diffusion and Lateral Segregation in Oriented Lipid Membranes with the Help of PFG NMR*, AMPERE NMR School, Bukowina Tatranska, Poland, June 2007

4.22 Graduations

Doctorate

- Dennis Schneider
  NMR investigations on ^{17}O nuclei in porous solids
  September 2007

Diploma

- Jakob Mauritz
  Diffusion Studies of Probe Particles in Channels with Comparable Diameter
  August 2007
- Mario Grossmann
  Entwicklung und Einsatz eines Probenkopfes für PFG-NMR-Massungen
  December 2007

4.23 Guests

- Alexander Skripov
  Academy of Sciences, Ekaterinburg, Russia
  June – September 2007
- Alexander Stepanov
  Boreskov Institute of Catalysis, Novosibirsk, Russia
  November 2007 – April 2008

5

Soft Matter Physics

5.1 General Scientific Goals – Polymers and Membranes in Cells

In his book "What is Life?", Schrödinger recognized the immense challenge to explain biological processes by basic physics and chemistry. Consequentially, traditional medical physics had predominately the role to develop devices for medicine such as sophisticated imaging solutions (X-ray, NMR, multiphoton) or laser scalpels. Commencing with Watson and Crick, science has gained tremendous insight into the molecular basis of biological cells. Over 25 000 genes encode the information of human life, and their subsequent transcription and translation add to the complexity of molecular interactions resulting in an insurmountable combinatorial number of relations. Recent progress in biosciences towards a more quantitative description opens a challenging and new pathway for medical physics to use physics underlying biological processes to directly impact diagnosis and therapy. Despite that this approach is still in its infancy, it may redefine medical physics. This kind of research is based on fundamental biological physics and has in its ideal case applied aspects in medical physics. By identifying cellular subunits acting as independent functional modules this complexity becomes tractable and the fundamental physical principles of these modules can be studied.

A prototypical example for such a module is the intracellular scaffold known as the cytoskeleton. The cytoskeleton is the key structural element in cellular organization and is an indicator of pathological changes in cell function. It is a compound of highly dynamic polymers and molecular motors as active nano-elements inside cells. The cytoskeleton mechanically and chemically senses a cell's environment achieving a high sensitivity by using processes such as stochastic resonance. This active polymeric scaffold generates cellular motion and forces in the tens of nanoNewton sufficiently strong to push rigid AFM cantilevers out of the way. These forces are generated by molecular motor-based nano-muscles and by polymerization through mechanisms similar to Feynman's hypothetical thermal ratchet. A new type of polymer physics describes these active polymer networks since the nano-sized motors overcome the inherently slow, often glass-like Brownian polymer dynamics. This results in novel self-organization of the polymer scaffolds and rapid switching between different ordered states. This organization of the cytoskeleton is tightly controlled in cells. Thus, suspended cells' biomechanical properties are well-defined and distinguish different cellular states and

cell types with confidence levels of more than 95 % (metastatic from non-metastatic cancer cells, stem cells from differentiated cells in adult tissues, etc.). Since cell elasticity depends highly nonlinear on cytoskeletal composition already small changes in a cell's state are measurable by biomechanical changes and recent polymer theories can be used to deduce the cytoskeletal part of a cell's proteomic condition. The cytoskeleton uses up to 30 % of cellular ATP, which is a cell's fuel. Optical gradient forces due to cells' dielectric nature can manipulate the cytoskeleton's consequential active and dynamical state. Opto-molecular coupling between laser light and cytoskeletal processes permits optical control of neuronal growth. The specific opto-molecular influence on membrane and cytoskeletal transport is complex. Cells cannot modulate diffusion by the parameters found in the Einstein equation (temperature, viscosity, molecular size). Consequentially, cells exhibit rich multifaceted intracellular transport including motor-driven motion and anomalous subdiffusion, which can be probed by the use of nanoparticles as tracers. The cytoskeleton as active, soft condensed matter, with structures on nanometer and micron scales representative of individual proteins and cells, calls forth new biological and polymer physics. Our research group's goals center on unraveling this new physics of the cytoskeleton. The current and future research goals are summarized in the following sections.

Josef A. Käs

5.2 Reconstituted Active Polymer Networks

B. Gentry, D. Smith, B. Stuhrmann, F. Huber, D. Strehle, M. Steinbeck, J. Alvarado, L. Hild, M.-F. Carlier*, J.A. Käs

*LEBS, Gif-sur-Yvette, France

Active remodelling of the cell's internal scaffold, the cytoskeleton, is crucial for many different biological processes. Cells have developed a variety of different active network systems that have been optimized for their respective purposes. Some of the most important of these independent intracellular functional modules are studied using reconstituted model systems [1]. We report a mechanism whereby the molecular motor myosin II can cause near-instantaneous order–disorder transitions in reconstituted cytoskeletal actin solutions. When motor-induced filament sliding diminishes, the actin network structure rapidly and reversibly self-organizes into various assemblies. Addition of stable cross linkers was found to alter the architectures of the resulting structural patterns [2].

Cells achieve directed locomotion making use of two very different active structural elements, an extending flat actin network (lamellipodium), and protruding actin bundles (filopodia), both of which we study in vitro. We investigate quasi-2D actin networks by combining several microfabrication techniques that allow selective functionalization with the polymerization inducing peptide VCA. The emerging actin networks are restricted to sub-micron sized structures and are visualized with fluorescence microscopy (Fig. 5.1). This model system is complemented by a Monte-Carlo simulation of actin network growth.

Cellular actin bundles are responsible for both structural support and the active generation of forces for protrusion and contraction. These structures are held together

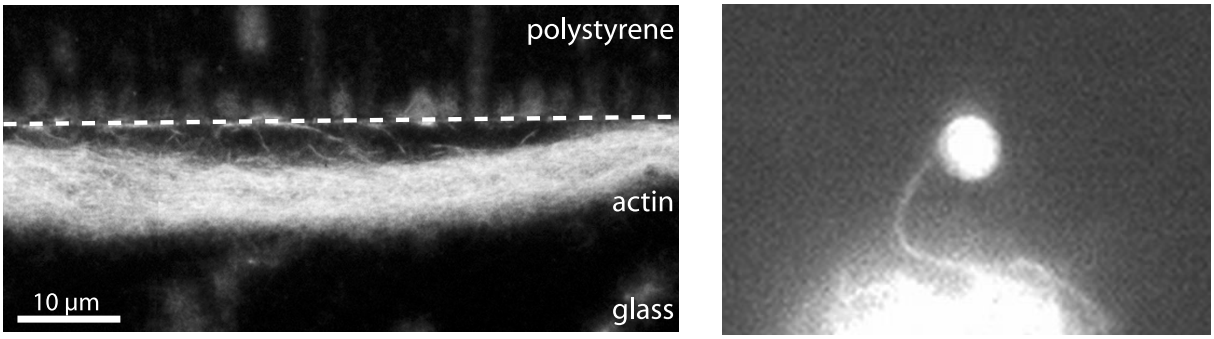

Figure 5.1: *Left*: Fluorescence image of a 2D actin network growing off a polystyrene wall. *Right*: F-actin bundle bent by an attached bead held by laser tweezers.

by transient cross-linking molecules, which enable differential response to mechanical stresses and ultimately result in bundle viscoelasticity. We actively probe their mechanic properties using optical tweezers and demonstrated that on long time scales actin bundles show plastic deformations. In addition, we create artificial contractile structures termed nanomuscles using actin bundles and molecular motors in order to further understand cellular force generation.

[1] D. Smith et al.: Biophy. J. **93**, 4445 (2007)
[2] D. Humphrey et al.: Nature **416**, 413 (2002)

5.3 Laser-Stretching in Opto-Fluidic Microsystems: A New Method for Cell Diagnosis and Cell Separation in the Field of Life Science

S. Ebert, T. Kießling, C. Stüber, K.D. Nnetu, J. Guck[*], S. Howitz[†], A. Emmendörffer[‡], C. Wenzel[§], J.A. Käs

[*]Department of Physics, University of Cambridge, UK
[†]GeSiM, Großerkmannsdorf
[‡]euroderm GmbH, Leipzig
[§]Department of Electrical Engineering, Technical University Dresden

Microfluidics is a fast growing field, since there is great demand to integrate many biological analysis methods on a so-called "lab on a chip". The microscopic dimensions of reservoirs, channels, and reaction chambers account for the often small substance volumes yield more accurate, and faster reactions than on the macroscopic scale.

Soft lithography is a suitable and widely used technique to manufacture such microfluidic chips. It comprises the fabrication of an SU-8 master on a silicon wafer used as a mold for silicon rubber (polydimethylsiloxane). On our chip we combine a microfluidic channel system (cf. Fig. 5.2) with an optical cell analysis tool, the optical stretcher [1, 2]. The laser profile of two opposing optical fibers can be used to trap and analyze living cells. A new pumping system was developed allowing to stop the

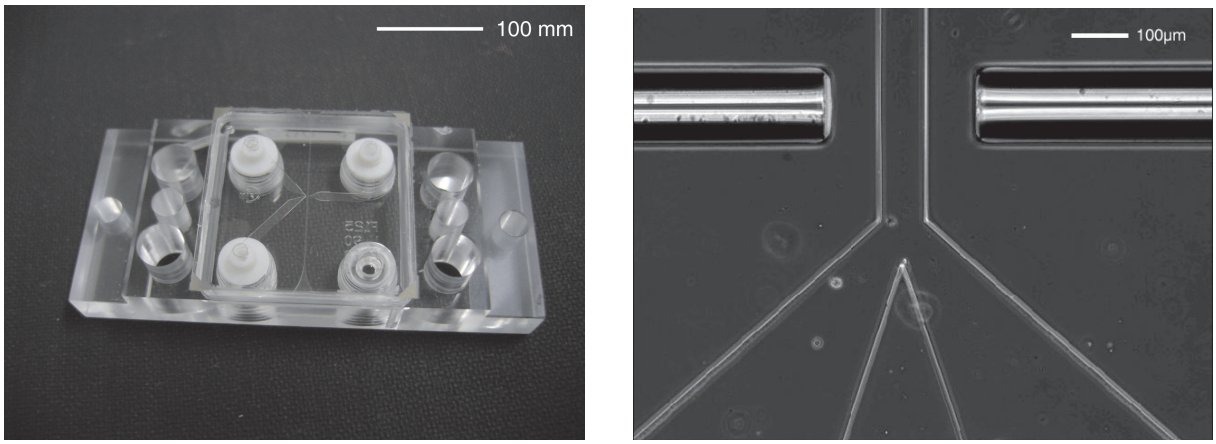

Figure 5.2: *Left*: Microfluidic Chip for the optical stretcher produced by GeSiM. *Right*: Close view of the optical fibers (*horizontal*) in the PDMS-layer of the chip and the integrated channel system for sorting cells. The flow of cells (visible as *small bright spheres*) is directed from top to bottom.

flow completely once a cell is delivered to the optical trap. The greatest benefit of the microfluidic chip will be the ability to sort the cells after analysis in order to isolate a subpopulation of cells for further analysis. For instance, stem cells identified by their characteristic deformability could be sorted out and used for further research or even therapeutic studies. In addition, it will be possible to do high resolution imaging of cells in suspension and to correlate the images with the deformability of the cells. This might help to reveal the origin of changes in cellular viscoelasticity.

[1] B. Lincoln et al.: Cytom. Part A **59**, 203 (2004)
[2] J. Guck et al.: Biophys. J. **81**, 767 (2001)

5.4 Biophotonic Non-Invasive Sorting of Mesenchymal Stem Cells

K. Müller, M. Zscharnack*, J. Galle†, J.A. Käs

*Biotechnological Biomedical Center, University of Leipzig
†Interdisciplinary Center for Bioinformatics, University of Leipzig

The aims the of MS-CartPro – Program are (i) the coordinated development of a production system for cartilage implants from adult mesenchymal stem cells (MSC) and (ii) the establishment of protocols for stem cell differentiation in a bioreactor. Our contribution within the biophysics project group focuses on characterizing MSC by their mechanical properties. These measurements should make it possible to isolate the cells with the highest chondrogenic potential.

The specific goal of this project is to establish the deformability of cells as a sensitive, non-invasive marker to characterize and sort mesenchymal stem cells. The deformability of cells will be measured by a new kind of laser trap – an Optical Stretcher – that

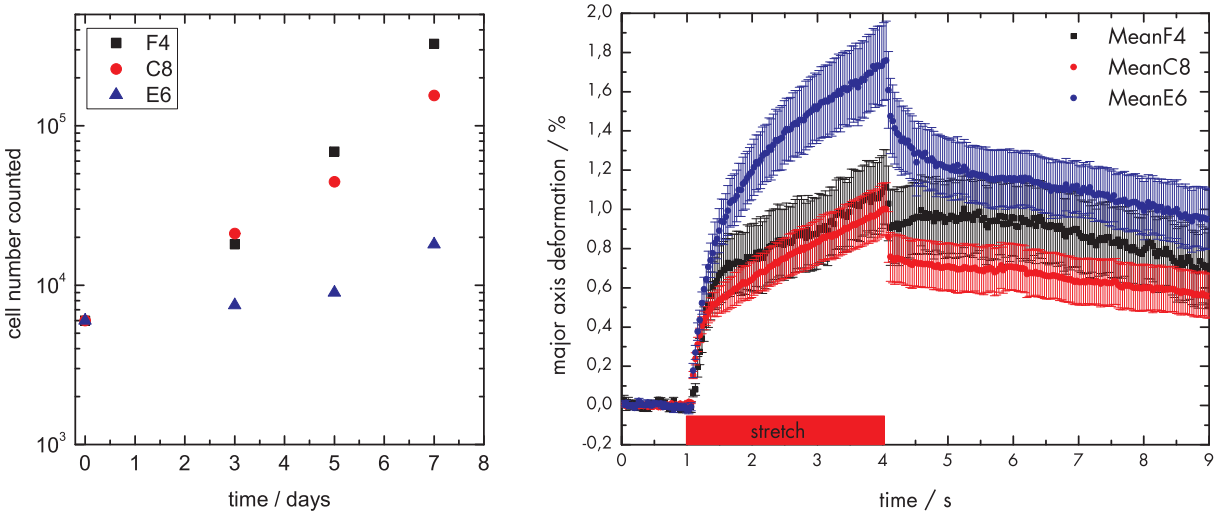

Figure 5.3: *Left*: Comparison of ovine MSC single cell clones. From an MSC population single cell clones were established and compared according to their cell growth rate. The cell clones exhibited different cell growth rates with C8 and F4 showing comparably fast growth rates while E6 is significantly slower. *Right*: The different proliferation rates are reflected in the mechanical properties of the cells measured by the optical stretcher. Again, clones C8 and F4 exhibited similar optical deformability which was significantly smaller than the one of E6.

catches and deforms single suspended cells individually [1, 2]. The correlation between cell deformability and the actual degree of differentiation should be verified. Preliminary data on cell growth and corresponding elasticity for various MSC is depicted in Fig. 5.3. Making use of an inherent habit of cells which is defined non-invasively offers the only opportunity to sort living cells without changing them allowing for subsequent application for the production of cartilage.

[1] M. Martin et al.: Proc. SPIE **6080**, 60 800P (2006), doi:10.1117/12.637899
[2] F. Wottawah et al.: Phys. Rev. Lett. **94**, 98 103 (2005)

5.5 Laser Directed Growth Cone Motility: A Study on How Optomolecular Mechanisms Influence Cytoskeletal Activity

A. Ehrlicher, T. Betz, M. Gögler, D. Koch, M. Knorr, U. Behn*, J.A. Käs

*Institute for Theoretical Physics, Theory of Condensed Matter Workgroup

Fundamental knowledge about neuronal growth and the ability to control it is invaluable in solving the enigma of nerve regeneration and the challenge of in vitro formation of neuronal circuits with defined architectures. The neuronal growth cone is a small dynamic structure at the tip of neuronal extensions that guides each neurite extension to its correct partner cell. To reach the designated target, the growth cone integrates chemical signals with high accuracy and reliability. This signal detection operates close

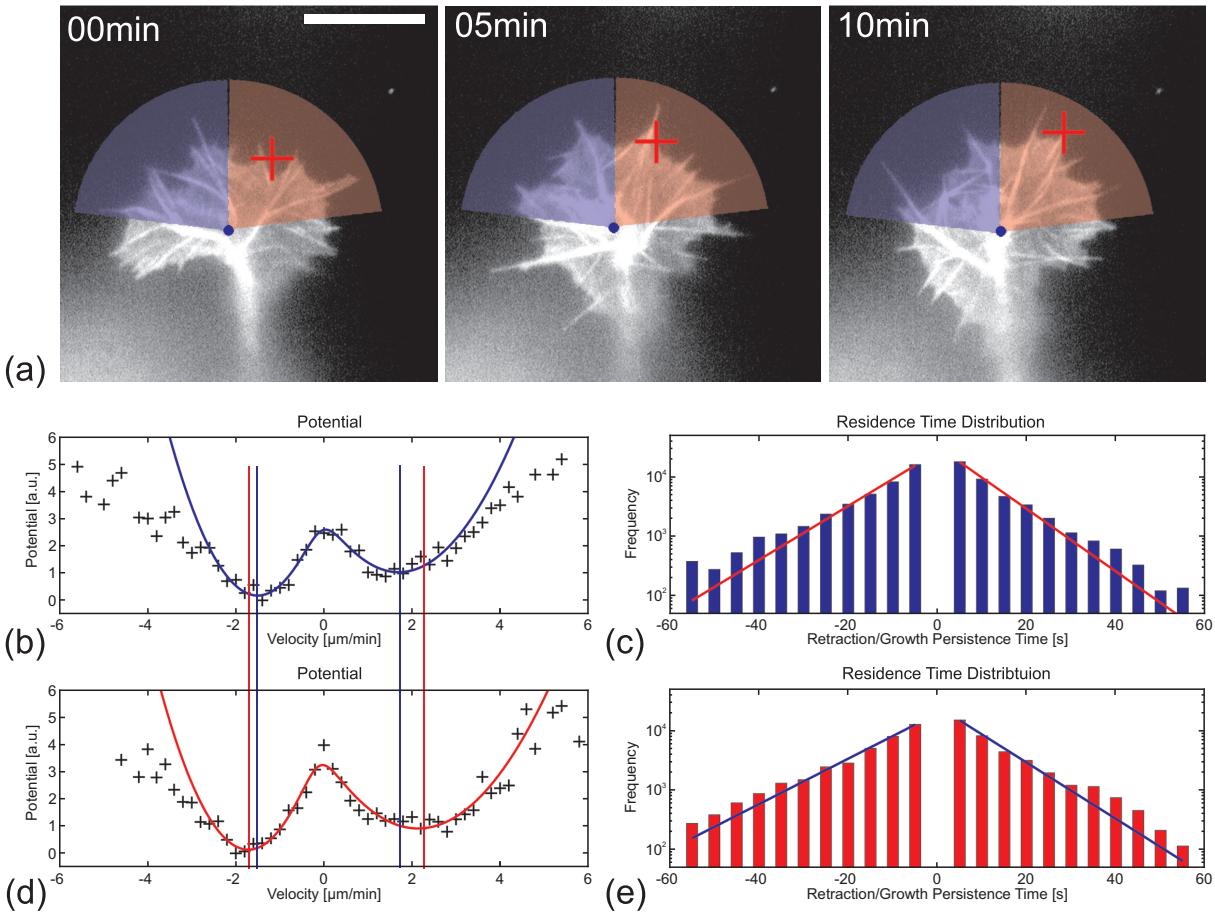

Figure 5.4: Growth statistics of a growth cone guided by a focused laser. The time series (**a**) gives the change of the growth cone, and the *red cross* defines the position of the laser spot. Images were recorded with a time lag of 5 s. (**b**) and (**c**) present the inferred potential and the residence time distribution for protusion and retraction states in the control direction and (**d**) and (**e**) in the direction of the laser. The *shaded red and blue lines* illustrate the changes in the potential dips in the different edge directions. Scale bar: 10 µm.

to the thermal noise limit and is, therefore of high interest not only to understand neuronal growth, but also to investigate the biological mechanisms of signaling and information processing under the influence of noise.

To further study neuronal growth, a focused laser positioned at the leading edge of the growth cone is used to bias growth direction and detailed measurements and analysis of the leading edge dynamics of laser treated and control growth cones is performed [1, 2]. Based on the edge motility measurements, we can consistently describe neuronal growth by a stochastic model that allows to extract a bistable potential of the stochastic process (cf. Fig. 5.4). The analysis quantifies the edge dynamics in growth cones manipulated by a laser in comparison to control growth cones. Growth cones that actively follow the laser show a tilt of the bistable potential in the direction of the laser favoring protrusions, but no significant changes in the leading edge growth velocity. This is in contrast to the potential changes observed in stationary growth cones that were influenced by the laser. Here, the laser does not tilt the potential shape, but increases the edge velocities, probably by an increase in actin polymerization ve-

locity [3, 4]. These measurements provide new quantitative insight into the dynamics underlying growth cone protrusion and movement. Based upon this knowledge, new strategies to shape neuronal networks and for optically controlled biomimetic machines will emerge.

[1] B. Stuhrmann et al.: Rev. Sci. Inst. **76**, 035 105 (2005)
[2] A. Ehrlicher et al.: Proc. Natl. Acad. Sci. USA **99**, 16 024 (2002)
[3] T. Betz et al.: Phys. Rev. Lett. **96**, 098 103 (2006)
[4] T. Betz et al.: New J. Phys. **9**, 11 426 (2007)

5.6 Light-Guiding Properties of Retinal Cells

K. Franze, S. Agte, J. Guck*, A. Reichenbach†, P. Wiedemann‡, J. Eilers§, J.A. Käs

*Department of Physics, University of Cambridge, UK
†Paul-Flechsig-Institute for Brain Research, University of Leipzig
‡University Hospital Leipzig
§Carl-Ludwig-Institute for Physiology, University of Leipzig

In contrast to the retina of many animals (such as the squids), the retina of vertebrates is "inverted". This means that the photoreceptor cells are turned away from light which enters the eye from environment. Thus, light must first pass all inner retinal layers before it can be absorbed by the outer segments of the photoreceptor cells. This should have consequences for both the quality of the optical image and the amount of photons that can be caught (it has been said that 'it is equivalent to placing a thin diffusing screen directly over the film in your camera'). The project is aimed at finding out whether the optical properties of retinal cells may be suitable to minimize this

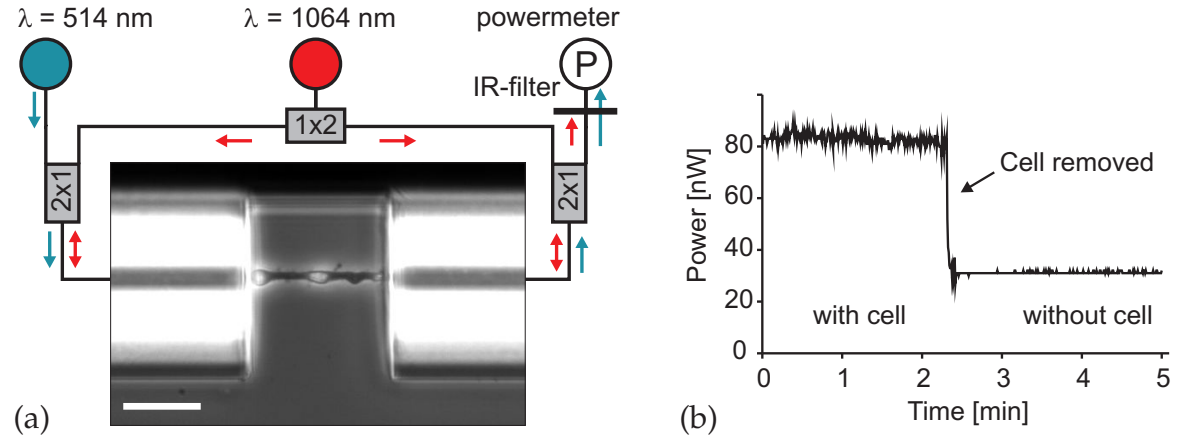

Figure 5.5: (**a**) The Müller cell (*central structure*) is trapped, aligned and stretched-out by two counterpropagating near-infrared laser beams (λ = 1064 nm) diverging from the optical fibers in contact with the cell. Visible light (λ = 514 nm) emerges from the left fiber and is collected and guided by the cell to the right output fiber. The recollected light is measured by a power meter. Scale bar length: 50 µm. (**b**) When the cell is removed from the trap, the measured power drops considerably.

problem. A significant part of the answer to this question might be already found. In one of our recent publications, we demonstrated that Müller cells from the vertebrate retina can guide light, acting as living optical fibers [1]. A key experiment for this finding, utilizing a modified two-beam optical trap, is illustrated in Fig. 5.5.

[1] K. Franze et al.: Proc. Natl. Acad. Sci. USA **104**, 8287 (2007)

5.7 Protrusion Force Generation of Motile Cells

C. Brunner, A. Ehrlicher, M. Gögler, D. Koch, T. Fuhs, J.A. Käs

Cell motilitiy is a fundamental process associated with many phenomena in nature, such as immune response, wound healing, and metastasis. On the molecular level, actin polymerization and molecular motors, such as myosin, are involved in cell motility. However, the mechanism as a whole is not very well understood. Rapidly migrating cells, such as keratocytes, move forward via active protrusion at the leading edge, and additionally by retraction/deadhesion of the cell's rear, indicating two force generating centers.

Our scanning-force microscopy (SFM) based technique uses the vertical and lateral deflection of a modified cantilever and allows direct measurements of the forces exerted by the cell. A polystyrene bead (blue) glued to a cantilever-tip of an SFM is positioned on the substrate in front of a migrating cell as illustrated in Fig. 5.6 [1]. The cell moves towards the bead, crawls under it, and pushes the cantilever upwards. Alternatively the cell pushes against the bead perpendicular to the cantilever's long axis which leads to a twist of the cantilever and is detected as lateral deflection. Direct measurements of the forward forces generated at the leading edge of the lamellipodium, the cell body and retrograde forces within the lamellipodium are possible, cf. Fig. 5.6 [2]. Application of different drugs, such as jasplakinolide, cytochalasin D, and ML-7 allows for selective manipulation of molecular components. Comparison of the measured forces and velocity changes leads to new insights concerning the importance of different force generating processes and reveals actin polymerization as the dominant force

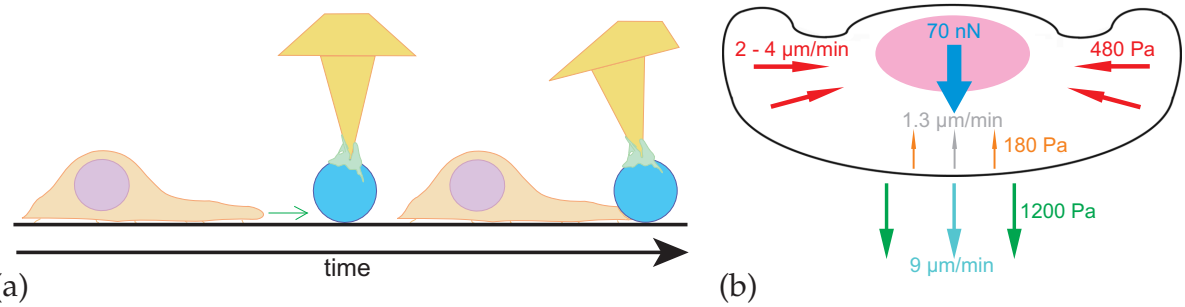

Figure 5.6: Cellular forces probed by a SFM. Schematic view of the detection (**a**), measured forces in fish keratocytes (**b**). In the sketch the nucleus is drawn in *pink*. Arrows in *red*: retrograde pressure and flow velocity in flanks; *orange*: retrograde pressure in center lamellipodium; *turquoise*: forward speed of lamellipodium; *grey*: retrograde flow velocity; *green*: protrusion pressure of the lamellipodium; *blue*: whole cell stall force.

generating process at the leading edge. On the other hand, from these results myosin can not be concluded to be responsible for the retrograde flow in the central lamellipodium. Our future research will focus particularly on the further characterization of malignant cells' increase in motility during metastasis and on the role of cell biomechanics during tumor growth.

[1] S. Park et al.: Biophys. J. **89**, 4330 (2005)
[2] C. Brunner et al.: Eur. Biophys. J. **35**, 713 (2006)

5.8 Single Particle and Polymer Tracking in Two-Dimensional Energy Landscapes

P. Rauch, L. Woiterski, F. Rückerl, C. Selle, J.A. Käs

Membranes of biological cells exemplify a complex film for diffusive transport of proteins and lipids (i.e. nano-sized objects) and can teach us how to control diffusive 2D transport from the nano- to micro-scale. In inhomogeneous lipid membranes a wide variety of interactions from simple steric repulsion to complex viscous or electrostatic interactions can locally influence the motion of a probe particle. Here, we focus on the impact of the interplay between steric repulsion of rigid domains and attractive dipole–dipole/charge interactions on local diffusion. Our previous results indicate that changes in the domain structure in Langmuir monoplayers, supported bilayers, and giant vesicles can switch between one- and two-dimensional diffusion as well as Brownian and subdiffusion [1, 2]. First, we will track the motions of point-like probes (latex spheres, quantum dots, quantum dots coupled to lipids) in changing energy landscapes modulated by domain-size and shape (cf. Fig. 5.7). We will not only learn how to switch in a controlled fashion between one- and two dimensional as well as Brownian and

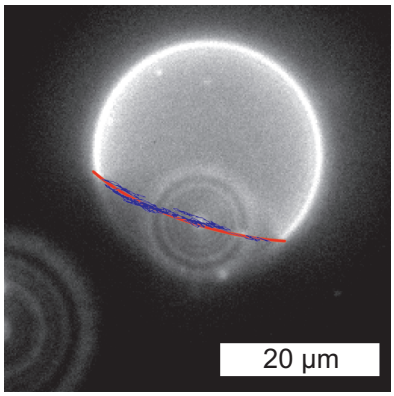

Figure 5.7: A fluorescence microscopic picture of a giant unilamellar vesicle (GUV) with an adsorbed point diffuser. The GUV is prepared from a lipid mixture, exhibiting phase separation. The liquid-disordered phase is recognized by its brighter appearance due to the partition of a suitable fluorescence label molecule in contrast to the darker liquid-ordered phase. A polymer nanoparticle on the vesicle surface typically diffuses at the phase boundary which is marked by a red line. Strongly associated to the latter, the blue trajectory of the nanoparticle is observed.

subdiffusive transport, but we will also catalogue the complex energy landscapes in these complex films. Secondly, we analyzed the diffusive behavior of polymers in such an energy landscape. Polymers as connected chain of point diffusors (DNA, actin filaments) have internal degrees of freedom. Their behavior can be better understood knowing first what a single point diffusor does. For many biological processes nature prefers two-dimensional diffusive over directed molecular motor-based transport. Understanding how diffusion in membranes can be modulated will help to comprehend why evolution has frequently chosen this route.

[1] C. Selle et al.: Phys. Chem. Chem. Phys. **6**, 5535 (2004)
[2] M. B. Forstner et al.: Langmuir **19**, 4876 (2003)

5.9 Interaction of Coated Nanoparticles with Amyloid Peptides

T. Siegemund, W. Härtig*, H. Schmiedel,

*Paul-Flechsig-Institute for Brain Research, University of Leipzig

The aim of this project is an exact analysis of the enzymatic degradation of nanoparticles by means of small-angle neutron scattering (SANS) [1, 2]. Enzymatic degradation of nanoparticles covered by the pharmaceutical agent thioflavin T should be investigated by SANS carried out at reactors located at Dubna (Russia), Berlin and Budapest (Hungary). Specifically, a 15 nm thick shell from polybutylcyanoacrylate (PBCA) is degraded by esterase (within the model porcine liver esterase) which leads to release of thioflavin T to the particle's environment. Core deutaration of the particle should provide sufficient contrast between particle core and shell allowing to study structural and kinetic details of the degradation. This analytical assay is considered a methodological novelty and very promising. Another project goal is the development of a new evaluation program for SANS data. Evaluation of SANS scattering curves requires a clear discrimination of (i) effects due to the polydispersity of the particle radius and (ii) effects resulting from the inhomogeneus scattering length profile along the particle radius. This problem should be managed by a software written in DELPHI accounting for the special case of an isotropic scattering length density profile when Gaussian distributed polydispersity occurs. Special attention is paid to user-friendliness in order to enable an application by other users.

[1] B.-R. Paulke et al.: Acta Polym. **43**, 288 (1992)
[2] H. Schmiedel et al.: J. Phys. Chem. B **105**, 111 (2001)

5.10 Funding

MS CartPro – Multiparametric Monitoring and Steering of Mesenchymal Stem Cell derived Cartilage Formation in 3D Production Systems, Projektbereich 2
Prof. Dr. J.A. Käs, Dr. J. Guck
BMBF-Project MS CartPro (FKZ: PTJ–BIO/31P4282)

Untersuchungen der altersabhängigen Modulation der Elastizität von Hautzellen durch physiologische Stressoren
Prof. Dr. J.A. Käs, F. Wetzel
Beierdorf AG – Forschungsvertrag

Leipziger Schule der Naturwissenschaften – Bauen mit Molekülen und Nano- Objekten (BuildMoNa)
Prof. Dr. E. Hey-Hawkins, Prof. Dr. M. Grundmann, Prof. Dr. J.A. Käs
BuildMoNa - Graduiertenschule

Single Particle and Polymer Tracking in Two-Dimensional Energy-Landscapes
Prof. Dr. J. Kärger, Prof. Dr. F. Cichos, Prof. Dr. J.A. Käs
DFG-Forschergruppe

Optical Stretcher zur hochaufgelösten Darstellung und Analyse von einzelnen Zellen
Prof. Dr. J.A. Käs
Carl-Zeiss MicroImaging GmbH – OSDA - Forschungsvertrag

Molecular structure and function of biopolymer networks, characterized by novel laser trapping tools, nanorheology and single polymer microscopy
Prof. Dr. J.A. Käs
Alexander von Humboldt Foundation

Laser Directed Growth Cone Motility: A Study on How Optomolecular Mechanisms Influence Cytoskeletal Activity
Prof. Dr. J.A. Käs
DFG-Project KA 1116/3-1 and 3-2

Untersuchung der Diffusion von Nanosonden in inhomogenen Monoschichten als Modell für diffusiven Transport in Lipidmembranen
Prof. Dr. J.A. Käs, Dr. C. Selle
DFG-Project KA 1116/4-1 and 4-2

DFG Graduiertenkolleg "InterNeuro"
Prof. Dr. J.A. Käs, Dr. J. Guck
GRK 1097

EU-Project "Active Biomimetic Systems" (Active BIOMICS)
Prof. Dr. J.A. Käs, Dr. J. Guck
Projektnr.: 2312 0 385

Sächsische AufbauBank (SAB)-Forschungsvorhaben "Identifikation und Isolierung von biologischen Zellen mittels Laser-Stretching in opto-fluidischen Mikrosystemen"
Prof. Dr. J.A. Käs, Dr. J. Guck
SAB-Projekt, Projektnr.: 9889/1519

Donation to the Softmatter Physics Division from Ms. H. Reifert
Prof. Dr. J.A. Käs

Donation to the Softmatter Physics Division from Ms. M. Duda
Prof. Dr. J.A. Käs

5.11 Organizational Duties

J.A. Käs

- Advisory committee for soft matter physics, NASA, USA
- Chair, scientific advisory board, Evacyte Inc., USA
- CNRS review committee, Institute Curie, Paris, France
- Referee: Nature, Phys. Rev. Lett., Phys. Rev. E, Biophys. J., Biophys. Biochem. Acta, Biochemistry, Proc. Natl. Acad. Sci. USA, Eur. Biophys. J., Langmuir
- Reviewer: National Science Foundation – Div. of Materials Research, Div. of Cellular Organization, Div. of Computational Biology, Div. of Physics, Special Programs; Deutsche Forschungsgemeinschaft, Alexander von Humboldt Foundation, Deutsche Studienstiftung, Centre National de Reserche

5.12 External Cooperations

Academic

- MD Anderson Cancer Center, Houston, USA
  Prof. Dr. Michel Follen
- Center for Nonlinear Dynamics, Austin, USA
  Prof. Dr. Harry Swinney
- University of Texas at Austin, USA
  Prof. Dr. Ken Shih, Prof. Dr. Mark Raizen, Prof. Dr. Tess Moon
- Institute Curie, Paris, France
  Prof. Dr. Jean-Francois Joanny
- ESPCI, Paris, France
  Prof. Dr. Jacques Prost
- CEA/Saclay, France
  Prof. Dr. Marie-France Carlier
- Princeton University, USA
  Prof. Dr. Robert Austin
- University of Saarbrücken, Germany
  Prof. Dr. Walter Zimmermann
- Max-Planck-Institute for Colloids and Interfaces, Potsdam-Golm, Germany
  Prof. Dr. Reinhardt Lipowsky
- Max-Planck-Institute for Complex Systems, Dresden, Germany
  Prof. Dr. Frank Jülicher

Industry

- Carl Zeiss MicroImaging GmbH, Jena, Germany
  Dr. C. Dietrich

- Beiersdorf AG, Hamburg, Germany
  Dr. T. Blatt
- EuroPhoton GmbH, Berlin, Germany
- Euroderm GmbH, Leipzig, Germany
  Dr. A. Emmendörffer
- Evacyte Inc., Austin, Texas, USA
- Evotec GmbH, Dresden, Germany
  Dr. T. Bauer
- FAUN GmbH, Leipzig, Germany
  F. Fischer
- GeSim GmbH, Dresden, Germany
  Dr. S. Howitz
- JPK Instruments, Berlin, Germany
  T. Jähnke
- LPI GmbH, Berlin, Germany
  Dr. S.P. Heyn
- Niendorf & Hamper, Hamburg, Germany
  Prof. A. Niendorf
- Nimbus GmbH, Leipzig, Germany
- Qiagen GmbH, Hilden, Germany
  Dr. T. Singer

5.13 Publications

Journals

T. Betz, D. Koch, B. Stuhrmann, A. Ehrlicher, J.A. Käs: *Statistical analysis of neuronal growth: edge dynamics and the effect of a focused laser on growth cone motility*, New J. Phys. **9**, 426 (2007), doi:10.1088/1367-2630/9/11/426

S. Ebert, K. Travis, B. Lincoln, J. Guck: *Fluorescence ratio thermometry in a microfluidic dual-beam laser trap*, Opt. Express **15**, 15493 (2007), doi:10.1364/OE.15.015493

K. Franze, J. Grosche, S.N. Skatchkov, S. Schinkinger, C. Foja, D. Schild, O. Uckermann, K. Travis, A. Reichenbach, J. Guck: *Müller cells are living optical fibers in the vertebrate retina*, Proc. Natl. Acad. Sci. USA **104**, 8287 (2007), doi:10.1073/pnas.0611180104

J. Fuhrmann, J.A. Käs, A. Stevens: *Initiation of cytoskeletal asymmetry for cell polarization and movement*, J. Theor. Biol. **249**, 278 (2007), doi:10.1016/j.jtbi.2007.08.013

M. Gögler, T. Betz, J.A. Käs: *Simultaneous manipulation and detection of living cell membrane dynamics*, Opt. Lett. **32**, 1893 (2007), doi:10.1364/OL.32.001893

B. Lincoln, S. Schinkinger, K. Travis, F. Wottawah, S. Ebert, F. Sauer, J. Guck: *Reconfigurable microfluidic integration of a dual-beam laser trap with biomedical applications*, Biomed. Microdevices **9**, 703 (2007), doi:10.1007/s10544-007-9079-x

D. Smith, F. Ziebert, D. Humphrey, C. Duggan, M. Steinbeck, W. Zimmerman, J.A. Käs: *Molecular motor-induced instabilities and crosslinkers determine biopolymer organization*, Biophys. J. **93**, 4445 (2007), doi:10.1529/biophysj.106.095919

Books

A. Ehrlicher, T. Betz, B. Stuhrmann, M. Gögler, D. Koch, K. Franze, Y. Lu, J.A. Käs: *Optical Neuronal Guidance*, in *Cell Mechanics*, Methods in Cell Biology Vol. 83, ed. by Y.-L. Wang, D. Discher (Academic Press, San Diego 2007), p 495, doi:10.1016/S0091-679X(07)83021-4

B. Lincoln, F. Wottawah, S. Schinkinger, S. Ebert, J. Guck: *High-throughput rheological measurements with an optical stretcher*, in *Cell Mechanics*, Methods in Cell Biology Vol. 83, ed. by Y.-L. Wang, D. Discher (Academic Press, San Diego 2007), p 397, doi:10.1016/S0091-679X(07)83017-2

Talks

J.A. Käs: *Can Polymer Physics Help Cellular Biomedicine*, 71st DPG Spring Meeting, Regensburg, 26. – 30. March 2007

J.A. Käs: *Can Polymer Physics Help Cellular Biomedicine*, Conf. "Trends in Optical Micromanipulation", Obergurgl, Austria, 05. – 09. February 2007 (invited)

J.A. Käs: *Chair Symposium S4: Cellular Mechanics*, Conf. "German Society for Cell Biology", University of Frankfurt a.M., 15. – 17. March 2007 (invited)

J.A. Käs: *Feeling for Cells with Light*, 8th Int. Topical Meeting and Workshop "Optics and Laser Applications in Medicine and Environmental Monitoring for Sustainable Development", Cape Coast, Ghana, 19. – 24. November 2007 (invited)

J.A. Käs: *Feeling for Cells with Light*, Sächsischer Biotechnologietag 2007, BIOTEC Dresden und BBZ Leipzig, Dresden, 28. November 2007 (invited)

J.A. Käs: *Optical deformability as a new cell marker*, Eur. Conf. Biomedical Optics, Munich, 19. – 21. June 2007 (invited)

J.A. Käs: *Optical deformability as a new cell marker*, Lecture on Biophysics at Technical University Chemnitz, 29. January 2007 (invited)

J.A. Käs: Organizer, PWM Winter School, Spindler-Mühle, Czech-Republic, 17. – 24. February 2007

J.A. Käs: *Probing individual elements of actin scaffolds by optical tweezers*, EU-STREP workshop "Bio Systems", Potsdam-Golm, 10./11. September 2007 (invited)

Patents

J.A. Käs, M. Raizen, V. Milner, T. Betz, A. Ehrlicher: *Optical Cell Guidance*, Preliminary U.S. Patent # 05670.P005, the European and Asian patents are pending.

5.14 Graduations

Doctorate

- Timo Betz
  Actin Dynamics and Forces of Neuronal Growth
  January 2007
- Allen Ehrlicher
  A Physical Perspective on Movement and Force Production in Animal Cells
  October 2007
- Kristian Franze
  Mechanical and Optical Properties of Nervous Tissue and Cells
  October 2007

Diploma

- Marc Großerüschkamp
  Biomechanical Cell Markers and their Role in the Isolation of Metastatic Cancer Cells from Blood
  December 2007
- Florian Huber
  Biomimetic Active Polymer Network Films
  December 2007
- Moritz Kreysing
  Optically induced rotation of dielectric particles in a dual beam laser trap
  October 2007
- Philipp Rauch
  A novel Physical Method for Monitoring of Giant Unilamellar Vesicle Phase Behaviour Under Rapid Medium Variation
  May 2007
- Maximilian Semmling
  Uptake Mechanisms of Microsized Polyelelctrolyte Capsules by Biological Cells
  December 2007
- Cornel Wolf
  Measurement of Nonlinear Dynamics in Single Cells
  Oktober 2007

Master

- Thomas Fuhs
  Investigating the Phase Space of Cell Motility using RNA Interference
  December 2007
- David Smith
  Molecular Motor-Induced Instabilities and Crosslinkers Determine Biopolymer Organization
  December 2007

5.15 Awards

- Prof. Dr. Josef A. Käs
  Wolfgang-Paul Prize awarded by the Alexander von Humboldt Foundation
- Prof. Dr. Josef A. Käs
  Distinguished Lecturer, SigmaXi Academic Honor Society, USA
- Prof. Dr. Josef A. Käs
  Adjunct Professor, Department of Biomedical Engineering, University of Texas at Austin, USA
- Kristian Franze
  Doktorandenpreis der Research Academy Leipzig (RAL)
- Franziska Lautenschläger
  Scientific Award 2007, BMW Group

II

Institute for Experimental Physics II

6

Magnetic Resonance of Complex Quantum Solids

6.1 Introduction

The electronic properties of quantum-solids in which the electrons exhibit strong correlations with each other or with the lattice are particularly rich and will be of special importance in future functional materials. In addition, such solids are challenging for experiment, as well as theory, as the twenty-year history of high-temperature superconductivity shows: we still do not understand the electronic structure of these systems. One particular aspect of strongly correlated electronic materials is their tendency towards nano-scale electronic phase separation. Even in perfect lattices, electronic nanostructures can form. The investigation of such materials requires the use of methods that can give detailed information. Here, magnetic resonance, on nuclei and electrons, is of particular interest as they not only have atomic scale resolution, but also yield bulk information in contrast to surface techniques. As one might expect, the material properties can be quite different from the bulk near the surface.

Jürgen Haase

6.2 NMR-Studies of High-Temperature Superconductivity – Evidence for a Two-Component Model

J. Haase, C.P. Slichter*, G.V.M. Williams†

*Department of Physics, University of Illinois at Urbana-Champaign, USA
†The MacDiarmid Institute and Industrial Research Limited, Wellington, New Zealand

A main subject of the group is the investigation of the electronic properties of high-temperature superconductors with Nuclear Magnetic Resonance (NMR). After more than 20 years, neither their superconducting, nor their normal state properties are understood and NMR is a key player in this area since it delivers bulk information with atomic scale resolution. We can observe NMR of the various nuclei in the unit cell and

thus get detailed information that can be used to test theories proposed for these materials. Since most nuclei in these high-temperature superconductors possess quadrupolar moments, we can investigate electronic charge and spin degrees of freedom. Recent progress in the group consists in proving that some materials cannot be described with the assumption of a simple electronic fluid, rather at least two fluids must be at work and cause intricate changes of the NMR parameters. Our results could be presented at the 50 years celebration for the famous Bardeen-Cooper-Schrieffer theory of superconductivity, one of the greatest theories of the last century. While this theory clearly plays an important role in understanding high-temperature superconductors, it is not clear yet whether it will suffice in explaining the new materials with minor additional changes. Our investigations are now extended to other classes of materials, hole as well as electron doped systems. These measurements comprise especially careful studies of NMR quadrupole splittings, magnetic shifts, intensities as a function of temperature in different materials. New results also show the uniqueness of NMR intensity loss also for electron doped materials at low doping levels, pointing to a quantum critical behavior close to the superconducting transition. In this work we mainly cooperate with groups in the USA, Australia, and New Zealand.

6.3 Vanadium(IV) Complexes on Solid Surfaces and in Frozen Solutions as Studied by Pulsed EPR Spectroscopy

G. Vijayasarthi, A. Pöppl

Immobilization of transition metal ions (TMI) and their complexes have been studied in catalytic research for many years because of their outstanding potential for catalyzing various industrially important reactions. There are several procedures available for the immobilization process such as impregnation, framework substitution, ion exchange, and defined chemical grafting by methods of surface organo-metallic chemistry (SOMC). In particular SOMC techniques are supposed to provide well dispersed species with uniform structure. However, SOMC involves various challenges such as the verification of a successful grafting and the elucidation of the structure of the grafted complexes as the necessary precondition to understand the catalytic mechanism.

The objective of this work is the spectroscopic characterization of chemically grafted paramagnetic V(IV) complexes, VO(II)$(acac)_2$, VO(II)(pc), and V(IV)$[NMe_2]_4$, by pulsed electron paramagnetic (EPR) spectroscopy in combination with quantum chemical calculations using density functional theory (DFT). Silica, alumina, and aluminium fluorides have been employed as solid supports. The major spectroscopic information used were ^{1}H, ^{14}N, and ^{27}Al ligand hyperfine couplings (hfc) with magnetic nuclei in the organic ligands and in the solid supports, which were measured by pulsed electron nuclear double resonance (ENDOR) and hyperfine sublevel correlation spectroscopy (HYSCORE). These magnetic interactions provided direct access to the specific grafting site and geometry of the TMI complexes. For the analysis of the ligand hfc's DFT computations were employed with the aim to interpret experimentally obtained data in terms of model structures of the grafted complexes.

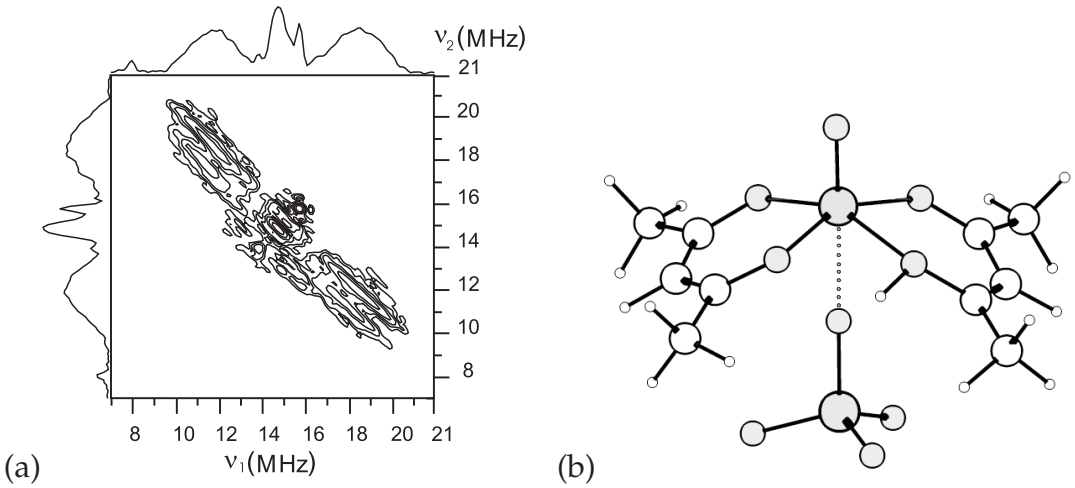

Figure 6.1: VO(II)$(acac)_2$ grafted over aluminum fluoride: (**a**) HYSCORE spectrum at 6 K showing ^{1}H and ^{19}F ligand hfc's and (**b**) optimized geometry of a corresponding VO(II)$(acac)_2$/AlF model complex.

The experiments on grafted vanadyl and non-vanadyl V(IV) moieties confirmed the structural integrity of the grafted TMI complexes. But the specific grafting process was found to be different for the two types of vanadium complexes. Whereas non-vanadyl complexes are chemically grafted by a typical ligand exchange reaction with a terminal proton of an active surface site, the vandyl complexes are coordinating to the surface via an open binding site at the metal ion (Fig. 6.1). Furthermore the geometrical structure of the surface complexes was successfully explored on the basis of the ligand hfc's.

Indeed, supplementary studies of $V[NMe_2]_4$ and $VO(acac)_2$ in frozen solution verified that the structure of the TMI complexes can be determined with sufficient accuracy by a comparison of experimental ^{1}H and ^{14}N ligand hfc parameters deduced from pulsed ENDOR and HYSCORE experiments with quantum chemically computed hfc data from model complexes [1]. In the DFT calculations of the ^{1}H and ^{14}N hfc's, it is essential to employ unrestricted methods as the spin polarization effects are a major source for the observed ligand hfc, whereas the omission of spin orbit coupling effects was not crucial for such light ligand atoms. The DFT calculations provided even reliable hfc parameters of the ligand nuclei within the limit of the experimental accuracy if no symmetry restrictions were imposed in the computations. This is especially noteworthy as surface TMI complexes exhibit low symmetries in general.

[1] V. Nagarajan et al.: Res. Chem. Intermed. **33**, 705 (2007)

6.4 Solid-State NMR Characterization of the Photodimerization of Cinnamic Acid and its Derivatives

I. Fonseca, M. Bertmer

Trans-cinnamic acid and its derivatives exhibit polymorphism and are known to photodimerize under UV irradiation. Their highly stereospecific reaction in the solid state

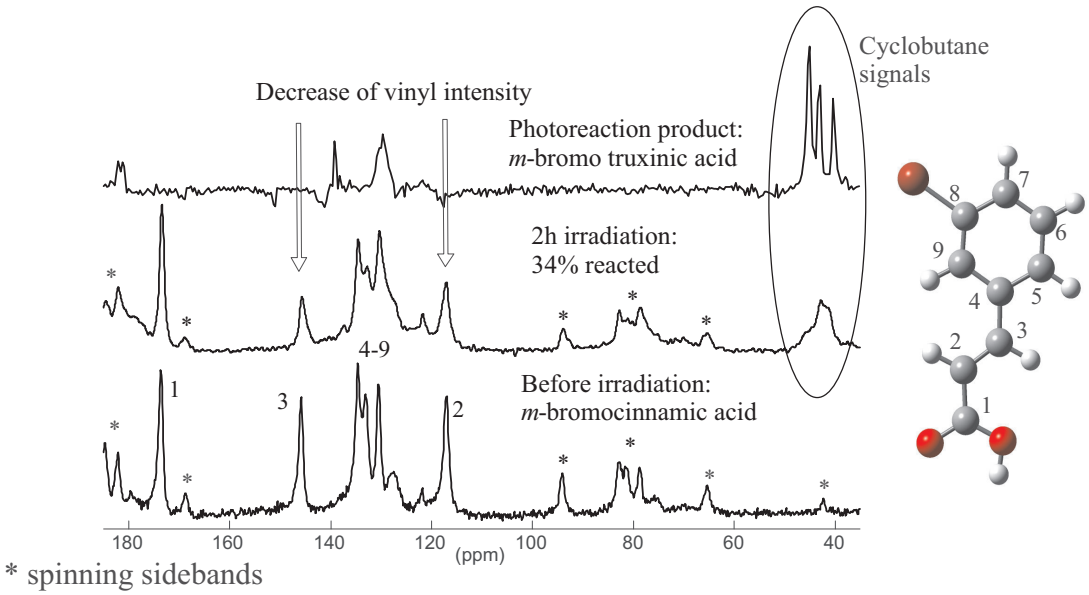

Figure 6.2: ^{13}C CPMAS spectra of *m*-bromocinnamic acid at different stages of photoreaction.

can also be used synthetically. Furthermore, this type of compounds or this type of reaction may also have potential applications in data storage systems. The photodimerization reaction has been studied by means of solid-state NMR, where the reaction kinetics can be monitored via ^{13}C CPMAS spectroscopy, since the olefinic signals of the reactant and the cyclobutane ring signals of the photoproduct have distinct chemical shifts (see the example given in Fig. 6.2). The relative intensities of the signals from those carbons that take place in reaction are plotted against the irradiation time to obtain the photoreaction kinetics curve. This can then be fitted to a Johnson–Mehl–Avrami–Kolmogorov nucleation and growth model. By comparing different derivatives of cinnamic acid – varying substituents on the aromatic ring and at different positions – information can be obtained to which factors influence the reaction kinetics. Further investigations include the study of the chemical shift anisotropy (CSA) tensors and their changes during the reaction. With this we want to obtain a better understanding of these solid-state reactions.

6.5 Structural and Optical Properties of Chromium-Doped Hexagonal Barium Titanate Ceramics

H.T. Langhammer*, R. Böttcher

*Physikalisches Institut, Martin-Luther-Universität Halle-Wittenberg

The influence of chromium on the crystallographic phase and the microstructure of $BaTiO_3$ ceramics was investigated by systematic studies of X-ray diffraction (XRD), electron paramagnetic resonance (EPR) and optical spectroscopy. At Cr concentrations of about 0.1 mol % a hexagonal phase appears (room temperature). For nominal concentrations > 0.1 mol % the material is 100 % hexagonal and its microstructure exhibits

exaggerated, plate-like grains with a mean grain size > 100 μm (sintering temperature 1400 °C). In the hexagonal phase the EPR-active Cr_{Ti}^{3+} ions substitute both for Ti(1) (corner-sharing octahedron) and Ti(2) (face-sharing octahedron) sites. In air-sintered ceramics chromium is incorporated with valence states 3+ and 4+, whereas for reduced samples the valence state 3+ predominates. Optical transmission both of air-sintered and reduced samples doped with nominally 5.0 mol % Cr was measured in the visible light region. The absorption spectra exhibit distinct absorption bands. Their assignment to chromium defects with different valence states is discussed. The Jahn–Teller distortion caused by the electron configuration d^2 (Cr_{Ti}^{4+}) is proposed as the driving force for the high-temperature phase transition cubic → hexagonal.

6.6 Funding

Controlling Mesoscopic Phase Separation
J. Haase
EU-FP6,CoMePhS, NMP4-CT-2005-517039

Advanced Signal-Processing for Ultra-Fast Magnetic Resonance Spectroscopic Imaging, and Training
J. Haase
EU-CORDIS-FP6, MRTN-CT-2006-035801

EuroMagNET, JRA NMR
J. Haase
EU, RII3CT-2004-506239

Magnetic Ground State and Dynamics in High-Temperature Superconductors
J. Haase, O.P. Sushkov, B. Keimer
EU, DP0881336

Quasi One-Dimensional Ferroelectrica
R. Böttcher, E. Hartmann
DFG BO 1080/8-2 within DFG Forschergruppe FOR 522

Identification of the paramagnetic centers in nano- and micrometer-sized SiC perspectives for photonic and biotechnology application by pulsed EPR spectroscopy
A. Pöppl
DFG PO 426/6-1

Characterization of the [2+2] Photodimerization of cinnamic acid and its derivatives with solid-state NMR
M. Bertmer
DFG BE 2434/2-1

Fabrication and physical properties of ferroelectrics confined in nanoporous materials
D. Michel, E.V. Charnaya
DFG Mi 390/25-1

6.7 Organizational Duties

M. Bertmer
- Referee: Angew. Chemie, Chem. Mater., Solid State Nucl. Magn. Res.

R.-M. Böttcher
- Referee: Phys. Rev., J. Phys. Cond. Matter, Langmuir, J. Magn. Res.

J. Haase
- Direktor des Zentrums für magnetische Resonanz, Universität Leipzig
- Referee: Phys. Rev.

A. Pöppl
- Referee: J. Magn. Res., J. Am. Chem. Soc., Phys. Chem. Chem. Phys., Chem. Phys. Lett.
- Project Reviewer: German-Israel-Foundation for Scientific Research and Development (GIF)

6.8 External Cooperations

Academic

- Laboratoire National des Champs Magnétiques Pulsés, Toulouse, France
  Prof. Dr. G. Rikken
- Department of Physics, University of Illinois at Urbana-Champaign, USA
  Prof. Dr. C.P. Slichter
- School of Physics, University of New South Wales, Sydney, Australia
  Prof. Dr. O.P. Sushkov
- Department of Electrical and Computer Engineering, University of Illinois at Urbana-Champaign, USA
  Prof. Dr. A.G. Webb
- The MacDiarmid Institute and Industrial Research Limited, Wellington, New Zealand
  Dr. G.V.M. Williams
- Dresden High Magnetic Field Laboratory, Forschungszentrum Dresden-Rossendorf, Germany
  Prof. Dr. J. Wosnitza
- Department of Chemistry, Washington University, St. Louis, USA
  Sophia E. Hayes
- Abteiltung Chemie, Universität Koblenz-Landau, Koblenz, Germany
  G.E. Schaumann
- Physikalisches Institut, Martin-Luther-Universität Halle–Wittenberg, Germany
  Dr. H.T. Langhammer
- Faculty of Physics, University of Vilnius, Lithuania
  Prof. Dr. J. Banys

- Advanced Materials Science, Institut für Physik, Universität Augsburg, Germany
  Prof. Dr. M. Hartmann
- Anorganisch-chemisches Institut, Technische Universität München, Germany
  Prof. Dr. K. Köhler
- Institute of Semiconductor Physics, National Academy of Sciences of Ukraine (NASU), Kiev, Ukraine
  Prof. Dr. E.N. Kalabukhovaa
- Laboratoire de Physique de l'Etat Condenseé, Faculté des Sciences, Université du Maine, Le Mans, France
  Prof. Dr. A. Kassiba

Industry

- NMR-Service, Erfurt, Germany
  M. Braun
- Bruker BioSpin, Rheinstetten, Germany
  F. Engelke

6.9 Publications

Journals

J. Banys, M. Kinka, G. Völkel, W. Böhlmann, V. Umamaheswari, M. Hartmann, A. Pöppl: *Dielectric Spectroscopy of Nano $BaTiO_3$ Betaine Phosphite Confined in MCM-41 Mesoporous Molecular Sieve Materials*, Ferroelectrics **353**, 97 (2007)

A.E. Berns, M. Bertmer, A. Schäffer, R.J. Meier, H. Vereecken, H. Lewandowski: *The ^{15}N-CPMAS spectra of simazine and its metabolites: measurements and quantum chemical calculations*, Eur. J. Soil Sci. **58**, 882 (2007)

M. Bertmer, M. Wang, M. Krüger, B. Blümich, V. Litvinov, M. van Es: *Structural Changes from the Pure Components to Nylon 6 - Montmorillonite Nanocomposites observed by Solid-State NMR*, Chem. Mater. **19**, 1089 (2007)

V. Degirmenci, Ö.F. Erdem, A. Yilmaz, D. Michel, D. Uner: *Sulfated zirconia in SBA-15 structures with strong Brønsted acidity as observed by ^1H MAS NMR spectroscopy*, Catal. Lett. **115**, 79 (2007)

R.-A. Eichel, R. Böttcher: *Chararcterization of the high-spin Mn^{2+}-functional centre in $BaTiO_3$ by means of right-angle wiggling electron paramagnetic resonance spectroscopy*, Mol. Phys. **105**, 2195 (2007)

U. Gerstmann, E. Rauls, S. Greulich-Weber, E.N. Kalabukhova, D.V. Savchenko, A. Pöppl, F. Mauri: *Nitrogen Donor Aggregation in 4H-SiC: g-Tensor Calculations*, Mater. Sci. Forum **556-557**, 391 (2007)

E.N. Kalabukhova, S.N. Lukin, D.V. Savchenko, W.C. Mitchel, S. Greulich-Weber, U. Gerstmann, A. Pöppl, J. Hoentsch, E. Rauls, Y. Rozentzveig, E.N. Mokhov, M. Syväjärvi, R. Yakimova: *EPR, ESE and Pulsed ENDOR Study of Nitrogen Related Centers in 4H-SiC Wafers Grown by Different Technologies*, Mater. Sci. Forum **556-557**, 355 (2007)

C. Li, R. Ji, R. Vinken, G. Hommes, M. Bertmer, A. Schäffer, P.F.X. Corvini: *Role of dissolved humic acids in the biodegradation of a single isomer of nonylphenol by Sphingomonas sp.*, Chemosphere **68**, 2172 (2007)

V. Nagarajan, B. Müller, O. Storcheva, K. Köhler, A. Pöppl: *Coordination of solvent molecules to VO(acac)$_2$ complexes in solution studied by hyperfine sublevel correlation sprectroscopy and pulsed electron nuclear double resonance*, Res. Chem. Intermed. **33**, 705 (2007)

J. Nelles, D. Sendor, M. Bertmer, A. Ebbers, F.-M. Petrat, U. Simon: *Surface Chemistry of n-Octane Modified Silicon Nanoparticles Analyzed by IR, ^{13}C CPMAS NMR, EELS, and TGA*, J. Nanosci. Nanotechnol. **7**, 2818 (2007)

L. Rodríguez-González, F. Hermes, M. Bertmer, E. Rodríguez-Castellón, A. Jiménez-López, U. Simon: *The acid properties of H-ZSM-5 as studied by NH_3-TPD and ^{27}Al-MAS-NMR spectroscopy*, Appl. Catal. A **328**, 174 (2007)

G.V.M. Williams, J. Haase: *Doping-Dependent Reduction of the Cu Nuclear Magnetic Resonance Intensity in the Electron-Doped Superconductor $Pr_{2-x}Ce_xCuO_4$*, Phys. Rev. B **75**, 172 506 (2007)

X.-W. Yan, J.-D. Wang, X.-H. Ren, Y.-R. Yang, B.-B. Jiang, M.A. Voda, M. Bertmer, S. Stapf: *Phase Structures of Nascent Polyethylene Powder Studied by Wideline Proton NMR*, J. Chem. **25**, 863 (2007)

in press

G.E. Schaumann, M. Bertmer: *Do water molecules bridge soil organic matter molecule segments?*, Eur. J. Soil Sci., available online on 18. September 2007

Talks

M. Bertmer: *Physicochemical characterization of heterogeneous catalysts: NMR methods in catalysis*, Mitteldeutscher Katalyselehrverbund, Universität Leipzig, 2007

M. Bertmer: *Multinukleare Festkörper-Spektroskopie an Hybridmaterialien und Photoreaktionen im festen Zustand*, 20. Mitteldeutsches Resonanztreffen, Analytische Chemie, Universität Leipzig, 2007

J. Haase: *NMR of Correlated Electron Superconductors*, Bardeen-Cooper-Schrieffer Theory of Superconductivity@50, University of Illinois at Urbana-Champaign, USA, October 2007

J. Haase: *Two Electronic Components in High-Temperature Superconductivity from NMR*, Washington University, St. Louis, USA, October 2007

J. Haase: *Two Fluids in high-temperature superconductivity from NMR*, International Conference: Modern Development of Magnetic Resonance, Kazan, Russia, September 2007

J. Haase: *Proof of Two-Component Behavior in Cuprate Superconductivity*, AMN-3, Advanced Materials and Nanotechnology, Wellington, New Zealand, February 2007

A. Pöppl: *EPR Spectroscopy of Vanadium(IV) Complexes On Solid Surfaces*, Université du Maine, Faculté des Sciences, Le Mans, France, September 2007

A. Pöppl: *Impuls-ESR Spektroskopie von Vanadium(IV)-Ionen in Heteropolysäuren und deren Salzen*, Universität Augsburg, Institut für Physik, June 2007

Posters

I. Fonseca, M. Bertmer, R.C. Nieuwendaal, S.E. Hayes: *Evaluation of Hydrogen-Bond Strengths with* ^{1}*H Solid State NMR in the Photodimerization of Cinnamic Acid Derivates*, 48th Experimental NMR Conference, Daytona Beach, USA, April 2007

Patents

J. Haase: *Method and apparatus for magnetic resonance spectroscopy*, US-2007-0273374-A1 patent (pending)

6.10 Graduations

Doctorate

- Özlen Ferruh Erdem
  Molecular Dynamics of Ethylene Glycol Adsorbed in Zeolites: Nuclear Magnetic Resonance and Broadband Dielectric Spectroscopy Investigations
  September 2007
- Vijayasarathi Nagarajan
  Vanadium(IV) Complexes on Solid Surfaces and in Frozen solutions as Studied by Pulsed EPR Spectroscopy
  March 2007

Bachelor

- Toni Rupprecht
  Measuring NMR Signals - A closer View on the Spectrometer
  September 2007

6.11 Guests

- Prof. O.P. Sushkov
  School of Physics University of New South Wales, Australia
  June – August 2007
- G.V.M. Williams, PhD
  The MacDiarmid Institute and Industrial Research Limited, New Zealand
  July – August 2007
- V. Ivanshin, PhD
  Physics Faculty, Kazan State University, Russia
  December 2007

7

Nuclear Solid State Physics

7.1 Introduction

Research in material and life sciences profits from modern and established methods like ion beam analysis and modification as well as nuclear probes.

We use the high-energy-nano-probe LIPSION with specifications which are unique in Germany. Current research is focused on spatially resolved quantitative trace elements analysis in neuroscience, determination of the response of living cells to single ion bombardment, ion beam analysis of micro- and nano-structures, as well as ion beam writing.

The perturbed angular correlation of γ-rays (TDPAC) is used to determine the nuclear quadrupole interactions of materials like TiO_2 bulk and TiO_2 nano-particles. This method is also able to determine in-vitro the solubility of these nano-particles in body fluids without separation of the particles and solution. This information is absolutely necessary to determine probable health risks after incorporation of nano-particles.

Tilman Butz

7.2 The New Irradiation Platform at LIPSION

M. Rothermel, T. Reinert

Following a well prepared planning phase, the former target chamber at the LIPSION nanoprobe has been replaced (Fig. 7.1). This change includes a new seven axis sample positioning system (stage) which can be mounted modularly, e.g. as eucentric goniometer. The stage allows linear and rotary motion with high precision. To control the stage a graphical user interface has been developed, which even permits remote control from the workstation. The accuracy and reproducibility of the stage has been tested, resulting in an accuracy of ±150 nm for the piezo motors and ±1.5 μm for the stepper motor. Additionally, a high resolution microscope with three different optics (overview, region of interest, focusing mode with a field of view of 2.6 mm, 0.33 mm and about 50 μm, respectively) and cameras for rear views have been installed. The modularity of the stage allows variable arrangements necessary for e.g. tomography, channeling and single ion experiments as well as proton beam writing.

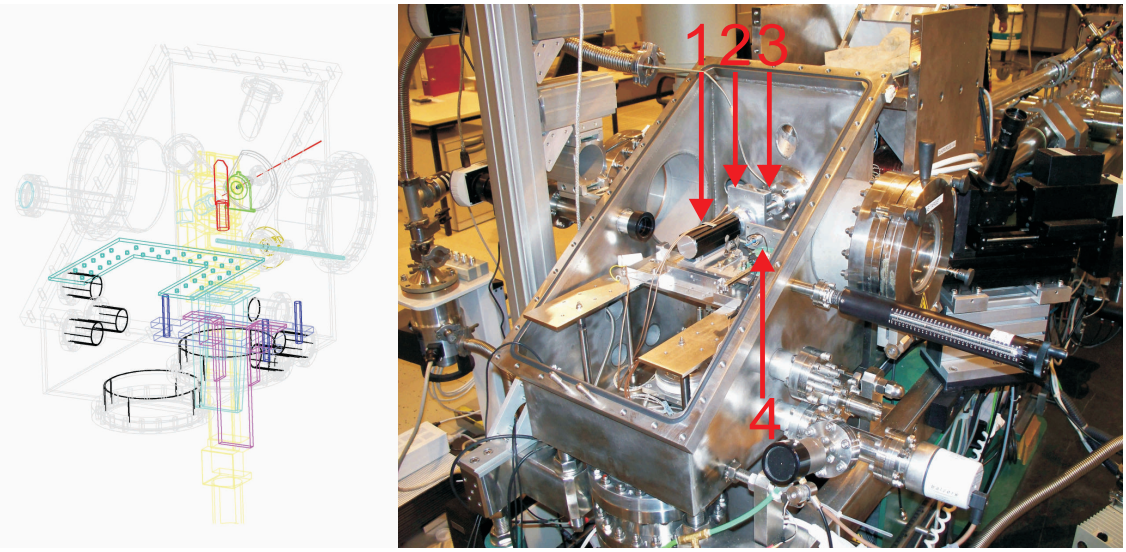

Figure 7.1: The new irradiation chamber at the LIPSION nanoprobe. *Left*: CAD drawing of the chamber (*grey*, without top) with the standard sample holder (*red*), stage (*yellow*) and stage mounting elements (*blue, violett*). *Right*: Fully implemented target chamber with exit nozzle and removed top for external beam applications (*1*: objective of the new optical microscope, *2*: holder for Petri dishes, *3*: exit nozzle, *4*: PIN-Diode for STIM measurements).

7.3 Ion Beam Analysis of ZnO:(Mg,P,Al,Mn,Cr,Fe,Co,Cu) Thin Films Grown on *c*-Plane Sapphire

C. Meinecke, A. Müller*, N. Gosh*, Q. Xu*, M. Brandt*, J. Vogt, T. Butz

*Semiconductor Physics Workgroup

ZnO thin films, nominally undoped, alloyed with Mg, P, Al, Mn, Cr, Fe, Co and Cu grown epitaxially on *c*-plane sapphire by pulsed laser deposition (PLD) were investigated. The films were analysed by Rutherford Backscattering Spectrometry (RBS) and Particle Induced X-ray Emission (PIXE) using a H^+ ion beam.

The knowledge of the composition of the Mg and P doped ZnO films is required to understand the optical properties (e.g. luminescence and band gap energy) with respect to the dopant concentration. The electric and magnetic properties, like anomalous Hall effect and magnetoresistance, are relevant for the Al, Mn, Cr, Fe, Co and Cu doped ZnO films. The determined elemental compositions could rule out other influences by impurities.

It was found that the element transfer from the PLD target to the film varies significantly for the individual doping and alloying elements, with concentration ratios between film and target ranging from less then 5 % for Al and Cu, over 10 – 20 % for Mn, to 200 – 400 % for Mg and Co.

Furthermore, the crystalline quality of the ZnO:P films was investigated using ion channeling. The deposited ZnO:P films showed a normalized minimum RBS yield of χ_{min} = 3.4 % under channeling conditions, which is nearly the same for undoped ZnO. This indicates that the dopant atoms do reside on regular Zn lattice sites. (More details can be found in the reports of the Semiconductor Physics division)

7.4 Development of New Techniques to Arrange and Recognise Cells for Radiobiological Ion Microbeam Experiments

T. Koal, M. Hohlweg, F. Menzel, T. Reinert, T. Butz

Apart from a few references the signal pathways of the cell–cell communication (Bystander effects) in microbeam experiments are still unknown. Two possibilities exist: direct cell–cell communication via gap junctions and cell–cell communication via media. A promising start for the investigation of the mediated pathways is the compartmentalization of Petri dishes. It allows spatially separated cell-subpopulations to communicate indirectly via medium borne factors only. Therefore, agar, a polysaccharide, was spin coated on Mylar or silicon nitride (Si_3N_4) irradiation windows. The compartmentalization was achieved by proton beam writing on the cell repellent substrate agar. The irradiated areas can be dissolved in water. It could be shown that cells exclusively grow in the agar-free areas (see Fig. 7.2). An arrangement in stripes could be useful to detect Bystander effects by using the Fast Fourier Transformation (see Fig. 7.3). All cells in

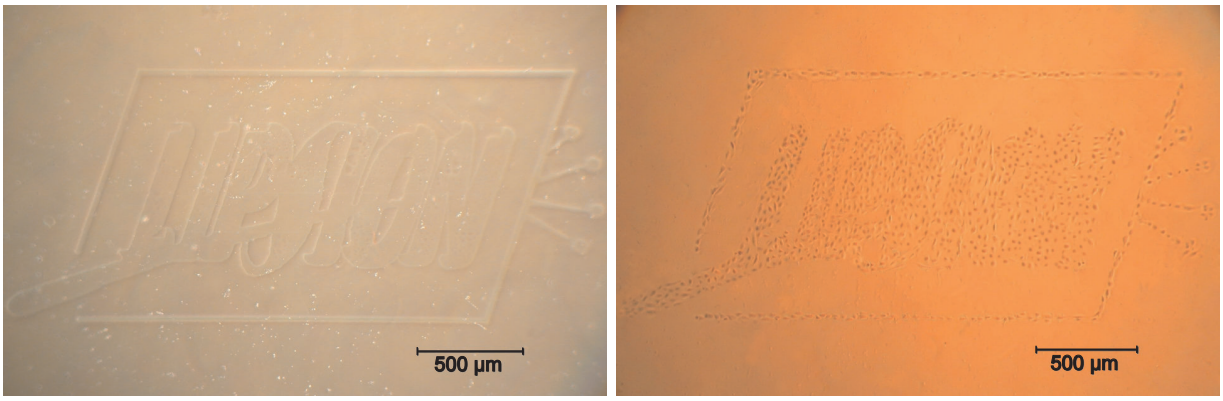

Figure 7.2: *Left*: The LIPSION logo as an agar-free area. *Right*: Cells are grown as LIPSION logo on the areas without agar.

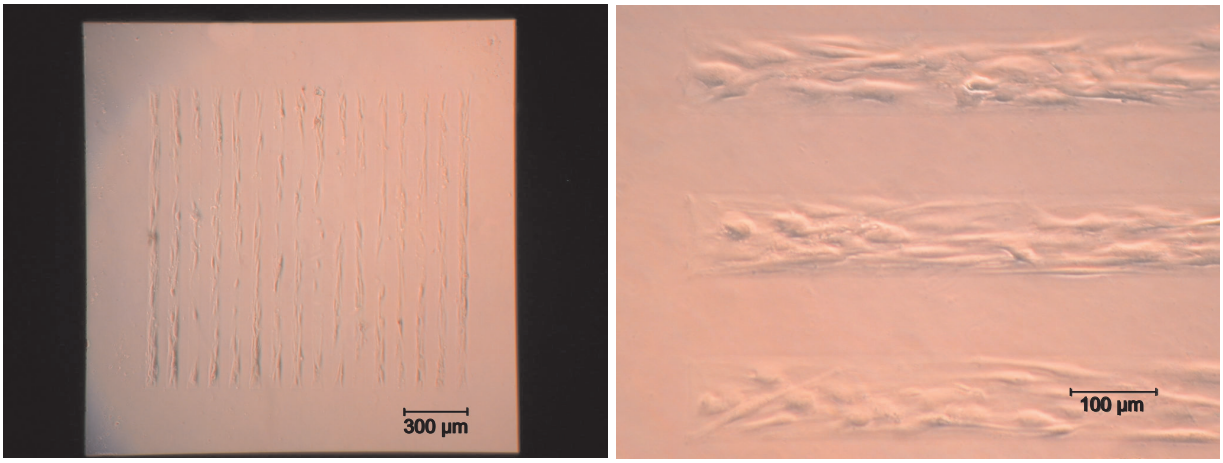

Figure 7.3: *Left*: Cells grown in 16 agar depleted stripes. *Right*: Expanded view of three stripes.

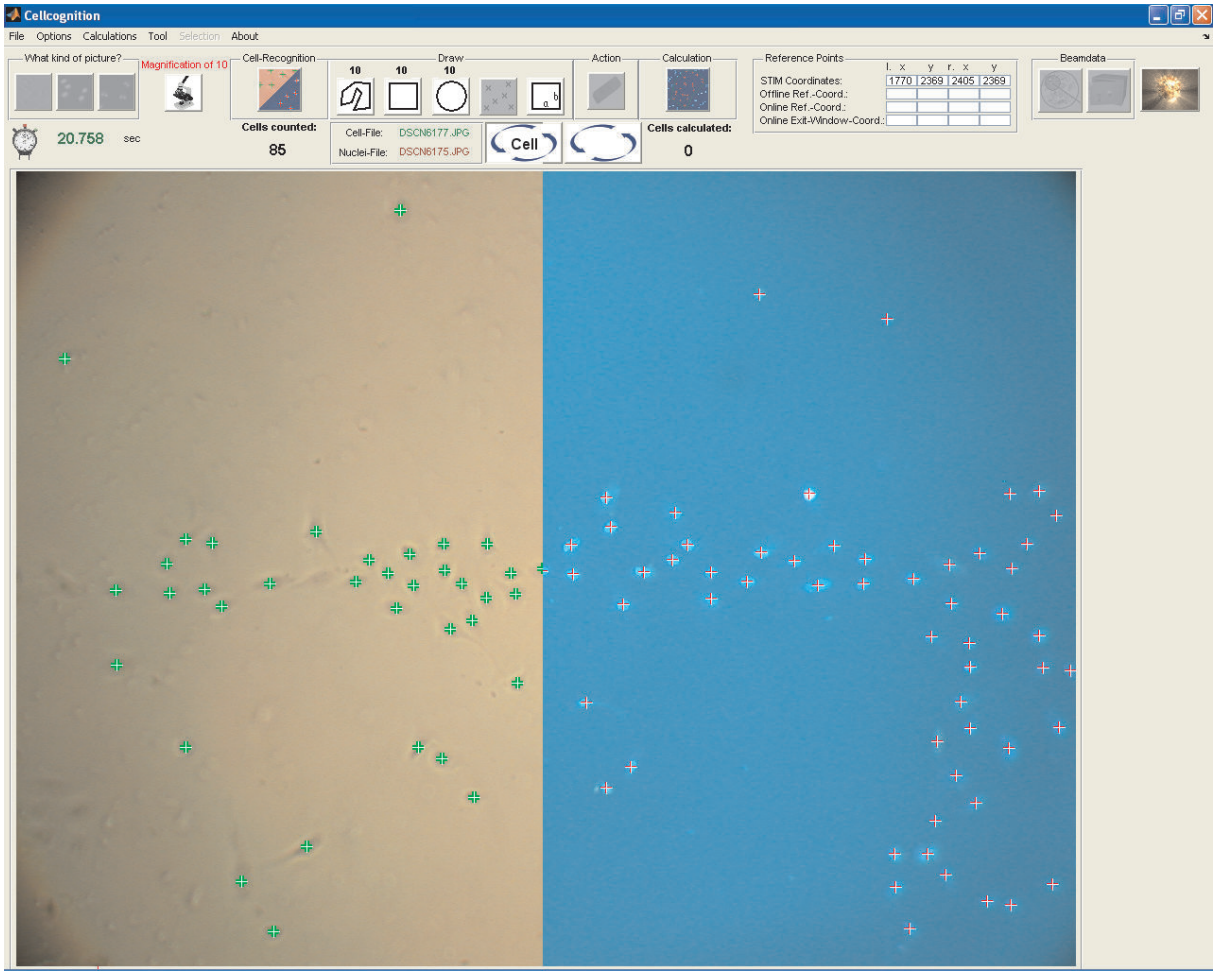

Figure 7.4: Screenshot of the Cellcognition software.

every second stripe will be irradiated. If cell–cell communication takes place, the non irradiated cells will exhibit foci as well as the irradiated cells. For targeted irradiation of cells, a recognition software named Cellcognition is being developed. Cellcognition can detect cells (especially the nuclei) with and without UV-illumination and with a reliability of more than 95 % (see Fig. 7.4). Cellcognition transforms the located cell positions into beam coordinates by using micro imprinted fiducial markers. First tests have shown that the procedure of transforming the data is reliable but requires further automatization.

7.5 Proton Irradiation of Living Cells in Structured Petri-Dishes

M. Hohlweg, J. Skopek, T. Reinert, T. Butz

Petri-dishes for radiobiological experiments have been especially designed for a structured cell growth. The structure consisted of five quadratic areas of $1 \times 1\,\mathrm{mm}^2$, one in the center, the others arranged in four directions around the center. The areas are

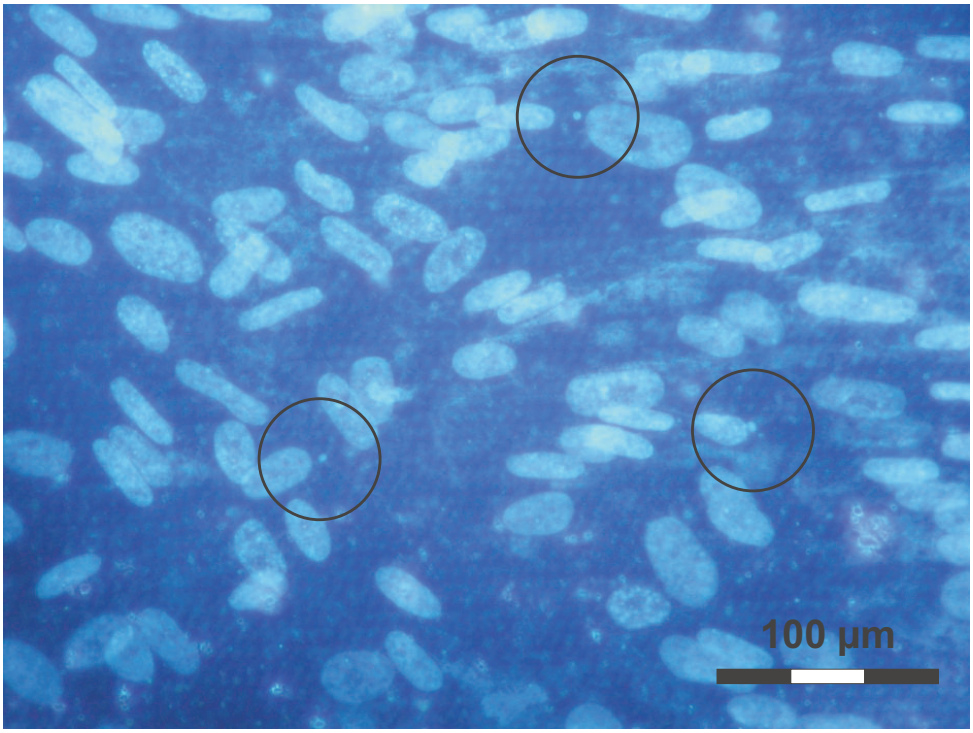

Figure 7.5: Nuclei of fibroblasts (DNA staining with DAPI) after low dose irradiation with 2 MeV protons. Micronuclei formation (*encircled*) was chosen as endpoint for the cellular response to ionizing radiation.

spatially separated by 1 mm. Thus, five sub-populations of cells without direct cell–cell contact in a single Petri-dish were created. The cell communication between the sub-populations can only be mediated via the cell medium. This arrangement was chosen to establish an experimental set-up to study cell medium mediated Bystander signals for a cellular response to ionizing radiation (counted number of single H^+ or He^{2+} ions). The irradiation induced production of micronuclei was chosen as endpoint for the cellular response.

In a first experiment, primary human fibroblasts were seeded in the specially designed Petri-dishes. The sub-population in the center was irradiated with 2 MeV protons at a low energy dose (on average 1.25 protons/μm^2). After irradiation cytochalasin B was added to suppress the cell division after mitosis in order to recognize micronuclei in mitotic cells (Fig. 7.5). Due to an extraordinary slow growth rate the number of cells in the mitotic phase was too low for a significant statistical analysis. The experiments will be repeated in 2008.

7.6 STIM Tomography of Biological Samples

T. Andrea, M. Rothermel, T. Reinert, T. Butz

Tomography experiments using scanning transmission ion microscopy (STIM) in the past have suffered from a limited resolution mostly due to an insufficient accuracy of goniometer motion which resulted in a blurred alignment of the projections. The

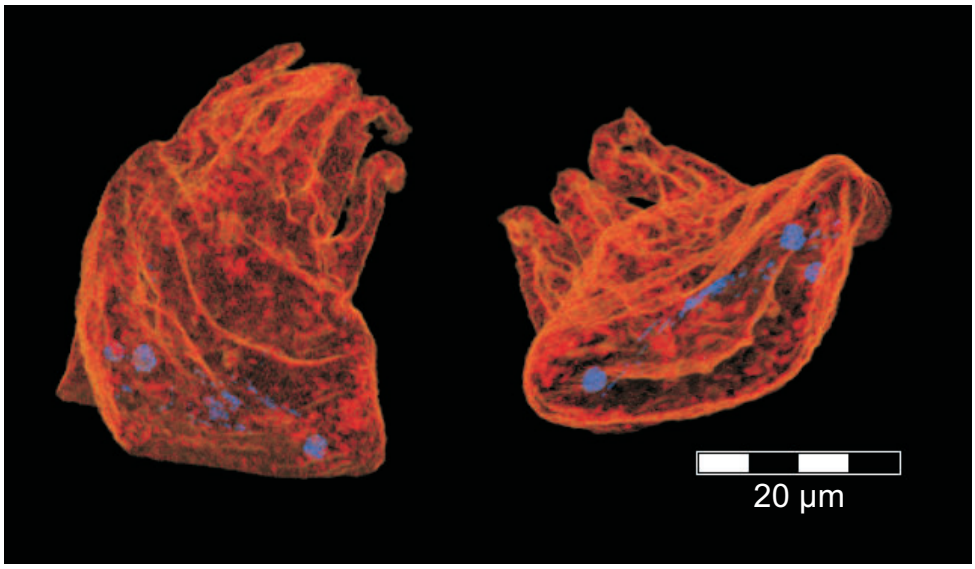

Figure 7.6: Tomogram of a rust mite. *Blue regions* are 25 % more dense than the surrounding area.

new stage and goniometer at the LIPSION accelerator laboratory allow a more precise rotation of the sample. For the STIM measurements a rust mite (Aculus schlechtendali) with an average thickness of 25 µm was mounted on the tip of a steel needle and was examined using a 2.25 MeV proton beam. Over an angular range of 180 degrees 360 projections were taken. By measuring the energy loss information about the density distribution was obtained. The three-dimensional image was reconstructed via back-projection of filtered projections (bfp) revealing spherical dense grains of yet unknown origin inside the mite's body (see Fig. 7.6). These structures are invisible in the 2D slices due to insufficient contrast.

7.7 Creation of Resist and Semiconductor Microstructures by Proton Beam Writing

F. Menzel, D. Spemann, T. Koal, J. Lenzner*, W. Böhlmann†, T. Butz

*Semiconductor Physics Workgroup
†Superconductivity and Magnetism Workgroup

For the easy and fast creation of complicated arbitrary shaped structures by proton beam writing (PBW) a new program called `Im2Dat` was developed in our group which converts arbitrary bitmap-files into dat-files used for scanning the ion beam over the samples (Fig. 7.7a).

First investigations of the application of PBW for grayscale lithography in negative resist materials were carried out. This technique allows to process the surface topography of microstructures without masks, usually needed for optical grayscale lithography, and without the limitations of low structure height connected with grayscale lithography by electron beam writing. In addition, the increasing linear energy transfer (LET)

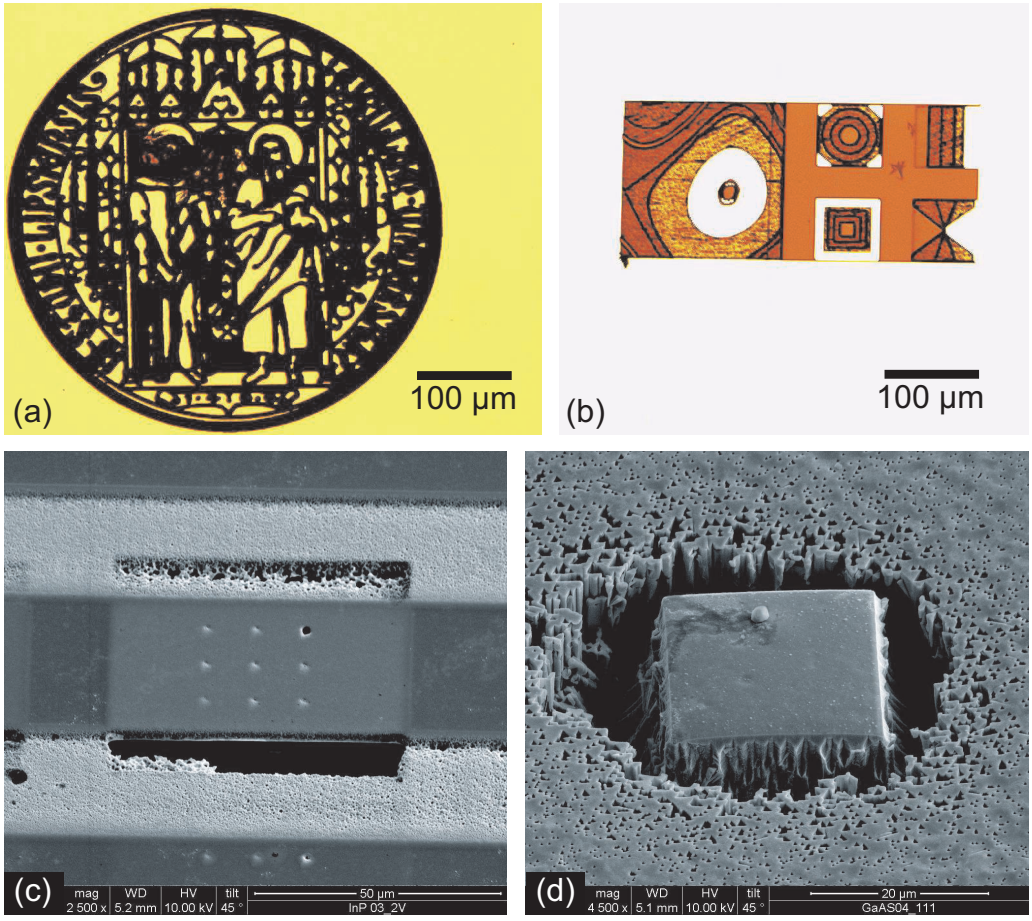

Figure 7.7: Optical micrographs of (**a**) the seal of the University of Leipzig created with PBW and (**b**) of a multilevel test structure produced with proton beam grayscale lithography, both in the negative resist ma-N 440, and REM images of (**c**) underetched membranes in InP after He irradiation and subsequent electrochemical etching and (**d**) of the non-etching effect of unirradiated material inside of closed square-shaped irradiation patterns in $(\bar{1}\bar{1}\bar{1})_{As}$-oriented GaAs.

towards the end of the ion range in the irradiated material leads to an easy control of the structure height via the irradiation fluence. First test structures in negative resists show multi step structures, where the step height depends on the irradiation dose and varies between 0 µm up to 42 µm (Fig. 7.7b).

Furthermore, among other things octagonal Ni-structures as test sample for the focusing of the high energy ion beam were produced by using resist templates created with PBW. The Ni-structures are smaller (~ 2.8 µm) and more precise than commercially available Cu-grids. In addition, first tests for the creation of 3D-Ni-microstructures were carried out in order to fabricate microsolenoids.

Further experiments on the irradiation of different types and orientations of InP and GaAs crystals with protons and helium ions and subsequent electrochemical etching show the formation of different microstructures depending on the material, the ion type and the irradiation dose. At *p*-type and SI InP as well as at SI GaAs the irradiated material is preferentially dissolved during the etching procedure, leading e.g. to underetched membranes in He-irradiated SI material (Fig. 7.7c). In *p*-type InP an increased

formation of porous material is stimulated by proton irradiation while in $(\bar{1}\bar{1}\bar{1})_{As}$ *n*-type GaAs porous material was formed in the unirradiated areas and a different etching behaviour ranging from amplified to a reduced dissolution depending on the irradiation fluence can be observed. Furthermore, it was determined that for InP and GaAs unirradiated material encircled by irradiated structures exhibit a similar etching behaviour like irradiated material (Fig. 7.7d).

7.8 Synthesis of TiO_2 Nanomaterials

S. Ghoshal, L.S. Chang, T. Butz

In order to study the biodistribution, translocation and eventual accumulation of TiO_2, we started to synthesize TiO_2-nanoparticles labeled with ^{44}Ti ($t_{1/2}$ = 60 y). The use of this label eliminates concerns about the stability of the label, as is relevant e.g. for ^{99m}Tc.

Time Differential Perturbed Angular Correlation (TDPAC) studies were carried out on bulk anatase and rutile. TiO_2-nanoparticles with dimensions between 2 and 5 nm were synthesized. The nuclear quadrupole interaction was determined both for bulk and nano-TiO_2.

The present research focuses on the synthesis of nanomaterials (particles and rods) using shape controllers which can be converted to monodisperse suspensions. Most synthesis routes use organic solvents under exclusion of moisture. Since the carrier free ^{44}Ti activity is available in 4 M HCl only, these routes are not useful for the labeling with ^{44}Ti. Recently we succeeded to produce nanorods with a diameter of about 2 nm and a length of about 50 nm (see Fig. 7.8) via an aqueous route, which will allow to label the rods with ^{44}Ti.

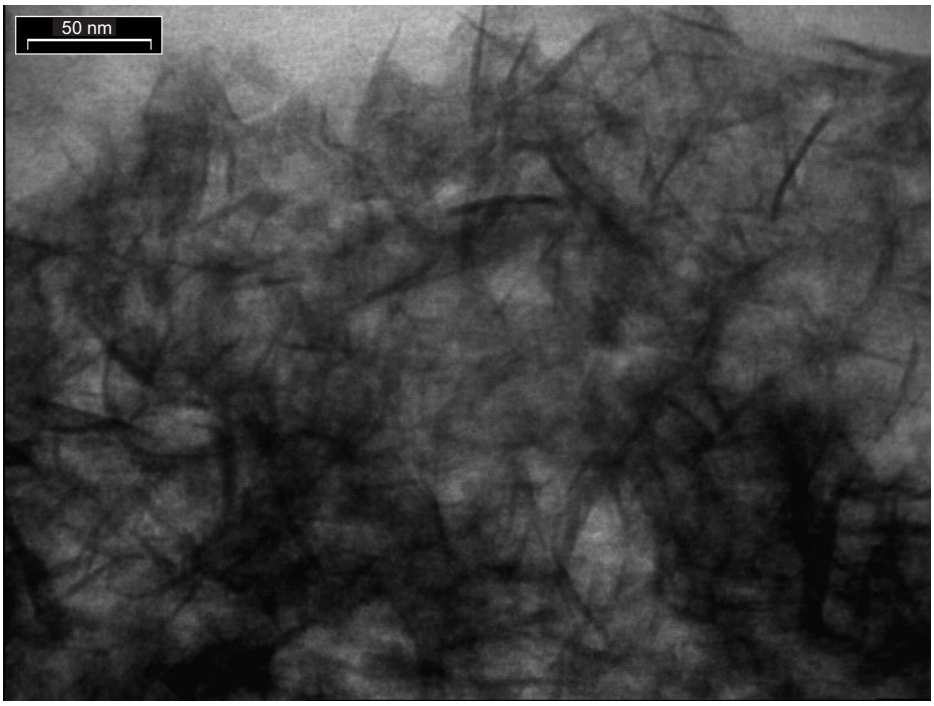

Figure 7.8: TEM image of TiO_2 nanorods (courtesy G. Wagner).

7.9 ESRF: Development of a Spectrometer for SRPAC for ^{61}Ni Spectroscopy in Biomolecules

Y. Manzhur, D. Spemann, S.K. Das, T. Butz

Synchrotron-based Perturbed Angular Correlation (SRPAC) spectroscopy is a rapidly growing field because it complements nuclear forward scattering. For ^{61}Ni spectroscopy efficient detectors for photon energies around 60 keV are required. The detectors have to withstand a huge prompt burst and yet be able to register delayed signals in the ns range.

Four different detectors are presently tested:

1. BaF_2-scintillators doped with La in order to suppress the 600 ns fluorescence mounted on XP2020a photomultipliers; here, the 220 nm fluorescence is used.
2. MPPC's with plastic scintillators; thus far, the active area of these MPPC's is by far too small to achieve an acceptable efficiency. However, larger MPPC's will be available within a few months. The decay time of plastic scintillators, e.g. here NE111, is short enough, but the low Z requires larger volumes.
3. Last year, solar blind photomultipliers became available which have a high quantum yield around 220 nm and about two orders of magnitude less at 315 nm; hence ordinary BaF_2-scintillators can be used.
4. The brand-new $LaBr_3$(Ce)-scintillators have decay times between 20 ns and 40 ns, depending on the Ce-concentration. This seems much too long for SRPAC-applications. However, it should be possible to detect a delayed pulse on the trailing edge of the prompt burst by suitable electronic differentiation in close analogy to the dynode signal processing.

7.10 ISOLDE: Development of a Fully-Digital PAC-Spectrometer

Y. Manzhur, S. Jankuhn, S.K. Das, T. Butz

The Fully-digital PAC-spectrometer consists of 6 $LaBr_3$(Ce)-scintillators on XP2020URQ-multipliers and 3 dual digitizers with 1 GSample/s (AC240 acqiris). The anode pulse analysis is carried out on field programmable gated arrays (FPGAs). For the the energy determination the area under the pulse is determined; once the lower threshold is passed, the channels are summed up to a user-determined time. The time-stamp is generated by calculating the centroid. The time resolution using a pulse-generator was 30 ps FWHM (see Fig. 7.9). The energy resolution for the 60 keV/70 keV pair in ^{44}Ti was still sufficiently good in order to separate start-stop coincidences of two detectors.

The system is presently under extensive tests before it will be installed at ISOLDE/CERN.

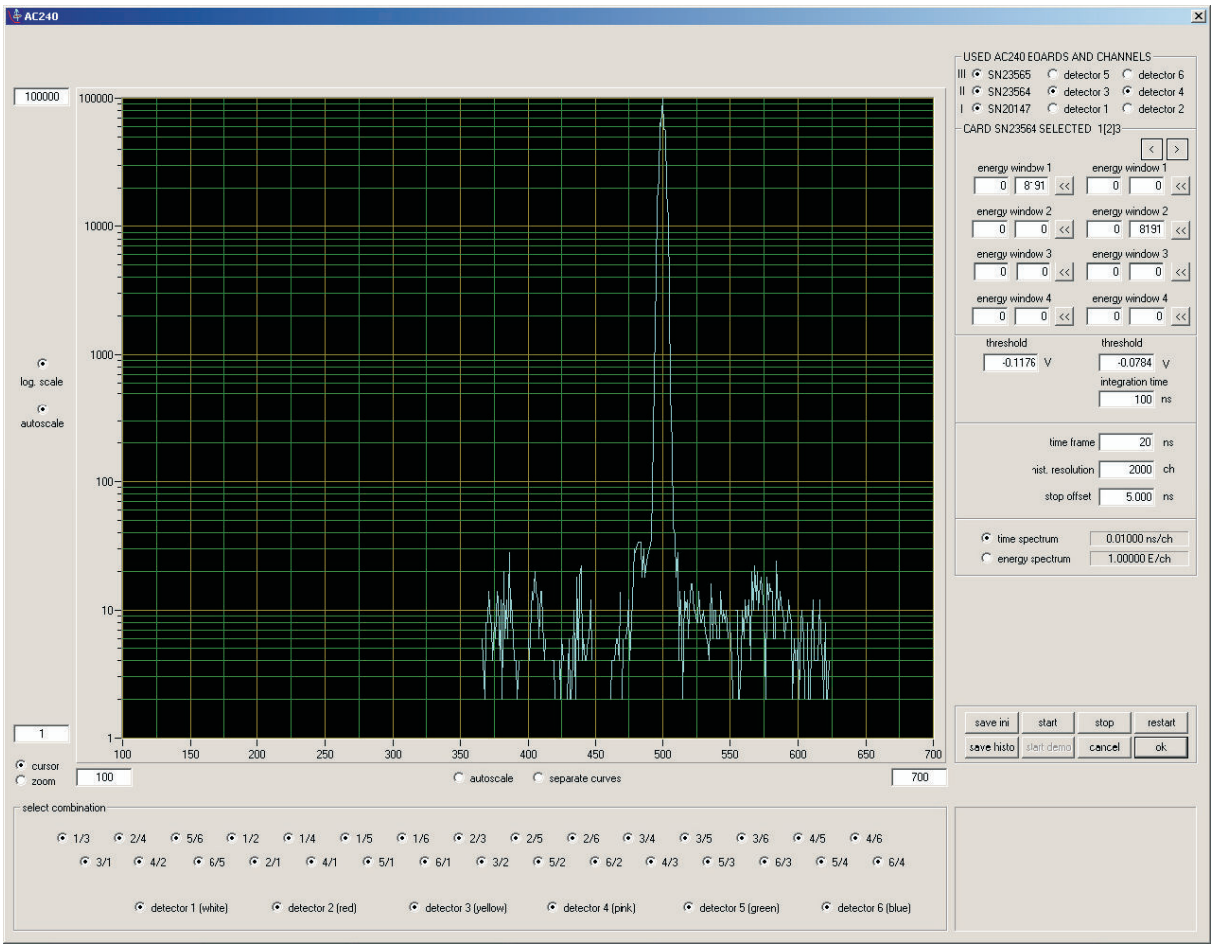

Figure 7.9: Screenshot of the time measurement with 130 kHz pulse-generator. Time per channel 10 ps.

7.11 Local Ordering Effects in Hafnium with 110 ppm Zirconium

S.K. Das, T. Butz

We used the ^{181}Hf(β^-)^{181}Ta nuclear probe in Hf-metal with 110 ppm Zr in order to study local ordering effects. At this low Zr-concentration, the probability to have a single Zr atom in the first coordination shell is 0.1 % for a random distribution. Hence, 99.9 % of the TDPAC-signal should correspond to a ^{181}Ta probe with 12 Hf nearest neighbours. On the contrary, about 90 % of the observed signal corresponds to 12 Hf nearest neighbours only. Three further signals of roughly equal intensity are observed with asymmetry parameters $\eta = 0$, $\eta \approx 0.9$ and $\eta \approx 0.4$. These three signals are assigned to three Zr nearest neighbours with three-fold rotation axis, to two Zr nearest neighbours in trans-configuration, and to one Zr nearest neighbour, all within the hexagonal plane. After the nuclear transmutation of ^{181}Ta, the lattice relaxation around the impurity results in the attraction of distant Zr atoms. The start level of the γ–γ-cascade in ^{181}Ta is sufficiently longlived ($t_{1/2} = 17\,\mu s$) to attract Zr atoms and to form preferred $TaZr_n$ ($n = 1, 2, 3$) configurations. These observations have implications for other alloys.

7.12 Funding

Non-Targeted Effects of ionising Radiation – NOTE
Prof. T. Butz
FI6R-036465

CELLION: Studies of cellular response to targeted single ions using nanotechnology
Prof. T. Butz
EU-Project:MRTN-CT-2003-503923 2

ESRF: Aufbau eines SRPAC Spektrometers zur Untersuchung der Koordination und Dynamik von Nickel-Zentren in biologischen Systemen
Prof. T. Butz
BMBF, 05KS40LA/3

NANODERM – Quality of Skin as a barrier to ultra-fine particles
Prof. T. Butz
EU-Project, QLK4-CT-02678

ISOLDE: Aufbau eines volldigitalen, nutzerfreundlichen PAC-Spektrometers
Prof. T. Butz
BMBF, 05KK4OL1/4

7.13 Organizational Duties

T. Butz
- Member of the ISOLDE and Neutron Time of Flight Committee, CERN
- Vertrauensdozent der Studienstiftung des deutschen Volkes
- Sprecher der Ortsgruppe Leipzig des deutschen Hochschulverbandes
- Co-tutor for students of Tautenburg (astrophysics), LMU München (astrophysics), DESY/Zeuthen (particle physics)
- external Expert Scientific Committee on Consumer Products, DG Sanco, Brüssel
- Reviewer: DFG, Studienstiftung des deutschen Volkes, US Immigration Service, CNRS (France)
- Referee: J. Phys. C, Phys. Rev. B, Chem. Rev., Phys. Rev. Lett., J. Biol. Inorg. Chem., Nucl. Instrum. Meth. B, Hyperfine Interact., Israeli Science Foundation, Alexander von Humboldt Foundation

C. Meinecke
- Referee: Nucl. Instrum. Meth. B

F. Menzel
- Referee: Nucl. Instrum. Meth. B
- Materials Today

C. Nilsson
- Referee: Nucl. Instrum. Meth. B

T. Reinert
- Referee: Nucl. Instrum. Meth. B

D. Spemann
- Referee: Nucl. Instrum. Meth. B

7.14 External Cooperations

Academic

- Centre d'Etudes Nucléaires de Bordeaux Gradignan (CENBG), Bordeaux, France
  Prof. P. Moretto
- European Organization for Nuclear Research (CERN), Genf, Switzerland
  ISOLDE Collaboration
- Commonwealth Scientific and Industrial Research Organisation (CSIRO), Exploration and Mining, Sydney, Australia
  Dr. C. Ryan
- Froschungsreaktor FRM II, Garching, Germany
  Prof. E. Wagner, Dr. U. Wagner
- Gray Cancer Institute, London, UK
  Prof. B. Michael
- Gesellschaft für Schwerionenforschung (GSI), Darmstadt, Germany
  Dr. D. Dobrev, Dr. B. Fischer
- Hahn–Meitner Institut (HMI), Berlin, Germany
  Dr. D. Alber, Dr. H. Haas
- Institute of Physics, Kraków, Poland
  Dr. Z. Stachura
- Institute of Nuclear Technology, Sacavém, Portugal
  Dr. T. Pinheiro
- Leibniz-Institut für Oberflächenmodifizierung (IOM), Leipzig, Germany
  Dr. K. Zimmer, Dr. J. Gerlach
- Royal Veterinary and Agricultural University (KVL), Copenhagen, Denmark
  Dr. L. Hemmingsen
- Max-Planck-Institute for Demographic Research, Rostock, Germany
  A. Fabig
- Max-Planck-Institut für Mikrostrukturphysik, Halle/Saale, Germany
  Dr. J. Heitmann
- National University of Singapore
  Prof. F. Watt, Dr. T. Osipowicz
- Universität Leipzig, Paul-Flechsig-Institut, Germany
  Prof. T. Arendt, Dr. M. Morawski, Dr. G. Brückner

- The University of Melbourne, Microanalytical Research Centre, Australia
  Prof. D. Jamison
- Technische Universität Wien, Austria
  Prof. K. Schwarz, Prof. P. Blaha
- Universität Hannover, Germany
  Arbeitskreis Prof. P. Behrens, Arbeitskreis Prof. C. Vogt
- Universität Leipzig, Germany
  Prof. R. Hoffmann
- Universität Zürich, Switzerland
  Prof. Vašak, Dr. P. Faller, Prof. R. Alberto
- Universitätskliniken Leipzig, Germany
  PD Dr. G. Hildebrandt, Dr. J. Tanner

Industry

- Infineon Technologies Dresden GmbH & Co. OHG, Germany
  M. Jerenz
- Dechema, Germany
  Dr. E. Zschau, Self-employed expert in materials research

7.15 Publications

Journals

J. Barzola-Quiquia, P. Esquinazi, M. Rothermel, D. Spemann, T. Butz, N. Garcia: *Experimental evidence for two-dimensional magnetic order in proton bombarded graphite*, Phys. Rev. B **76**, 161 403(R) (2007)

J. Barzola-Quiquia, P. Esquinazi, M. Rothermel, D. Spemann, A. Setzer, T. Butz: *Proton-induced magnetic order in carbon: SQUID measurements*, Nucl. Instrum. Meth. B **256**, 412 (2007)

A. Fiedler, T. Reinert, M. Morawski, G. Brückner, T. Arendt, T. Butz: *Intracellular ion concentration of neurons with and without perineuronal nets*, Nucl. Instrum. Meth. B **260**, 153 (2007)

A. Fiedler, T. Reinert, J. Tanner, T Butz: *DNA double strand breaks and HSP70 expression in proton irradiated cells*, Nucl. Instrum. Meth. B **260**, 169 (2007)

S. Heitsch, G. Benndorf, G. Zimmermann, C. Schulz, D. Spemann, H. Hochmuth, H. Schmidt, T. Nobis, M. Lorenz, M. Grundmann: *Optical and structural properties of MgZnO/ZnO hetero- and double heterostructures grown by pulsed laser deposition*, Appl. Phys. A **88**, 99 (2007)

S. Heitsch, G. Zimmermann, D. Fritsch, C. Sturm, R. Schmidt-Grund, C. Schulz, H. Hochmuth, D. Spemann, G. Benndorf, B. Rheinländer, T. Nobis, M. Lorenz, M. Grundmann: *Luminescence and surface properties of $Mg_xZn_{1-x}O$ thin films grown by pulsed laser deposition*, J. Appl. Phys. **101**, 083 521 (2007)

O. Iranzo, P.W. Thulstrup, S.-B. Ryu, L. Hemmingsen, V.L. Pecoraro: *The Application of ^{199}Hg NMR and ^{199m}Hg Perturbed Angular Correlation Spectroscopy to Define the Biological chemistry of HgII: A case study with Designed Two- and Three-stranded Coiled Coils*, Chem. Eur. J. **13**, 9178 (2007)

J. Lekki, Z. Stachura, W. Dabros, J. Stachura, F. Menzel, T. Reinert, T. Butz, J. Pallon, E. Gontier, M.D. Ynsa, P. Moretto, Z. Kertesz, Z. Szikszai, A.Z. Kiss: *On the follicular pathway of percutaneous uptake of nanoparticles: Ion microscopy and autoradiography studies*, Nucl. Instrum. Meth. B **260**, 174 (2007)

C. Meinecke, J. Vogt, J. Bauer, V. Gottschalch T. Butz: *Stoichiometry investigations of interlayer of GaAs/AlAs*, Nucl. Instrum. Meth. B **260**, 314 (2007)

C. Meinecke, J. Vogt, R. Kaden, K. Bente, T. Butz: *Investigation of synthetic cylindrite-microstructures*, Nucl. Instrum. Meth. B **260**, 317 (2007)

F. Menzel, D. Spemann, S. Petriconi, J. Lenzner, T. Butz: *Proton beam writing of submicrometer structures at LIPSION*, Nucl. Instrum. Meth. B **260**, 419 (2007)

M. Morawski, A. Fiedler, T. Reinert, G. Brückner, T. Arendt: *Iron compartmentalisation in the rat brain: do perineuronal net-ensheathed neurons play a special role?*, J. Neurochem. **101**, 35 (2007)

C. Nilsson, S. Petriconi, T. Reinert T. Butz: *The new target chamber at LIPSION: The new translation stage and goniometer and the new irradiation platform for single cell experiments*, Nucl. Instrum. Meth. B **260**, 71 (2007)

H. Ohldag, T. Tyliszczak, R. Höhne, D. Spemann, P. Esquinazi, M. Ungureanu, T. Butz: *π-Electron Ferromagnetism in Metal-Free Carbon Probed by Soft X-Ray Dichroism*, Phys. Rev. Lett. **98**, 187 204 (2007)

A. Rahm, E.M. Kaidashev, H. Schmidt, M. Diaconu, A. Pöppl, R. Böttcher, C. Meinecke, T. Butz, M. Lorenz, M. Grundmann: *Growth and characterization of Mn- and Co-doped ZnO nanowires*, Microchim. Acta **156**, 21 (2007)

T. Reinert, A. Fiedler, M. Morawski, T. Arendt: *High resolution quantitative trace element mapping of neuromelanin-containing neurons*, Nucl. Instrum. Meth. B **260**, 227 (2007)

R. Salzer, D. Spemann, P. Esquinazi, R. Höhne, A. Setzer, K. Schindler, H. Schmidt, T. Butz: *Possible pitfalls in search of magnetic order in thin films deposited on single crystalline sapphire substrates*, J. Magn. Magn. Mater. B **317**, 53 (2007)

M. Ungureanu, H. Schmidt, Q. Xu, H. von Wenckstern, D. Spemann, H. Hochmuth, M. Lorenz, M. Grundmann: *Electrical and magnetic properties of RE-doped ZnO thin films (RE = Gd, Nd)*, Superlatt. Microstruct. **42**, 231 (2007)

Q. Xu, L. Hartmann, H. Schmidt, H. Hochmuth, M. Lorenz, R. Schmidt-Grund, C. Sturm, D. Spemann, M. Grundmann: *The magnetotransport properties of Co-doped ZnO films*, AIP Conf. Proc. **893**, 1187 (2007)

Q. Xu, L. Hartmann, H. Schmidt, H. Hochmuth, M. Lorenz, R. Schmidt-Grund, C. Sturm, D. Spemann, M. Grundmann, Y. Liu: *Magnetoresistance and anomalous Hall effect in magnetic ZnO films*, J. Appl. Phys. **101**, 063 918 (2007)

Q. Xu, L. Hartmann, H. Schmidt, H. Hochmuth, M. Lorenz, A. Setzer, P. Esquinazi, C. Meinecke, M. Grundmann: *Room temperature ferromagnetism in Mn-doped ZnO films mediated by acceptor defects*, Appl. Phys. Lett. **91**, 092 503 (2007)

Q. Xu, L. Hartmann, H. Schmidt, H. Hochmuth, M. Lorenz, D. Spemann, M. Grundmann: *s-d exchange interaction induced magnetoresistance in magnetic ZnO*, Phys. Rev. B **76**, 134 417 (2007)

Books

T. Butz et al: *Nuclear Solid State Physics*, in: *Report 2006 - Institute für Physik*, ed. by M. Grundmann (Universität Leipzig, Leipzig 2007)

L. Hemmingsen, T. Butz: *Perturbed Angular Correlation (PAC) Spectroscopy*, in: *Applications of Physical Methods to Inorganic and Bioinorganic Chemistry*, ed. by R.A. Scott, C.M. Lukehart (Wiley, Chichester 2007) p 423

Talks

J. Barzola-Quiquia, P. Esquinazi, A. Setzer, M. Ziese, M. Rothermel, D. Spemann, T. Butz: *High-temperature magnetic order in an aromatic polyimide*, 71st DPG Spring Meeting, Regensburg, 26. – 30. March 2007

T. Butz: *Aufnahme und Speicherung von Nanopartikeln durch die Haut*, 3. Erfurter Staatswissenschaftliche Tagung "Nanotechnologie als Innovation und Risiko", Erfurt, 11.,– 12. October 2007

T. Butz: *Hautpenetration von Nanopartikeln: Die Ergebnisse des NANODERM-Projekts*, MSII-Fachforum: "Risiken von Nanometerialien realistisch bewerten", Frankfurt am Main, 23. October 2007

T. Butz: *Ionenstrahlanalytik und Ionenstrahlbearbeitung in den Material- und Lebenswissenschaften*, Technische Universität Bergakademie Freiberg, 02. May 2007

T. Butz: *Quality of Skin as a Barrier to Percutaneous Uptake of TiO_2 Nanoparticles from Sunscreens*, 3rd Int. Symp. Nanotechnology, Occupational and Environmental Health, Taipei, Taiwan, 29. August 2007

T. Butz: *Quality of Skin as a Barrier to Nanoparticles – The NANODERM-Project*, European Chemical Industry Council (CEFIC), Brussels, Belgium, 06. March 2007

T. Butz: *Quality of Skin as a Barrier to Nanoparticles – The NANODERM-Project*, Nanotechnology and Toxicology in Environment and Health, Helmholtz Centre for Environmental Research (UFZ), Leipzig, 27. March 2007

L. Hartmann, Q. Xu, H. Schmidt, H. Hochmuth, M. Lorenz, C. Sturm, C. Meinecke, A. Setzer, P. Esquinazi, M. Grundmann: *Spin polarization in $Zn_{0.95}Co_{0.05}O$:(Al, Cu) thin films*, 71st DPG Spring Meeting, Regensburg, 26. – 30. March 2007

T. Koal, T. Butz: *FFT to prove and characterize Bystander effects on cells*, 13th ICRR, San Francisco, USA, 10. July 2007.

D. Kolbe: *Microdosimetry of single cells*, Cellion Meeting, Padua, Italy, 20./21. April 2007

C. Meinecke, A. Rahm, J. Vogt, T. Butz: *Elemental Characterisation of Mn-, Mg- and Co-doped ZnO nanostructures*, 71st DPG Spring Meeting, Regensburg, 26. – 30. March 2007

Posters

A. Müller, G. Benndorf, S. Heitsch, H. Hochmuth, C. Sturm, R. Schmidt-Grund, C. Meinecke, M. Grundmann: *Optical characterization of hexagonal $Mg_xZn_{1-x}O$. thin films grown by pulsed laser deposition*, 71st DPG Spring Meeting, Regensburg, 26. – 30. March 2007

D. Kolbe, M. Hohlweg, T. Reinert, T. Koal, T. Butz: *Microdosimetry of single cells at the nanoprobe LIPSION*, Int. Conf. Biomed. Appl. High Energy Ion Beams, Surrey, UK, 30. July – 2. August 2007

7.16 Graduations

Doctorate

- Daniel Spemann
  Anwendung hochenergetischer Ionenstrahlen in den Materialwissenschaften
  June 2007

Diploma

- Peter Steinbach
  Vector Meson Production in the Forward and Backward Region of the H1 Experiment at HERA
  November 2007
- Roman Follert
  Astronomische Interferometrie – Anwendung und Perspektiven
  November 2007
- Frank Heymann
  Numerische Simulation zu möglichen Auswirkungen des gravitativen Mikrolinsen-effekts auf die Langzeitvariabilität einer flussbegrenzten Quasarsteilprobe
  November 2007

Master

- Nirav Barapatre
  In-situ Trace Element Analysis of Neuromelanin
  February 2007
- Draco Szathmáry
  Comparison of the Quasar Selection in the Sloan Digital Sky Survey and Tautenburg-Calar Alto Variability and Proper Motion Survey
  June 2007

7.17 Guests

- Dr. C.C. Dey
  Saha Institute of Nuclear Physics, Kolkata, India
  April – May 2007
- Dr. S. Dey
  Bose Institute, Kolkata, India
  April – May 2007
- Prof. Dr. Subhash Bedi
  Panjab University, Department of Physics, Chandigarh, India
  June – August 2007
- Dr. J. Skopek
  Charles University, Praha, Czech Republic
  since September 2007
- Shamik Ghoshal
  Bhabha Atomic Research Centre, Mumbai, India
  June – August 2007 and since November 2007
- Dr. Ling-Shao Chang
  Sun Yat Sen University, Taipei, Taiwan
  since October 2007

8

Semiconductor Physics

8.1 Introduction

In the year 2007 our highly esteemed colleague Prof. Dr. Bernd Rheinländer retired from his duties at the university. He continues to work part time in our labs, in order to finish his on-going projects as well as to support and offer guidance to students formerly under his tutelage. In a memorable colloquium on the occasion of Bernd's retirement, Prof. Daniel Le Si Dang from CNRS Grenoble presented a talk on his work about Bose–Einstein condensation of exciton-polaritons in selenide-based micro-cavities. This talk highlighted one of the many areas of scientific achievement for which we have to be grateful to Bernd, alongside his contributions made in teaching and administration (the latter sometimes being the more difficult part). We wish Bernd well in his retirement.

Based on our work on oxide heterostructures within FOR 522 we have applied to the German Science Foundation (DFG) for the establishment of Sonderforschungsbereich SFB 762 (Collaborative Research Project) titled "Functionality of Oxide Interfaces". This application is a joint project between the Faculty of Chemistry and Mineralogy and foremost our colleagues from Martin-Luther-Universität Halle–Wittenberg and Max-Planck-Institute for Microstructures Physics in Halle.

After a successful evaluation in September 2007, the SFB 762 commenced in January 2008. As part of the SFB, the semiconductor physics group will investigate interface effects in multi-functional oxide heterostructures, as well as multiferroic heterostructures, such as ZnO/$BaTiO_3$/ZrO_2:Mn. We are currently establishing an ultra-high vacuum pulsed laser deposition (UHV-PLD) with in-situ RHEED and a Raman scattering set-up optimized for the UV spectral range for high bandgap materials.

We have achieved significant progress in homoepitaxy of ZnO. Using ZnO substrate preparation involving high-temperature annealing, PLD layers can be grown with excellent structural properties and low defect concentration (see Sect. 8.3). In a certain window of growth conditions, 2D step-flow growth is obtained. Currently we are fabricating various homoepitaxial heterostructures. Preliminary investigations show well-controlled quantum wells and 2D electron gases.

In order to establish high-quality oxide micro-cavities for the investigation of strong coupling between ZnO excitons and light, we have optimized all-oxide Bragg reflectors. A reflectivity of 99.8 % at the ZnO band-edge for 10.5 pairs is sufficient to now proceed to the optimization of surface roughness and the properties of the ZnO cavity material (see Sect. 8.7).

Our efforts on *p*-doping of ZnO have been again rewarded. We have achieved phosphorous-doped ZnO micro- and nanowires and we demonstrated *p*-type conductivity via the gate-voltage dependence of MISFETs fabricated from the ZnO wires (see Sect. 8.5). The incorporation of ZnO/MgZnO quantum wells on top of ZnO nanowires led to the surprising discovery of quantum dot formation, as deducted from emission in sharp spectral lines. This work has benefited tremendously from our collaboration with Le Si Dang's group in Grenoble. The journal Nanotechnology has chosen this paper as featured article on its cover page of volume 19(11) in 2008.

Our previous work on whispering gallery modes (WGM) in the green spectral range (transparency regime) of ZnO nanowires with hexagonal cross-section could be extended to the UV spectral range near the band gap. We found that lasing in ZnO microwires occurs via such WGM as proven with micro-photoluminescence spectroscopy under pulsed high optical excitation.

Finally, I would like to direct your attention to our work on space charge spectroscopy. We have developed a model to fit the temperature dependence of admittance spectra and extract defect level properties. Various electron traps in ZnO have been investigated in detail (Sects. 8.14 and 8.15). Using the very best Schottky contacts on ZnO based on silver oxide as gates we have fabricated ZnO MESFET's with record performance (see Sect. 8.4).

We have enjoyed the cooperation with many colleagues and guests. We are grateful to the funding agencies supporting our work; they are acknowledged individually in the short notes. I like to note that some of our doctoral students are now supported by the Leipzig Graduate School of Natural Sciences - BuildMoNa (Building with Molecules and Nano-objects) which is supported within the German Excellence Initiative. We hope that the following short notes find your interest and keep you informed about our progress. If you have further questions we would be more than happy to discuss these with you.

Marius Grundmann

8.2 Quantum Dot Like Emission from ZnO Nanowire Quantum Wells

C. Czekalla, B.Q. Cao, C. Hanisch, J. Lenzner, A. Travlos*, D. Le Si Dang†, M. Lorenz, M. Grundmann

*National Center of Scientific Research Demokritos, Greece

†CEA-CNRS group "Nanophysique et Semiconducteurs", Grenoble, France

MgZnO/ZnO quantum wells (QWs) were grown on top of ZnO nanowires using a two-step pulsed laser deposition process [1]. Optical emission originating from the QW and the barrier was observed up to room temperature. Figure 8.1a shows cathodoluminescence (CL) intensity images for the emission energies of the ZnO wire, the ZnO QW and the MgZnO barrier. It can be seen that the barrier and the QW were only grown on top of the wires. Furthermore, the QW emission is not homogeneously distributed over the top of the wire. Ensembles of spatially fluctuating and narrow CL peaks with individual widths down to 1 meV were found at the spectral position of the quantum

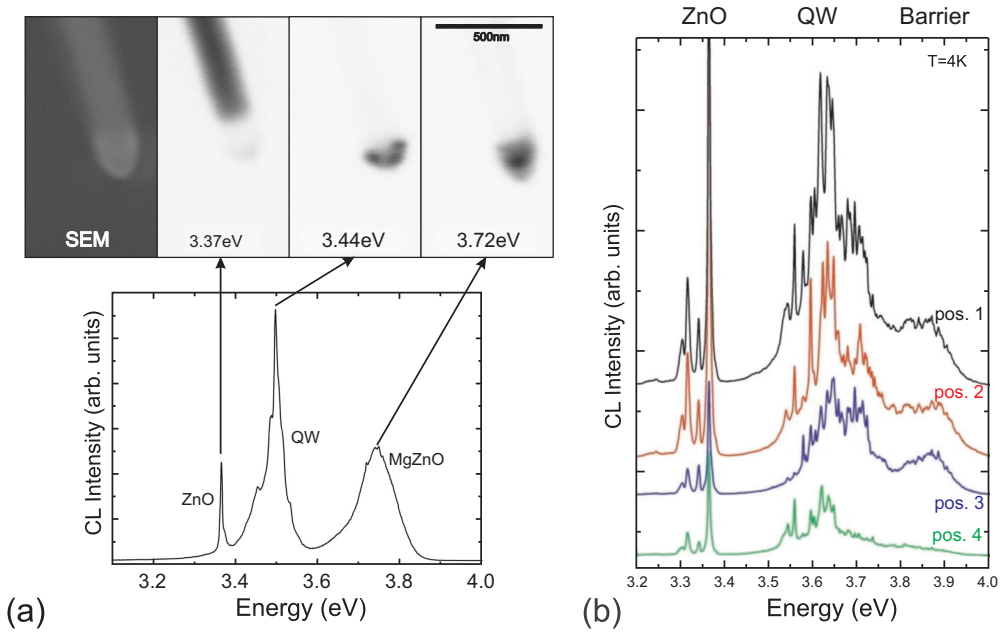

Figure 8.1: (**a**) Cathodoluminescence intensity images corresponding to the spectral range of the ZnO wire body, the MgZnO barrier and the ZnO QW. (**b**) Spatially fluctuating and narrow CL peaks are found at the energetic position of the QW band.

well emission at 4 K, as depicted in Fig. 8.1b. The spectra were taken at positions few tens of nanometers apart. The number of these narrow QW peaks increases with increasing excitation power in micro-photoluminescence, thus pointing to quantum dot recombination centers.

By means of high-resolution transmission electron microscopy, laterally strained areas of about 5 nm diameter were identified at the quantum well positions on top of the nanowires. These spatially fluctuating structures may act as quantum dot-like recombination centers for excitons as indicated by the emission spectroscopy results.

This work was supported by the DFG within FOR522 and the EU within NANDOS and SANDiE.

[1] C. Czekalla et al.: Nanotechnology **19**, 115 202 (2008)

8.3 Growth of High Quality Doped Homoepitaxial ZnO Thin Films by Pulsed Laser Deposition

M. Brandt, H. von Wenckstern, G. Zimmermann H. Schmidt*, A. Rahm†, G. Biehne, G. Benndorf, H. Hochmuth, M. Lorenz, C. Meinecke, T. Butz, M. Grundmann

*now at Forschungszentrum Rossendorf, Dresden
†now at Solarion AG, Leipzig

Homoepitaxial growth represents a promising approach for the fabrication of ZnO thin films with both high structural quality and low impurity concentration. However, the quality of the ZnO substrates available makes the deposition of high quality thin films

a challenging process. As-received substrates show serious polishing damage. An additional annealing step is required for substrate preparation [1] before growth. Undoped samples grown by PLD show a very high structural and optical quality, as well as a very low residual donor concentration of about 6×10^{14} cm^{-3}. However, even without out-of-plane mismatch a small in-plane mismatch of the film against the substrate was observed [2]. This was ascribed to an increase of the lattice constant of the substrate due to the high concentration of mostly metallic impurities in the substrate accumulating at the surface during the annealing process [3]. A large concentration of residual donors in ZnO is often an obstacle for the formation of stable *p*-type ZnO. The high purity of the undoped homoepitaxially grown thin films makes them ideal for experiments aiming for *p*-doping. Within this study ZnO:P thin films with target phosphorous concentrations of 0.01, 0.1 and 1 wt. % P_2O_5 have been deposited by PLD at a substrate temperature of 650 °C and oxygen partial pressures ranging from 3×10^{-4} mbar to 0.1 mbar. The film thickness was determined to be about 1 µm from Pendelloesung-oscillations in the $2\Theta-\omega$ scan of the (0002) ZnO reflection. With increasing phosphorous concentration the lattice constant of the thin films increases compared to that of the substrate [2]. However for the smallest phosphorous concentration of 0.01 wt. % P_2O_5 in the target, and an oxygen partial pressure of 0.1 mbar perfect lattice match between the thin film and the substrate was obtained as well in plane (Fig. 8.2a) as out of plane (Fig. 8.2b). Further, 2D growth was confirmed by atomic force microscopy investigations for that particular film (Fig. 8.2c).

Rutherford backscattering channeling experiments have been carried out at the LIPSION ion beamline. A channeling axis perpendicular to the sample surface was observed for the sample showing the 2D growth mode. This provides further evidence for the single crystalline nature of this ZnO:P thin film. A χ_{min} as low as 0.034 can be seen for the film grown at 0.1 mbar oxygen partial pressure which is comparable to the value obtained for the substrate (χ_{min} = 0.033), indicating very good crystal quality (cf. for pure single crystalline Si χ_{min} = 0.03). All of the samples investigated show *n*-type conduction with superior transport properties. However, samples showing *p*-type conductivity and having good structural properties simultaneously have not been reported so far. An extended defect (V_{Zn}–P_{Zn}–V_{Zn}) has been proposed as an origin of the *p*-type conductivity, leading to high lattice distortions [4]. For the smallest phosphorous concentration of 0.01 wt. % P_2O_5 in the target, and a oxygen partial pressure of 3×10^{-4} mbar a peak electron mobility of 800 cm^2/Vs was observed. The

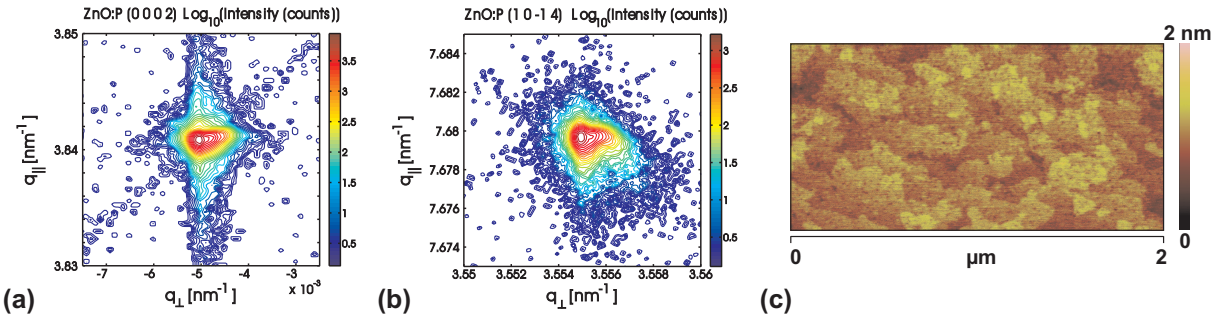

Figure 8.2: Reciprocal space maps of the (0002) (**a**) and (10$\bar{1}$4) (**b**) reflex and AFM height image with $c/2$ monolayer steps (**c**) of the very smooth sample E1327 (0.01 % P_2O_5) with 2D growth mode.

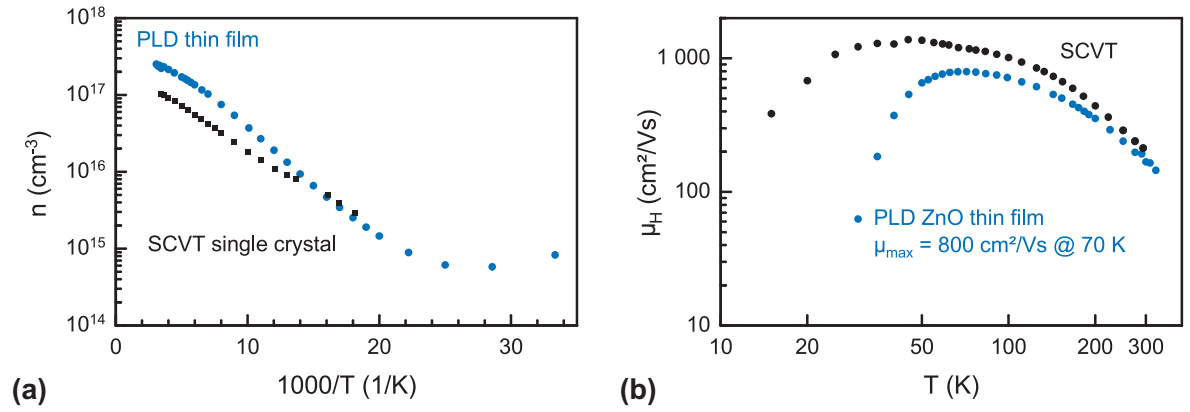

Figure 8.3: Temperature dependence of the free electron concentration (**a**) and mobility (**b**) of a homoepitaxial ZnO:P thin film (0.01 % P_2O_5) and of a SCVT ZnO single crystal.

value is the highest value ever reported in phosphorous doped ZnO. The temperature dependence of the free electron concentration (Fig. 8.3a) and the mobility (Fig. 8.3b) are compared to that of a single crystal grown by seeded chemical vapor transport (SCVT). The lower values of the mobility can be ascribed to two mechanisms. First of all, the free electron concentration is higher than that in the single crystal, leading to an increased influence of ionized impurity scattering. Further, at low temperatures an increase of the apparent electron concentration is observed, which can result from a degenerate parallel conduction channel in the sample, most likely situated at the sample surface. The existence of this parallel channel reduces the apparent mobility and therefore the data displayed in (Fig. 8.3b) represents a lower limit of the actual bulk mobility in the ZnO:P thin film. In summary, an appropriate phosphorous doping of homoepitaxial ZnO thin films enhanced the thin film lattice constant such that a perfect fit with the substrate was achieved. A single-crystalline 2D growth was observed as well as a very high peak electron mobility of 800 cm^2/Vs.

This work has been supported by Deutsche Forschungsgemeinschaft in the framework of FOR 404.

[1] H. von Wenckstern et al.: Phys. Stat. Sol. RRL **1**, 129 (2007)
[2] M. Lorenz et al.: *Homoepitaxial ZnO thin films by PLD: Structural properties*, Phys. Stat. Sol. C, in press
[3] N. Volbers: Disseration, Universität Giessen (2007)
[4] W.-J. Lee: Phys. Rev. B **73**, 024 117 (2006)

8.4 ZnO Metal-Semiconductor Field-Effect Transistors with Ag Schottky-Contacts

H. Frenzel, A. Lajn, M. Brandt, H. von Wenckstern, H. Hilmer, C. Sturm, G. Biehne, H. Hochmuth, M. Lorenz, M. Grundmann

Metal-semiconductor field-effect transistors (MESFET) were fabricated by reactive DC-sputtering of Ag Schottky-contacts on ZnO thin-film channels grown by pulsed-laser deposition (PLD) on sapphire.

The key advantage of MESFETs is the higher mobility of carriers in the channel as compared to metal-insulator-semiconductor field-effect transistors (MISFET). Since the carriers in the channel of a MISFET are accelerated towards the semiconductor/insulator interface by the gate electric field and suffer from interface scattering, their mobility is less than half of the mobility of bulk material. As the depletion region in MESFETs separates the carriers from the surface their mobility is close to that of bulk material [1].

The ZnO thin films were grown on *a*-plane sapphire substrates at a growth temperature of about 630 ℃ and oxygen partial pressure of 0.02 mbar. Four layer configurations have been used: 10 thousand pulses (kP) ZnO, 3 kP ZnO, grown directly on the substrate and on a MgO buffer layer, respectively. The MgO buffer reduces Al diffusion from the substrate into the ZnO layer drastically. The thicknesses d of the ZnO layers measured by spectroscopic ellipsometry are shown in Table 8.1.

Three steps of photolithography were used to produce the MESFETs. First the ZnO channels were etched into a mesa structure. Then the source and drain contacts were deposited by dc-sputtering of Au. Last, highly rectifying Ag Schottky gate-contacts were fabricated using reactive DC-sputtering under a 50/50 ratio of O_2 and Ar at 0.02 mbar. Subsequently, an Au-capping-layer was sputtered for passivation.

I–V characteristics of the gate Schottky-contacts show an excellent rectification behaviour with leakage currents in the range of picoamperes. For Sample 1 and 3 a rectification ratio of 10^8 at ±2 V is achieved whereas it is 10^6 for sample 2 and 10^3 for sample 4. The forward current is thereby limited by the series resistances of the ZnO layers, which are 4 kΩ and 6 kΩ for samples 1 and 3 as well as 1 MΩ and 300 MΩ for samples 2 and 4, respectively. Here, the effect of the MgO buffer layer avoiding Al diffusion from the substrate [2] is obvious.

The output characteristics of sample 3 are shown in Fig. 8.4a. There are clear pinch-off points following a quadratic behaviour as predicted by MESFET theory. At these points, the depletion layer of the Schottky-contact is deformed by the source-drain voltage such that it completely closes the channel and only a diffusive saturation current flows.

A comparison of transfer characteristics for samples 1, 2 and 3 is shown in Fig. 8.4b. Sample 2 and 3 show a strong field-effect whereas the larger layer thickness and higher doping concetration of sample 1 inhibit full depletion of the channel. In the case of sample 4 it was not possible to reduce the depletion layer and open the channel in a gate voltage range without leakage gate-current due to the extremely low doping concentration and small layer thickness. The channel current of sample 3 can be tuned over 8 orders of magnitute in a gate-voltage range of 2.5 V. All MESFETs except sample 4 exhibit 'normally-on' behaviour with a low off-voltage of −1.5 V. The off-current is limited by the Schottky-contact's leakage current whereas the on-current reflects the channel's series resistance. The forward gate voltage does not exceed 1 V, which is

Table 8.1: Overview of the measured sample properties.

Sample	Layers	d [nm]	n_{Hall} [cm^{-3}]	μ_{Hall} [cm^2/Vs]	$N_{\mathrm{D,CV}}$ [cm^{-3}]	μ_{FE} [cm^2/Vs]	g_{max} [S/cm]
S1	10 kP ZnO	131	1.5×10^{18}	15.4	1×10^{18}	19.1	10.2
S2	10 kP ZnO + MgO	117	2.9×10^{13}	29.4	3×10^{14}	27.4	0.026
S3	3 kP ZnO	20	5.5×10^{17}	9.3	5×10^{18}	11.3	30.3
S4	3 kP ZnO + MgO	32	4.7×10^{12}	9.7	-	-	-

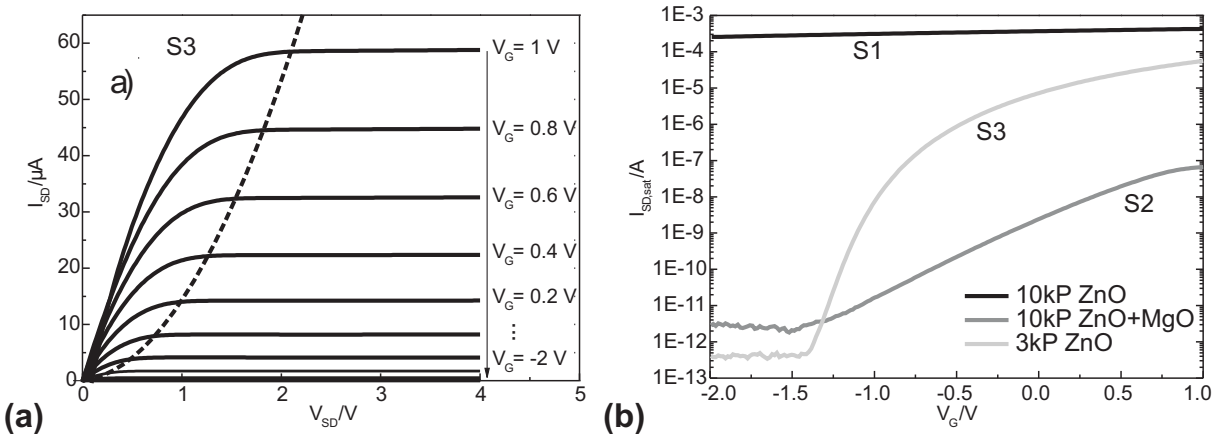

Figure 8.4: a) source–drain *I–V* output characteristic of sample 3 for different gate voltages. The *dashed line* is a quadratic fit of the pinch-off points. (**b**) Transfer characteristics of samples 1, 2 and 3 (cf. Table 8.1).

the approximate built-in voltage of the Schottky-contact. Then, the depletion layer is reduced to zero and the channel is completely open. A further increase of the gate voltage leads to an exponentially increase of gate leakage current.

In Table 8.1 the carrier densities obtained at 300 K from Hall effect measurements on the as-grown layers are compared to doping densities from *C–V* measurements performed at the final MESFET structures. One can see, that the doping concentration of samples 2 and 3 are ten times higher than the free carrier concentration due to the effect of deep defect levels, whereas it is equal in case of the higher doped sample 1. The channel mobilities μ_{FE} are calculated from the FET's maximum drain transconductance g_{max} using the doping concentrations obtained from *C–V* measurements [3]:

$$\mu_{\mathrm{FE}} = \frac{g_{\mathrm{max}}}{\frac{W}{L} e N_{\mathrm{D}} d} \,, \tag{8.1}$$

where $W/L = 200\,\mu\mathrm{m}/60\,\mu\mathrm{m}$ is the channel width to length ratio, e is the elementary charge, N_{D} is the doping concentration and d is the channel depth. The channel mobilities are in good agreement with the Hall mobilities of the unstructured ZnO layers.

[1] B. Van Zeghbroeck: ece-www.colorado.edu/ bart/book/book/index.html
[2] H. von Wenckstern et al.: Adv. Sol. State Phys. **45**, 263 (2005)
[3] M. Grundmann: *The Physics of Semiconductors* (Springer, Heidelberg 2006)

8.5 p-Type Conducting ZnO:P Microwires Prepared by Direct Carbothermal Growth

B.Q. Cao, M. Lorenz, M. Brandt, H. von Wenckstern, J. Lenzner, G. Biehne, M. Grundmann

Phosphorous-doped (ZnO:P) and undoped ZnO wires with diameter of several micrometers and length of several hundred micrometers were thermally grown directly

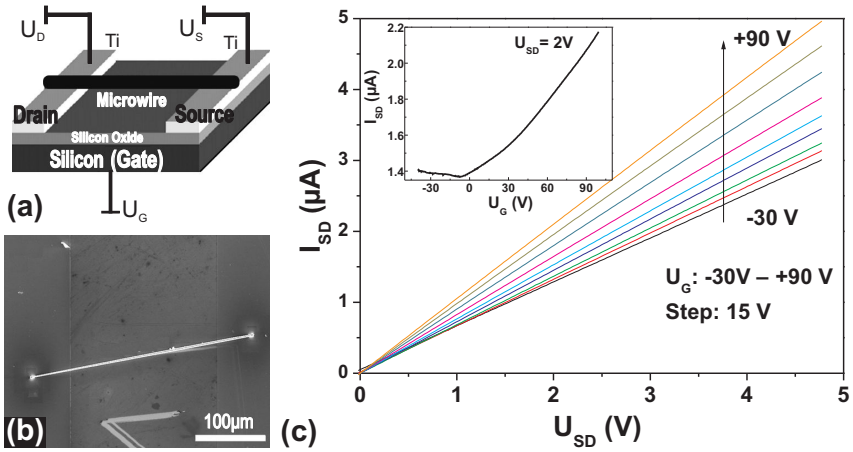

Figure 8.5: a) Schematic illustration of the back-gate FET configured with a microwire as conductive channel. (**b**) SEM image of an undoped ZnO microwire fixed on titanium electrodes with FIB-tungsten deposition. (**c**) Output characteristics (I_{SD}–U_{SD}) and transfer characteristics (I_{SD}–U_G, *inset*) of the *n*-type undoped ZnO-FET.

on phosphorus pentoxide doped and undoped ZnO:graphite targets, respectively. The low-temperature (T = 11 K) cathodoluminescence spectra of single ZnO:P microwires show three typical acceptor-related emissions which can be attributed to ($A^0$0,X), (e,A^0), and DAP [1]. It means that phosphorus acceptor levels were introduced by doping.

Next, these microwires were used as channels to build back-gated field effect transistors (FET) on silicon substrate, as shown in Fig. 8.5a and 8.5b). Electrical measurements were performed with the FET configuration. The change in conductance of ZnO wires as a function of gate voltage can be used to distinguish the conductive type of a given wire since the conductance will vary oppositely for increasing gate voltages [2]. Figure 8.5c shows the FET characteristics of undoped ZnO microwire-FET. The I_{SD} increases with increasing U_{SD} and the slopes of the I_{SD} versus U_{SD} curves increases with the gate voltages (U_G) posi(c)tively. The corresponding transfer characteristics [I_{SD}–U_G, inset of Fig. 8.6c] shows a positive slope of the I_{SD} vs. U_G curve, indicating that the undoped ZnO wire is *n*-type conducting. Figure 8.6 shows the FET characteristics of

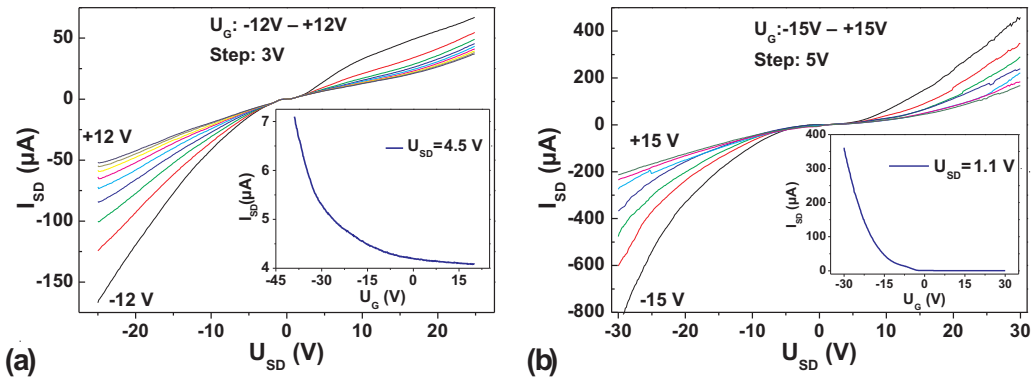

Figure 8.6: Output characteristics (I_{SD}–U_{SD}) and transfer characteristics (I_{SD}–U_G, *inset*) of two different ZnO:P wire-FETs, indicating *p*-type conductivity: (**a**) not fully depleted; (**b**) fully depleted.

doped ZnO:P microwire-FET. All curves are slightly nonlinear, which indicates that the contacts between wire and titanium electrodes are not ideally ohmic. However, the I_{SD}–U_{SD} curves show an inverse arrangement concerning the gate voltage compared to that of the undoped *n*-type wire FET in Fig. 8.5c. This is further demonstrated by the insets of Fig. 8.6, where the corresponding transfer characteristics of the ZnO:P wire FETs are shown. The source–drain current decreases with increasing gate voltages. This negative I_{SD}–U_G slope is opposite to that of the undoped (*n*-type) ZnO-FET in Fig. 8.5c. It indicates unambiguously that the conductivity of the phosphorus doped ZnO wires is *p*-type. The *p*-type conductivity was found to be stable over six months after their growth.

[1] B.Q. Cao et al.: Phys. Stat. Sol. RRL **2**, 37 (2008)
[2] B. Xiang, et al.: Nano Lett. **7**, 323 (2007)

8.6 Improved $BaTiO_3$–ZnO Heterojunctions Grown by Pulsed Laser Deposition

M. Brandt, G. Biehne, H. Hochmuth, M. Lorenz, M. Grundmann, V. Voora*, M. Schubert*

*Department of Electrical Engineering, University of Nebraska-Licoln, Lincoln, USA

Ferroelectric materials play an important role in present days technology. Their high dielectric, piezoelectric and pyroelectric makes them relevant for electric, electromechanic and electrooptic applications. However one of the most promising fields is the application in nonvolatile memory elements, due to the switchable spontaneous polarization. Crystallizing in the wurtzite structure, ZnO shows a spontaneous polarization, which is oriented antiparallel to the crystallographic *c*-axis. There are numerous calculations giving a value for the spontaneous polarization of ZnO [4, 6], but only a few experimental values are known [7]. A coupling of the materials and their polarizations gives rise to a variety of applications as polarization probes, optical switches, transparent non-volatile memory elements and transparent field effect transistors [1, 2].

Previously, BTO layers have been deposited by PLD on Si(100) and sapphire substrates, using a Pt back-contact in some cases [2]. The expected polarization coupling [3] has been observed in the junctions, but was only partially understood.

In order to understand the observed coupling effects in detail, and to quantify the spontaneous polarization in ZnO, a quantity only reported in very few publications up to now, a polarization coupling model has been. The model is based on the continuity of dielectric displacement, and the summation of the potentials across each of the layers. Finally the total surface charge of the structure is calculated assuming a metal–insulator (BTO)–semiconductor (ZnO) junction. Two simplifying assumptions have therefore been introduced:

- Complete insulation of the BTO layer, a condition, which cannot be completely fulfilled in an experimental situation.
- A potential build-up in the ZnO is present in the depletion regime, whereas no potential drop exists across the ZnO layer in the accumulation regime.

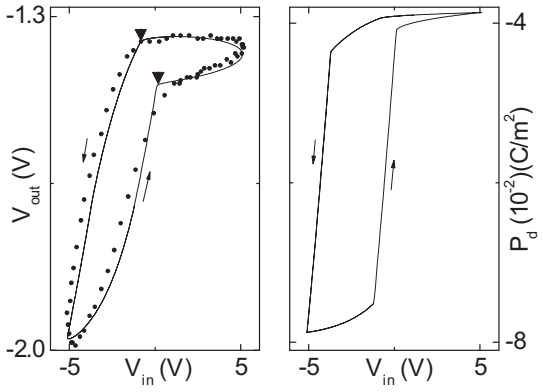

Figure 8.7: *Left*: Experimental (*dotted line*) and calculated data (*solid line*) for the Sawyer–Tower response of a BTO–ZnO heterostructure. *Right*: calculated ferroelectric polarization in the BTO layer. *Arrows* indicate the voltage sweep direction, *triangles* show the points where the depletion layer begins to form.

A detailed description of the model is given in [5]. The calculations were used to model the behavior of the samples in the Sawyer-Tower circuit measurement, and an excellent qualitative agreement was achieved (Fig. 8.7). From the model, a value for the spontaneous polarization of ZnO $P_{sz} = -4.1\ \mu\mathrm{Ccm}^2$ could be extracted, being in very good agreement with theoretical data previously published [4]. A very good qualitative agreement could also be achieved between frequency and excitation voltage dependent experimental data and the model predictions varying the respective parameter. A quantitative analysis of the measured data is the scope of ongoing investigations.

This work has been supported by Deutsche Forschungsgemeinschaft in the framework of FOR 404

[1] B.N. Mbenkum et al.: Appl. Phys. Lett. **86**, 091 904 (2005)
[2] J. Siddiqui et al.: Appl. Phys. Lett. **88**, 212 903 (2006)
[3] N. Ashkenov et al.: Thin Solid Films **486**, 153 (2005)
[4] F. Bernardini et al.: Phys. Rev. B **56**, R10 024 (1997)
[5] V. Voora et al.: *Interface-charge-coupled polarization response of Pt-ZnO-BaTiO3-Pt heterojunctions: A physical model approach*, J. Electron. Mat., in press
[6] Y. Kim et al.: Appl. Phys. Lett. **90**, 101 904 (2007)
[7] J. Jerphagnon et al.: Appl. Phys. Lett. **18**, 245 (1971)

8.7 Highly Reflective Oxide Material UV-Bragg Reflectors Grown by Pulsed Laser Deposition

J. Sellmann, H. Hilmer, C. Sturm, H. Hochmuth, J. Lenzner, B. Rheinländer, M. Lorenz, M. Grundmann

Low-threshold exciton-polariton lasers based on semiconductor microcavity-resonators are interesting devices for classical and quantum communication. For this purpose, resonator structures consisting of a ZnO microcavity embedded between an upper and a lower all-oxide Bragg reflector (BR) are very promising structures [1–3]. Because of

their large binding energy of approximately 60 meV, excitons in ZnO are stable at temperatures above room temperature [4]. Therefore, ZnO based resonators are applicable for the realisation of cavity coupled exciton-polariton lasers operating at room temperature and are predicted to work at temperatures up to 560 K [1]. In order to reach a high exciton-polariton lifetime in the microcavity, highly reflective BR are needed. For this, BR consisting of ZrO_2/Al_2O_3 layer pairs and Yttrium stabilised ZrO_2(YSZ)/Al_2O_3 layer pairs have been grown by means of pulsed laser deposition (PLD) on *c*-plane sapphire substrates. These high band-gap oxide materials are appropriate candidates for BR because of the large difference between the respective indices of refraction. For highly reflective BR smooth interfaces are necessary. As the optical properties of the ZnO cavity depend strongly on the surface morphology of the subjacent layer, the top layer of the substrate sided BR should exhibit a smooth surface and high crystal quality.

The BR layers have been deposited by means of pulsed laser deposition (PLD) on (0001)-sapphire substrates applying growth temperatures of about 600 °C and oxygen partial pressures in the range of 0.002 mbar to 0.02 mbar. The structural and optical properties of the layers were studied by X-Ray diffraction (XRD) measurements, atomic force microscopy (AFM), scanning transmission electron microscopy (STEM) and spectroscopic ellipsometry.

Low average surface roughnesses of $R_a = 0.7$ nm were achieved for 12.5 pair ZrO_2/Al_2O_3. STEM measurements revealed that the BR interfaces are well defined and smooth (Fig. 8.8). Thicknesses obtained by means of ellipsometry and STEM agree very well with each other with an average deviation of ±2 nm. The variations of the layer thicknesses throughout the whole layer stack were found to be ±4 nm for each material respectively. The reflectivity of the BR has to be very near to 1. We achieved the growth of BR with a maximum reflectivity R_{max} = 99.8 % at 3.31 eV (Fig. 8.9). This reflectivity value is sufficient for our laser application. We have fabricated many other BR with such high reflectivity and were able to adjust the spectral position of the stop-band by changing the layer thicknesses.

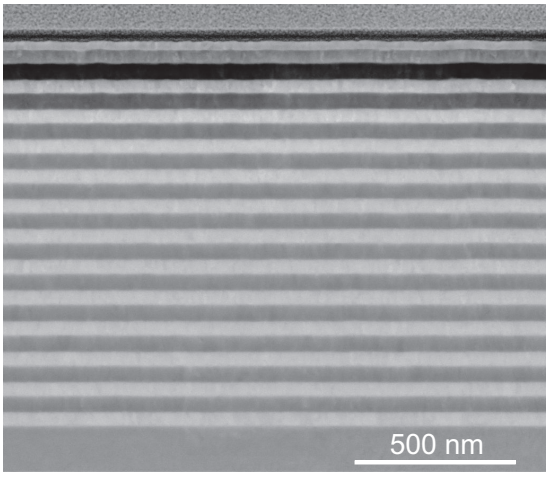

Figure 8.8: Scanning transmission electron microscopy image of a 12.5 pair ZrO_2/Al_2O_3 Bragg reflector on *c*-plane sapphire. The bright layers are ZrO_2 (thickness (42 ± 3) nm), the dark layers Al_2O_3 (thickness (52 ± 3) nm).

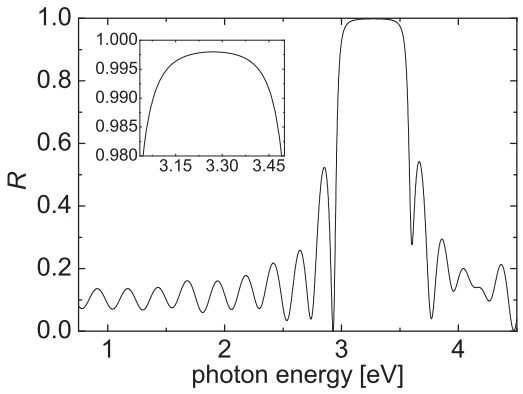

Figure 8.9: Reflectivity at normal incidence of a 12.5 pair ZrO_2/Al_2O_3 Bragg reflector optimised for the ZnO near band edge emission calculated from ellipsometry model fit.

XRD measurements revealed the YSZ layers to crystallise only in the (111) cubic phase opposed to the multi-phase crystal structure of ZrO_2. The full width at half maximum (FWHM) of XRD rocking curve scans (ω-scans) of the ZrO_2 and the YSZ layers are $FWHM(\omega)_{ZrO_2} = 6.5^\circ$ and $FWHM(\omega)_{YSZ} = 1.3^\circ$. Due to the higher quality of the YSZ crystal structure compared to ZrO_2 it is favourable to grow ZnO on YSZ-based BR. Applying low growth temperatures for the ZnO-layer leads to surface roughnesses down to $R_a = 0.7$ nm on the top of 10.5 pair YSZ/Al_2O_3 BR.

[1] M. Zamfirescu et al.: Phys. Rev. B **65**, 161 205 (2002)
[2] R. Schmidt-Grund et al.: Superlatt. Microstruct. **41**, 360 (2007)
[3] R. Schmidt-Grund et al.: Proc. SPIE **6038**, 603 827 (2005)
[4] Ü. Özgur et al.: J. Appl. Phys. **98**, 041 301 (2005)

8.8 Calculations of the Optical Properties of ZnO Microcavities for Bose–Einstein Condensation

C. Sturm, R. Schmidt-Grund, B. Rheinländer, M. Grundmann

Exciton-polaritons are quasi particles, which are formed due to the coupling between photons and excitons. Since photons as well as excitons are bosons, exciton-polaritons can undergo a Bose–Einstein Condensation (BEC). In contrast to diluted gases of atoms exciton-polaritons in high bandgap semiconductors can condensate even at room temperature and higher temperature [1]. A promising material for the realisation of BEC of exciton-polaritons at room temperature is ZnO due to its large exciton binding energy of approx. 60 meV so that the excitons are stable at room temperature. Another advantage of ZnO is its large exciton oscillator strength which will lead to a huge exciton-photon coupling (Rabi splitting) of about 120 meV [1]. Usually the exciton-polaritons are formed in microresonators, e.g. a ZnO based cavity embedded between two Bragg reflectors. For the optimization of these resonators the understanding of the coupling mechanism is important. We calculated the polariton branches as well as the critical exciton-polariton density in dependence on the Rabi splitting for ZnO based resonators in order to investigate the exciton-photon coupling on these structures. These investigations are based on the theoretical works reported by D. Porras et al., G. Rochat et al., V. Savona et al., and A. Kavokin et al. [2–5].

The exciton-polariton modes of the ZnO based resonator were calculated using a standard transfer-matrix approach. The resonator consists of a $\lambda/2$ ZnO-cavity as active medium embedded between two Bragg reflectors (BR). Both BR consist of 10.5 pair layer stacks of Al_2O_3 and ZrO_2. The dielectric function of the materials which were used for the calculation was determined by spectroscopic ellipsometry on BR as well as on ZnO films which were grown by pulsed laser deposition (PLD).

The calculated exciton-polariton branches are shown in Fig. 8.10. It can be seen that besides the ground-state exciton the first excited exciton states also couple with the photon modes, i.e. 6 exciton modes must be considered for describing the exciton-photon coupling. There is more than one photon mode which couples to each exciton mode. Such photon-modes are the Bragg band edge modes as well as a second (and/or third) first order cavity mode which also fulfill the condition $n(\lambda) \times d = \lambda/2$. The

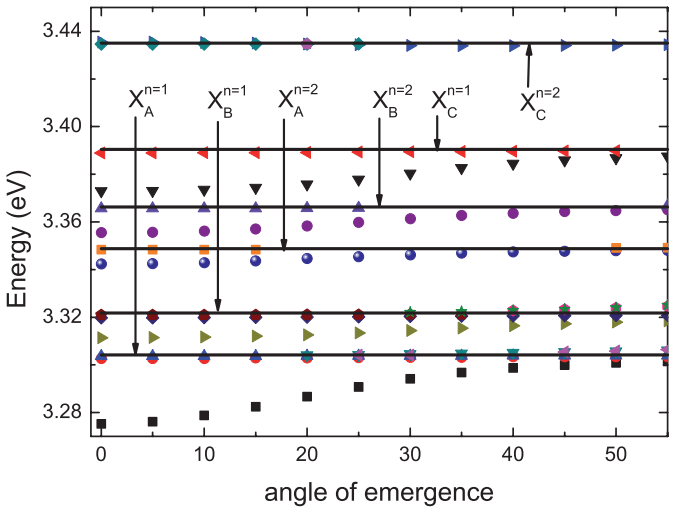

Figure 8.10: Calculated angular dispersion of the exciton-polariton modes in a λ-half ZnO resanontor. The cavity mode is tuned to the resonance of the B exciton of the ZnO. The *solid lines* represent the uncoupled exciton modes.

abbreviations $n(\lambda)$, d and λ denote the index of refraction, the thickness of the cavity and the vacuum wavelength of the cavity mode. Responsible for the occurrence of two or three cavity modes is the large change of the refraction index of ZnO in the spectral vicinity of the excitons. E.g., if the cavity is tuned to the resonance of the B-exciton, cavity modes can be found at 3.246 eV and at 3.322 eV. Further investigations are necessary for understanding of the whole coupling mechanism.

Furthermore, we investigated the critical exciton-polariton density (n_{crit}) for a BEC in dependence on the Rabi-splitting. It was found that for a Rabi-splitting Ω smaller than 40 meV BEC is not possible since n_{crit} is larger than the saturation density (n_{sat}). For densities larger than n_{sat} the density of the excitons is too large and thereby the fermionic character of the electrons and the holes dominates the excitonic behaviour and avoid BEC.

[1] M. Zamfirescu et al.: Phys. Rev. B **65**, 161 205R (2005)
[2] D. Porras et al.: Phys. Rev. B **66**, 085 304 (2002)
[3] G. Rochat et al.: Phys. Rev. B **61**, 13 856 (2000)
[4] V. Savona et al.: Phase Transitions **68**, 169 (1999)
[5] A. Kavokin, G. Malpuech: *Cavity Polaritons* (Elsevier, Amsterdam 2003)

8.9 Phosphorous Acceptor Doped ZnO Nanowires Prepared by Pulsed Laser Deposition

B.Q. Cao, M. Lorenz, A. Rahm, H. von Wenckstern, C. Czekalla, J. Lenzner, G. Benndorf, M. Grundmann

The lack of *p*-type conducting ZnO is the main bottleneck for its potential optoelectronic device applications. Up to now, there are only very few reports on doped ZnO

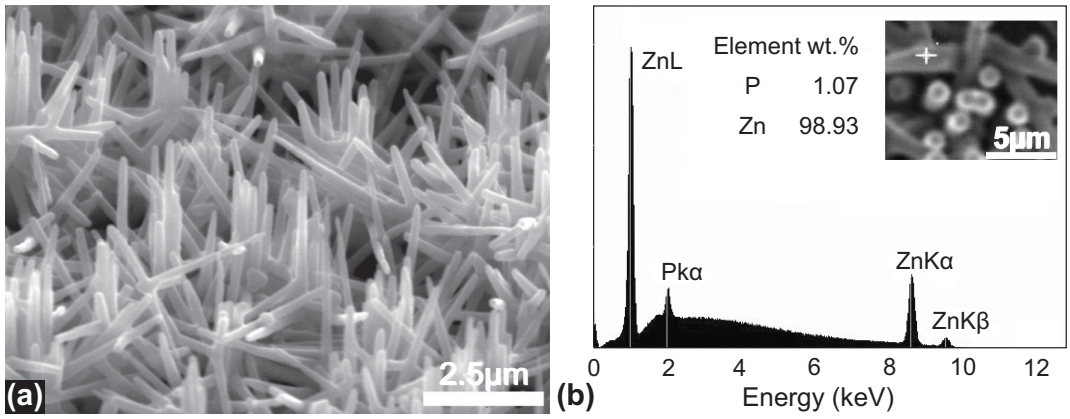

Figure 8.11: (**a**) SEM image of doped ZnO:P nanowires grown on sapphire substrate with 10 nm gold colloids as catalysts. (**b**) EDX spectrum of a single doped ZnO:P wire (see *inset*) showing clearly phosphorus signal.

nanowires for *p*-type conductivity in comparison with numerous published data on doped films. Phosphorous-doped ZnO (ZnO:P) nanowires were successfully prepared by a novel high-pressure pulsed-laser deposition process using phosphorus pentoxide (P_2O_5) as dopant source. Figure 8.11a) shows the SEM image of doped ZnO nanowires. The phosphorous doping leads to a more random growth of the doped wires. The phosphorous signal is clearly observed in the energy dispersive X-ray (EDX) spectrum, as shown in Fig. 8.11b), and the weight percentage of phosphorous in the nanowire is about 1 wt. %.

Low-temperature cathodoluminescence (CL) spectrum of single ZnO:P nanowire exhibits characteristic acceptor-related peaks: neutral acceptor-bound exciton emission

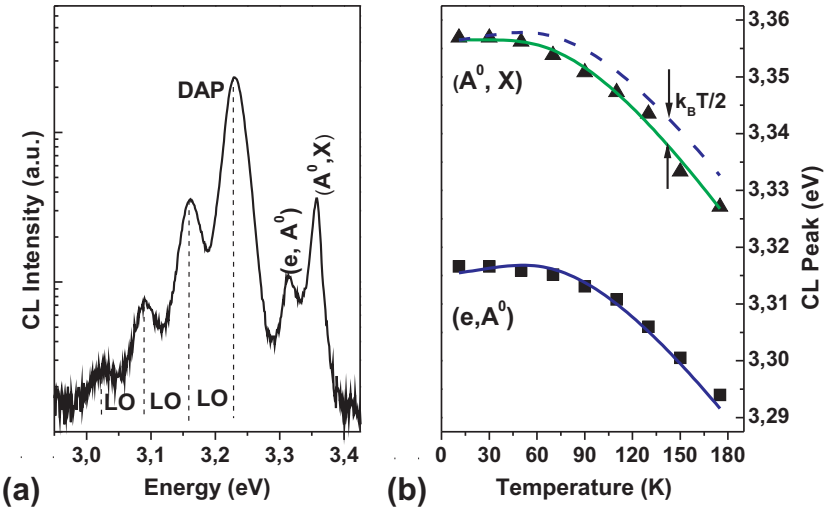

Figure 8.12: (**a**) Low-temperature (T = 11 K) CL spectrum of a single ZnO:P nanowire. (A^0,X), (e,A^0) and DAP with strong LO phonon replicas are observed. (**b**) CL peak energies versus temperature for the (e,A^0) and (A^0,X) peaks. *Solid symbols* are experimental data and *solid lines* are fitted with equations $E_{A^0,X}(T) = E_{A^0,X}(0) - 2\alpha_B\Theta_B[\coth(\Theta_B/2T) - 1]$ and $E_{e,A^0}(T) = E_g(T) - E_A + k_BT/2$, respectively. The *dashed line* is shifted to demonstrate the slope of the (e,A^0) fitted line (*blue*) near the (A^0,X) data points.

($E_{A^0,X}$ = 3.356 eV), free-to-neutral-acceptor emission (E_{e,A^0} = 3.314 eV), and donor-to-acceptor pair emission (E_{DAP} = 3.24 eV), as shown in Fig. 8.12a. These typical emissions can not be observed from undoped ZnO nanowires. It means that they are due to the intentional phosphorus doping. Temperature-dependent behavior of these new characteristic emissions proves their acceptor-related origin, as shown in Fig. 8.12b. Therefore, stable acceptor levels with a binding energy of about 122 meV are induced into the nanowires by phosphorus doping. CL intensity maps also prove that the distribution of the phosphorus acceptors is homogeneous along the nanowires [1].

[1] B.Q. Cao et al.: Nanotechnology **18**, 455 707 (2007)

8.10 Electronic Properties of Homoepitaxial ZnO:P Thin Films Grown by Pulsed Laser Deposition

H. von Wenckstern, M. Brandt, J. Zippel, G. Benndorf, H. Hochmuth, M. Lorenz, M. Grundmann

We investigated the low temperature recombination properties of homoepitaxial ZnO:P thin films grown by pulsed laser deposition on hydrothermal ZnO wafers. The wafers are not epi-ready in the as-delivered state and were, therefore, annealed in oxygen at 1000 °C for two hours resulting in a vicinal surface perfectly suited for epitaxy. Samples with nominal phosphorous doping concentrations of 0.01, 0.1 and 1 wt. % were deposited on the heat-treated ZnO wafers using oxygen partial pressures of 3×10^{-4}, 2×10^{-3}, 1.6×10^{-2} and 10^{-1} mbar, respectively.

Low temperature recombination spectra are shown for the phosphorous doped samples in Fig. 8.13. The samples were excited by an electron beam; the acceleration voltage was 10 kV and the beam current 400 pA. Already for the lowest phosphorous doping level investigated (Fig. 8.13a) clear differences compared to the recombination spectra of undoped homoepitaxial layers are observed [1]. The most evident differences are the recombination involving deep defects and the comparatively unstructured near band edge emission. A luminescence band centered at about 1.9 eV (r–o band) is observed independent of the oxygen partial pressure used during growth. It is assigned to a shallow donor to deep acceptor transition; the deep acceptor involved is an intrinsic acceptor preferably forming under oxygen rich conditions like V_{Zn}, O_i or O_{Zn} [2, 3]. For oxygen partial pressures of 2×10^{-3} mbar or lower a blue–violet (b–v) band centered at about 2.85 eV is observed. The appearance of the b–v band is accompanied by diminishing of the near band edge (NBE) emission. The intensity of the ro band seems not to be influenced by the b–v band. The recombination spectra of the sample series nominally containing 0.1 wt. % phosphorous (Fig. 8.13) show similar trends as the series containing 0.01 wt. %. However, the b-v band is already observable for an oxygen partial pressure of 0.016 mbar. The series nominally containing 1 wt. % phosphorous (Fig. 8.13c) behaves different than the two series discussed above. For oxygen partial pressures $\geq$ 0.016 mbar the r–o band dominates the recombination spectra. The NBE emission is comparatively weak and its maximum is shifted to lower energies. Only for this series the relative intensity of the NBE emission increases for the lower oxygen partial pressures, it is now structured and its maximum is shifted towards higher

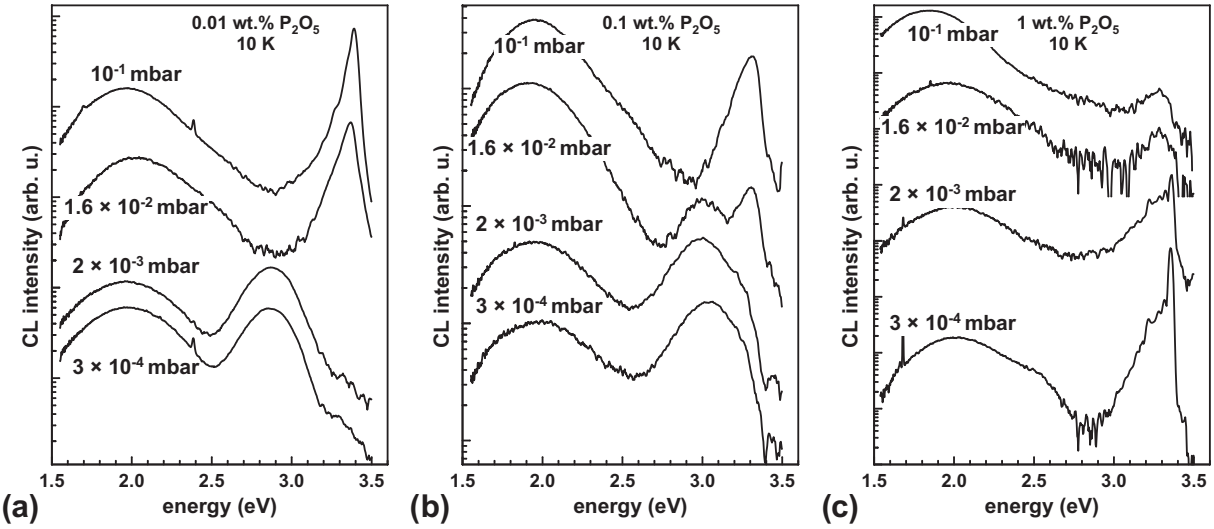

Figure 8.13: Low temperature cathodoluminescence spectra of ZnO:P thin films with nominal phosphorous content of (**a**) 0.01 wt. %, (**b**) 0.1 wt. %, and (**c**) 1 wt. % in dependence on the oxygen partial pressure.

energies. This behavior is opposite to that observed for the lower nominal phosphorous contents. Another difference is that the b-v band is not observed for the samples with 1 wt. % phosphorous.

Overall the low temperature recombination spectra indicate that the behavior of ZnO:P thin films is clearly different if the phosphorous content is below or equal and above 0.1 wt. %, respectively. The changes observed might be due to different lattice position of the phosphorous dopant. One might speculate that the phosphorous is incorporated at oxygen lattice site for low and at the zinc lattice site for high doping concentrations of phosphorous.

[1] H. von Wenckstern et al.: Phys. Stat. Sol. RRL **1**, 129 (2007)
[2] H. von Wenckstern et al.: Appl. Phys. A **88**, 125 (2007)
[3] H. von Wenckstern et al.: Proc. SPIE Int. Soc. Opt. Eng. **6895**, 689 505 (2008)

8.11 Absorption of MgZnO Determined from Transmission Measurements

A. Müller, G. Benndorf, H. Hochmuth, M. Grundmann

Temperature dependent transmission measurements have been performed on MgZnO thin films with Mg contents between 0 and 33 %. In the spectra of films with low Mg content, multiple minima are visible. These can be attributed to exciton phonon complexes (EPC) [1]. To calculate the exciton transition energy, the transmission spectra were fitted using the Adachi model dielectric functions (MDF) [2].

The dielectric function of the film is a sum of contributions from band-to-band transitions, discrete exciton states, unbound exciton scattering and EPC. Gaussian-like broadening was used for the MDF. The EPC are described by exciton-like transitions. It

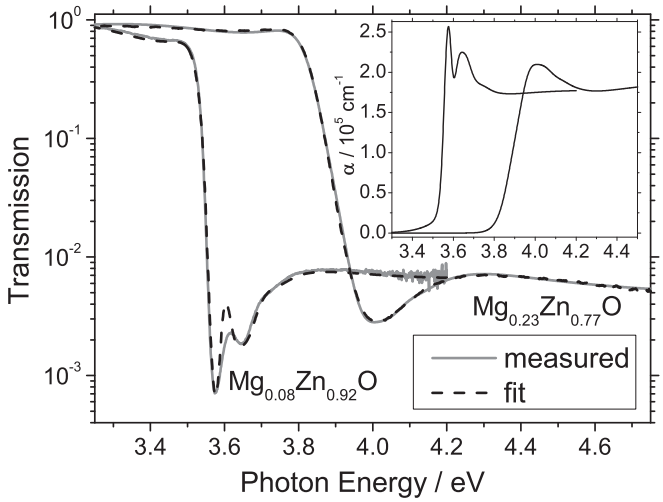

Figure 8.14: Fitted transmission spectra of two MgZnO samples at $T = 4$ K. The *inset* shows the calculated absorption coefficient.

was assumed that the transition strength shows a Poisson distribution and the transition energy as well as the broadening parameter depend linearly on the number of phonons.

A matrix formalism was used to calculate the transmission of the sample in dependence on the photon energy. As model, the layer sequence air/film/substrate was used. The thickness of the thin films was determined by room temperature ellipsometry. To fit the modeled curves to the transmission spectra, the MDF parameters were varied manually. Two sample specta are shown in Fig. 8.14.

For low Mg contents, a good description of the transmission minima was achieved, while the intervals between these show a poor fit. This may result from depth inhomogeneities, which were disregarded within the model. The fit for higher Mg contents is in very good agreement with the spectrum, but shows a high correlation between the parameters.

[1] W.Y. Liang, A.D. Yoffe: Phys. Rev. Lett. **20**, 59 (1968)
[2] S. Adachi, T. Taguchi: Phys. Rev. B **43**, 9569 (1991)

8.12 Photoluminescence Investigations of $Cd_xZn_{1-x}O$ Grown by Pulsed Laser Deposition

M. Lange, J. Zippel, H. Hochmuth, G. Benndorf, M. Lorenz, M. Grundmann

ZnO-based optoelectronic devices are well suited for possible applications like light emitting diodes or laser diodes working at wavelengths in the blue and UV spectral range. A bandgap range from about 2.3 to 8 eV can be covered by using the ternary alloys $Cd_xZn_{1-x}O$ (bandgap energy E_g decreases with increasing x) and $Mg_yZn_{1-y}O$ (E_g increases with growing y). The combination of $Cd_xZn_{1-x}O$ and $Mg_yZn_{1-y}O$ is auspicious for lattice matched heterostructures (for special pairs of x and y values [1]), such as quantum well structures with $Cd_xZn_{1-x}O$ as well material. In order to gain experience

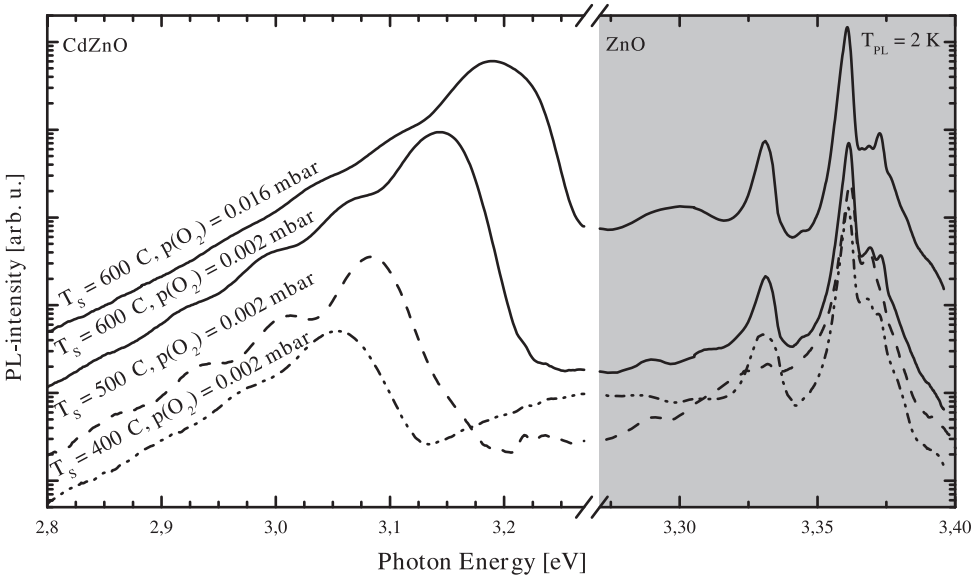

Figure 8.15: PL spectra of selected ZnO/CdO/ZnO DHS deposited under different conditions. The scale is stretched in the ZnO range and the baselines are shifted for clarity.

with the material system we deposited a number of double heterostructures (DHS) and investigated their PL-properties. Due to the thermodynamic solubility limit of Cd in ZnO, which is as low as $x = 0.02$ [1], the deposition of $Cd_xZn_{1-x}O$ with larger x is extremely difficult. On the other hand $Cd_xZn_{1-x}O$ changes from wurzite into rock-salt structure for $x > 0.8$, which results in a totally different band structure [2]. Therefore we deposited a ZnO/CdO/ZnO DHS by pulsed laser deposition. A very thin CdO layer was used. During the deposition the substrate temperature T_s was chosen within a range of 400 – 600 °C and oxygen partial pressure $p(O_2)$ between 0.002 and 0.16 mbar.

The photoluminescence (PL) spectra of some DHS are shown in Fig. 8.15. For photon energies greater than 3.27 eV the ZnO luminescence is observed, while at lower energies the PL is showing a broad and intensive peak followed by a number of phonon replica appearing at low energies. Similar luminescence features were reported for $Mg_yZn_{1-y}O$ thin films [3] but at higher energies. Until now there are two possibilities for the origin of $Cd_xZn_{1-x}O$ related luminescence: one is that there is a confinement effect because of the ZnO/CdO/ZnO DHS and we observe a quantum well PL. The other possibility is that the luminescence is due to an $Cd_xZn_{1-x}O$ alloy, that is formed by Cd diffusion during the PLD growth. If we assume an alloy of $Cd_xZn_{1-x}O$ one can estimate a value of $x \sim 0.04$. Further studies will clarify this point.

The energy of the $Cd_xZn_{1-x}O$ related luminescence was tuned from 3.0 to 3.2 eV by variation of T_s and $p(O_2)$. For smaller T_s the peak shifts to lower energies, maybe due to a better incorporation of Cd [4]. Changes in $p(O_2)$ result in the same tendency. The full width at half maximum could be minimized down to a value of 39 meV with setting $T_s = 500$ °C and $p(O_2) = 0.002$ mbar.

[1] T. Makino et al.: Appl. Phys. Lett. **78**, 1237 (2001), doi:10.1063/1.1350632
[2] J. Ishihara et al.: Appl. Surf. Sci. **244**, 381 (2005), doi:10.1016/j.apsusc.2004.10.094
[3] S. Heitsch et al.: J. Appl. Phys. **101**, 083 521 (2007), doi:10.1063/1.2719010
[4] S.Y. Lee et al.: Appl. Phys. Lett. **85**, 218 (2004), doi:10.1063/1.1771810

8.13 Simulation of Capacitance–Temperature Measurements on ZnO Schottky Diodes

M. Schmidt, M. Ellguth, A. Lajn, H. von Wenckstern, R. Pickenhain, M. Grundmann

Capacitance spectroscopic measurements are a powerful tool for the investigation of point defects in semiconductors. A space charge region (SCR) is required and can be provided by a metal–semiconductor interface, a Schottky contact. The SCR and thus its capacitance depends on the three experimentally tunable parameters: temperature, reverse bias voltage and probing frequency of the capacitance bridge. Typically, a series of capacitance–temperature (*C*–*T*) measurements is recorded for varying probing frequencies at fixed reverse bias.

In the measured *C*–*T* data, steps are visible that occur at different temperatures, depending on the probing frequencies. If the electron capture and emission rate of a defect is small compared to the probing frequency, the defect cannot be charged and decharged by the probing voltage, if the rates are much greater than the probing frequency, the defect is in a quasi equilibrium at each time and contributes to the capacitance. Since the electron capture and emission rate of a defect depends exponentially on the temperature, there is a (probing frequency dependent) temperature range in which the defect starts to follow the probing voltage, so each step in the capacitance temperature curve represents the activation of a (donor-like) defect. Standard analysis makes use of single points in the measured *C*–*T* curves and gains information about energetical depth, and, with large errors, concentration and electron capture cross section. Our aim was to model the entire curve and gain more precise information about the defect concentrations and electron capture cross sections.

The simulation is based on two main steps, the solution of Poisson's equation inside the SCR, from which the potential as well as the charge density distribution can be obtained, and the solution of the donor occupancy time evolution equation by a Fourier ansatz. The time evolution of the donor occupancy includes the information about charging and decharging of the defects during one period of the probing voltage. The simulation results for the *C*–*T* measurements of a ZnO single crystal are shown

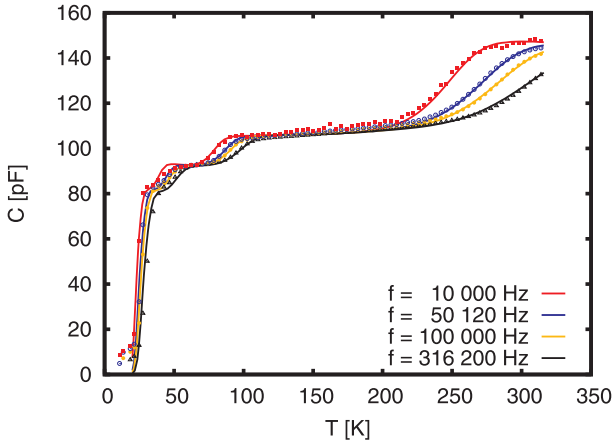

Figure 8.16: Measured (*dots*) and simulated (*lines*) *C*–*T* curves of a ZnO single crystal for four different probing frequencies. Simulation parameters can be found in Tab. 8.2.

Table 8.2: Traps found in the ZnO single crystal. Parameter values obtained from the simulation shown in Fig. 8.16.

trap	N_d [cm^{-3}]	$E_C - E_d$ [meV]	σ_n [cm^2]
	6×10^{15}	36	1×10^{-13}
	2×10^{16}	40	1×10^{-15}
E1 [3]	1×10^{16}	102	6×10^{-15}
E3 [3]	4×10^{16}	330	7×10^{-16}

in Fig. 8.16. The possible ambiguity of the chosen impurity parameters is strongly reduced by the request that all simulated curves with varying probing frequencies fit to the measurement data using only a single set of impurity parameters for *all* frequencies. It is also possible to distinguish between two energetically close lying defects, which is impossible by means of standard analysis.

[1] P. Blood, J.W. Orton: *The Electrical Characterization of Semiconductors: Majority Carriers and Electron States* (Academic Press, San Diego 1992)
[2] M. Schmidt: Diploma Thesis, Universität Leipzig, 2006
[3] F.D. Auret et. al.: Sup. Latt. Microsruc. **39**, 17 (2006)

8.14 Electronic Properties of Defects in ZnO with Levels at 300 and 370 meV below the Conduction Band

H. von Wenckstern, F.D. Auret*, W.E. Meyer*, P.J. Janse van Rensburg*, M. Hayes*, J.M. Nel*, G. Biehne, H. Hochmuth, M. Lorenz, M. Grundmann

*Physics Department, University of Pretoria, South Africa

High-quality Pd/ZnO Schottky diodes were realized on ZnO thin films grown heteroeptaxially on *a*-plane sapphire substrates by pulsed laser deposition. First, a 50 nm thick n^{++} ZnO:Al layer was deposited. The main layer, with a thickness of 1 µm, deposited on top of the n^{++} layer, is nominally undoped and was grown at a temperature of 650 °C at an oxygen partial pressure of 0.016 mbar. Circular Schottky contacts, having areas ranging from 4×10^{-4} to 5×10^{-3} cm^2, were realized by resistive evaporation of Pd on the nominally undoped ZnO layer. The n^{++} ZnO:Al layer was contacted by sputtered Au and serves as an ohmic back contact [1]. We have used deep level transient spectroscopy (DLTS) as well as high-resolution Laplace DLTS for the characterization of defects with DLTS peaks in the range from 165 K to 185 K. Figure 8.17a depicts high-resolution LDLTS spectra measured at 165 K, 175 K and 185 K. The signatures of two defects labelled E3 and E3′ are observed; the features appearing to the right of E3 are noise-related artifacts. From the temperature dependence of the defect emission rates the thermal activation energy $E_c - E_t$ of E3 and E3′ is obtained to be 300 meV and 370 meV, respectively. Next, we have performed high resolution Laplace DLTS using variable pulse widths shown in Fig. 8.17b. Because the peak heights of E3 are the same within the measurement accuracy for 165 K, 175 K and 185 K, only the data obtained for 175 K is depicted. It can be seen that there is little variation in the peak height of E3 for changes in the filling pulse between 2×10^{-5} and 8×10^{-1}s. This is typical for a point

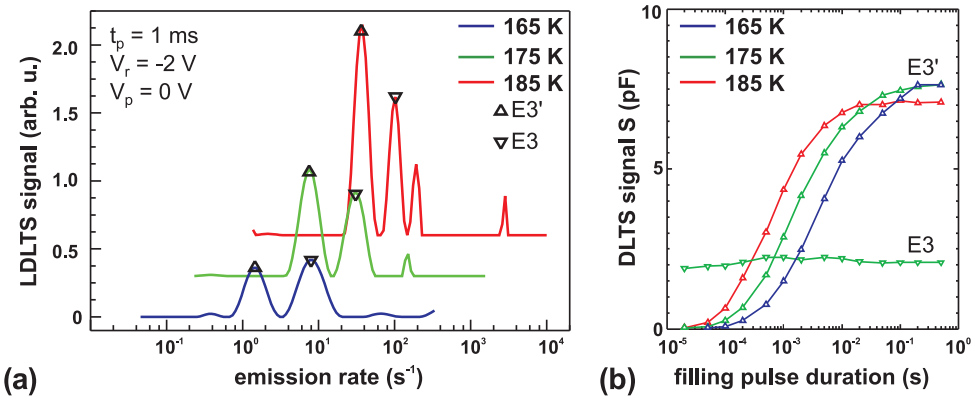

Figure 8.17: Laplace DLTS spectra of the E3 and E3′ defects (**a**) and peak heights of the E3 and E3′ peaks measured by Laplace DLTS as a function of filling pulse duration (**b**). For the E3 defect this dependence is similar for the different measuring temperatures.

defect with a temperature independent capture cross-section. The defect E3′ on the other hand, displays a strong dependence on filling pulse duration and temperature. For a given pulse filling width, the peak height of E3′ increases strongly with increasing temperature. For example, at a temperature of 165 K, its height increases by a factor of about 40 if the pulse width is increased from 200 μs to 200 ms, i.e. in the typical range of pulse widths used for DLTS. Also, for a typical DLTS pulse width of 1 ms, the E3′ peak height increases from 1.6 to 6 pF if the measurement temperature increases from 165 to 195 K. The data above indicates that electron capture onto E3′ is strongly temperature dependent. This behavior is often associated with a defect that has a capture barrier for carrier capture [2].

[1] H. von Wenckstern et al.: Appl. Phys. Lett. **88**, 092 102 (2006)
[2] F.D. Auret et al.: Physica B **401-402**, 378 (2007)

8.15 Defects in Hydrothermally Grown Bulk ZnO

H. von Wenckstern, H. Schmidt*, M. Grundmann, M.W. Allen†, P. Miller†, R.J. Reeves†, S.M. Durbin†

*now with Forschungszentrum Rossendorf, Dresden
†The MacDiarmid Institute for Advanced Materials and Nanotechnology, University of Canterbury, Christchurch, New Zealand

Hydrothermally grown ZnO wafers are the most frequently used substrates for the homoepitaxy of ZnO. The natural *n*-type conductivity of such single crystalline ZnO wafers is a topic of current interest. Candidates for the source of this *n*-type conductivity include intrinsic point defects, such as Zn_i or V_O and impurity atoms, such as group III elements, hydrogen, iron and nickel unintentionally introduced during crystal growth. We have used high-quality Ag/ZnO Schottky contacts on hydrothermal (HT) ZnO single crystalline wafers of *Tokyo Denpa Ltd.* to apply the space charge region based spectroscopic methods thermal admittance spectroscopy (TAS) and deep level transient

spectroscopy (DLTS). The room temperature free carrier density and Hall mobility of the wafer is $10^{14}\,\mathrm{cm}^{-3}$ and $200\,\mathrm{cm}^2/\mathrm{Vs}$, respectively. Prior to the TAS and DLTS measurements the sample was kept 24 h in the cryostat under dark conditions.

For admittance spectroscopy the diodes were held at zero bias during cooling and warm-up. The measurements were performed in the temperature range from 20 K to 330 K. Figure 8.18 depicts $C(T)$ and $G(\omega)/\omega$ for $\omega = 94\,000\,\mathrm{s}^{-1}$. Three shallow defect levels labeled T1, T2, and T3 are visible in $C(T)$ and $G(\omega)/\omega$ below 150 K. T3 is only visible as a comparatively small step in C and as a broadening on the high temperature side of T2 in $G(\omega)/\omega$. This indicates that T3 has a significantly lower concentration than T1 or T2. T1 and T2 were evaluated using an Arrhenius plot (Fig. 8.19b) from which we find $E_t(T1) = (13 \pm 2)$ meV and $E_t(T2) = (52 \pm 3)$ meV. For temperatures higher than 150 K, a broad double peak structure is visible in $G(\omega)/\omega$. This is related to the simultaneous thermal activation of two defects labeled E3 and E3′.

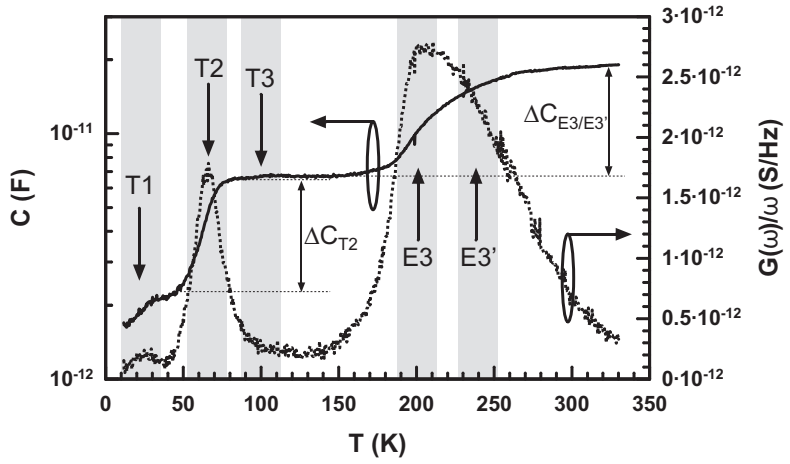

Figure 8.18: Temperature dependence of C and $G(\omega)/\omega$ of hydrothermal ZnO single crystal using a fixed test signal frequency of 15 kHz ($\omega = 94\,000\,\mathrm{s}^{-1}$).

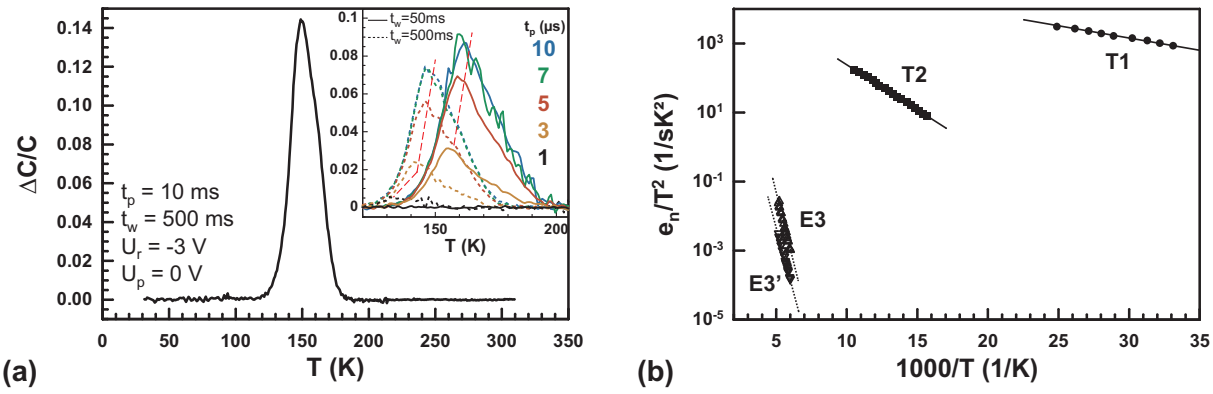

Figure 8.19: (**a**) DLTS signal of a hydrothermally grown ZnO single crystal (rate window: 2 Hz); the *inset* shows the DLTS signal due to E3/E3′ for different filling pulse lengths t_p and two different time windows t_w of 50 ms and 500 ms, respectively. (**b**) Arrhenius plot of the levels T1 and T2 of Fig. 8.18 yielding unambiguously their thermal activation energy and Arrhenius plots of E3 and E3′ as obtained from (**a**). Note that the high concentration of E3/E3′ and their superposition cause a large experimental error.

A typical DLTS signal is shown in Fig. 8.19a using a bias $U_r = -3\,\mathrm{V}$, a filling pulse height of 3 V ($U_p = 0\,\mathrm{V}$), and a filling pulse length $t_p = 10\,\mathrm{ms}$. The only deep levels observed are E3 and E3′. The inset of Fig. 8.19a shows the DLTS signal for two different time windows ($t_w = 50\,\mathrm{ms}$ and $t_w = 500\,\mathrm{ms}$) obtained for different filling pulse lengths t_p. The level E3 is visible for the shortest filling pulses applied ($t_p = 1\,\mu\mathrm{s}$), whereas the level E3′ is only visible for $t_p \geq 3\,\mu\mathrm{s}$. This is evident from the shift of the maxima of the DLTS peaks to higher temperatures with increasing t_p (indicated by the dashed red lines). It implies that the capture cross sections of the two defects are clearly different. A two-level fit was applied to DLTS signals recorded using different rate windows and the maxima used to construct an Arrhenius plot (shown in Fig. 8.19b) from which the thermal activation energies E_t are 318 meV for E3 and 321 meV for E3′. Their concentrations are approximately 8×10^{14} and $4\times10^{14}\,\mathrm{cm}^{-3}$, respectively. However, the values derived from the Arrhenius analysis of E3/E3′ have large experimental uncertainties.

However, the TAS and DLTS results unambiguously demonstrate that Tokyo Denpa hydrothermally grown ZnO contains three shallow defect levels, T1 ($E_t = 13\,\mathrm{meV}$), T2 ($E_t = 51\,\mathrm{meV}$), and T3 (T3 in a very low concentration), and two closely lying deep defect levels, E3 and E3′, with activation energies in the region of 320 meV [1].

[1] H. von Wenckstern et al.: Appl. Phys. Lett. **91**, 022 913 (2007)

8.16 Selective Area Growth of GaAs and InAs Nanowires – Homo- and Heteroepitaxy Using SiN_x Templates

H. Paetzelt*, V. Gottschalch*, J. Bauer*, G. Benndorf

*Fakultät für Chemie und Mineralogie, AK Halbleiterchemie

We have fabricated GaAs, InAs nanowires and QW-structures using selective-area metalorganic vapor phase epitaxy (SA-MOVPE) [1, 2]. The nanowires were grown on various oriented GaAs substrates partially covered with SiN_x. We used plasma enhanced chemical vapor deposition (PECVD) for deposition of 15 nm SiN_x on (100), (110), (111)A and (111)B GaAs substrates [3]. The SiN_x was partially removed by electron beam lithography (EBL) and wet chemical etching using NH_4F:HF:H_2O solutions. The SA-MOVPE growth was carried out in a horizontal reactor using trimethylgallium (TMG), trimethylindium (TMI) as group-III sources and arsine (AsH_3) as group-V source. The total flow into the reactor was amounted to 7 slm and the pressure was 50 mbar. The circular openings in the SiN_x were arranged in a triangular lattice with a pitch of 0.6 – 1 μm. The diameter of the nanowires is related to the openings diameter in the SiN_x-layer which were in the range of 200 nm.

At optimized conditions, a combination of $T_{\mathrm{growth}} = 800\,^{\circ}\mathrm{C}$ and a V/III ratio of 260 results in uniform and high density arrays of GaAs nanowire on (111)B GaAs substrate. Figure 8.20 shows such a nanowire-array with a pitch of 0.6 μm, a nanowire diameter of 200 nm and a length of 1.8 μm for a growth time of 20 min. The sidewalls of the wires are six {110} facets [4] which yield to a hexagonal cross section of the GaAs nanowires grown in (111)B direction. For the growth of InAs nanowire arrays with high aspect ratio nanowires on (111)B GaAs substrate we used lower temperatures

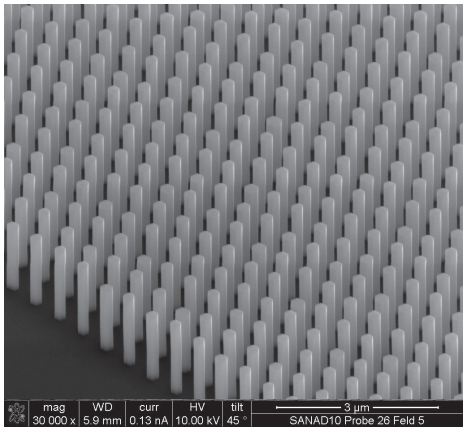

Figure 8.20: SEM image of selective-area grown GaAs nanowires on (111)B substrate.

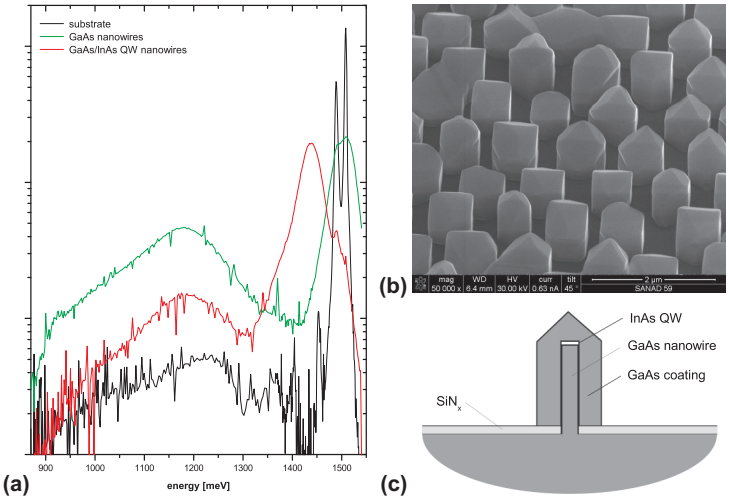

Figure 8.21: a) PL spectra at 4 K of GaAs nanowire-array with and without InAs QW, (**b**) nanowire-array with InAs QW, (**c**) shematic illustration of GaAs/InAs QW structure.

(600 ℃) and a higher V/III ratio of 550. In a combination of GaAs and InAs SA-growth a InAs quantum well (QW) was embedded into GaAs. Therefor the GaAs bottom barrier nanowire was grown (T = 800 ℃, V/III = 260, t = 10 min), cooling down to 600 ℃ under arsine flow, InAs QW (T = 600 ℃, V/III = 140, t = 2.5 s), GaAs coating (T = 600 ℃ to 800 ℃, V/III = 260, t = 2 min) and finally the growth of GaAs top barrier (T = 800 ℃, V/III = 263, t = 10 min). Due to the InAs QW and the GaAs coating the nanowires lose their hexagonal shape. Figure 8.21b and 8.21c show a SEM image of a GaAs/InAs QW array and a schematic illustration of the structure. Figure 8.21a shows photoluminescence (PL) spectra at low temperatures (4 K) for GaAs nanowires with and without InAs QW from $500 \times 500\ \mu m^2$ arrays with a pitch of 1 µm. The peak observed at energy of 1438 meV is due to the InAs QW with a thickness of around one monolayer formed on the (111)B facet of the GaAs bottom barrier nanowire.

[1] T. Hamano et al.: Jpn. J. Appl. Phys. **36**, L286 (1997)
[2] J. Motohisa et al.: J. Cryst. Growth **272**, 180 (2004)
[3] V. Gottschalch et al.: Thin Solid Films **416**, 224 (2002)
[4] K. Ikejiri et al.: J. Cryst. Growth **298**, 616 (2007)

8.17 Growth of β-Ga_2O_3 on Al_2O_3(0001) Using Metal-Organic Vapor-Phase Epitaxy

V. Gottschalch*, K. Mergenthaler*, R. Bindig*, J. Bauer*, H. Paetzelt*, U. Teschner

*Fakultät für Chemie und Mineralogie, AK Halbleiterchemie

Monoclinic β-Ga_2O_3 is a wide band gap semiconductor with a direct bandgap of 4.9 eV [1–3]. Epitaxial β-Ga_2O_3 is applicable to deep-ultraviolet (DUV) photodetectors [3, 4] and as a substrate for the growth of GaN-based compounds [5]. Monoclinic

β-Ga_2O_3 epitaxial layers and nano-structures have been prepared by several methods, such as sol-gel techniques, pulsed spray pyrolysis, molecular beam epitaxy and pulsed laser deposition.

In this paper we have studied the MOVPE growth of β-Ga_2O_3 on differently oriented Al_2O_3 substrates. The epitaxial growth of Ga_2O_3 was carried out in a horizontal cold wall reactor at atmospheric pressure. The precursors were separatly introduced into the growth region of the reactor. We used triethylgallium (TEG) as gallium precursor and N_2O as oxygen source. We have studied the growth on *a*-, *c*- and *r*-plane Al_2O_3 substrates within a temperature range between 700 and 800 ℃ and applied N_2 as carrier gas. The flow rates of TEG and N_2O were 5.2 μmol/min and 22 μmol/min, respectively. The growth rate was 0.7 μm/h.

The Ga_2O_3 films were analyzed by means of X-ray diffraction, scanning electron microscopy, cathodoluminescence and transmission measurements. The XRD-patterns (Fig. 8.22a) show three Ga_2O_3 peaks, indicating that the epitaxial material consists of stable β-Ga_2O_3. The XRD scans (Ω–2Θ- and ϕ-scan) definitely indicate the stable β-Ga_2O_3 phase and the epitaxial relationship between Ga_2O_3 layer and substrate (Fig. 8.22):

$$(\bar{2}01)\,\beta\text{–}Ga_2O_3 \parallel (0001)\,Al_2O_3\,, \qquad [010]\,\beta\text{–}Ga_2O_3 \parallel [10\bar{1}0]\,Al_2O_3\,. \tag{8.2}$$

The indicated sixfold rotational symmetry of asymmetric reflexions (Fig. 8.22b) of monoclinic β-Ga_2O_3 results from differently oriented rotational domains. The orientation of the domains is caused by the threefold symmetry of the Al_2O_3 (0001) surface.

Figure 8.23a shows a SEM image of the surface of a 500 nm thick β-Ga_2O_3 film grown at 800 ℃, mirror-like surfaces have been observed. The surface steps probably originate from the differently oriented rotational domains. Figure 8.23b shows the optical transmittance spectra for β-Ga_2O_3 taken from a 500 nm thick layer. The *c*-plane sapphire substrate was used as a reference material. This nominally undoped β-Ga_2O_3

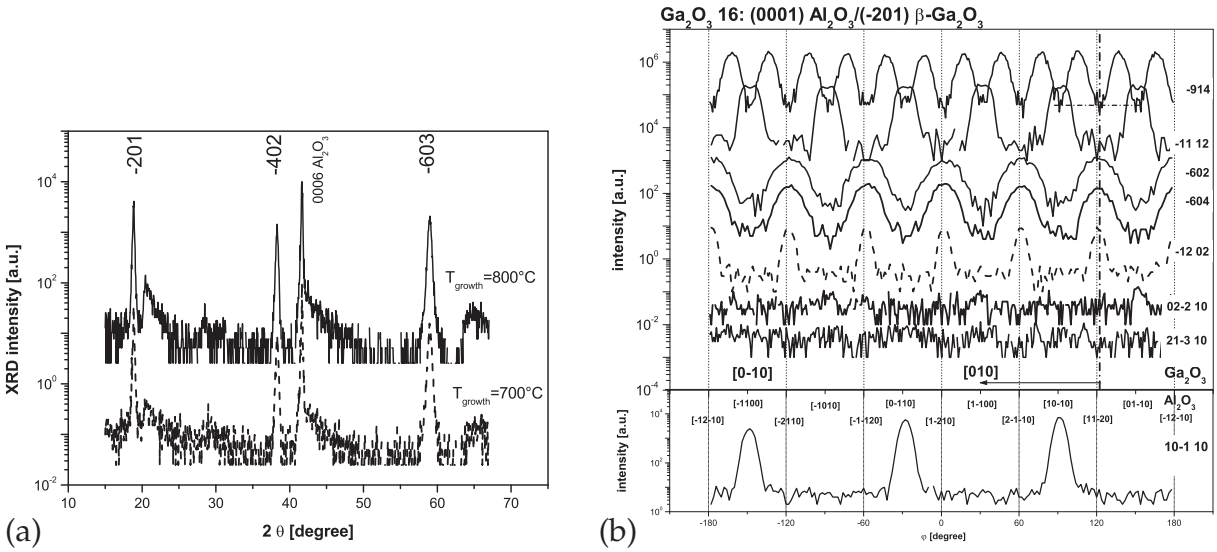

Figure 8.22: (**a**) XRD Ω–2Θ scan of 500 nm thick β-Ga_2O_3 layer on Al_2O_3 (0001) substrate. (**b**) ϕ-scans of the β-Ga_2O_3 layer and the Al_2O_3 substrate.

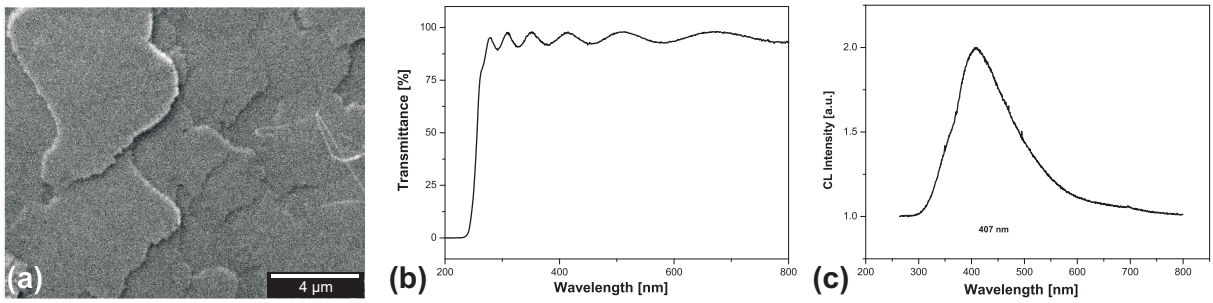

Figure 8.23: SEM images (**a**), transmission spectrum (**b**) and cathodoluminescence spectrum (**c**) of a β-Ga_2O_3 layer deposited on Al_2O_3 (0001) at 800 °C.

layer shows high optical transmittance in the visible wavelength region. We observed a high optical transmittance of over 90 %. Emission from UV to green could be detected using cathodoluminescence technique (Fig. 8.23c). This is in good agreement with the reported different radiative recombination processes [6].

[1] M. Orita et al.: Appl. Phys. Lett. **77**, 4166 (2000)
[2] N. Suzuki et al.: Phys. Stat. Sol. C **4**, 2310 (2007)
[3] T. Oshima et al.: Thin Solid Films **416**, 224 (2002)
[4] T. Oshima et al.: Appl. Phys. Express **1**, 011 202 (2008)
[5] S. Ohira et al.: Phys. Stat. Sol. C **4**, 2306 (2007)
[6] E.G. Villora et al.: Solid State Comm. **120**, 455 (2001)

8.18 Growth of ZnO Quantum Dots Embedded Films Using Metal-Organic Vapor-Phase Epitaxy

K. Mergenthaler*, V. Gottschalch*, H. Paetzelt*, J. Bauer*, G. Wagner†, G. Benndorf

*Fakultät für Chemie und Mineralogie, AK Halbleiterchemie
†Institut für Mineralogie, Kristallographie und Materialwissenschaften

Because of the wide band gap (3.37 eV) and the large exciton binding energy (60 meV) ZnO is a very promising material for future applications. ZnO nanoparticles smaller than about 10 nm in diameter exhibit a so-called quantum size effect, an enlargement of the band gap that is typically measured by blue shift of light absorbance and emission [1]. Such nanoparticles can be synthesized by various methods [2–5]. In this paper we studied the atmospheric pressure metal-organic vapor-phase epitaxial growth of ZnO nanocrystal embedded into amorphous ZnO films on sapphire substrates. We used the precursor diethylzinc (DEZn) as zinc source and iso-propanol (i-PrOH) as oxygen source, the carrier gas was N_2. We have studied the growth within a temperature range between 300 and 450 °C and an oxygen to zinc ratio (VI/II) range between 45 and 720. The TEM image (Fig. 8.24) shows the grown ZnO nanocrystals for growth temperature T_{growth} = 400 °C and VI/II = 45. The nanocrystal size ranges for this sample between 5 and 10 nm. The electron diffraction image in Fig. 8.24 shows the polycrystalline nature of the quantum dots and the amorphous state of the embedding layer.

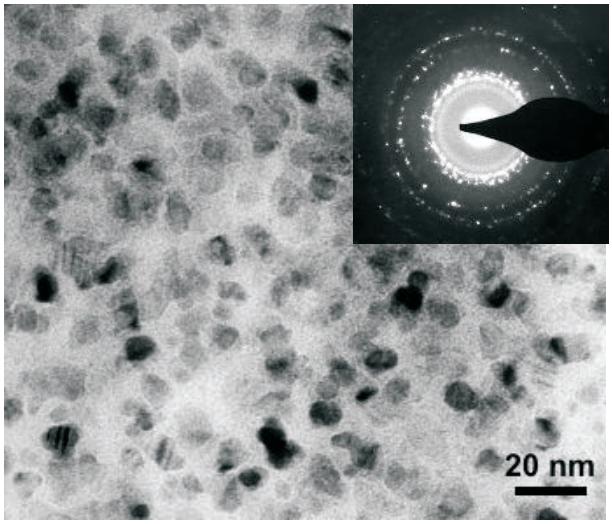

Figure 8.24: TEM image of ZnO nanocrystals embedded into amorphous ZnO and corresponding SAD pattern in the *inset*.

The amorphous layer has a higher band gap than the bulk material, so in the nanocrystals quantum confinement effects are possible. For low quantum dot diameters the measured energy gap is shifted to higher energies depending on the dot diameter [6]. The size-dependence can be described by the following equation [2, 6]:

$$E_{(\text{gap,QDs})} = E_{(\text{gap,bulk})} + \frac{\pi^2\hbar^2}{2R^2}\left(\frac{1}{m_e^*} + \frac{1}{m_h^*}\right) - 0.248E_{\text{Ryd}}^* \tag{8.3}$$

The bulk band gap $E_{(\text{gap,bulk})}$ is taken as 3.37 eV and the bulk exciton binding energy E_{Ryd}^* as 60 meV. According to [7] the effective masses of electrons and holes are taken as $m_e^* = 0.24m_0$ and $m_h^* = 0.59m_0$, respectively.

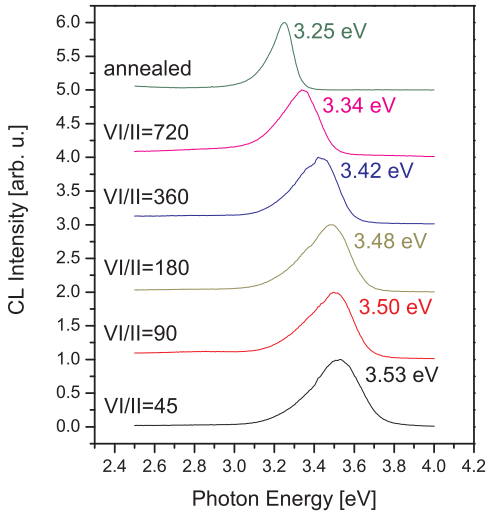

Figure 8.25: Room temperature cathodoluminescence spectra of samples grown at different VI/II ratios and a sample annealed in N_2O at 800 °C.

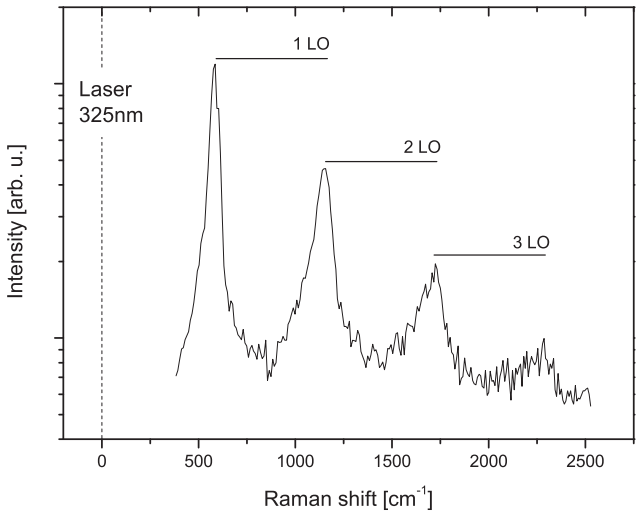

Figure 8.26: Resonant Raman scattering of a sample grown at T_{growth} = 400 °C and VI/II = 45.

In Fig. 8.25 the cathodoluminescence spectra of samples grown at different VI/II ratios are shown. It is believed [5], that the nanocrystals are formed in gaseous phase and than incorporated into the ZnO film during growth. So the size of the nanocrystals is highly dependent of the composition in the gas phase. This can be seen in the different energy shifts of the luminescence in Fig. 8.25. Higher growth rates (lower VI/II) causes smaller diameters. For lower growth rates (higher VI/II) the measured energy lies closer to the bulk value. The measured QD diameter (5 to 10 nm, see Fig. 8.24) fits well to the calculated value of 6.6 nm (for VI/II = 45). An annealing step at 800 ℃ with N_2O atmosphere leads to partly recrystallisation of the amorphous ZnO. The crystal size increases and no longer a blue shift can be measured (top graph in Fig. 8.25).

By observing the size dependence of intensity ratio between the second- and the first-order Raman scattering one can evaluate the coupling strength of the electron-phonon interaction. This ratio was found to increase remarkably while an increase of crystallite size [4]. The resonant Raman scattering for the sample grown with VI/II = 45 can be seen in Fig. 8.26. The very low intensity ratio of ≈ 0.38 observed herein is therefore also an indication for the quantum dot formation.

[1] U. Koch et al.: Chem. Phys. Lett. **122**, 507 (1985)
[2] K.K. Kim et al.: Appl. Phys. Lett. **84**, 3810 (2004)
[3] L. Mädler et al.: J. Appl. Phys. **92**, 6537 (2002)
[4] H.M. Cheng et al.: Appl. Phys. Lett. **88**, 261 909 (2006)
[5] S.T. Tan et al.: J. Cryst. Growth **290**, 518 (2006)
[6] Y. Kayanuma: Phys. Rev. B **38**, 9797 (1988)
[7] K. Hümmer: Phys. Stat. Sol. B **56**, 249 (1973)

8.19 Heteroepitaxial MOVPE Growth of InAs Nanowires on GaAs $(\bar{1}\bar{1}\bar{1})_B$

J. Bauer*, V. Gottschalch*, H. Paetzelt*, G. Wagner†, U. Pietsch‡, J. Lenzner

*Fakultät für Chemie und Mineralogie, AK Halbleiterchemie
†Institut für Mineralogie, Kristallographie und Materialwissenschaften
‡Universität Siegen, Festkörperphysik

Semiconductor nanowires (NW) acquire recently attraction because of promising new application fields in electronics and optoelectronics. We applied the vapor–liquid–solid (VLS) mechanism with gold seeds in combination with low-pressure metal-organic vapor phase epitaxy (LP-MOVPE) to achieve reproducible growth of InAs single crystal NWs with high growth rates. While the growth of heterojunctions with group-V material change has been successfully demonstrated [1], the growth of the desirable III-As heterostructures is problematic. Frequently, heterostructure growth is accompanied by characteristic phenomena like kinking, increased twin density, the formation of diffuse heterojunctions with alloy crystal gradients instead of abrupt interfaces [2], and growth along a side facet of the already grown NW [3, 4]. However, sharp axial InAs/GaAs heterojunctions have been reported [5], which motivates a more detailed investigation of the material system.

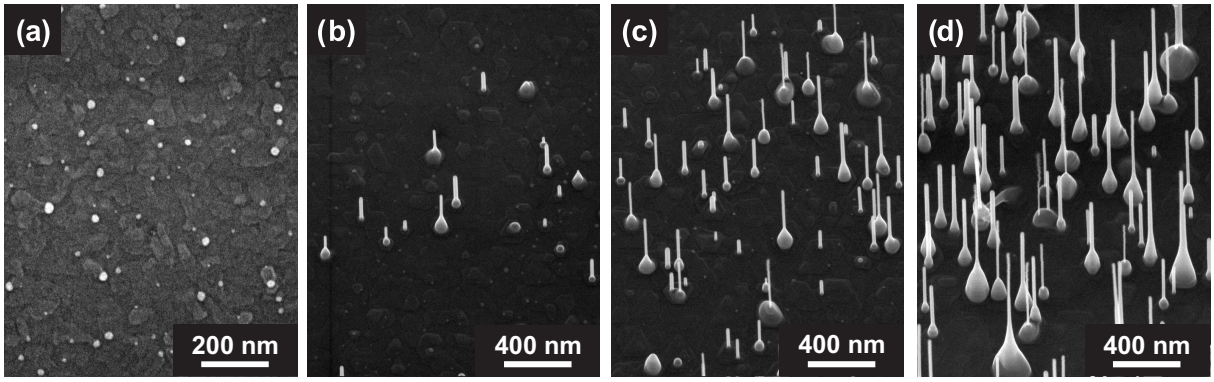

Figure 8.27: Temporal evolution of InAs NW growth on GaAs$(\bar{1}\bar{1}\bar{1})_{As}$ substrate (450 °C, V/III = 10, gold film thickness < 1 nm). The growth duration was set to (**a**) 20 s, (**b**) 40 s, (**c**) 60 s and (**d**) 120 s. The sample in (**a**) is shown in top view, while those in (**b**)–(**d**) are tilted by 20°.

The nanoheteroepitaxial growth was studied at the initial growth of InAs NWs on GaAs$(\bar{1}\bar{1}\bar{1})_B$ substrate. At elevated temperatures the gold seeds alloy with the substrate material resulting in Au–Ga alloy droplets. Hence, the starting situation prior to InAs NW growth is comparable to the situation of GaAs/InAs NW heterostructure growth. With the precursors TMI and arsine the effect of growth temperature, V/III ratio and growth duration were investigated. Figure 8.27 shows the time dependence of InAs NW growth at 450 °C. The V/III ratio was set to 10 with a TMI partial pressure of 0.36 Pa. A time delay was observed before which no NW growth occurs. In this initial growth duration droplets move over the substrate surface. After about 40 s NW start to

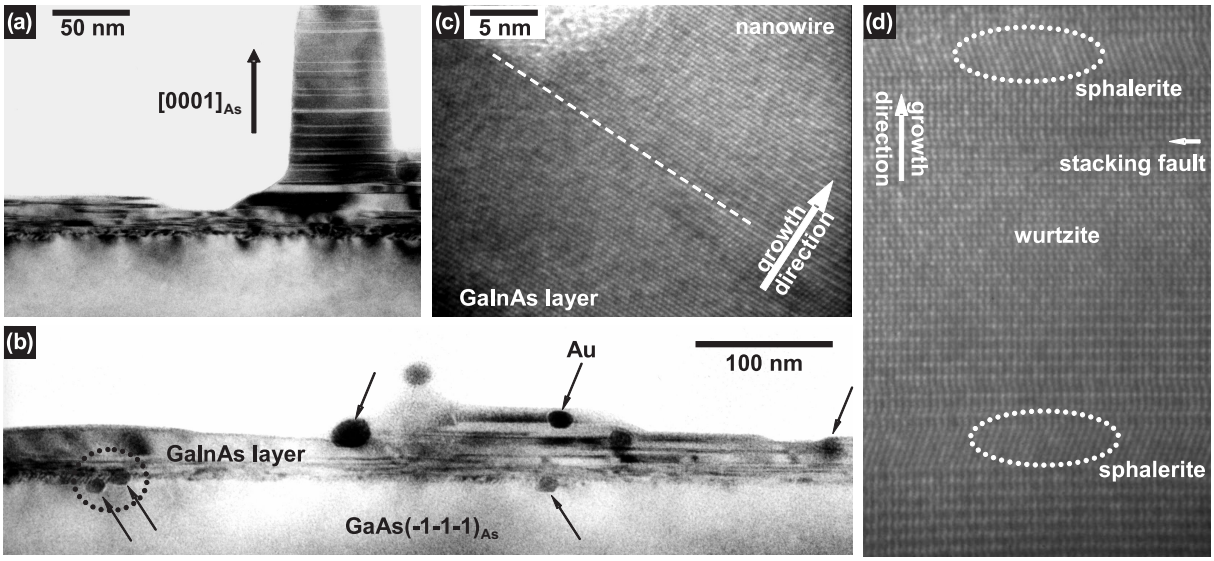

Figure 8.28: TEM investigation of InAs NW growth on GaAs$(\bar{1}\bar{1}\bar{1})_{As}$ substrate (450 °C, V/III = 80, 2 min, gold film thickness < 1 nm). (**a**) TEM bright-field image ($(\bar{1}10)$ cross-section) of the sample structure. (**b**) GaInAs layer below the InAs NW. Embedded gold particles are indicated by arrows. (**c**) HRTEM image of the structural transition between the cubic GaInAs layer and a hexagonal InAs NW. (**d**) Real-structure of an InAs NW showing stacking faults and sphalerite type structure lamella.

grow. With increasing growth time the NW length is enhanced but also the dimensions of the NW foot sections. While the first observation confirms the expected steady-state NW growth process, the second one gives advice for InAs gas-phase deposition. The influence of V/III ratio on the surface diffusion length of the precursor molecules and atoms is discussed controversial in literature. Related results concerning the InAs NW morphology suggest, that group-III elements have a short surface diffusion length at low V/III ratios. The NW foot seems to be preferred nucleation site and because of the short surface diffusion length at V/III = 10 InAs vapor-phase deposition is concentrated in the NW foot region. Related to the observed time delay TEM and grazing-incidence XRD experiments revealed the formation of a graduated $Ga_xIn_{1-x}As$ alloy layer on the substrate out of which the NW growth starts (Fig. 8.28a). This alloy layer has a thickness of about 40 nm with a Ga-content ranging from 6 to 22 at. %. Gold particles alloyed with indium were found embedded into this layer (Fig. 8.28b). While the $Ga_xIn_{1-x}As$ layer has sphalerite type crystal structure the InAs NWs are wurtzite (Fig. 8.28c). At 450 °C, a V/III-ratio of 80, and 2 min growth duration the InAs NWs have a length up to 4 μm and diameters from 35 to 70 nm. In the NW foot region a Ga content of 11 at. % was verified at a single NW. The mainly hexagonal InAs NW contain stacking faults and sphalerite type structure lamella (Fig. 8.28d). The lattice parameters of the InAs NWs were determined by a combination of conventional XRD (out-of-plane lattice parameters) and gracing incidence XRD (in-plane lattice parameters). Thus, the lattice constants $a = 4.243$ Å and $c = 7.025$ Å ($c/a = 1.656$) were obtained.

[1] M.T. Björk et al.: Nano Lett. **2**, 87 (2002)
[2] K. Hiruma et al.: J. Cryst. Growth **163**, 226 (1996)
[3] K.A. Dick et al.: Nano Lett. **7**, 1817 (2007)
[4] M. Paladugu et al.: Small **3**, 1873 (2007)
[5] B.J. Ohlsson et al.: Physica E **13**, 1126 (2002)
[6] J. Bauer et al.: J. Cryst. Growth **298**, 625 (2007)

8.20 Funding

One-dimensional heterostructures and nanowire arrays
Prof. Dr. M. Grundmann, Dr. M. Lorenz
DFG Gr 1011/11-1 within DFG Forschergruppe FOR 522 *Architecture of nano- and microdimensional building blocks*

Lateral optical confinement of microresonators
Prof. Dr. B. Rheinländer, Dr. V. Gottschalch
DFG Rh 28/4-1 within DFG Forschergruppe FOR 522 *Architecture of nano- and microdimensional building blocks*

Transferability of the codoping concept to ternary ZnO:(Cd,Mg)
Prof. Dr. M. Grundmann, Dr. H. Schmidt
DFG Gr 1011/10-2 within DFG-Schwerpunktprogramm 1136 *Substitutionseffekte in ionischen Festkörpern*

Self-assembled Semiconductor Nanostructures for New Devices in Photonics and Electronics (SANDiE)
Coordinator: Universität Leipzig, Prof. Dr. M. Grundmann
Sixth Framework Programme, European Network of Excellence, Contract NMP4-CT-2004-500101

Leipzig School of Natural Sciences – Building with Molecules and Nano-objects (BuildMoNa)
Prof. Dr. M. Grundmann
GSC 185/1

III-V-Semiconductor Nano-Heterostructures for Advanced Opto-Electronic Devices
Prof. Dr. B. Rheinländer
BMBF: Bilaterale Zusammenarbeit BRD-Slowakei: SVK 01/001

New gallium phosphide grown by vertical gradient freeze method for light emitting diodes
Prof. Dr. B. Rheinländer
(VGF GaP - LED's) No. IST - 2001-32793, EU-FP5-Projekt and BMBF: Bilaterale Zusammenarbeit BRD-Slowakei: SVK 01/001

Interface-related properties of oxide quantum wells
Prof. Dr. M. Grundmann, Dr. V. Gottschalch
DFG Gr 1011/14-1 within DFG Forschergruppe FOR 404 *Oxidic interfaces*

Interface-induced electro-optical properties of oxide semiconductor-ferroelectric thin film heterostructures
Dr. M. Schubert, Dr. M. Lorenz
DFG Schu 1338/4-1 within DFG Forschergruppe FOR 404 *Oxidic interfaces*

Semiconductor oxides for UV optoelectronics, surface acoustics and spintronics
Prof. Dr. M. Grundmann, Dr. M. Lorenz
SOXESS European Network on ZnO (Thematic Network), Fifth Framework Programme, Competitive and sustainable growth, Contract G5RT-CT-2002-05075

Nanophotonic and nanoelectronic Devices fom Oxide Semiconductors (NANDOS)
Prof. Dr. M. Grundmann, Dr. M. Lorenz
EU STReP Contract No. 016 424

BMBF-Nachwuchsgruppe "Nano-Spinelektronik"
Dr. H. Schmidt
BMBF FKZ 03N8708

Deutsch-Chinesische Kooperation zur Entwicklung von transparenten und halbleitenden GMR und TMR Prototyp-Bauelementen
Dr. H. Schmidt
BMBF CH05/010

Ferromagnetism in transition metal doped ZnO
Dr. H. Schmidt
DFG Schm 1663/1-1

8.21 Organizational Duties

M. Grundmann

- Direktor des Institut für Experimentelle Physik II
- Coordinator of the European Network of Excellence on 'Self-Assembled semiconductor Nanostructures for new Devices in photonics and Electronics' (SANDiE, www.sandie.org)
- Sprecher der DFG Forschergruppe 'Architektur von nano- und mikrodimensionalen Strukturelementen' (FOR 522), http://www.uni-leipzig.de/~for522
- Stellvertredender Sprecher der Graduiertenschule 'Leipzig School of Natural Sciences – Building with Molecules and Nano-objects' (BuildMoNa), http://www.buildmona.de
- 1. Stellvertretender Sprecher des Sonderforschungsbereiches zur "Funktionalität Oxidischer Grenzflächen" (SFB 762), http://www.physik.uni-halle.de/FG
- Sprecher der Fächerübergreifenden Arbeitsgemeinschaft Halbleiterforschung Leipzig (FAHL), http://www.uni-leipzig.de/~fahl
- Mitglied des Beirat Ionenstrahlzentrum, FZR, Rossendorf
- Project Reviewer: Deutsche Forschungsgemeinschaft (DFG), Alexander-von-Humboldt Stiftung (AvH), Schweizerischer Nationalfonds zur Förderung der wissenschaftlichen Forschung (FNSNF), Fonds zur Förderung der Wissenschaften (FWF)
- Referee: Appl. Phys. Lett., Electr. Lett., J. Appl. Phys., Nature, Physica E, Phys. Rev. B., Phys. Rev. Lett., Phys. Stat. Sol., Science

M. Lorenz

- Project Reviewer: United States – Israel Binational Science Foundation (BSF)
- Referee: Appl. Phys. Lett., IEEE Transact. Appl. Supercond., J. Am. Chem. Soc., J. Phys. D Appl. Phys., Thin Solid Films, J. Cryst. Growth, Mater. Lett., Appl. Surf. Sci., Appl. Phys. A, J. Phys. Chem., Mat. Sci. Eng. B, Semicond. Sci. Technol., Nanotechnology

H. Schmidt

- Referee: Phys. E, Appl. Phys. Lett., Phys. Stat. Sol. A, J. Appl. Phys., Opt. Mat., J. Phys. Cond. Matter

8.22 External Cooperations

Academic

- Leibniz-Institut für Oberflächenmodifizierung e.V., Leipzig, Germany
  Prof. Dr. B. Rauschenbach
- Universität Leipzig, Fakultät für Biowissenschaften, Pharmazie und Psychologie, Germany
  Prof. Dr. A. Beck-Sickinger
- Universität Leipzig, Fakultät für Chemie und Mineralogie, Germany
  Dr. V. Gottschalch, Prof. Dr. H. Krautscheid, Prof. Dr. K. Bente

- Universität Halle-Wittenberg, Germany
  Prof. Dr. I. Mertig, Prof. Dr. W. Widdra, Prof. Dr. H. Graener
- Max-Planck-Institut für Mikrostrukturphysik, Halle/Saale, Germany
  Prof. Dr. U. Gösele, Dr. O. Breitenstein, Dr. A. Ernst, Dr. P. Werner, Dr. D. Hesse
- Forschungszentrum Dresden-Rossendorf, Germany
  Prof. Dr. M. Helm
- Technische Universität Berlin, Germany
  Prof. Dr. D. Bimberg, Dr. A. Hoffmann
- Universidade de Aveiro, Portugal
  Prof. Dr. N. Sobolev
- Kinki University, Dept. of Electronics Systems and Information Engeneering, Japan
  Dr. M. Kusunoki
- Chinese Academy of Sciences, Institute of Physics, Beijing, P.R. China
  Prof. Dr. Yusheng He
- Universität Gießen, Germany
  Prof. Dr. B. Meyer, Dr. D. Hofmann, Prof. Dr. J. Janek
- Universität Magdeburg, Germany
  Prof. Dr. A. Krost, Dr. A. Dadgar, Prof. Dr. J. Christen
- Universität Bonn, Germany
  Prof. Dr. W. Mader
- Universität Hannover, Germany
  Prof. Dr. M. Binnewies
- Göteborg University, Sweden
  Prof. Dr. M. Willander
- NCSR "Demokritos", Institute of Materials Science, Greece
  Prof. Dr. A. Travlos
- Univerité Joseph Fourier, Grenoble, France
  Prof. Dr. D. Le Si Dang
- University of Pretoria, South Africa
  Prof. F.D. Auret
- University of Canterbury, Christchurch, New Zealand
  Prof. S. Durbin

Industry

- Solarion GmbH, Leipzig, Germany
  Dr. Alexander Braun, Dr. Andreas Rahm
- El-Mul Technologies, Yavne, Israel
  Dr. Armin Schön
- OSRAM Opto-Semiconductors GmbH, Regensburg, Germany
  Dr. V. Härle, Dr. S. Lutgen

- Freiberger Compound Materials GmbH, Freiberg, Germany
  Dr. G. Leibiger
- Q-Cells AG, Thalheim, Germany
  Dr. K. Petter, P. Clemens

8.23 Publications

Journals

A.O. Ankiewicz, M.C. Carmo, N.A. Sobolev, W. Gehlhoff, E.M. Kaidashev, A. Rahm, M. Lorenz, M. Grundmann: *Electron paramagnetic resonance in transition metal-doped ZnO nanowires*, J. Appl. Phys. **101**, 024 324 (2007), doi:10.1063/1.2402095

A.O. Ankiewicz, W. Gehlhoff, E.M. Kaidashev, A. Rahm, M. Lorenz, M. Grundmann, M.C. Carmo, N.A. Sobolev: *Electron Paramagnetic Resonance Characterization of Mn- and Co-Doped ZnO Nanowires*, AIP Conf. Proc. **893**, 63 (2007), doi:10.1063/1.2729771

F.D. Auret, W.E. Meyer, P.J. Janse van Rensburg, M. Hayes, J.M. Nel, H. von Wenckstern, H. Schmidt, G. Biehne, H. Hochmuth, M. Lorenz, M. Grundmann: *Electronic properties of defects in pulsed-laser deposition grown ZnO with levels at 300 meV and 370 meV below the conduction band*, Physica B **401-402**, 378 (2007), doi:10.1016/j.physb.2007.08.192

G. Brauer, W. Anwand, W. Skorupa, J. Kuriplach, O. Melikhova, J. Cizek, I. Prochazka, C. Moisson, H. von Wenckstern, H. Schmidt, M. Lorenz, M. Grundmann: *Comparative characterization of differently grown ZnO single crystals by positron annihilation and Hall effect*, Superlatt. Microstruct. **42**, 259 (2007), doi:10.1016/j.spmi.2007.04.003

B.Q. Cao, M. Lorenz, A. Rahm, H. von Wenckstern, C. Czekalla, J. Lenzner, G. Benndorf, M. Grundmann: *Phosphorus acceptor doped ZnO nanowires prepared by pulsed-laser deposition*, Nanotechnology **18**, 455 707 (2007), doi:10.1088/0957-4484/18/45/455707

C. Czekalla, J. Lenzner, A. Rahm, T. Nobis, M. Grundmann: *A Zincoxide Microwire Laser*, Superlatt. Microstruct. **41**, 347 (2007), doi:10.1016/j.spmi.2007.03.027

H. Frenzel, H. von Wenckstern, A. Weber, G. Biehne, H. Hochmuth, M. Lorenz, M. Grundmann: *Measurements of deep intrinsic defects in thin ZnO films via mid-infrared photocurrent spectroscopy*, AIP Conf. Proc. **893**, 301 (2007), doi:10.1063/1.2729887

H. Frenzel, H. von Wenckstern, A. Weber, H. Schmidt, G. Biehne, H. Hochmuth, M. Lorenz, M. Grundmann: *Photocurrent spectroscopy of deep levels in ZnO thin films*, Phys. Rev. B **76**, 035 214 (2007), doi:10.1103/PhysRevB.76.035214

D. Fritsch, H. Schmidt, M. Grundmann: *Calculated optical properties of wurtzite GaN and ZnO*, AIP Conf. Proc. **893**, 325 (2007), doi:10.1063/1.2729899

K. Goede, M. Bachmann, W. Janke, M. Grundmann: *Specific adhesion of peptides on semiconductor surfaces in experiment and simulation*, AIP Conf. Proc. **893**, 611 (2007), doi:10.1063/1.2730040

S. Heitsch, G. Benndorf, G. Zimmermann, C. Schulz, D. Spemann, H. Hochmuth, H. Schmidt, T. Nobis, M. Lorenz, M. Grundmann: *Optical and structural properties of MgZnO/ZnO hetero- and double heterostructures grown by pulsed laser deposition*, Appl. Phys. A **88**, 99 (2007), doi:10.1007/s00339-007-3953-5

S. Heitsch, G. Zimmermann, D. Fritsch, C. Sturm, R. Schmidt-Grund, C. Schulz, H. Hochmuth, D. Spemann, G. Benndorf, B. Rheinländer, T. Nobis, M. Lorenz, M. Grundmann: *Luminescence and surface properties of $Mg_xZn_{1-x}O$ thin films grown by pulsed laser deposition*, J. Appl. Phys. **101**, 083 521 (2007), doi:10.1063/1.2719010

S. Heitsch, G. Zimmermann, J. Lenzner, H. Hochmuth, G. Benndorf, M. Lorenz, M. Grundmann: *Photoluminescence of $Mg_xZn_{1-x}O$/ZnO Quantum Wells Grown by Pulsed Laser Deposition*, AIP Conf. Proc. **893**, 409 (2007), doi:10.1063/1.2729939

D. Hofstetter, Y. Bonetti, F.R. Giorgetta, A.-H. El-Shaer, A. Bakin, A. Waag, R. Schmidt-Grund, M. Schubert, M. Grundmann: *Demonstration of an ultraviolet ZnO-based optically pumped third order distributed feedback laser*, Appl. Phys. Lett. **91**, 111 108 (2007), doi:10.1063/1.2783965

R. Johne, M. Lorenz, H. Hochmuth, J. Lenzner, H. von Wenckstern, G. Zimmermann, H. Schmidt, R. Schmidt-Grund, M. Grundmann: *Cathodoluminescence of large-area PLD grown ZnO thin films measured in transmission and Reflection*, Appl. Phys. A **88**, 89 (2007), doi:10.1007/s00339-007-3939-3

Y. Liu, Q. Xu, H. Schmidt, L. Hartmann, H. Hochmuth, M. Lorenz, M. Grundmann, X. Han, Z. Zhang: *Co location and valence state determination in ferromagnetic ZnO:Co thin films by atom-location-by-channeling-enhanced-microanalysis electron energy-loss spectroscopy*, Appl. Phys. Lett. **90**, 154 101 (2007), doi:10.1063/1.2720713

M. Lorenz, M. Brandt, J. Schubert, H. Hochmuth, H. von Wenckstern, M. Schubert, M. Grundmann: *Polarization coupling in epitaxial ZnO/$BaTiO_3$ thin film heterostructures on $SrTiO_3$ (100) substrates*, Proc. SPIE **6474**, 64 741S (2007), doi:10.1117/12.715217

M. Lorenz, R. Johne, H.P.D. Schenk, S.I. Borenstain, A. Schön, C. Bekeny, T. Voß, J. Gutowski, T. Nobis, H. Hochmuth, J. Lenzner, M. Grundmann: *Self absorption in the room-temperature cathodoluminescence of ZnO scintillator thin films on sapphire*, Appl. Phys. Lett. **89**, 243 510 (2007), doi:10.1063/1.2405392

T. Nobis, A. Rahm, C. Czekalla, M. Lorenz, M. Grundmann: *Optical whispering gallery modes in dodecagonal zinc oxide microcrystals*, Superlatt. Microstruct. **42**, 333 (2007), doi:10.1016/j.spmi.2007.04.031

T. Nobis, A. Rahm, M. Lorenz, M. Grundmann: *Temperature dependence of the whispering gallery effect in ZnO nanoresonators*, AIP Conf. Proc. **893**, 1057 (2007), doi:10.1063/1.2730261

A. Rahm, M. Lorenz, T. Nobis, G. Zimmermann, M. Grundmann, B. Fuhrmann, F. Syrowatka: *Pulsed Laser Deposition and characterization of ZnO nanowires with regular lateral arrangement*, Appl. Phys. A **88**, 31 (2007), doi:10.1007/s00339-007-3979-8

H. Schmidt, M. Diaconu, H. Hochmuth, G. Benndorf, H. von Wenckstern, G. Biehne, M. Lorenz, M. Grundmann: *Electrical and optical spectroscopy on ZnO:Co films*, Appl. Phys. A **88**, 157 (2007), doi:10.1007/s00339-007-3992-y

M. Schmidt, R. Pickenhain, M. Grundmann: *Exact Solutions for the Capacitance of Space Charge Regions at Semiconductor Interfaces*, Solid State Electr. **51**, 1002 (2007), doi:10.1016/j.sse.2007.04.004

R. Schmidt-Grund, N. Ashkenov, M.M. Schubert, W. Czakai, D. Faltermeier, G. Benndorf, H. Hochmuth, M. Lorenz, M. Grundmann: *Temperature-dependence of the refractive index and the optical transitions at the fundamental band-gap of ZnO*, AIP Conf. Proc. **893**, 271 (2007), doi:10.1063/1.2729872

R. Schmidt-Grund, B. Rheinländer, C. Czekalla, G. Benndorf, H. Hochmut, A. Rahm, M. Lorenz, M. Grundmann: *ZnO based planar and micropillar resonators*, Superlatt. Microstruct. **41**, 360 (2007), doi:10.1016/j.spmi.2007.03.010

R. Schmidt-Grund, B. Rheinländer, T. Gühne, H. Hochmuth, V. Gottschalch, A. Rahm, J. Lenzner, M. Grundmann: *ZnO micro-pillar resonators with coaxial Bragg reflectors*, AIP Conf. Proc. **893**, 1137 (2007), doi:10.1063/1.2730298

C. Sturm, R. Schmidt-Grund, R. Kaden, H. von Wenckstern, B. Rheinländer, K. Bente, M. Grundmann: *Optical Properties of Cylindrite*, AIP Conf. Proc. **893**, 1483 (2007), doi:10.1063/1.2730468

M. Ungureanu, H. Schmidt, H. von Wenckstern, H. Hochmuth, M. Lorenz, M. Grundmann, M. Fecioru-Morariu, G. Güntherodt: *A comparison between ZnO films doped with 3d and 4f magnetic ions*, Thin Solid Films **515**, 8761 (2007), doi:10.1016/j.tsf.2007.04.010

M. Ungureanu, H. Schmidt, Q. Xu, H. von Wenckstern, D. Spemann, H. Hochmuth, M. Lorenz, M. Grundmann: *Electrical and magnetic properties of RE-doped ZnO thin films (RE = Gd, Nd)*, Superlatt. Microstruct. **42**, 231 (2007), doi:10.1016/j.spmi.2007.04.022

H. von Wenckstern, M. Allen, H. Schmidt, P. Miller, R. Reeves, S. Durbin, M. Grundmann: *Defects in hydrothermally grown bulk ZnO*, Appl. Phys. Lett. **91**, 022 913 (2007), doi:10.1063/1.2757097

H. von Wenckstern, G. Benndorf, S. Heitsch, J. Sann, M. Brandt, H. Schmidt, J. Lenzner, M. Lorenz, A.Y. Kuznetsov, B.K. Meyer, M. Grundmann: *Properties of phosphorus doped ZnO*, Appl. Phys. A **88**, 125 (2007), doi:10.1007/s00339-007-3965-1

H. von Wenckstern, M. Brandt, H. Schmidt, G. Biehne, R. Pickenhain, H. Hochmuth, M. Lorenz, M. Grundmann: *Donor like defects in ZnO substrate materials and ZnO thin films*, Appl. Phys. A **88**, 135 (2007), doi:10.1007/s00339-007-3966-0

H. von Wenckstern, R. Pickenhain, H. Schmidt, M. Brandt, G. Biehne, M. Lorenz, M. Grundmann, G. Brauer: *Investigation of acceptor states in ZnO by junction DLTS*, Superlatt. Microstruct. **42**, 14 (2007), doi:10.1016/j.spmi.2007.04.014

H. von Wenckstern, H. Schmidt, C. Hanisch, M. Brandt, C. Czekalla, G. Benndorf, G. Biehne, A. Rahm, H. Hochmuth, M. Lorenz, M. Grundmann: *Homoepitaxy of ZnO by Pulsed-Laser Deposition*, Phys. Stat. Sol. RRL **1**, 129 (2007), doi:10.1002/pssr.200701052

Q. Xu, L. Hartmann, H. Schmidt, H. Hochmuth, M. Lorenz, R. Schmidt-Grund, C. Sturm, D. Spemann, M. Grundmann: *Magnetoresistance and anomalous Hall effect in magnetic ZnO films*, J. Appl. Phys. **101**, 063 918 (2007), doi:10.1063/1.2715846

Q. Xu, L. Hartmann, H. Schmidt, H. Hochmuth, M. Lorenz, R. Schmidt-Grund, C. Sturm, D. Spemann, M. Grundmann: *The magnetotransport properties of Co-doped ZnO films*, AIP Conf. Proc. **893**, 1187 (2007), doi:10.1063/1.2730322

Q. Xu, L. Hartmann, H. Schmidt, H. Hochmuth, M. Lorenz, D. Spemann, M. Grundmann: *s–d exchange interaction induced magnetoresistance in magnetic ZnO*, Phys. Rev. B **76**, 134 417 (2007), doi:10.1103/PhysRevB.76.134417

Q. Xu, H. Schmidt, L. Hartmann, H. Hochmuth, M. Lorenz, A. Setzer, P. Esquinazi, C. Meinecke, M. Grundmann: *Room temperature ferromagnetism in Mn-doped ZnO films mediated by acceptor levels*, Appl. Phys. Lett. **91**, 092 503 (2007), doi:10.1063/1.2778470

J. Zúñiga-Pérez, A. Rahm, C. Czekalla, J. Lenzner, M. Lorenz, M. Grundmann: *Ordered growth of tilted ZnO nanowires: morphological, structural and optical characterization*, Nanotechnology **18**, 195 303 (2007), doi:10.1088/0957-4484/18/19/195303

Books

S. Heitsch, G. Zimmermann, A. Müller, J. Lenzner, H. Hochmuth, G. Benndorf, M. Lorenz, M. Grundmann: *Interface and Luminescence Properties of Pulsed Laser Deposited MgZnO/ZnO Quantum Wells with Strong Confinement*, in: *Zinc Oxide and Related Materials*, ed. by J. Christen, C. Jagadish, D.C. Look, T. Yao, F. Bertram, Mater. Res. Soc. Symp. Proc. **957** (MRS, Warrendale 2007) p 229

M. Grundmann (Ed.): *The Physics Institutes of Universität Leipzig, Report 2006* (Universität Leipzig, Leipzig 2007)

M. Grundmann, A. Rahm, T. Nobis, H. von Wenckstern, C. Czekalla, J. Lenzner, M. Lorenz: *Growth and Characterization of Optical and Electrical Properties of ZnO Nano- and Microwires*, in: *Zinc Oxide and Related Materials*, ed. by J. Christen, C. Jagadish, D.C. Look, T. Yao, F. Bertram, Mater. Res. Soc. Symp. Proc. **957** (MRS, Warrendale 2007) p 107

H. von Wenckstern, M. Brandt, J. Lenzner, G. Zimmermann, H. Hochmuth, M. Lorenz, M. Grundmann: *Temperature dependent Hall measurements on PLD thin films*, in: *Zinc Oxide and Related Materials*, ed. by J. Christen, C. Jagadish, D.C. Look, T. Yao, F. Bertram, Mater. Res. Soc. Symp. Proc. **957** (MRS, Warrendale 2007) p 23

in press

M. Grundmann, A. Rahm, T. Nobis, M. Lorenz, C. Czekalla, E.M. Kaidashev, J. Lenzner: *Growth and characterization of ZnO nano- and microstuctures*, in: *Handbook of Self-Assembled Semiconductor Nanostructures for Novel Devices in Photonics and Electronics*, ed. by M. Henini (Elsevier)

J. Sellmann, C. Sturm, R. Schmidt-Grund, C. Czekalla, J. Lenzner, H. Hochmuth, B. Rheinländer, M. Lorenz, M. Grundmann: *Structural and optical properties of ZrO_2 and Al_2O_3 thin films and Bragg reflectors grown by pulsed laser deposition*, Phys. Stat. Sol. C, doi:10.1002/pssc.200777875

V.M. Voora, T. Hofmann, M. Brandt, M. Lorenz, M. Grundmann, M. Schubert: *Electrooptic ellipsometry study of spontaneous polarization coupling in piezoelectric $BaTiO_3$–ZnO heterostructures*, Phys. Stat. Sol. C, doi:10.1002/pssc.200777908

Talks

M. Allen, H, von Wenckstern, M. Grundmann, S. Hatfield, P. Jefferson, P. King, T. Veal, C. McConville, S. Durbin: *Mechanisms in the Formation of High Quality Schottky Contacts to n-type ZnO*, MRS Fall Meeting 2007, Boston, USA, 26. – 30. November 2007

M. Brandt, H. von Wenckstern, C. Hanisch, H. Hochmuth, M. Lorenz, H. Schmidt, M. Grundmann: *Homoepitaxial growth of ZnO thin film by pulsed laser deposition (PLD)*, 71st DPG Spring Meeting, Regensburg, 26. – 30. March 2007

B. Cao, M. Lorenz, A. Rahm, H. von Wenckstern, C. Czekalla, G. Benndorf, J. Lenzner, M. Grundmann: *Acceptor Doping of ZnO Nanowires*, 71st DPG Spring Meeting, Regensburg, 26. – 30. March 2007

C. Czekalla: *ZnO Microwire Lasers*, SANDiE Optics Meeting, Berlin, 12. January 2007

C. Czekalla, J. Guinard, C. Hanisch, B. Cao, E. Kaidashev, N. Boukos, A. Travlos, D. Le Si Dang, M. Lorenz, M. Grundmann: *Quantum-dot like narrow cathodoluminescence emission from ZnO-MgZnO nano quantum wells*, Quantum Dot Optoelectronics Symposium (QDOS-2007), Limassol, Cyprus, 16. November 2007

C. Czekalla, A. Rahm, J. Lenzner, M. Grundmann: *Lasing emission from Zincoxide Microwire Structures*, 71st DPG Spring Meeting, Regensburg, 26. – 30. March 2007

H. Frenzel, H. von Wenckstern, A. Weber, H. Schmidt, G. Biehne, H. Hochmuth, M. Lorenz, M. Grundmann: *Photocurrent spectroscopy of deep levels in ZnO thin films*, 71st DPG Spring Meeting, Regensburg, 26. – 30. March 2007

M. Grundmann: *Nanowhiskers and their applications*, 1st Saxon Biotechnology Symposium, Technische Universität Dresden, 28. November 2007 (invited)

M. Grundmann: *Solarzellen aus Verbindungshalbleitern: Stand und Perspektiven*, 1. Photovoltaik-Symposium TGZ Bitterfeld "Neue Photovoltaiktechnologien – Innovation durch Synergie", Bitterfeld, 15. November 2007 (invited)

N. Ghosh, H. Schmidt, Q. Xu, L. Hartmann, H. Hochmuth, M. Lorenz, G. Wagner, M. Grundmann: *Conductivity measurements on ZnO/YBCO heterostructures*, 71st DPG Spring Meeting, Regensburg, 26. – 30. March 2007

L. Hartmann, Q. Xu, H. Schmidt, H. Hochmuth, M. Lorenz, C. Sturm, C. Meinecke, A. Setzer, P. Esquinazi, M. Grundmann: *Spin polarization in $Zn_{0.95}Co_{0.05}O$:(Al,Cu) thin Films*, 71st DPG Spring Meeting, Regensburg, 26. – 30. March 2007

S. Heitsch, G. Zimmermann, A. Müller, J. Lenzner, H. Hochmuth, G. Benndorf, M. Lorenz, M. Grundmann: *Interface and Luminescence Properties of Pulsed Laser Deposited $Mg_xZn_{1-x}O$/ZnO Quantum Wells with Strong Confinement*, 71st DPG Spring Meeting, Regensburg, 26. – 30. March 2007

M. Lorenz: *Advanced Pulsed Laser Deposition of hetero- and homoepitaxial ZnO thin films and nanostructures*, Workshop Laser Processing for Semiconductor Devices: Science and Technology, Saint Malo, 01./02. October 2007

M. Lorenz: *Pulsed Laser Deposition of hetero- and homoepitaxial ZnO thin films and nanostructures*, II. Physikalisches Institut, Georg August Universität Göttingen, 14 December 2007 (invited)

M. Lorenz, H. Schmidt, C. Ronning, S. Müller, M. Ungureanu, G. Benndorf, M. Grundmann: *Photoluminescence of vanadium-implanted and annealed ZnO thin films*, 71st DPG Spring Meeting, Regensburg, 26. – 30. March 2007

H. Schmidt, M. Wiebe, B. Dittes, M. Grundmann: *The influence of entropy on the capture cross-section determination in ZnO*, 71st DPG Spring Meeting, Regensburg, 26. – 30. March 2007

M. Schmidt, R. Pickenhain, M. Grundmann: *Exact solution for the capacitance of a current free Schottky diode*, 71st DPG Spring Meeting, Regensburg, 26. – 30. March 2007

R. Schmidt-Grund, B. Rheinländer, C. Czekalla, G. Benndorf, H. Hochmuth, M. Lorenz, M. Grundmann: *Exciton-Polaritons at room temperature in a planar ZnO resonator structure*, 71st DPG Spring Meeting, Regensburg, 26. – 30. March 2007

R. Schmidt-Grund, J. Sellmann, C. Sturm, C. Czekalla, B. Rheinländer, J. Lenzner, H. Hochmuth, G. Zimmermann, M. Lorenz, M. Grundmann: *Exciton-Polaritons in All-oxide ZnO-based Resonator Structures*, MRS Fall Meeting 2007, Boston, USA, 26. – 30. November 2007

M. Schubert, T. Hofmann, R. Voora, M. Brandt, H. Hochmuth, M. Lorenz, M. Grundmann, N. Ashkenov, J. Schubert: *Spontaneous polarization in ferroelectric wurtzite (ZnO) perovskite (BaTiO3) heterostructures: theory, experiments and further prospects*, SPIE Photonics West 2007, San Jose, California, USA, 20. – 25 January 2007

C. Sturm, R. Schmidt-Grund, T. Chavdarov, B. Rheinländer, H. Hochmuth, M. Lorenz, M. Grundmann: *The anisotropy of the dielectric function of ZnO films*, 71st DPG Spring Meeting, Regensburg, 26. – 30. March 2007

C. Sturm, R. Schmidt-Grund, T. Chavdarov, B. Rheinländer, A. Rahm, H. Hochmuth, M. Lorenz, J. Zúñiga-Pérez, M. Grundmann: *Band-gap energy shift of non-polar ZnO thin films*, 4th Int. Conf. Spectroscopic Ellipsometry (ICSE-4), Stockholm, Sweden, 11. – 15. June 2007

V.M. Voora, T. Hofmann, M. Brandt, M. Lorenz, M. Grundmann, N. Ashkenov, M. Schubert: *Interface-charge-coupled polarization response of Pt–ZnO–$BaTiO_3$–Pt heterojunctions: A physical model approach*, 2007 Electronic Materials Conference (EMC 2007), Notre Dame, USA, 20. – 22. June 2007

R. Weirauch, R. Pickenhain, H. von Wenckstern, M. Lorenz, G. Biehne, M. Grundmann: *Optical Deep Level Transient Spectroscopy on ZnO*, 71st DPG Spring Meeting, Regensburg, 26. – 30. March 2007

H. von Wenckstern, F.D. Auret, W.E. Meyer, P.J. Janse van Rensburg, G. Biehne, H. Hochmuth, M. Lorenz, M. Grundmann: *Electrical characterization of defects in ZnO grown by pulsed-laser deposition*, MRS Fall Meeting 2007, Boston, USA, 26. – 30. November 2007

H. von Wenckstern, G. Biehne, M. Lorenz, M. Grundmann, F.D. Auret, W.E. Meyer, P.J. Janse van Rensburg, M. Hayes, J.M. Nel: *Dependence of trap concentrations in ZnO thin films on annealing conditions*, 13th Int. Conf. II–VI Compounds, Jeju, Korea, 10. – 14. September 2007

H. von Wenckstern, M. Brandt, H. Schmidt, C. Hanisch, G. Benndorf, H. Hochmuth, M. Lorenz, M. Grundmann: *Homoepitaxy of ZnO thin films by Pulsed-Laser Deposition*, 13th Int. Conf. II–VI Compounds, Jeju, Korea, 10. – 14. September 2007

H. von Wenckstern, H. Schmidt, G. Biehne, R. Pickenhain, M. Lorenz, M. Grundmann: *Depletion layer spectroscopy on bulk and thin film ZnO*, 71st DPG Spring Meeting, Regensburg, 26. – 30. March 2007

H. von Wenckstern, H. Schmidt, C. Hanisch, M. Brandt, C. Czekalla, G. Benndorf, A. Müller, S. Heitsch, G. Biehne, R. Schmidt-Grund, A. Rahm, H. Hochmuth M. Lorenz, M. Grundmann: *Properties of Homoepitaxial ZnO thin films grown by pulsed-laser deposition*, MRS Fall Meeting 2007, Boston, USA, 26. – 30. November 2007

Q. Xu, L. Hartmann, H. Schmidt, H. Hochmuth, M. Lorenz, M. Grundmann: *Magnetoresistance in n-type conducting magnetic ZnO films*, 71st DPG Spring Meeting, Regensburg, 26. – 30. March 2007

Posters

F.D. Auret, W.E. Meyer, P.J. Janse van Rensburg, M. Hayes, J.M. Nel, H. von Wenckstern, H. Schmidt, G. Biehne, H. Hochmuth, M. Lorenz, M. Grundmann: *Electronic properties of defects in pulsed-laser deposition grown ZnO with levels at 300 meV and 370 meV below the conduction band*, 24th Int. Conf. Defects in Semiconductors (ICDS-24), Albuquerque, USA, 22. – 27. July 2007

B. Bastek, J. Christen, F. Bertram, M. Noltemeyer, H. Frenzel, H. Hochmuth, M. Lorenz, M. Brandt, M. Grundmann: *Excitonic Transport in ZnO – Investigated by Temperature, Time, and Spatially Resolved Cathodoluminescence*, MRS Fall Meeting 2007, Boston, USA, 26. – 30. November 2007

M. Brandt, H. Hochmuth, M. Lorenz, M. Grundmann, M. Schubert, T. Hoffman, R. Voora, N. Ashkenov, J. Schubert: *Electrical and Electro-optical Investigations on the Polarization Coupling in Epitaxial Ferroelectric BTO/ZnO Heterostructures*, MRS Fall Meeting 2007, Boston, USA, 26. – 30. November 2007

M. Brandt, H. von Wenckstern, H. Hochmuth, M. Lorenz, M. Grundmann, J. Schubert, V. Voora, M. Schubert: *Ferroelectric Properties of $BaTiO_3$–ZnO heterojunctions*, 71st DPG Spring Meeting, Regensburg, 26. – 30. March 2007

C. Bundesmann, A. Rahm, D. Spemann, M. Lorenz, M. Grundmann, M. Schubert: *Infrared dielectric tensor studies of $Mg_xZn_{1-x}O$ ($0 < x < 1$) thin films*, 4th Int. Conf. Spectroscopic Ellipsometry (ICSE-4), Stockholm, Sweden, 11. – 15. June 2007

T. Chavdarov, C. Sturm, R. Schmidt-Grund, B. Rheinländer, H. Hochmuth, M. Lorenz, M. Schubert, C. Bundesmann, M. Grundmann: *Investigation of the free charge carrier properties at the ZnO-sapphire interface in a-plane ZnO films by generalized infrared ellipsometry*, 4th Int. Conf. Spectroscopic Ellipsometry (ICSE-4), Stockholm, Sweden, 11. – 15. June 2007

D. Fritsch, H. Schmidt, R. Schmidt-Grund, M. Grundmann: *Intensity of optical absorption close to the band edge in strained ZnO films*, 13th Int. Conf. II–VI Compounds, Jeju, Korea, 10. – 14. September 2007

N. Ghosh, H. Schmidt, L. Hartmann, G. Biehne, H. Hochmuth, M. Lorenz, G. Wagner, J.L. Barzola Quiquia, P.D. Esquinazi, M. Grundmann: *Study of interface and modelling of subgap conductivity fluctuations of magnetic ZnO/YBCO heterostructure*, 10th Int. Conf. Advanced Materials (IUMRS-ICAM 2007), Bangalore, India, 08. – 13. October 2007

N. Ghosh, H. Schmidt, H. Hochmuth, M. Lorenz, Q. Xu, M. Grundmann, G. Wagner: *Current voltage measurements on magnetic ZnO/$Y_1Ba_2Cu_3O_{7-\delta}$*, APS March Meeting 2007, Denver, USA, 05. – 09. March 2007

L. Hartmann, Q. Xu, H. Schmidt, H. Hochmuth, M. Lorenz, M. Grundmann, P. Esquinazi, M. Saenger, T. Hofmann, M. Schubert, S.-H. Liou: *Optical and structural properties of NiO and NiMnO thin films grown on ZnO and sapphire substrates*, 71st DPG Spring Meeting, Regensburg, 26. – 30. March 2007

C. Henkel, H. Schmidt, C. Sturm, M. Grundmann, A. Krtschil, A. Krost, P. Pelzing, A. Möller: *Scanning capacitance microscopy measurements on Si epilayers*, 71st DPG Spring Meeting, Regensburg, 26. – 30. March 2007

A. Müller, S. Heitsch, G. Benndorf, H. Hochmuth, G. Zimmermann, C. Meinecke, C. Sturm, R. Schmidt-Grund, M. Grundmann: *Optical characterization of hexagonal $Mg_xZn_{1-x}O$ thin films grown by pulsed laser deposition*, 71st DPG Spring Meeting, Regensburg, 26. – 30. March 2007

A. Rahm, H. von Wenckstern, J. Lenzner, M. Lorenz, M. Grundmann: *Electrical Characterization of ZnO Microcrystals*, 71st DPG Spring Meeting, Regensburg, 26. – 30. March 2007

M. Saenger, L. Hartmann, H. Schmidt, M. Hetterich, M. Lorenz, H. Hochmut, M. Grundmann, T. Hofmann, M. Schubert: *Comparison of giant Faraday effects in ZnMnSe and ZnMnO studied by magneto-optic ellipsometry*, 71st DPG Spring Meeting, Regensburg, 26. – 30. March 2007

M. Schmidt, H. von Wenckstern, R. Pickenhain, M. Grundmann: *Simulation of capacitance - temperature measurements on ZnO Schottky diodes*, 71st DPG Spring Meeting, Regensburg, 26. – 30. March 2007

R. Schmidt-Grund, D. Fritsch, M. Schubert, B. Rheinländer, H. Schmidt, C.M. Herzinger, H. von Wenckstern, E.M. Kaidashev, M. Lorenz, M. Grundmann: *Vacuum ultraviolet dielectric function and band-structure of ZnO*, 13th Int. Conf. II–VI Compounds, Jeju, Korea, 10. – 14. September 2007

R. Schmidt-Grund, S. Heitsch, B. Rheinländer, A. Müller, C. Czekalla, G. Benndorf, H. Hochmuth, M. Lorenz, M. Brandt, M. Grundmann: *Towards Bose-Einstein condensation of exciton-polaritons at room temperature in ZnO resonator structures*, SPIE Photonics West 2007, San Jose, California, USA, 20. – 25 January 2007

R. Schmidt-Grund, B. Rheinländer, C. Czekalla, H. Hochmuth, C. Sturm, J. Sellmann, A. Rahm, M. Lorenz, H. von Wenckstern, M. Grundmann: *ZnO based resonators*, 13th Int. Conf. II–VI Compounds, Jeju, Korea, 10. – 14. September 2007

R. Schmidt-Grund, B. Rheinländer, V. Gottschalch, M. Grundmann: *Generalized ellipsometry applied to micro-structures with curved geometry*, 4th Int. Conf. Spectroscopic Ellipsometry (ICSE-4), Stockholm, Sweden, 11. – 15. June 2007

R. Schmidt-Grund, C. Sturm, M. Schubert, N. Ashkenov, B. Rheinländer, D. Faltermeier, H. Hochmuth, A. Rahm, J. Bläsig, C. Bundesmann, J. Zúñiga-Pérez, T. Chavdarov, M. Lorenz, M. Grundmann: *Valence Band Structure of ZnO and* $Mg_xZn_{1-x}O$, MRS Fall Meeting 2007, Boston, USA, 26. – 30. November 2007

J. Sellmann, C. Sturm, R. Schmidt-Grund, C. Czekalla, J. Lenzner, H. Hochmuth, B. Rheinländer, M. Lorenz, M. Grundmann: *Optical and structural properties of* ZrO_2 *and* Al_2O_3 *on (0001) and (1-120) sapphire and silicon substrates*, 4th Int. Conf. Spectroscopic Ellipsometry (ICSE-4), Stockholm, Sweden, 11. – 15. June 2007

C. Sturm, T. Chavdarov, R. Schmidt-Grund, B. Rheinländer, C. Bundesmann, H. Hochmuth, M. Lorenz, M. Schubert, M. Grundmann: *The Charge Sheet Density in Non-polar ZnO Films at the ZnO-Sapphire Interface Determined by Generalized Ellipsometry*, MRS Fall Meeting 2007, Boston, USA, 26. – 30. November 2007

S.B. Thapa, E. Angelopoulos, J. Hertkorn, F. Scholz, A. Reiser, K. Thonke, R Sauer, H. Hochmuth, M. Lorenz, M. Grundmann: *Heteroepitaxial Growth of GaN on ZnO by MOVPE*, 12th Eur. Workshop Metalorganic Vapour Phase Epitaxy (EW-MOVPE 2007), Bratislava, Slovakia, 03. – 06. June 2007

N. Volbers, S. Lautenschläger, J. Sann, S. Zhou, K. Potzger, F. Bertram, A. Krtschil, J. Christen, A. Krost, H. von Wenckstern, M. Grundmann, B.K. Meyer: *Annealing Studies on Arsenic Implanted Zinc Oxide*, MRS Fall Meeting 2007, Boston, USA, 26. – 30. November 2007

V. Voora, T. Hofmann, M. Schubert, M. Brandt, M. Lorenz, M. Grundmann: *Polarization coupled response of ZnO–$BaTiO_3$: Determination of ZnO Spontaneous Polarization*, 71st DPG Spring Meeting, Regensburg, 26. – 30. March 2007

8.24 Graduations

Doctorate

- Daniel Fritsch
  Investigation of Nitride and Oxide Semiconductors by means of the Empirical Pseudopotential Method
  May 2007
- Andreas Rahm
  Growth and Characterization of ZnO-based Nanostructures
  März 2007
- Rüdiger Schmidt-Grund
  Dielectric Function of ZnO and MgZnO and Application to Bragg Reflectors and Micro-Resonators
  September 2007
- Mariana Ungureanu
  ZnO-based diluted magnetic semiconductors for applications in the field of spintronics
  July 2007

Diploma

- Christoph Henkel
  Kapazitätsspektroskopie an SiGe-Heterostrukturen
  Oktober 2007
- Kilian Mergenthaler
  Metallorganische Gasphasenepitaxie von ZnO und $ZnGa_2O_4$
  November 2007
- Alexander Müller
  Optische Untersuchungen an $Mg_xZn_{1-x}O$-Schichten im UV-Bereich
  September 2007
- Jan Sellmann
  PLD-Wachstum und Eigenschaften von ZrO_2/Al_2O_3-Schichtstrukturen in Bragg-Spiegeln für ZnO-Resonatoren
  November 2007

- Matthias Schirnow
  Heteroepitaxie von GaN: MOVPE-Wachstum und Characterisierung von nadelförmigen GaN-Kristallen
  May 2007
- Robin Weirauch
  Photostrom- und optische DLTS-Untersuchungen an Zinkoxid
  September 2007

Master

- Ahmed Abdelrahman
  Determination of Magneto Optical Constants in Metals and Semiconductors Using Magneto Optical Kerr Effect Measurements
  November 2007

8.25 Guests

- Prof. Dr. Ahmed Mohamed El-Sayed
  Inorganic Chemistry Department, National Research Centre, Cairo, Egypt
  18. September – 13. December 2007
- Dr. Evgeny Kaydashev
  Rostov-on-Don State University, Russia
  12. May – 11. August 2007
- Dr. Jesús Zúñiga Pérez
  Centre de Recherche sur l'Hétéro-Epitaxie et ses Applications (CNRS-CRHEA), Valbonne, France
  01. September – 30. November 2007
- Dr. Xiaona Zhang
  Institute of Microstructures and Properties of Advanced Materials, Beijing University of Technology, China
  01. May – 30. June 2007

9

Superconductivity and Magnetism

9.1 Introduction

The research of the Division of Superconductivity and Magnetism is concerned with the study of magnetic ordering and superconductivity in a range of materials. The present focus is on ferromagnetic and superconducting ordering phenomena in carbon-based materials, superconductivity in MgB_2 and magnetotransport properties of ferromagnetic oxide heterostructures. Research highlight of the year 2007 was the discovery of superconductivity in multigraphene with a critical temperature around 25 K.

Pablo Esquinazi

9.2 Intrinsic Superconductivity at 25 K in Highly Oriented Pyrolytic Graphite

P. Esquinazi, N. García*, J. Barzola-Quiquia, J.C. González*, M. Muñoz*, P. Rödiger, K. Schindler, J.-L. Yao, M. Ziese

*CSIC Madrid, Spain

High resolution magnetoresistance data in highly oriented pyrolytic graphite thin samples manifest non-homogenous superconductivity with a critical temperature $T_c \sim 25$ K. These data exhibit:

1) hysteretic loops of resistance versus magnetic field similar to Josephson-coupled grains,
2) quantum Andreev resonances, see Fig. 9.1, and
3) the absence of Schubnikov-de Haas oscillations.

The results indicate that graphite is a system with non-percolative superconducting domains immersed in a semiconducting-like matrix. As possible origin of the superconductivity in graphite we discuss interior-gap superconductivity when two very different electronic masses are present.

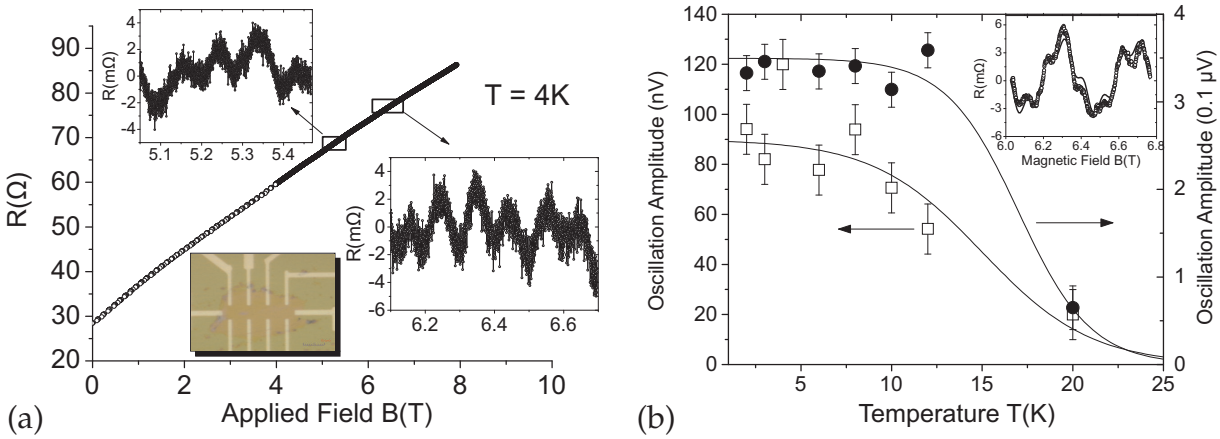

Figure 9.1: (**a**) The main panel shows the resistance of a multigraphene sample at 4 K as a function of magnetic field. The *lower inset* to that panel shows a microscopy image of the sample. The other two *insets* are magnifications of the magnetoresistance behaviour, showing the presence of fine oscillations, interpreted as Andreev resonances. The oscillations were analyzed by Fourier analysis, see *inset* to panel (**b**), and the amplitudes of two oscillation frequencies are shown in (**b**) as a function of temperature. These decrease strongly with temperature and vanish around 25 K, with the latter temperature being interpreted as critical temperature for the local superconductivity.

9.3 Intrinsic Spin Filtering in a $La_{2/3}Ca_{1/3}MnO_3$/Nb(1.0 %):$SrTiO_3$ Junction

Y.F. Chen, M. Ziese

The nonlinear transport properties and the magnetoresistance of a junction between $La_{2/3}Ca_{1/3}MnO_3$ and Nb(1.0 %)-doped $SrTiO_3$ were studied. The striking feature in the present magnetoresistance data is the appearance of a step-like magnetoresistance hysteresis that typically occurs in magnetic tunnelling junctions with two ferromagnetic electrodes. This is unexpected, since the structures under study contain only one ferromagnetic layer. Therefore this tunnelling magnetoresistance is attributed to spin filtering by an insulating, but ferromagnetic interfacial layer in this manganite/Nb:$SrTiO_3$ bilayer system. From the measured values for the tunnelling magnetoresistance the spin polarization of the interfacial layer is derived with a value of about 25 %. The spin polarization vanishes at 110 K far below the Curie temperature of $La_{2/3}Ca_{1/3}MnO_3$.

9.4 Spin Filtering in $La_{0.7}Sr_{0.3}MnO_3/CoFe_2O_4$/Nb(0.5%):$SrTiO_3$ Heterostructures

Y.F. Chen, M. Ziese

The magnetotransport properties of $La_{0.7}Sr_{0.3}MnO_3/CoFe_2O_4$/Nb(0.5 %):$SrTiO_3$ junctions were investigated. At low temperatures, these junctions show a magnetoresistance strongly dependent on current bias, temperature, and magnetic field. Figure 9.2

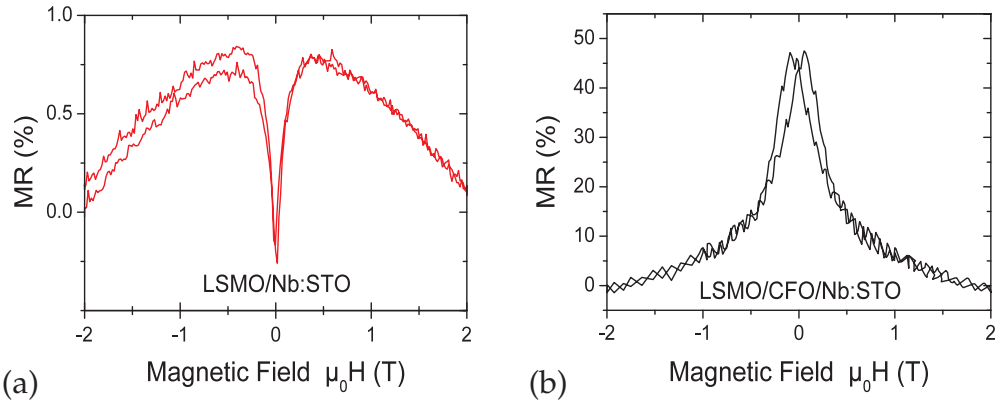

Figure 9.2: Magnetoresistance of (**a**) a bare $La_{0.7}Sr_{0.3}MnO_3$/Nb(0.5 %) : $SrTiO_3$ junction and (**b**) a $La_{0.7}Sr_{0.3}MnO_3/CoFe_2O_4$/Nb(0.5 %) : $SrTiO_3$ junction, both measured at 5 K.

shows a comparison of the magnetoresistance of a spin-filter junction and a bare $La_{0.7}Sr_{0.3}MnO_3$/Nb(0.5 %):$SrTiO_3$ junction, elucidating the strong magnetoresistance enhancement by the $CoFe_2O_4$ layer. This is attributed to spin filtering in the $CoFe_2O_4$ layer. Moreover, the apparent coercive field of the junctions depends on the applied bias current due to the interplay of magnetic switching and the bias dependent transport in the $CoFe_2O_4$ layer. A spin filter efficiency of 20 % was derived for the $CoFe_2O_4$ layer from the magnetoresistance values.

9.5 Transport Properties and Growth Parameters of PdC and WC Nanowires Prepared in a Dual Beam Microscope

D. Spoddig, K. Schindler, P. Rödiger, J. Barzola-Quiquia, K. Fritsch, H. Mulders*, P. Esquinazi

*FEI Electron Optics, Eindhoven, The Netherlands

In this work we investigate the electrical transport properties and growth conditions of Tungsten Carbon (WC) and Palladium Carbon (PdC) nanostructures on Si substrates using a focused ion beam and scanning electron microscope. The nanowires were grown by ion and electron beam induced deposition (IBID/EBID), see Fig. 9.3a. Due to the higher metal content in IBID structures than in EBID these nanowires show a more metallic behaviour. In-situ resistance measurements of the nanowires as function of thickness reveal a minimum around ~ 200 nm (Fig. 9.3b). Temperature dependent resistance measurements on WC nanowires exhibit a superconducting critical temperature of ~ 5 K.

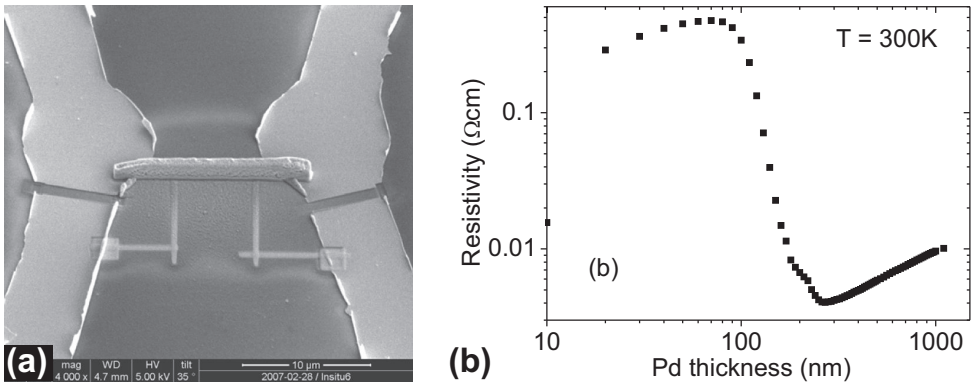

Figure 9.3: (**a**) SEM image of an IBID PdC nanowire. (**b**) In situ resistivity measurement as function of PdC thickness (IBID).

9.6 Funding

Room Temperature Ferromagnetism in Graphite and Fullerenes (FERROCARBON)
Prof. P. Esquinazi
EU Strep No. 012881

The origin of carbon-based magnetism and the role of hydrogen
Prof. P. Esquinazi
DFG ES 86/11-1

Magnetotransport Properties of Oxide Interfaces
Prof. P. Esquinazi and Dr. M. Ziese
DFG Es 86/7-4

Studies on interfacial effects in magnetite-based heterostructures
Dr. J. Yao, Prof. P. Esquinazi, Dr. M. Ziese
Humboldt-Stiftung

9.7 Organizational Duties

P. Esquinazi

- Project Reviewer: Deutsche Forschungsgemeinschaft (DFG), National Science Foundation (USA), German-Israeli Foundation
- Referee: Phys. Rev. Lett, Phys. Rev. B., Physica C, Phys. Lett. A, Phys. Stat. Sol., J. Low Temp. Phys., Carbon, J. Chem. Phys., Eur. J. Phys. B, J. Magn. Magn. Mater.

M. Ziese

- Project Reviewer: U.S.-Israel Binational Science Foundation, European Science Foundation
- Referee: APS Outstanding Referee, Phys. Rev. Lett., Phys. Rev. B., J. Phys. Condens. Matter, J. Phys. D Appl. Phys., Phys. Stat. Sol., J. Magn. Magn. Mater., Eur. J. Phys. B, Thin Solid Films

9.8 External Cooperations

Academic

- State University of Campinas, Campinas, Brazil
  Prof. Dr. Y. Kopelevich
- Umea University, Sweden
  Dr. T. Makarova
- Universidad Autónoma de Madrid, Spain
  Prof. Dr. M.A. Ramos, Prof. Dr. S. Vieira
- Institute for Metal Physics, National Academy of Sciences of Ukraine, Kiev, Ukraine
  Prof. Dr. V.M. Pan
- Max-Planck-Institut für Metallforschung, Stuttgart, Germany
  Dr. E.H. Brandt
- University of Ioannina, Greece
  Prof. I. Panagiotopoulos
- Institute for Materials Science, National Center of Scientific Research "Demokritos", Athens, Greece
  Dr. N. Moutis
- Trinity College, Dublin, Ireland
  Prof. J.M.D. Coey
- Leibniz-Institut für Festkörper- und Werkstoffforschung, Dresden, Germany
  Dr. Kathrin Dörr
- University of Sheffield, UK
  Prof. G. Gehring
- University of the Negev, Beer Sheva, Israel
  Dr. E. Rozenberg
- Leibniz-Institut für Oberflächenmodifizierung, Leipzig, Germany
  Dr. K. Zimmer

9.9 Publications

Journals

J. Barzola-Quiquia, P. Esquinazi, M. Rothermel, D. Spemann, T. Butz, N. García: *Experimental evidence for two-dimensional magnetic order in proton bombarded graphite*, Phys. Rev. B **76**, 161 403(R) (2007)

J. Barzola-Quiquia, P. Esquinazi, M. Rothermel, D. Spemann, A. Setzer, T. Butz: *Proton-induced magnetic order in carbon: SQUID measurements*, Nucl. Instrum. Meth. B **256**, 412 (2007)

J. Barzola-Quiquia, P. Häussler: *Electronic transport properties of amorphous and quasicrystals TM Al100-alloys*, J. Non-Cryst. Solids **353**, 3237 (2007)

A.J. Behan, J.R. Neal, R.M. Ibrahim, A. Mokhtari, M. Ziese, H.J. Blythe, A.M. Fox, G.A. Gehring: *Magneto-optical and transport studies of ZnO-based dilute magnetic semiconductors*, J. Magn. Magn. Mater. **310**, 2158 (2007)

Y.F. Chen, M. Ziese: *Intrinsic spin filtering in a $La_{2/3}Ca_{1/3}MnO_3/Nb(1.0\%):SrTiO_3$ junctions*, Eur. Phys. Lett. **77**, 47 001 (2007)

Y.F. Chen, M. Ziese: *Magnetotransport properties of Fe_3O_4-$La_{0.7}Sr_{0.3}MnO_3$ junctions*, J. Phys. D Appl. Phys. **40**, 3271 (2007)

Y.F. Chen, M. Ziese: *Nonlinear transport properties of $La_{2/3}Ca_{1/3}MnO_3$ and Fe_3O_4 films in the extreme Joule heating regime*, J. Appl. Phys. **101**, 103 902 (2007)

Y.F. Chen, M. Ziese: *Spin filtering in $La_{0.7}Sr_{0.3}MnO_3/CoFe_2O_4/Nb(0.5\%):SrTiO_3$ heterostructures*, Phys. Rev. B **76**, 014 426(R) (2007)

Y.F. Chen, M. Ziese, P. Esquinazi: *Interface capacitance of $La_{0.8}Ca_{0.2}MnO_3/Nb:SrTiO_3$ junctions*, J. Appl. Phys. **101**, 123 906 (2007)

Y.F. Chen, M. Ziese, P. Esquinazi: *Joule heating enhanced colossal magnetoresistance in $La_{0.8}Ca_{0.2}MnO_3$ films*, Appl. Phys. Lett. **89**, 082 501 (2006), doi:10.1063/1.2337280

Y.F. Chen, M. Ziese, P. Esquinazi: *Scaling analysis of an apparent metal-insulator transition in a $Fe_3O_4/Nb:SrTiO_3$ bilayer*, J. Magn. Magn. Mater. **316**, e674 (2007)

J.C. González, M. Muñoz, N. García, J. Barzola-Quiquia, D. Spoddig, K. Schindler, P. Esquinazi: *Sample-Size Effects in the Magnetoresistance of Graphite*, Phys. Rev. Lett. **99**, 216 601 (2007)

R. Höhne, P. Esquinazi, V. Heera, H. Weishart: *Magnetic properties of ion-implanted diamond*, Diam. Relat. Mater. **16**, 1589 (2007)

Y. Kopelevich, P. Esquinazi: *Graphene Physics in Graphite*, Adv. Mater. **19**, 4559 (2007)

H. Ohldag, T. Tyliszczak, R. Höhne, D. Spemann, P. Esquinazi, M. Ungureanu, T. Butz: *π-Electron Ferromagnetism in Metal-Free Carbon Probed by Soft X-Ray Dichroism*, Phys. Rev. Lett. **98**, 187 204 (2007)

R. Salzer, D. Spemann, P. Esquinazi, R. Höhne, A. Setzer, K. Schindler, H. Schmidt, T. Butz: *Possible pitfalls in search of magnetic order in thin films deposited on single crystalline sapphire substrates*, J. Magn. Magn. Mater. **317**, 53 (2007)

D. Spoddig, K. Schindler, P. Rödiger, J. Barzola-Quiquia, K. Fritsch, H. Mulders, P. Esquinazi: *Transport properties and growth parameters of PdC and WC nanowires prepared in a dual-beam microscope*, Nanotechnology **18**, 495 202 (2007)

A. Talyzin, A. Dzwilewski, L. Dubrovinsky, A. Setzer, P. Esquinazi: *Structural and magnetic properties of polymerized C_{60} with Fe*, Eur. Phys. J. B **55**, 57 (2007)

Q. Xu, H. Schmidt, L. Hartmann, H. Hochmuth, M. Lorenz, A. Setzer, P. Esquinazi, C. Meinecke, M. Grundmann: *Room temperature ferromagnetism in Mn-doped ZnO films mediated by acceptor defects*, Appl. Phys. Lett. **91**, 092 503 (2007)

Books

P. Esquinazi: *Magnetic Carbon*, in: *Handbook of Magnetism and Advanced Magnetic Materials*, ed. by H. Kronmüller, S. Parkin (Wiley, Chichester 2007)

Talks

J. Barzola-Quiquia, P. Esquinazi, A. Setzer, M. Ziese, M. Rothermel, D. Spemann, T. Butz: *Actual trends in Solid State Physics: a few examples*, Universidad Europea de Madrid, Spain, 10. – 15. December 2007

J. Barzola-Quiquia, P. Esquinazi, A. Setzer, M. Ziese, M. Rothermel, D. Spemann, T. Butz: *Graphene Physics in Graphite: Differences and Similarities*, Universidad Autonoma de Madrid, Spain, 23. November 2007

J. Barzola-Quiquia, P. Esquinazi, A. Setzer, M. Ziese, M. Rothermel, D. Spemann, T. Butz: *High-temperature magnetic order in an aromatic polymer?*, 71st DPG Spring Meeting, Regensburg, 26. – 30. March 2007

J. Barzola-Quiquia, P. Esquinazi, A. Setzer, M. Ziese, M. Rothermel, D. Spemann, T. Butz: *Magnetic order in Carbon*, Graphene-Graphite Workshop, Brasilia, Brazil, 10. June 2007

J. Barzola-Quiquia, P. Esquinazi, A. Setzer, M. Ziese, M. Rothermel, D. Spemann, T. Butz: *Magnetic order in Carbon*, Minerva Seminar, Kefar Hamaccabiah, Israel, 09. May 2007

J. Barzola-Quiquia, P. Esquinazi, A. Setzer, M. Ziese, M. Rothermel, D. Spemann, T. Butz: *Magnetischer Kohlenstoff: Eine wissenschaftliche Geschichte voller Skepsis, Vorurteile und Fallen*, Kolloquium zum Thema "Magnetischer Kohlenstoff", Technische Universität Braunschweig, 17. April 2007

J. Barzola-Quiquia, P. Esquinazi, A. Setzer, M. Ziese, M. Rothermel, D. Spemann, T. Butz: *Spintronics: Physics Nobel Prize 2007*, Universidad Europea de Madrid, 10. – 15. December 2007

9.10 Graduations

Diploma

- Peter Rödiger
  Fabrication and Characterization of Metallic and Superconducting Mesoscopic Structures
  November 2007

Master

- Yashwant Kumar Verma
  AC and DC Magnetization Studies of Cobalt-Ferrite-Magnetite Bilayers and Transport Measurements of Magnetite-Gold Double Layers
  January 2007

9.11 Guests

- Prof. Nicolás García
  CSIC Madrid, Spain
  07. – 20. June 2007
- Theeraphob Saengsri
  Maejo University, Thailand
  02. July – 31. August 2007
- Mari Elisabeth Wale
  University of Oslo, Norway
  18. June – 10. August 2007
- Salomon W. Pohl
  Wilhelm-Ostwald-Gymnasium, Leipzig, Germany
  03. – 16. May 2007
- Marcus Kuhnhardt
  Wilhelm-Ostwald-Gymnasium, Leipzig, Germany
  04. September 2006 – 31. July 2007

III

Institute for Theoretical Physics

10

Computational Quantum Field Theory

10.1 Introduction

The Computational Physics Group performs basic research into classical and quantum statistical physics with special emphasis on phase transitions and critical phenomena. In the centre of interest are currently the physics of spin glasses, diluted magnets and other materials with quenched, random disorder, soft condensed matter physics with focus on fluctuating paths and interfaces, and biologically motivated problems such as protein folding, aggregation and adhesion as well as related properties of semiflexible polymers. These projects are embedded into the joint international DFH-UFA Graduate School "Statistical Physics of Complex Systems" with the l'Université Henri Poincaré Nancy, France, supported by the Deutsch-Französische Hochschule. Investigations of a geometrical approach to the statistical physics of topological defects with applications to superconductors and superfluids and research into fluctuating geometries with applications to quantum gravity (e.g., dynamical triangulations) are conducted within the EC-RTN Network "ENRAGE": *Random Geometry and Random Matrices: From Quantum Gravity to Econophysics*. The statistical mechanics of complex networks is studied within the frame of an Institute Partnership with the Jagellonian University in Krakow, Poland, supported by the Alexander-von-Humboldt Foundation. And with the help of a Development Host grant of the European Commission, also research into the physics of anisotropic quantum magnets has been established.

The methodology is a combination of analytical and numerical techniques. The numerical tools are currently mainly Monte Carlo computer simulations and high-temperature series expansions. The computational approach to theoretical physics is expected to gain more and more importance with the future advances of computer technology, and will probably become the third basis of physics besides experiment and analytical theory. Already now it can help to bridge the gap between experiments and the often necessarily approximate calculations of analytical work. To achieve the desired high efficiency of the numerical studies we develop new algorithms, and to guarantee the flexibility required by basic research all computer codes are implemented by ourselves. The technical tools are Fortran, C, and C++ programs running under Unix or Linux operating systems and computer algebra using Maple or Mathematica. The

software is developed and tested at the Institute on a cluster of PCs and workstations, where also most of the numerical analyses are performed. Large-scale simulations requiring vast amounts of computer time are carried out at the Institute on the Linux cluster GRAWP with 40 Athlon MP1800+ processors, 60 dual-core Opteron 2218 processors, and 18 Opteron 242 processors. Further large-scale computations are performed on the parallel computers of the University computing center and upon grant application at the national supercomputing centres in Jülich and München on IBM and Hitachi parallel supercomputers. This combination of various platforms gives good training opportunities for the students and offers promising job perspectives in many different fields for their future career.

Within the University, our research activities are tightly bound to the Centre for Theoretical Sciences (NTZ) of the Centre for Advanced Study (ZHS) and the recently established "Sächsische Forschergruppe" FOR877 *From Local Constraints to Macroscopic Transport* and the Graduate School "BuildMoNa": Leipzig School of Natural Sciences – *Building with Molecules and Nano-objects* within the Excellence Initiative. These research structures are embedded into the priority research areas ("Profilbildende Forschungsbereiche (PbF)") and the Research Academy Leipzig (RAL), providing in particular the organizational frame for our cooperations with research groups in experimental physics and biochemistry. Also the international DFH-UFA Graduate School with Nancy is integrated into the RAL as a separate "Class". On a wider scale, our research projets are embedded in a wide net of national and international collaborations funded by network grants of the European Commission and the European Science Foundation (ESF), and by binational research grants with scientists in Sweden, China and Poland funded by the German Academic Exchange Service (DAAD) and the Alexander-von-Humboldt Foundation. Further close contacts and collaborations are also established with research groups in Armenia, Austria, France, Great Britain, Israel, Italy, Japan, Russia, Spain, Taiwan, Turkey, Ukraine, and the United States.

Wolfhard Janke

10.2 Free-Energy Barriers of Spin Glasses

M. Aust, F. Beyer, A. Nußbaumer, E. Bittner, W. Janke

A major open problem in statistical physics is the nature of the "glassy" low-temperature phase of finite-dimensional spin-glass systems. It is still unresolved whether the replica symmetry-breaking theory or the phenomenological droplet picture yields the correct description.

In the thermodynamic limit the frozen phase of the mean-field spin glass shows many stable and metastable states. Such a feature is the consequence of the disorder and the frustration characterising spin glasses in general, leading to a rugged free-energy landscape with probable regions (low free energy) separated by rare-event states (high free energy). But also for finite systems the free-energy landscape shows an intricate, corrugated structure. Therefore, it is hard to measure the free-energy barriers by means of conventional Monte Carlo simulations directly. The aim of this project is

to study the free-energy barriers of the Sherrington-Kirkpatrick (SK) mean field spin-glass model [1] and the three-dimensional Edwards-Anderson (EA) nearest-neighbour model [2] using a combination of the multioverlap Monte Carlo algorithm [3] with parallel tempering methods [4]. By using this combined algorithm we are able to perform simulations at much lower temperatures for the EA model than in previous studies [5]. This is necessary, because for temperatures close to the spin-glass transition significant deviations from the theoretical mean-field prediction were found in both the three- and four-dimensional EA model. Since one possible explanation for these deviations are strong finite-size effects close to the spin-glass transition, by measuring at lower temperatures these effects should become less pronounced.

The fact that there is no explicit order parameter which allows one to exhibit the free-energy barriers led us to use the Parisi overlap parameter [6],

$$q = \frac{1}{N} \sum_{i=1}^{N} s_i^{(1)} s_i^{(2)} \ , \tag{10.1}$$

where the spin superscripts label two independent (real) replicas for the same realization of randomly chosen exchange coupling constants $\mathcal{J} = \{J_{ij}\}$. For given $\mathcal{J}$ the probability density of q is denoted by $P_{\mathcal{J}}(q)$, and the function $P(q)$ is obtained as

$$P(q) = [P_{\mathcal{J}}(q)]_{\text{av}} = \frac{1}{\#J} \sum_{\mathcal{J}} P_{\mathcal{J}}(q) \ , \tag{10.2}$$

where $[\ldots]_{\text{av}}$ symbolises the quenched average and $\#J$ is the number of realizations considered. For a given realization of $\mathcal{J}$ the nontrivial (i.e., away from $q = \pm 1$) minima are related to the free-energy barriers of this disordered system. We are, therefore, interested in the whole range of the probability density $P_{\mathcal{J}}(q)$, for an example see Fig. 10.1.

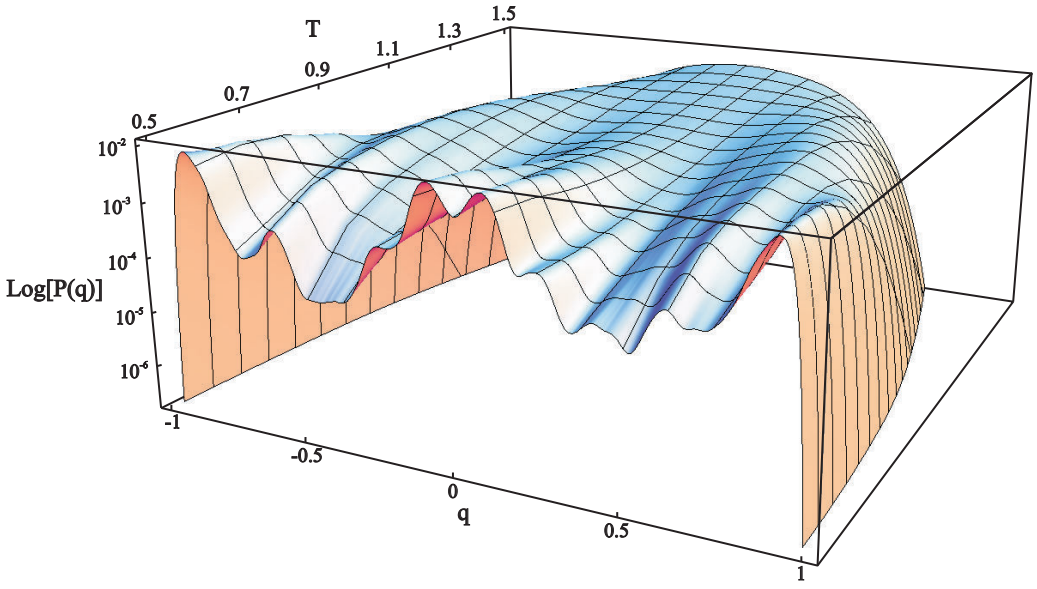

Figure 10.1: EA model: The logarithm of the canonical $P(q)$ distribution for a 8^3 lattice as a function of temperature for a typical disorder realisation.

We found that the free-energy barriers of the SK model are non-self-averaging and distributed according to the Fréchet extreme-value distribution [7]. These particular features were also found for the EA nearest-neighbour model [8] and such similarities support the position that the Parisi replica symmetry breaking solution of the SK model is the limit of the short-range model on a lattice in dimension d when $d \to \infty$, with a proper rescaling of the strength of the Hamiltonian. On the other hand, we also found that the free-energy barriers of the SK model diverge with the theoretically predicted value $\alpha = 1/3$, which is in contrast to our new results for the EA model in three dimensions [8] and previous findings for the three- and four-dimensional EA model [5].

This work is partially supported by the Deutsche Forschungsgemeinschaft (DFG) under grant No. JA483/22-1 and the JUMP supercomputer time grant hlz10 of NIC, Forschungszentrum Jülich.

[1] D. Sherrington, S. Kirkpartick: Phys. Rev. Lett. **35**, 1792 (1975)
[2] S.F. Edwards, P.W. Anderson: J. Phys. F Metal Phys. **5**, 965 (1975)
[3] B.A. Berg, W. Janke: Phys. Rev. Lett. **80**, 4771 (1998)
[4] K. Hukushima, K. Nemoto: J. Phys. Soc. Jpn. **65**, 1604 (1996)
[5] B.A. Berg et al.: Phys. Rev. B **61**, 12 143 (2000)
[6] G. Parisi: Phys. Rev. Lett. **43**, 1754 (1979)
[7] E. Bittner, W. Janke: Europhys. Lett. **74**, 195 (2006)
[8] E. Bittner et al.: in *NIC Symposium 2008*, NIC Series, Vol. **39**, ed. by G. Münster et al. (John von Neumann Institute for Computing, Jülich 2008) p 229

10.3 Self-Avoiding Walks on Percolation Clusters

V. Blavatska, W. Janke

The universal configurational properties of long, flexible polymer chains in a good solvent are perfectly described by the model of self-avoiding walks (SAWs) on a regular lattice [1]. In particular, the average square end-to-end distance $\langle R^2 \rangle$ and the number of configurations Z_N of SAWs with N steps obey the scaling laws:

$$\langle R^2 \rangle \sim N^{2\nu_{\mathrm{SAW}}} , \qquad Z_N \sim z^N N^{\gamma_{\mathrm{SAW}}-1} , \tag{10.3}$$

where ν_{SAW} and γ_{SAW} are the universal critical exponents that only depend on the space dimension d.

A question of great interest is how SAWs behave on randomly diluted lattices, which may serve as a model of linear polymers in a porous medium. This problem attracts a great attention of researchers [2]. Most interesting is the case when the concentration p of structural defects is exactly at the percolation threshold p_c. Studying properties of percolative lattices, one encounters two possible statistical averages. In the first, one considers only incipient percolation clusters whereas the other statistical ensemble includes all the clusters, which can be found in a percolative lattice. For the latter ensemble of all clusters, the SAW can start on any of the clusters, and for an N-step SAW, performed on the ith cluster, we have $\langle R^2 \rangle \sim l_i^2$, where l_i is the averaged size of the ith cluster. We are interested in the former case, when SAWs reside only on the

percolation cluster. In this regime, the scaling laws (10.3) hold with new exponents $\nu_{p_c} \neq \nu_{\mathrm{SAW}}, \gamma_{p_c} \neq \gamma_{\mathrm{SAW}}$ [2, 3]. A hint to the physical understanding of this phenomenon is given by the fact that weak disorder does not change the dimension of a lattice, whereas the percolation cluster itself is a fractal with fractal dimension $d^F_{p_c}$ dependent on d. In this way, scaling law-exponents of SAWs change with the dimension $d^F_{p_c}$ of the (fractal) lattice on which the walk resides.

Note that up to date there do also not exist many studies dedicated to Monte Carlo (MC) simulations of our problem and they do still exhibit some controversies. The value for ν_{p_c} was found in two dimensions to be in a new universality class in a study of Grassberger [4]. In the case of three and four dimensions, there also exist estimates indicating a new universality class, but no satisfactory numerical values have been obtained so far.

In our study, we use the pruned-enriched Rosenbluth method (PERM), proposed in the work of Grassberger [5], taking into account that a SAW can have its steps only on the sites belonging to the backbone of the percolation cluster. In the given problem, we have to perform two types of averaging: the first average is performed over all SAW configurations on a single backbone, the second average is carried out over different realizations of disorder, i.e. over many backbone configurations. We use lattices of size up to $L_{\mathrm{max}} = 300, 200, 50$ in $d = 2, 3, 4$, respectively, and perform averages over 1000 clusters in each case.

Since we can only construct lattices of a finite size L, it is not possible to perform very long SAWs on it. For each L, the scaling laws (10.3) hold only up to some "marginal" number of SAW steps N_{marg}. We take this into account when analyzing the data obtained; for each lattice size we are interested only in values of $N < N_{\mathrm{marg}}$, which results in effects of finite-size scaling for critical exponents. We find, that for a SAW confined inside a lattice with size L finite-size scaling holds:

$$\langle r \rangle \sim N^{\nu_{p_c}} g\left(\frac{N}{L^{1/\nu_{p_c}}}\right) , \tag{10.4}$$

where g is a scaling function.

Our results bring about numerical values of critical exponents, governing the end-to-end distance of SAWs in a new universality class in two-, three-, and four-dimensional lattices at the percolation thresholds. The effects of finite lattice size are discussed as well.

[1] J. des Cloizeaux, G. Jannink: *Polymers in Solution* (Clarendon Press, Oxford 1990); P.-G. de Gennes: *Scaling Concepts in Polymer Physics* (Cornell University Press, Ithaca 1979)
[2] K. Barat, B.K. Chakrabarti: Phys. Rep. **258**, 378 (1995)
[3] V. Blavatska et al.: Phys. Rev. E **70**, 035 104(R) (2004)
[4] P. Grassberger: J. Phys. A **26**, 1023 (1993)
[5] P. Grassberger: Phys. Rev. E **56**, 3682 (1997); H.-P. Hsu et al.: J. Chem. Phys. **118**, 444 (2003)

10.4 Percolation of Vortices and Monopoles in the 3D Abelian Lattice Higgs Model

S. Wenzel, E. Bittner, W. Janke, A.M.J. Schakel*

*Institut für Theoretische Physik, Freie Universität Berlin

The Abelian Higgs model with a compact gauge field formulated on a three-dimensional (3D) lattice possesses an intriguing phase structure. In addition to the Higgs state where the photon acquires a mass, it exhibits a state in which electric charges are confined. The richness of the model, which serves as a toy model for quark confinement, stems from the presence of two types of topological excitations: vortex lines and magnetic monopoles. The former are similar to the defect lines found in superfluid liquids. The latter are point defects in three dimensions which arise because of the compactness of the $U(1)$ gauge group. In the pure 3D compact Abelian gauge theory, these monopoles lead to confinement of electric charges for all values of the gauge coupling. The coupling to the scalar theory preserves this confinement state and gives in addition rise to a Higgs state. For sufficiently small values of the Higgs self-coupling parameter λ, the two ground states are separated by a first-order transition as sketched in Fig. 10.2. For λ larger than a critical value λ_c, which depends on the value of the gauge coupling, the two states are no longer separated by a transition where thermodynamic observables become singular, i.e., it is always possible to cross over from one ground state to the other without encountering a thermodynamic singularity. Because of this, the Higgs and confinement states were thought to constitute a single phase, despite profound differences in physical properties.

In [1], we argued that the phase diagram is more refined than implied by this picture. We conjectured that although analytically connected, the two ground states can be considered as two distinct phases. In the confinement phase the monopoles must form

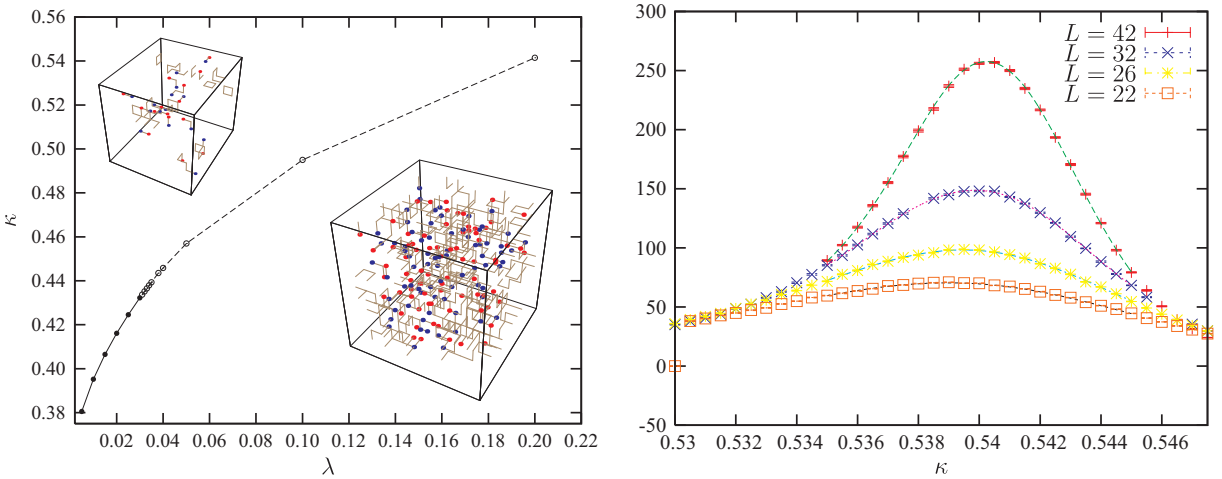

Figure 10.2: *Left:* Phase diagram of the $U(1)$ Lattice Higgs in dependence on two coupling constants. While for small λ the type of the transition line is of first order (*black dots*), the line continues as a Kertész line (*open dots*) with no thermal phase transition. The insets show typical configurations of the vortex network in the two phases. *Right:* Diverging susceptibility of the maximal cluster size at the Kertész line.

a plasma which means that they are no longer tightly bound in pairs as in the Higgs phase, cf. the typical configuration plots in Fig. 10.2. Since the tension of the vortex lines connecting the monopoles and antimonopoles is finite in the Higgs phase and zero in the confinement phase, we argued that the phase boundary is uniquely defined by the vanishing of the vortex line tension, irrespective of the order of the phase transition.

In addition to open vortex lines the system also possesses closed vortex lines which are expected to be characterized by the same line tension. Because of the finite line tension, large vortex loops are exponentially suppressed in the Higgs phase. Upon approaching the phase boundary, the line tension becomes smaller so that the vortex network can grow larger and the overall line density increases. Finally, at the phase boundary where the line tension vanishes, vortices can grow arbitrarily large at no energy cost. The phase boundary between the Higgs and confinement phase is therefore expected to be marked by a proliferation of (open and closed) vortex lines. The vortices proliferate both in the region where the transition is first-order and in the region where it is not. A line along which geometrical objects proliferate, yet thermodynamic quantities and other local gauge-invariant observables remain nonsingular has become known as a Kertész line [2]. Such a line was first discussed in the context of spin clusters in the 2D Ising model in an applied magnetic field.

In our Monte Carlo study [3] we investigated this vortex proliferation scenario by studying the behavior of the vortex network directly. Because vortices are geometrical objects, their analysis is amenable to the methods developed in percolation theory [4]. As one of our main results we find that along the Kertész line, percolation observables have the usual percolation exponents. In addition, we verified that the vortex network displays discontinuous behavior in the region where the phase boundary consists of a first-order transition.

This work is partially supported by the Studienstiftung des deutschen Volkes (S.W.).

[1] S. Wenzel et al.: Phys. Rev. Lett. **95**, 051 601 (2005)
[2] J. Kertész: Physica A **161**, 58 (1989)
[3] S. Wenzel et al.: Nucl. Phys. B **793**, 344 (2008)
[4] D. Stauffer, A. Aharony: *Introduction to Percolation Theory* (Taylor and Francis, London 1994)

10.5 Geometric Properties of the Three-Dimensional Ising and XY Models

F.T. Winter*, A.M.J. Schakel†, W. Janke

*John von Neumann-Institut für Computing (NIC), Forschungszentrum Jülich, Germany and Deutsches Elektron-Synchrotron (DESY), Zeuthen, Germany

†Institut für Theoretische Physik, Freie Universität Berlin

The relation between thermal phase transitions of lattice spin systems and the percolation problem has been in the focus of intense research for at least three decades. Clusters of spins are natural objects occurring in the analysis of phase ordering processes and nucleation [1], and a theory of critical phenomena in terms of purely geometrical objects

appears appealing. In this context, it had long been surmised that a continuous phase transition of a spin system might be accompanied (or, in fact, caused) by a percolation transition of the clusters of like spins (*geometric clusters*). While the geometric clusters are not yet the proper objects in general, it turned out that, in fact, a close relation between thermal phase transitions and percolation can be established by considering *stochastically* defined clusters (or droplets) as they occur in the Fortuin–Kasteleyn (FK) or Coniglio–Klein (CK) representation of the Potts model. Using this type of clusters, the Potts model can be shown to be equivalent to a site-bond correlated percolation problem [2] such that the corresponding critical exponents agree exactly.

In this sprit we have recently developed a new approach in which the high-temperature (HT) series expansion of lattice spin models is used to study their critical properties in a geometric percolation picture. In this approach, the partition function and correlation functions are calculated by counting graphs on the lattice, with each graph representing a certain contribution. Traditionally, such an expansion is carried out exactly to a given order by enumerating all possible ways a graph of given size and topology can be drawn on the lattice. This exact approach, involving combinatorial and graph-theoretical algorithms, is notoriously challenging and laborious, with each additional order requiring typically about the same amount of effort needed for all previous orders combined.

To circumvent this problem, we apply here Monte Carlo simulations to sample the graph configurations stochastically, cf. Fig. 10.3. At high temperatures, only a few small graphs generated this way can be found scattered throughout the lattice. As the temperature is lowered, graphs start to fill the lattice by growing larger and becoming more abundant. At temperatures below the critical temperature, the lattice becomes filled with graphs. A typical graph configuration now consists of one big graph spanning the entire lattice and a collection of much smaller graphs (see Fig. 10.4). The steady increase in the number of occupied links and the appearance of graphs spanning the lattice as the temperature is lowered are reminiscent of a percolation process. The use of percolation observables therefore suggests itself to analyze the graph configurations. For these observables to have bearing on the critical properties of the model under investigation, it is necessary that the HT graphs percolate right at the thermal critical point. The fractal structure of closed and open graphs then encodes the standard critical exponents [3].

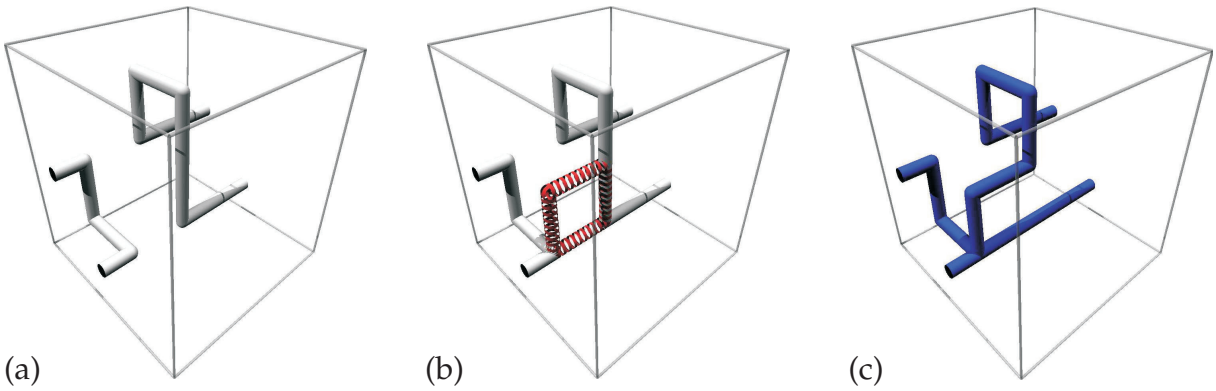

Figure 10.3: An existing Ising HT graph on a cubic lattice (**a**) is updated with the help of a chosen plaquette (**b**) into a new graph (**c**).

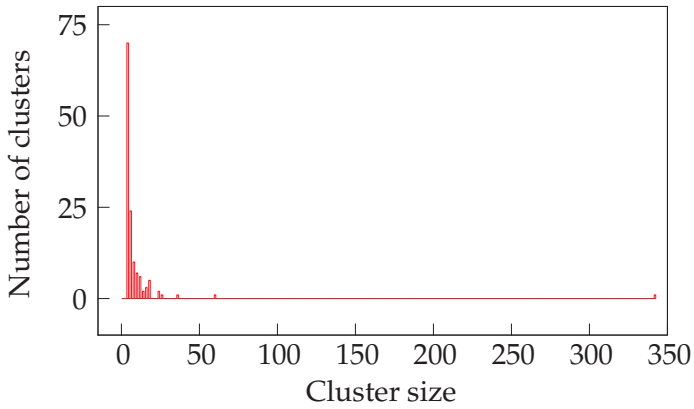

Figure 10.4: Distribution of Ising HT graphs on a cubic lattice of linear size $L = 24$ at the percolation threshold. Note the presence of a single big graph and many much smaller graphs.

We have verified this scenario for the HT graphs of the three-dimensional Ising and XY models on a simple cubic lattice with periodic boundary conditions [4]. The graphs are shown to indeed percolate right at the (thermal) Curie critical point. The diverging length scale relevant to the graphs in the vicinity of the percolation threshold is shown to be provided by the spin correlation length. By applying finite-size scaling techniques, the fractal dimension of the HT graphs at criticality is estimated to be $D = 1.7349(65)$ for the Ising and $D = 1.7626(66)$ for the XY model, which both are, via general scaling relations, in good agreement with the standard thermal critical exponents.

[1] K. Binder et al.: Phys. Rev. B **12**, 5261 (1976); A.J. Bray: Adv. Phys. **43**, 357 (1994)
[2] C.M. Fortuin, P.W. Kasteleyn: Physica **57**, 536 (1972); A. Coniglio, W. Klein: J. Phys. A **13**, 2775 (1980)
[3] W. Janke, A.M.J. Schakel: Nucl. Phys. B **700**, 385 (2004); Phys. Rev. E **71**, 036 703 (2005); Braz. J. Phys. **36**, 708 (2006); in *Order, Disorder and Criticality: Advanced Problems of Phase Transition Theory*, Vol. 2, ed. by Y. Holovatch (World Scientific, Singapore 2007) p 123
[4] F.T. Winter et al.: *Geometric Properties of the Three-Dimensional Ising and XY Models*, Phys. Rev. E (2008), in print

10.6 Statistical Mechanics of Complex Networks

B. Wacław, L. Bogacz*, Z. Burda*, W. Janke

*Institute of Physics, Jagellonian University, Krakow, Poland

Recent progress in understanding the structure and function of complex networks [1] has been largely influenced by the application of methods of statistical physics. We use these tools to investigate the properties of different models of networks as well as dynamical processes taking place on them. We also study matter-network interactions, that is situations when not only the network governs the behavior of some matter field placed on it, but also the matter field can have an influence on the network. For all problems, we apply both analytical and Monte Carlo methods.

An example of a problem we study in connection with structural properties of networks are finite-size effects in equilibrated graphs [2]. These are graphs which are maximally random under given constraints. The possible constraints are, for instance, fixing the total number of nodes and links, excluding multiple- and self-connections, or imposing a tree structure. Finite-size effects in graphs are very strong, much stronger than in more "typical" physical systems, where the number of degrees of freedom is of order 10^{23}. In networks, however, the typical number of nodes N is between 10^3 (transportation networks) to 10^9 (the World Wide Web). Moreover, since complex networks have in general infinite fractal dimension, their "surface" is very large in comparison to the volume. This, together with power-law degree distributions of many networks is the reason why very large corrections to solutions in the thermodynamic limit appear. We study these corrections by means of analytical methods and also with the help of advanced Monte Carlo procedures like, e.g., multicanonical simulations.

Apart from the structural properties we also study their influence on the dynamics on networks. A very simple model we consider is the zero-range process (ZRP) [3], where some particles hop between nodes along existing connections between them. Particles jump according to a very local rule: the probability that a particle will move to another site depends only on the occupation of the departure node. Because of its simplicity, this model can be treated analytically in many aspects. It has, however, a very rich behavior. For instance, in networks with inhomogeneous degrees of nodes, that is when nodes have various numbers of nearest neighbors, a phenomenon called condensation occurs. This means that a finite fraction of particles resides on a single node. This can be viewed as a prototype of traffic jamming. We study conditions under which the condensate is formed, a typical time it takes to build the condensate from a uniform background, and its mean life time [4].

We also investigate the interplay between the network and the matter. The prototype of such a system is a modified ZRP, where we allow the network to rearrange itself in parallel to the particle dynamics. Different rules for rewiring connections lead to different effects. But even if we rewire links at random, there is an interesting transition from the condensed to a liquid phase provided that the rewiring rate is large enough. It turns out that if the node with maximal number of neighbors migrates fast through the network, the condensate has no time to grow up [5].

On the other hand, if the network dynamics is very slow, it can be considered as quenched disorder from the particles point of view. The averaging over the disorder can lead to a very interesting effect: for networks with properly tuned degree distribution, the distribution of particles shows a power law, exactly as it has been observed in the ZRP on homogeneous networks [6].

This work is partially supported by a Fellowship of the German Academic Exchange Service (DAAD), an Institute Partnership grant "Krakow–Leipzig" of the Alexander-von-Humboldt Foundation and the EU Network "ENRAGE"

[1] S. Boccaletti et al.: Phys. Rept. **424**, 175 (2006)
[2] L. Bogacz et al.: Physica A **366**, 587 (2006)
[3] M.R. Evans, T. Hanney: J. Phys. A: Math. Gen. **38**, R195 (2005)
[4] B. Waclaw et al.: Phys. Rev. E **76**, 046 114 (2007)
[5] L. Bogacz et al.: Proc. SPIE **6601**, 66 010V (2007)
[6] B. Waclaw et al.: submitted to Eur. Phys. J. B (2008), arXiv:0802.2688

10.7 Studies of Structure Formation Processes Employing Mesoscopic Models for Polymers and Proteins

C. Junghans[*], A. Kallias[†], M. Möddel, J. Schluttig[‡], S. Schnabel, M. Bachmann[§], W. Janke

[*]Max-Planck-Institute for Polymer Research, Mainz
[†]Volkswagen AG, Wolfsburg
[‡]Center for Modelling and Simulation in the Biosciences (BIOMS), Ruprecht-Karls-Universität Heidelberg
[§]Universität Leipzig and Lunds Universitet, Lund, Sweden

With several thermodynamic and kinetic questions regarding polymer and protein folding, aggregation and adsorption at solid substrates in mind, we have investigated by means of sophisticated Monte Carlo [1–6] and thermostated Molecular Dynamics simulations [7] mesoscopic models for homo- and heteropolymers. Usually, polymer structure formation processes require semilocal or even nonlocal cooperativity of the monomers involved. In good solvents, secondary structures such as helices and sheets, for example, are formed on relatively small scales, whereas the hydrophobic collapse requires an optimal formation of all monomers in a highly compact shape. If it comes to crystallization, the monomers can even arrange in symmetric structures. Because of the mesoscopic nature of tertiary structure formations processes, simplified models can be employed to analyze characteristic features of such conformational transitions.

Therefore, we have likewise analyzed hydrophobic collapse, crystallization, as well as compact hydrophobic-core formation with mesoscopic models for the folding of flexible homopolymers and hydrophobic-polar heteropolymers, the aggregation of polymers, and the adsorption of polymers at attractive solid substrates. The main advantage of these models is the possibility to perform systematic, comparative studies regarding different aspects. In a detailed analysis of a simple heteropolymer model based on the effective attraction of nonbonded hydrophobic monomers (mimicking the "hydrophobic effect" in good solvents) [8], we could show that typical folding characteristics known from natural proteins are also observed on mesoscopic scales, i.e., without explicitly taking into account interactions on nanoscales [1, 2]. One such typical folding behavior is two-state folding, where only ensembles of folded and denatured protein structures occur. In this case, folding and unfolding times depend exponentially on the temperature near the transition state [3].

By investigating the nucleation transition of small peptides and polymers with mesoscopic models, we have also found that the aggregation of polymers and peptides is a phase separation process, in which the loss of entropy due to surface effects entails an decrease of temperature with increasing energy ("backbending effect") [4–6].

[1] S. Schnabel et al.: Phys. Rev. Lett. **98**, 048 103 (2007)
[2] S. Schnabel et al.: J. Chem. Phys. **126**, 105 102 (2007)
[3] A. Kallias et al.: J. Chem. Phys. **128**, 055 102 (2008)
[4] C. Junghans et al.: Phys. Rev. Lett. **97**, 218 103 (2006)
[5] C. Junghans et al.: J. Chem. Phys. **128**, 085 103 (2008)
[6] C. Junghans et al.: *Monte Carlo Study of Polymer Aggregation*, Mainz/Leipzig preprint (2008)

[7] J. Schluttig et al.: *Comparative Molecular Dynamics and Monte Carlo Study of Statistical Properties for Coarse-Grained Heteropolymers*, J. Comput. Chem. (2008), in print
[8] F.H. Stillinger et al.: Phys. Rev. E **48**, 1469 (1993); F.H. Stillinger, T. Head-Gordon: Phys. Rev. E **52**, 2872 (1995)

10.8 Conformational Transitions of Flexible Polymers

T. Vogel, S. Schnabel, M. Bachmann*, W. Janke

*Universität Leipzig and Lunds Universitet, Lund Sweden

The nature of conformational freezing transitions of single flexible polymers and their relations to colloidal systems is little understood. Systems of finite length that can computationally be studied do not reveal a clear picture at all. This is actually not surprising as the large conformational entropy of frozen polymer conformations leads to the assumption that the solid phase is largely amorphous and frustrated. In contrast, very large systems are known to form crystalline structures with long-range order in order to optimize energetically favored short-range monomer-monomer contacts. The reason for the complexity of the structural behavior of small polymers is the competition between surface effects in order to reduce interfacial free energy and the tendency to form lattice structures in the interior.

Even in lattice models, the diversity of lowest-energy conformations can be observed [1]. For polymers of different lengths on the simple-cubic lattice, we have found a remarkably systematic pattern of the freezing transition which can be explained by lattice effects of the finite-length systems. In fact, the high precision of our data allows us to reveal a noticeable difference in the behavior of "magic" chain lengths that allow for cubic or cuboid conformations. In these cases, an energy gap exists between the ground-state conformations and the first excitations. This peculiarity causes a first-order-like pseudotransition which is typically more pronounced than the separate freezing transition. Surprisingly, this effect vanishes widely for polymers with slightly longer chain lengths. The freezing temperature decreases with increasing chain length until the next "magic" length is reached. Polymers on the face-centered cubic lattice behave similarly, but the relevant geometries are more complex.

Employing a flexible polymer model with highly elastic covalent bonds, polymer freezing behaves similar like atomic cluster formation at low temperatures (Lennard–Jones cluster) [2]. There are also "magic numbers" of atoms or monomers, for which almost perfect geometric structures form (see Fig. 10.5 for an icosahedral structure of a 147mer). A particularly important shape is the regular icosahedron with 20 equilateral triangular faces and it is known to be the basic capsid structure of spherical viruses, on which the capsomer proteins assemble. For chain lengths different from "magic" numbers, overlayers form on the outer faces. Depending on the kind of monomer arrangement on the surface, so-called Mackay or anti-Mackay layers are distinguished. Actually, the different strategies how clusters grow with increasing chain lengths make a uniform description of the freezing transition for flexible polymers quite intricate. The situation seems to be even more difficult for polymers with nonflexible bonds (such as proteins), as regular tertiary structures can hardly be identified.

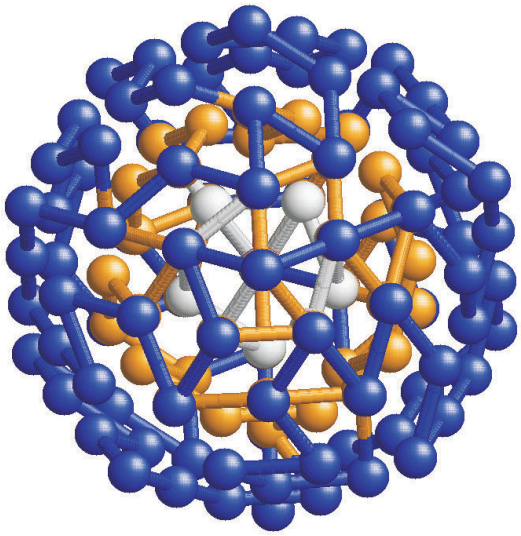

Figure 10.5: Optimal volume-filling icosahedral shape of a flexible polymer with elastic bonds. The linear polymer consists of 147 monomers and as such it is of "magic" length.

[1] T. Vogel et al.: Phys. Rev. E **76**, 061 803 (2007)
[2] S. Schnabel et al.: *Liquid-Solid Transitions of Flexible Polymers*, Leipzig preprint (2008)

10.9 Thickness-Dependent Secondary–Structure Formation of Tubelike Polymers

T. Vogel, T. Neuhaus*, M. Bachmann†, W. Janke

*John von Neumann-Institut für Computing (NIC), Forschungszentrum Jülich, Germany
†Universität Leipzig and Lunds Universitet, Lund, Sweden

By means of Monte Carlo methods, we have investigated conformational ground-state and thermodynamic properties of a simple model for flexible polymer classes with explicit thickness [1]. The thickness constraint, which is introduced via the global radius of curvature [2] of a polymer conformation, accounts for the excluded volume induced by the polymer side chains. In our detailed analysis of ground states and conformational phases of short tubelike polymers, we find that, depending on the thickness, known secondary structures like helices and turns, but also ringlike conformations and stiff rods are intrinsic topologies of such tubelike objects. Explicit dipole-dipole interactions resulting in the formation of hydrogen bonds, which in natural polymers stabilize secondary structures are, thus, not a necessary prerequisite for forming secondary structures. Furthermore, we clearly find that the thickness of polymers noticeably influences the ability to form structural segments which naturally occur in conformations of linear polymers, such as proteins.

For the identification of underlying *secondary* structure segments like helices and strands, the generic modeling of volume exclusion by means of pair potentials is not

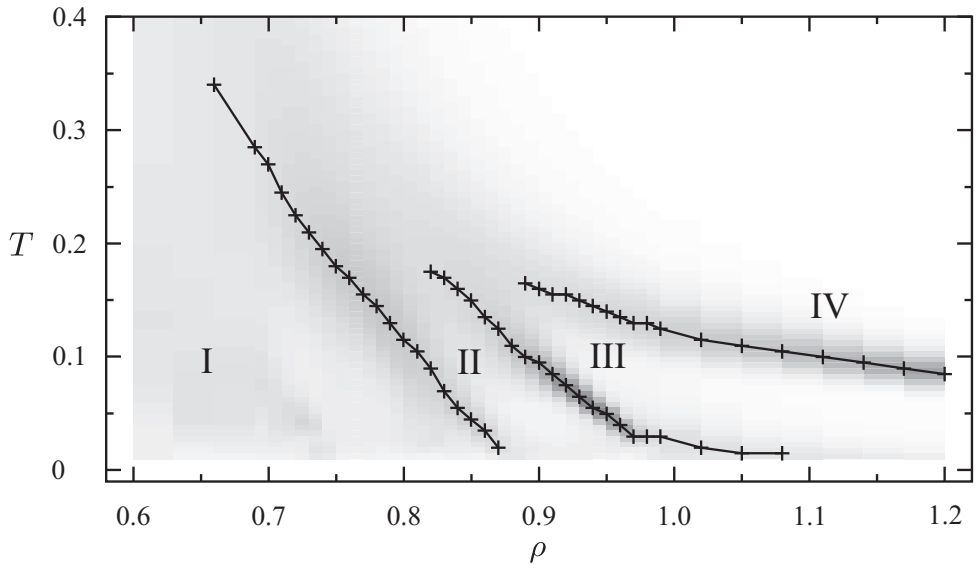

Figure 10.6: Hundreds of simulations revealed a clear structure of the temperature–thickness pseudophase diagram of secondary structures for classes of short tubelike polymers. Dominant structures in the principal phases are found to be helical (I), sheetlike (II), ringlike (III), or random coils/rods (IV).

sufficient. Rather, the formation of such segments requires the cooperative behavior of adjacent monomers, i.e., in addition to pairwise repulsion, information about the relative position of the monomers to each other in the chain is necessary to effectively model the competition between noncovalent monomeric attraction and short-range repulsion due to volume exclusion effects [3]. The simplest way to achieve this in a general, unspecific mesoscopic model is to introduce a hard single-parameter thickness constraint and, thus, to consider a polymer chain rather as a three-dimensional tube than as a one-dimensional, linelike object [4, 5].

We have also analyzed in detail the phase diagram of flexible polymers that does not only allow for the classification of possible thermodynamic conformational phases of a single polymer with fixed thickness (see Fig. 10.6). Performing various simulations for different thicknesses enabled us also to resolve the phase behavior with respect to the thickness constraint. This means that the we have identified the structure of the conformational space of *classes* of polymers, parametrized by their thickness. Although we employ a generic model for flexible polymers, we find that the thickness constraint is an intrinsic source of an effective stiffness. The main result of our analysis is that the tube thickness is also responsible for the capability of a polymer to form secondary structures. Indeed, we clearly find helical and sheet-like structures which are dominant in different pseudophases.

[1] T. Vogel et al.: *Thickness-Dependent Secondary Structure Formation of Tubelike Polymers*, Leipzig/Jülich preprint (2008)
[2] O. Gonzalez, J. Maddocks: Proc. Natl. Acad. Sci. USA **96**, 4769 (1999)
[3] J.R. Banavar et al.: J. Phys. Cond. Matter **15**, S1787 (2003)
[4] A. Maritan et al.: Nature **406**, 287 (2000); J.R. Banavar, A. Maritan: Rev. Mod. Phys. **75**, 23 (2003)
[5] T. Neuhaus et al.: Phys. Rev. E **75**, 051 803 (2007)

10.10 Computer Simulation and Experimental Analysis of Peptide Adhesion at Semiconductor Substrates

K. Goede*, M. Grundmann*, S. Mitternacht†, A. Irbäck†, S. Schnabel, M. Bachmann‡, W. Janke

*Semiconductor Physics Group, Institute for Experimental Physics II
†Lunds Universitet, Lund, Sweden
‡Universität Leipzig and Lunds Universitet, Lund, Sweden

In this project, we have investigated solvent properties and adsorption behavior of short synthetic proteins. From experiments [1–3], it is known that some of these peptides possess a specific adsorption characteristics at semiconductor surfaces like, for example, silicon (Si) and gallium-arsenide (GaAs) with certain crystal orientations at the surface. It could be shown in these experiments that permutations and pointwise mutations of the amino acid sequences can cause noticeably changes in the adsorption behavior of the peptides. In our simulation study, our main interest was devoted to an amino-acid sequence that exhibits good binding propensity to the (100) surface of GaAs and poor binding strength to Si(100) and to a peptide with the same amino acid contents but with randomly permuted sequence. In the latter case, the adsorption strength to Si(100) improved noticeably. It is one of the main objectives of our project to get deeper insights into specific properties of peptide binding to semiconductor substrates by means of single-molecule Monte Carlo computer simulations of a hybrid model that enables a detailed analysis of the thermodynamics of folding and adsorption properties on atomic scales. On the other hand, it is required that the model is sufficiently simple allowing for an efficient simulation. The particular complexity of the problem lies in the competition of the folding and the adsorption transitions, both affecting the conformational changes of the peptides under the influence of thermal fluctuations.

In a first step, we have analyzed solvent properties of these peptides [4]. For that purpose, we performed simulated tempering computer simulations employing a simplified implicit-water all-atom protein model that had recently been developed in the Lund group [5, 6]. Although unstructured conformations dominate at room temperature, we found surprisingly clear evidence that the peptide with good Si(100) binding strength and the peptides with small Si(100) binding propensities exhibit different tendencies in forming secondary-structure (i.e., α-helical and β-stranded) segments. We could also identify the amino acid proline and its different position in the sequences we compared with each other as being relevant for the different trends in structure formation. By a pairwise mutation regarding the proline positions, we could also show that then the trends of secondary-structure formation reverse.

In order to check our experimentally not yet verified prediction that this trend reversal also changes the binding propensity to Si(100) substrates, we have developed and analyzed in the second part of the project an extension of the peptide model, where the interaction with a Si(100) substrate has been incorporated [7]. In our model, the Si substrate is considered as bare and flat. This approach is justified, as our experiments revealed that the Si(100) substrate is not yet noticeably oxidized while the peptide adsorption process proceeds. The multicanonical computer

simulations we performed with this model not only confirmed qualitatively the experimentally observed Si(100) binding specificity of the different peptides; we also found that the position changes of proline in the sequences actually reverse also the binding propensity of the peptides as predicted from our studies of the peptides' solvent behavior.

[1] S.R. Whaley et al.: Nature **405**, 665 (2000)
[2] K. Goede et al.: Nano Lett. **4**, 2115 (2004)
[3] K. Goede et al.: Langmuir **22**, 8104 (2006)
[4] S. Mitternacht et al.: J. Phys. Chem. B **111**, 4355 (2007)
[5] A. Irbäck et al.: Biophys. J. **85**, 1466 (2003)
[6] A. Irbäck, S. Mohanty: Biophys. J. **88**, 1560 (2005)
[7] M. Bachmann et al.: *Sequence-Specific Peptide Adsorption at (100) Silicon Surfaces*, Lund/Leipzig preprint (2008)

10.11 Directional-Ordering in the Two-Dimensional Compass Model

S. Wenzel, W. Janke

The so-called compass model with quantum spin-degrees of freedom is a possible realization of a system that topologically protects Qbits from decoherence [1] and has, as such, prompted recent theoretical investigations. The model is a spin model on a simple square lattice (in two-dimensions), defined by the Hamiltonian

$$\mathcal{H} = \sum_i \left(J_x S_i^x S_{i+e_x}^x + J_y S_i^y S_{i+e_y}^y \right) , \tag{10.5}$$

where $S = (S^x, S^y)$ is a two-component spin on sites i and J_x, J_y are the coupling constants. This Hamiltonian looks very similar to an ordinary XY model but differs

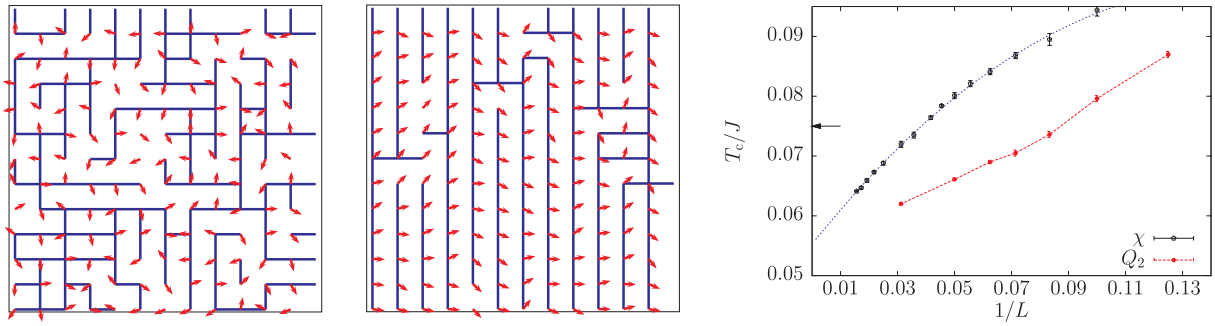

(a) (b) (c)

Figure 10.7: (**a**) Sketch of spin configurations in the disordered state and (**b**) in the ordered state where thick lines indicate bonds carrying the important energy contributions. The pictures are obtained from simulations of the classical model. (**c**) The critical temperature T_c obtained from finite-size scaling of the susceptibility at different lattice sizes L. Our result is at variance with a recent estimate (indicated by the arrow) in the literature.

from it crucially in that the interactions in the system are strangely non-isotropic. The x-component of the spin interacts only with nearest neighbor spins in x-direction and the y-component in y-direction, respectively.

We study this model for the case $J_x = J_z$ employing state-of-the-art quantum Monte Carlo methods based on the so-called stochastic series expansion (SSE) [2]. By investigating the quantity $D = |E_x - E_y|$ (the difference between mean energy in x and y direction), we show that there is a finite-temperature phase transition between a disordered state ($T > T_c$) and an ordered state. This ordered state is not magnetic but rather like a nematic phase oriented with equal probability in x or $y-$direction (see Fig. 10.7a,b). By performing comprehensive simulations of the model we were able to determine the critical temperature T_c and the critical exponents of this transition. Our results reported in [3] improve previous values in the literature considerably and provide a first real benchmark for future studies (see Fig. 10.7c).

[1] B. Douçot et al.: Phys. Rev. B **71**, 024 505 (2005)
[2] A.W. Sandvik, J. Kurkijärvi: Phys. Rev. B **43**, 5950 (1991); O.F. Syljuasen, A.W. Sandvik: Phys. Rev. E **66**, 046 701 (2002)
[3] S. Wenzel, W. Janke: Leipzig preprint (2008), arXiv:0804.2972

10.12 Quantum Critical Phenomena and Quantum Spin Systems

R. Bischof, S. Wenzel, I. Juhász Junger*, L. Bogacz†, D. Ihle*, W. Janke

*Theory of Condensed Matter Group
†Institute of Physics, Jagellonian University, Krakow, Poland

In this project we study the quantum Heisenberg model, which is one of the most fundamental models of quantum magnetism. Several aspects of this model are studied in relation to a theoretical understanding of quantum phase transition.

Firstly, so called mixed spin chains in one dimension (1D) are considered. The low temperature properties of those chains depend significantly on the size of spins involved. Uniform chains of half-odd integer spins have no energy gap between ground-state and first excited states (i.e. they are quantum critical), whereas chains with integer spins do show this gap [1]. However, even integer spin chains can be driven to quantum criticality by tuning the bond alternation of the coupling strength.

We have investigated quantum chains of mixed spins [2, 3]. By means of quantum Monte Carlo (QMC) simulations (continuous imaginary time loop algorithm) at low temperatures, the quantum phase transitions in antiferromagnetic Heisenberg spin chains consisting of two different kinds of spin, S_a and S_b, that appear alternatingly in pairs, have been studied for the cases $S_a = 1/2$ and $S_b = 1$, $S_a = 1/2$ and $S_b = 3/2$ as well as $S_a = 1$ and $S_b = 3/2$. The analysis of the QMC results is supplemented by exact Lanczos diagonalisation. Under the aspect of conformal invariance theory [4], extrapolation methods have been applied to determine central charge and critical exponents of the models under investigation.

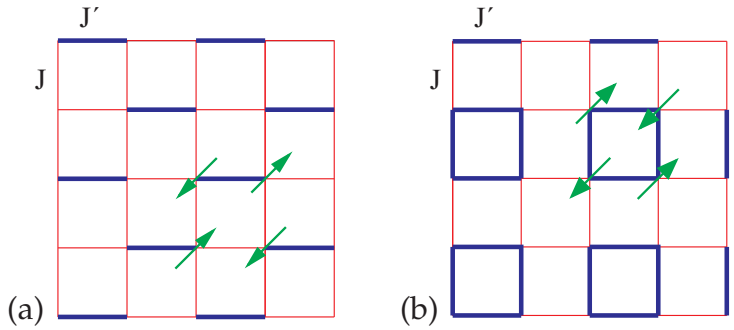

Figure 10.8: Two-dimensional Heisenberg models on the square lattice with antiferrogmagnetic couplings J and J'. Varying the ratio J/J' drives the system through a quantum phase transition, which is the main object of this project.

Secondly, we study the quantum phase transition from a Néel ordered to a disordered (dimer) state in two-dimensional antiferrogments possessing two different kinds of nearest neighbor interactions J and J' (see Fig. 10.8). To this end, we employ the stochastic series expansion (SSE) [5] algorithm. Our main interest is to study the critical exponents of the phase transitions. We compare the effect of several geometric arrangements of the bonds and our current high-precission data suggests that $O(3)$ Heisenberg universality class might be broken in case of Fig. 10.8a.

Thirdly, we have investigated quantum ferromagnets in an external magnetic field. Here we performed for one-dimensional chains and two-dimensional layers a careful comparison of analytical approaches with numerical quantum Monte Carlo simulations using the SSE method, paying special attention to a peculiar double-peak structure of the specific heat and the behaviour of correlation lengths as a function of temperature in dependence on the spin quantum number S [6].

[1] F.D.M. Haldane: Phys. Rev. Lett **50**, 1153 (1983)
[2] K. Takano: Phys. Rev. Lett. **82**, 5124 (1999); Phys. Rev. B **61**, 8863 (2000)
[3] Z. Xu et al.: Phys. Rev. B **67**, 214 426 (2003)
[4] M. Henkel: *Conformal Invariance and Critical Phenomena* (Springer, London 1999)
[5] A.W. Sandvik, J. Kurkijärvi: Phys. Rev. B **43**, 5950 (1991); O.F. Syljuasen, A.W. Sandvik: Phys. Rev. E **66**, 046 701 (2002)
[6] I. Juhász Junger et al.: Phys. Rev. B (2008), in print, arXiv:0802.3395

10.13 Evaporation/Condensation of Ising Droplets

E. Bittner, A. Nußbaumer, W. Janke

In our present research project we continued an ongoing approach to theoretically investigate the evaporation/condensation transition in liquid/gas or solid/gas mixtures by means of computer simulations. More precisely, we use the two and three-dimensional spin-1/2 Ising model, having a Hamiltonian

$$H = -J \sum_{\langle ij \rangle} \sigma_i \sigma_j \,, \qquad \sigma_i = \pm 1 \,, \tag{10.6}$$

where $J = 1$ is an interaction constant and $\sigma_i = \pm 1$ is a spin located at the lattice site i. The symbol $\langle ij \rangle$ denotes the pairs of interacting spins defined by the underlying lattice. In two dimensions we select the square lattice, triangular lattice and the next-nearest-neighbour lattice all of size $L \times L$ while in three dimensions only the cubic lattice of size $L \times L \times L$ was taken into account. Certainly, the idea is, that (e.g.) positive spins correspond to particles while negative spins correspond to vacancies. Then, an interpretation as lattice gas is possible.

For these systems it is known, that for temperatures T below the critical temperature T_c the magnetisation $m = M/V = \sum_i \sigma_i / V$ has in the infinite-volume limit ($V = L^2 \to \infty$) a value of $m_0(T) \neq 0$. Assuming that the majority of spins has a positive sign, i.e. $\sigma_i = +1$, then, on a microscopic level, at every given time there is a fixed amount of spins $V(1 - m_0)/2$ in the system that are overturned and therefore have a negative sign. If we artificially increase the number of overturned spins by a macroscopic amount, then the magnetisation decreases and we can pose the question what happens to the extra -1-spins. One possible answer is that the system forms a droplet of the "wrong phase" that has the same magnitude of the spontaneous magnetisation but the opposite sign, i.e., this phase consists of negative majority spins with some overturned spins within. If all additional -1-spins are "absorbed" into this phase, and if this phase is compact, then there is only one (large) droplet with negative magnetisation. The total magnetisation is then given by a contribution $m_0(V - v)$ from the positive phase (background) of volume $V - v$ and a contribution $-m_0 v$ from the negative phase of volume v giving

$$M = m_0(V - v) - m_0 v = m_0 V - 2m_0 v \; . \tag{10.7}$$

We can measure the volume of this droplet and it must hold

$$\frac{v}{V} = \frac{m_0 - m}{2m_0} \; . \tag{10.8}$$

In order to do so we performed simulations in the low-temperature phase at $T = 1.5$ at constant magnetisation (Kawasaki dynamics). The choice of the temperature is a trade-off between a fast spin-flip (pseudo-)dynamics and an increase of the correlation length in the vicinity of the critical temperature of the model. At a certain temperature, the infinite-system correlation length exceeds the system size L. Then, a percolating cluster builds up which effectively would prevent us from measuring a droplet in the system – which is our main interest.

Figure 10.9(a) shows the droplet size for various values of the magnetisation m (every point is a single simulation). Clearly, only for large system sizes and small values of the magnetisation m the theoretical value (10.8) of the droplet is approached. For $L \geq 160$ and large values of m, a kink in the droplet size becomes visible and the droplet size rapidly reaches zero. The position of this drop-off is moving for larger system sizes towards m_0 while the height of the drop-off is decreasing. Apparently, the assumption that *all* extra spins form a droplet is not correct but only a part of them form the droplet while the rest stays in the background. For values of the magnetisation larger than the drop-off value, there is no droplet at all, i.e., in this case all extra spins contribute to the fluctuations in the background and the maximal droplet volume is of the order one.

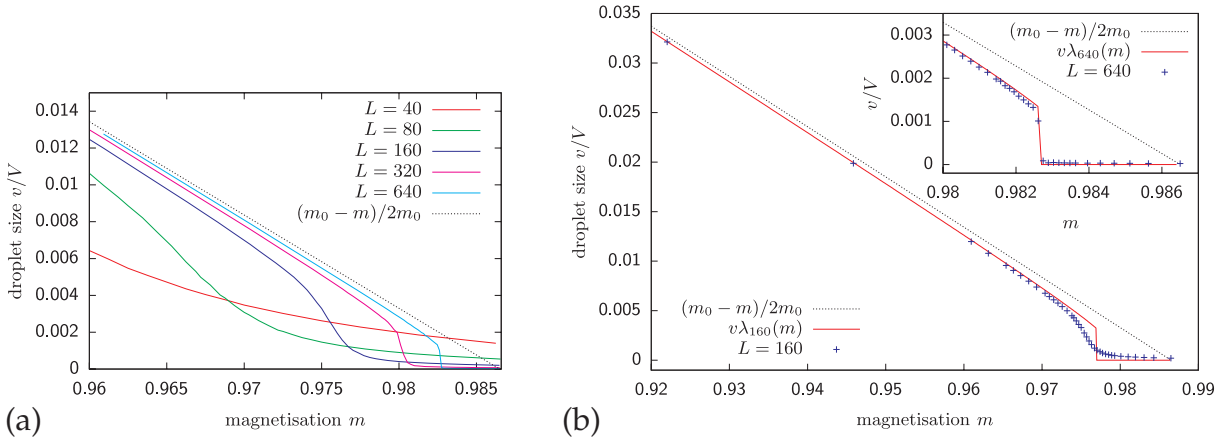

Figure 10.9: (**a**) Relative droplet volume v/V for the 2D Ising model at the temperature $T = 1.5$ and for different system sizes from $L = 40$ to $L = 640$. The abscissa ranges from $m_{\min} = 0.96$ to the value of the spontaneous magnetisation $m_{\max} = m_0(1.5) = 0.9865$. The *dashed line* shows (10.8); for the measured values a combination of Hoshen–Kopelman and flood-fill algorithm was used. Similar plots can be found in [1, 2]. (**b**) Relative droplet volume v/V for the 2D Ising model at the temperature $T = 1.5$ and system sizes $L = 160$ and $L = 640$ (*inset*). The *dashed line* shows (10.8) and the *blue '+' symbols* indicate the measured values. The *solid red line* represents the theoretical curve modified by the factor $\lambda_L(m)$.

In recent work Biskup et al. [3, 4] were able to proof this behaviour in the case of the two-dimensional Ising model rigorously. They give an analytic expression for $\lambda_L(m)$, the fraction of the additionally overturned spins that help to form the droplet. Then, the actual droplet volume is not $v(m)$ but $\lambda_L(m)v(m)$. Furthermore, for values $m > m_c$ there is no large minority droplet at all and consequently $\lambda_L(m) = 0$. At $m = m_c$ the value of λ_L jumps to 2/3, marking the position where the system makes a transition from a one-phase state (evaporated) to a two-phase state (evaporated/condensed), thereby absorbing 2/3 of the extra −1-spins into the droplet. For lower values of the magnetisation the fraction $\lambda_L(m)$ gradually increases to 1 and the actual droplet size approaches that of (10.8). In Fig. 10.9b we show the data for $L = 160$ and $L = 640$ (inset) from Fig. 10.9 again but additionally the (red) solid curve shows the finite size corrected theoretical value of the droplet size $\lambda_L(m)v(m)$.

More details can be found in [5] and the recent detailed work in [6].

Work supported by the Deutsche Forschungsgemeinschaft (DFG) under grants No. JA483/22-1/2 and No. JA483/23-1 and in part by the EU RTN-Network "ENRAGE" under grant No. MRTN-CT-2004-005616. Supercomputer time at NIC Jülich under grant No. hlz10 is also gratefully acknowledged.

[1] M. Pleimling, W. Selke: J. Phys. A: Math. Gen. **33**, L199 (2000)
[2] T. Neuhaus, J.S. Hager: J. Stat. Phys. **113**, 47 (2003)
[3] M. Biskup et al.: Europhys. Lett. **60**, 21 (2002)
[4] M. Biskup et al.: Comm. Math. Phys. **242**, 137 (2003)
[5] A. Nußbaumer et al.: Europhys. Lett. **75**, 716 (2006)
[6] A. Nußbaumer et al.: Phys. Rev. E **77**, 041 109 (2008)

10.14 Boundary Field Induced First-Order Transition in the 2D Ising Model

E. Bittner, W. Janke

Wetting transitions are phase transitions in the surface layer of bulk systems which are induced by symmetry-breaking surface fields. The Ising model with a boundary magnetic field is a simple model for such a wetting problem, because the Ising ferromagnets have the same critical behaviour as the analogous case of gas-fluid transitions, as has been pointed out by Nakanishi and Fisher [1]. The use of the Ising model with short range interactions for wetting studies has not only the advantage that one can use all the advanced simulation techniques, which have been developed for the Ising model. Especially in two dimensions (2D), there are also a lot of theoretical results available for comparison.

The Ising model with a uniform boundary magnetic field on one side of a square lattice has been completely solved by McCoy and Wu [2], whereas the Ising model with a uniform bulk field can only be solved at the critical temperature. For configurations with other fixed boundary spins or equivalently infinite boundary magnetic fields or finite boundary magnetic fields some exact results have also been found. In a recent paper, Clusel and Fortin [4] presented an alternative method to that developed by McCoy and Wu to obtain some exact results for the 2D Ising model with a general boundary magnetic field and for finite-size systems. Their method is based on the fermion representation of the Ising model using a Grassmann algebra. They applied this method to study the first-order transition induced by an inhomogeneous boundary magnetic field in the 2D Ising model [5]. By taking the thermodynamic limit exactly for a given geometry of the lattice, they obtained a simple equation for the transition line and also a threshold for the aspect ratio $\zeta_s = L_x/L_y \simeq 1/4$, where this line moves into the complex plane. This vanishing of the transition line indicates the crossover from 1D behaviour for $L_x \ll L_y$ to 2D behaviour at large ζ, which can be seen in the boundary spin-spin correlation function.

The aim of this work is to check some of the predictions by carrying out Monte Carlo simulations of this model and to extend the results to parameter ranges and for observables where analytic solutions cannot be found. Data were first obtained for $\zeta = 0.2 < \zeta_s$. For this value of the aspect ratio we find the phase diagram as predicted by Clusel and Fortin [5], cf. Fig. 10.10a. Here the thick line indicates the transition from the fully magnetized state to a state with an interface extended across the bulk. To check the nature of this transition we measured the probability density for the magnetization as a function of the boundary magnetic field H at constant temperature T and estimated the interface tension, cf. Fig. 10.10b. We find a good agreement with the infinite-volume transition boundary magnetic field given by Clusel and Fortin [5] and for all cuts of constant temperature T a clearly nonzero interface tension. We also performed simulations at various constant values of the boundary magnetic field $H > 0$ and chose the temperature such that the peaks of the probability density for the magnetization are of equal height. The infinite-volume extrapolation tends to increase with system size and yields a clearly nonzero interface tension and the transition point converges to the analytical value. Furthermore, we checked the critical behaviour along the line of second-order transitions at $T = T_c$. To this end we performed a finite-

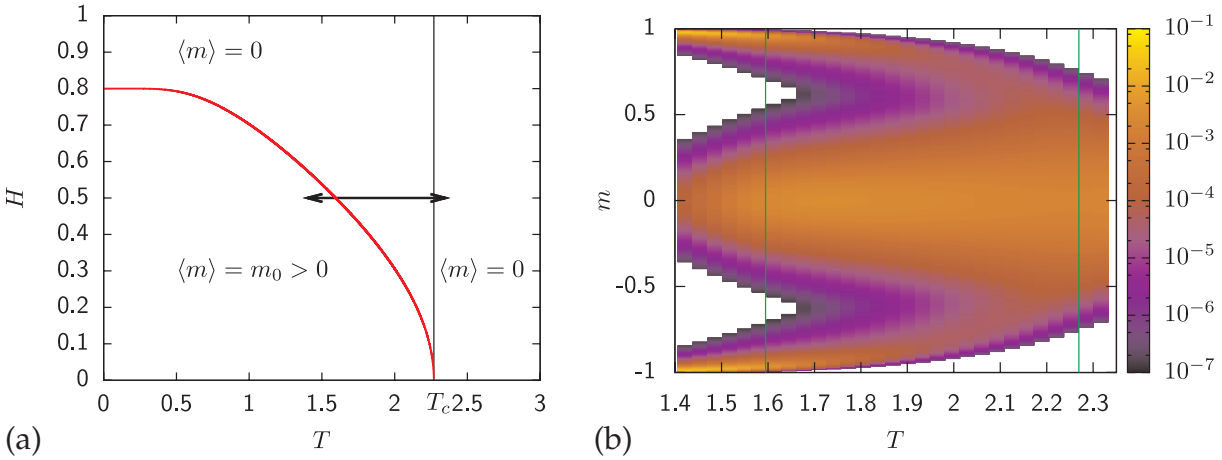

Figure 10.10: (**a**): The phase diagram for a system with $\zeta = 0.2$. The *thick line* shows the first-order transition given by Clusel and Fortin [5] and the *thin line* indicates the second-order bulk phase transition. The *double headed arrows* show the parameters of the Monte Carlo simulation. (**b**): The probability density for the magnetization as a function of temperature at the constant boundary magnetic field $H = 0.5$ for $L_x = 20$ and $L_y = 100$. The *vertical lines* indicate the value of the temperature T at which the peaks are of equal height and the critical temperature $T_c \approx 2.269$ of the bulk phase transition.

size scaling (FSS) analysis at $H = 0.5$ and determined the transition point and some critical exponents. Moreover, we studied the spin-spin correlation function for which no analytical results are available.

[1] H. Nakanishi, M.E. Fisher: J. Chem. Phys. **78**, 3279 (1983)
[2] B.M. McCoy, T.T. Wu: *The Two-Dimensional Ising Model* (Harvard Univerity Press, Cambridge 1973)
[3] A.B. Zamolodchikov: Adv. Stud. Pure Math. **19**, 641 (1989); Int. J. Mod. Phys. A **4**, 4235 (1989)
[4] M. Clusel, J.-Y. Fortin: J. Phys. A **38**, 2849 (2005)
[5] M. Clusel, J.-Y. Fortin: J. Phys. A **39**, 995 (2006)

10.15 Multibondic Cluster Algorithm with Wang–Landau Sampling for Finite-Size Scaling Studies of Critical Phenomena

B.A. Berg*, W. Janke

*Department of Physics, Florida State University, Tallahassee, USA

When studying equilibrium properties of statistical physics systems by means of Markov chain Monte Carlo (MCMC) simulations, it has turned out that it is often advantageous to work with so-called "generalized" ensembles [1]; for reviews see, e.g., [2, 3]. While the power of this approach is well documented for first-order phase transitions and complex systems such as spin glasses or peptides (small proteins) [4],

this is surprisingly not the case for second-order phase transitions and associated critical phenomena. In this case the critical energy range of interest is often larger than the energy range covered by a canonical Monte Carlo simulation close to the critical temperature. The desired extended energy range can, in principle, be covered by performing a Wang-Landau recursion for the spectral density followed by a multicanonical simulation with fixed weights. However, in the conventional approach one loses the advantage of cluster algorithms, which can reduce critical slowing down at second-order phase transitions dramatically.

We have therefore developed a combination of multibondic cluster simulations with the Wang-Landau recursion [5]. We furthermore show that by careful finite-size scaling considerations the relevant energy range to be covered by the simulations can be estimated a priori [6, 7]. This turned out to be an important aspect of our method. We have performed thorough tests of these ideas for 2D and 3D Ising models and obtained improvements over the conventional Wang-Landau/multicanonical approach by power laws in the lattice size [5–7].

[1] G.M. Torrie, J.P. Valleau: J. Comp. Phys. **23**, 187 (1977); B.A. Berg, T. Neuhaus: Phys. Rev. Lett. **68**, 9 (1992); A.A. Martsinovski et al.: J. Chem. Phys. **96**, 1776 (1992); E. Marinari, G. Parisi: Europhys. Lett. **19**, 451 (1992); F. Wang, D.P. Landau: Phys. Rev. Lett. **86**, 2050 (2001)
[2] B.A. Berg: *Markov Chain Monte Carlo Simulations and Their Statistical Analysis* (World Scientific, Singapore 2004)
[3] W. Janke: in *Computer Simulations of Surfaces and Interfaces*, NATO Science Series, II. Vol. **114**, p. 137
[4] W. Janke (ed.): *Rugged Free Energy Landscapes: Common Computational Approaches to Spin Glasses, Structural Glasses and Biological Macromolecules*, Lect. Notes Phys. **736** (Springer, Berlin 2008)
[5] B.A. Berg, W. Janke: Phys. Rev. Lett. **98**, 040 602 (2007)
[6] B.A. Berg, W. Janke: in *Computer Simulations in Condensed Matter Physics XX*, ed. by D.P. Landau et al. (Springer, Heidelberg 2008)
[7] B.A. Berg, W. Janke: *Multibondic Cluster Algorithm for Finite-Size Scaling Studies of Critical Phenomena*, Comp. Phys. Comm. (2008), in print

10.16 Funding

Numerical Studies of Protein Folding
M. Bachmann
Deutsche Forschungsgemeinschaft (DFG) Fellowship for extended research visit of the Computational Biology & Biological Physics Group at Lunds Universitet (Lund, Sweden)

Mesoscopic Models for Protein Folding
M. Bachmann
Wenner-Gren Research Fellowship in the group of Prof. Dr. A. Irbäck in the Computational Biology & Biological Physics Group at Lunds Universitet (Lund, Sweden)

Excellence Initiative, Graduate School "BuildMoNa": Leipzig School of Natural Sciences – Building with Molecules and Nano-objects

W. Janke (Principal Investigator)
Deutsche Forschungsgemeinschaft (DFG)

From Local Constraints to Macroscopic Transport
W. Janke (Principal Investigator)
Deutsche Forschungsgemeinschaft (DFG) "Forschergruppe 877"

International Conference ENRAGE – Random Geometry and Random Matrices: From Quantum Gravity to Econophysics, 17. – 22. May 2009
W. Janke (Organizer)
Max-Planck-Institut für Physik komplexer Systeme in Dresden

Host of the Alexander von Humboldt Research Prize Winner Bernd A. Berg (Florida State University, Tallahassee, USA)
W. Janke
Alexander von Humboldt Foundation

Host of EU Marie Curie Incoming Fellowship: SAWs on Fractals, Dr. Viktoria Blavatska (Lviv, Ukraine)
W. Janke
EU Grant No. MIF1-CT-2006-021867

"Deutsch-Französisches Doktorandenkollegium (DFDK)" with "Co-tutelle des Thèse", jointly with l'Université Henri Poincaré, Nancy I (with B. Berche): Statistical Physics of Complex Systems
W. Janke
Deutsch-Französische Hochschule

Random Geometry and Random Matrices: From Quantum Gravity to Econophysics
W. Janke
EU RTN-Network "ENRAGE", Grant No. MRTN-CT-2004-005616

Dynamik und Statik von Spingläsern
W. Janke
Deutsche Forschungsgemeinschaft (DFG), Grant No. JA483/22-1

Investigation of Thermodynamic Properties of Lattice and Off-Lattice Models for Proteins and Polymers
M. Bachmann and W. Janke
Deutsche Forschungsgemeinschaft (DFG), Grant Nos. JA483/24-1 and 2

Phasenübergänge in Systemen mit einschränkender Geometrie
W. Janke
Deutsche Forschungsgemeinschaft (DFG), Grant Nos. JA483/23-1 and 2

Two-Dimensional Magnetic Systems with Anisotropy
W. Janke
EU Marie Curie Development Host Fellowship, Grant No. IHP-HPMD-CT-2001-00108

Numerical Approaches to Protein Folding
W. Janke (with A. Irbäck)
DAAD-STINT Collaborative Research Grant with the University of Lund, Sweden, Grant No. D/05/26016

Quantum Monte Carlo Studies of Valence Bond Solid Transitions
W. Janke (with B. Zheng)
DAAD Collaborative Research Grant with the Zhejiang University, Hangzhou, P.R. China, Grant No. D/05/06935

Statistical Mechanics of Complex Networks
W. Janke (with Z. Burda)
Alexander von Humboldt Foundation "Institutspartnerschaft" with the Jagellonian University, Krakow, Poland

Monte Carlo Simulations of Self-Avoiding Walks on the Percolation Cluster
V. Blavatska (Lviv, Ukraine)
Host of Alexander von Humboldt Foundation Fellowship

Statistical Mechanics of Networks Interacting with Matter
B. Wacław (Jagellonian University, Krakow, Poland)
Host of DAAD Fellowship

Monte Carlo Simulationen der Statik und Dynamik von Spingläsern
E. Bittner and W. Janke
NIC Jülich (computer time grant for "JUMP"), Grant No. hlz10

Protein and Polymer Models
M. Bachmann and W. Janke
NIC Jülich (computer time grant for "JUMP"), Grant No. hlz11

Quantum Monte Carlo Simulations
W. Janke
NIC Jülich (computer time grant for "JUMP"), Grant No. hlz12

Quantum Monte Carlo Simulations
S. Wenzel
Studienstiftung des deutschen Volkes

10.17 Organizational Duties

M. Bachmann

- Scientific Secretary of the Workshop *CompPhys07 – 8th NTZ-Workshop on Computational Physics*, ITP, Universität Leipzig, 29. November – 01. December 2007
- Scientific Secretary of the Workshop *LEILAT08 – 18th Workshop on Lattice Field Theory and Statistical Physics* ITP, Universität Leipzig, 26. – 28. June 2008
- Scientific Secretary of the Workshop *CompPhys08 – 9th NTZ-Workshop on Computational Physics*, ITP, Universität Leipzig, 27. – 29. November 2008

- Referee: Phys. Rev. Lett., J. Am. Chem. Soc., IEEE/ACM Transact. Comp. Biol. Bioinf., Phys. Rev. A, Phys. Rev. E, J. Phys. A, Eur. J. Phys. D, Biophys. Rev. Lett., Comput. Phys. Commun., J. Comput. Chem.
- Reviewer: Engineering and Physical Sciences Research Council (EPSRC), UK; National Science Foundation (NSF), USA

E. Bittner

- Scientific Secretary of the Workshop *CompPhys07 – 8th NTZ-Workshop on Computational Physics*, ITP, Universität Leipzig, 29. November – 01. December 2007
- Scientific Coordinator of the Spring School on *Monte Carlo Simulations of Disordered Systems*, ITP, Universität Leipzig, 30. March – 04. April 2008
- Scientific Secretary of the Workshop *LEILAT08 – 18th Workshop on Lattice Field Theory and Statistical Physics* ITP, Universität Leipzig, 26. – 28. June 2008
- Co-organizer of the contribution *Football Feaver* to the "Wissenschaftssommer" exhibition within the frame of the "Jahr der Mathematik", Universität Leipzig, 28. Juni – 04. July 2008
- Scientific Secretary of the Workshop *CompPhys08 – 9th NTZ-Workshop on Computational Physics*, ITP, Universität Leipzig, 27. – 29. November 2008
- Referee: Phys. Rev. Lett., Phys. Rev. E, J. Phys. A, Eur. J. Phys. B, Comput. Phys. Commun.

W. Janke

- Director of the Naturwissenschaftlich-Theoretisches Zentrum (NTZ) at the Zentrum für Höhere Studien (ZHS), Universität Leipzig
- Chairperson of the Programme Committee "Scientific Computing" of Forschungszentrum Jülich
- Member of the Scientific-Technical-Council of the Supervisory Board ("Aufsichtsrat") of the Forschungszentrum Jülich GmbH
- Editor "Computational Sciences", Lecture Notes in Physics, Springer, Berlin, Heidelberg
- Editor "Computational Physics", Central European Journal of Physics
- Member of Editorial Board, Condens. Matter Phys.
- Permanent Member of "International Advisory Board", *Conference of the Middle European Cooperation in Statistical Physics (MECO)*
- Organizer of the Symposium *Finite-Size Effects at Phase Transitions* within the 71st German Physics Spring Meeting ("Physiker-Tagung") 2007 (with W. Selke, RWTH Aachen), Universität Regensburg, 27. – 28. March 2007
- Organizer of the 9th Int. Conf. *Path Integrals – New Trends and Perspectives* (with A. Pelster, Universität Duisburg-Essen) Max-Planck-Institut für Physik komplexer Systeme (MPI-PKS), Dresden, 23. – 28. September 2007
- Organizer of the Workshop *Statistical Mechanics of Complex Networks* (with P. Bialas, Z. Burda, J. Jurkiewicz, and G. Rodgers), Jagellonian University, Krakow, Poland, 02. – 04. November 2007
- Organizer of the Workshop *CompPhys07 – 8th NTZ-Workshop on Computational Physics*, ITP, Universität Leipzig, 29. November – 01. December 2007
- Organizer of the Spring School on *Monte Carlo Simulations of Disordered Systems*, ITP, Universität Leipzig, 30. March – 04. April 2008
- Organizer of the Workshop *LEILAT08 – 18th Workshop on Lattice Field Theory and*

Statistical Physics (with A. Schiller, ITP, TET) ITP, Universität Leipzig, 26. – 28. June 2008
- Co-organizer of the contribution *Football Feaver* to the "Wissenschaftssommer" exhibition within the frame of the "Jahr der Mathematik", Universität Leipzig, 28. Juni – 04. July 2008
- Organizer of the Workshop *CompPhys08 – 9th NTZ-Workshop on Computational Physics*, ITP, Universität Leipzig, 27. – 29. November 2008
- Organizer of the The 34th Conference of the Middle European Cooperation in Statistical Physics *MECO34* (with S. Trimper, Martin-Luther-Universität Halle-Wittenberg), ITP, Universität Leipzig, 29. March – 01. April 2009
- Organizer of the International Conference *ENRAGE – Random Geometry and Random Matrices: From Quantum Gravity to Econophysics*, Max-Planck-Institut für Physik komplexer Systeme in Dresden, 17. – 22. May 2009
- Member of International Organization Committee of the 10th International Conference *Path Integrals*, planned for Seoul, South Korea, August 2009
- Chair of the Review Panel: Mid-Term Evaluation of the Research Programme "Scientific Computing" of the Helmholtz-Gemeinschaft, Forschungszentrum Jülich, June 2007
- Member of the Review Panel: Mid-Term Evaluation of the Research Programme "Condensed Matter Physics, PNI and Nanoelectronics" of the Helmholtz-Gemeinschaft, Forschungszentrum Jülich, October 2007
- Member of the Review Panel of the AQAS "Akkreditierungsverfahren" of the Master Studies Curriculum "Computer Simulation in Science", Bergische Universität Wuppertal, January 2008
- Reviewer: Humboldt-Stiftung; Deutsche Forschungsgemeinschaft; Studienstiftung des deutschen Volkes; Jeffress Memorial Trust, Bank of America, Virginia, USA; "Fond zur Förderung der wissenschaftlichen Forschung (FWF)", Österreich; "The Royal Society", UK; The "Engineering and Physical Sciences Research Council (EPSRC)", UK; The University of Warwick, UK; Coventry University, UK; CECAM, Lyon, France; National Science Foundation (NSF), USA; Israel Science Foundation, Israel
- Referee: Phys. Rev. Lett., Phys. Rev. B, Phys. Rev. E, J. Chem. Phys., Europhys. Lett., Phys. Lett. A, Phys. Lett. B, Eur. Phys. J. B, Physica A, Proc. R. Phys. Soc., J. Physics A, Comput. Phys. Commun., J. Stat. Mech., New J. Phys., Int. J. Mod. Phys. C

10.18 External Cooperations

Academic

- EU RTN-Network "ENRAGE" – *Random Geometry and Random Matrices: From Quantum Gravity to Econophysics*
  research collaboration with 13 teams throughout Europe
- Deptartment of Physics, Florida State University, Tallahassee, USA
  Prof. Dr. Bernd A. Berg
- CEA/Saclay, Service de Physique Théorique, France
  Dr. Alain Billoire

- Laboratoire de Physique des Matériaux (UMR CNRS No 7556), Université Henri Poincaré, Nancy, France
  Prof. Dr. Bertrand Berche, Dr. Christophe Chatelain, Prof. Dr. Malte Henkel, Dr. Dragi Karevski
- Groupe de Physique des Matériaux (UMR CNRS No 6634), Université de Rouen, France
  Dr. Pierre-Emmanuel Berche
- School of Mathematical and Computer Sciences, Heriot-Watt University, Edinburgh, UK
  Prof. Dr. Desmond A. Johnston, Dr. Martin Weigel
- School of Mathematical and Information Sciences, Coventry University, England, UK
  Dr. Ralph Kenna, PD Dr. Christian von Ferber
- Department of Physics, Hacettepe University, Ankara, Turkey
  Prof. Dr. Tarik Çelik, Dr. Handan Arkin, Gökhan Gökoğlu
- Institute for Condensed Matter Physics, National Academy of Sciences, Lviv, Ukraine
  Prof. Dr. Yurij Holovatch
- Complex Systems Division, Department of Theoretical Physics, Lund University, Lund, Sweden
  Prof. Dr. Anders Irbäck, Simon Mitternacht
- John von Neumann-Institut für Computing (NIC), Forschungszentrum Jülich, Germany
  Prof. Dr. U. Hansmann, Prof. Dr. Peter Grassberger, PD Dr. Thomas Neuhaus
- Institut für Physik, Universität Mainz
  Prof. Dr. Kurt Binder, Dr. Hsiao-Ping Hsu, Dr. Martin Weigel
- Atominstitut, TU Wien, Austria
  Prof. Dr. Harald Markum, Dr. Rainer Pullirsch
- Brunel University of West London, UK
  Dr. Gernot Akemann
- Institut für Theoretische Physik, FU Berlin, Germany
  Prof. Dr. Hagen Kleinert, Dr. Adriaan M.J. Schakel
- IAC-1, Universität Stuttgart, Germany
  PD Dr. Rudolf Hilfer
- Universität Duisburg-Essen, Germany
  PD Dr. Axel Pelster
- Institut für Theoretische Physik, Universität Bielefeld, Germany
  PD Dr. Thomas Neuhaus, Prof. Dr. Friderike Schmid
- Jacobs Universität Bremen, Germany
  Prof. Dr. Hildegard Meyer-Ortmanns
- Institute of Physics, Jagellonian University, Kraków, Poland
  Prof. Dr. Zdzisław Burda, Prof. Dr. Piotr Bialas, Dr. Leszek Bogacz
- Landau Institute for Theoretical Physics, Chernogolovka, Russia
  Prof. Dr. Lev N. Shchur

- Yerevan Physics Institute, Yerevan, Armenia
  Prof. Dr. David B. Saakian
- University of Sri Jayewardenepura, Sri Lanka
  Dr. Ranasinghe P.K.C. Malmini
- Department of Physics, Sri Venkateswara College, University of Delhi, New Delhi, India
  Dr. Bibudhananda Biswal
- Department of Mechanical Engineering and Intelligent Systems, Tokyo University of Electro-communications, Chofu, Tokyo, Japan
  Prof. Dr. Hans-Georg Mattutis
- Zhejiang Institute of Modern Physics, Zhejiang University, Hangzhou, P.R. China
  Prof. Dr. He-Ping Ying, Prof. Dr. Bo Zheng

10.19 Publications

Journals

B.A. Berg, W. Janke: *Wang-Landau Multibondic Cluster Simulations for Second-Order Phase Transitions*, Phys. Rev. Lett. **98**, 040 602 (2007)

E. Bittner, A. Nußbaumer, W. Janke, M. Weigel: *Self-Affirmation Model for Football Goal Distributions*, Europhys. Lett. **78**, 58 002 (2007)

L. Bogacz, Z. Burda, W. Janke, B. Wacław: *Balls-in-Boxes Condensation on Networks*, Chaos **17**, 026 112 (2007)

L. Bogacz, Z. Burda, W. Janke, B. Wacław: *Free Zero-Range Processes on Networks*, Proc. SPIE **6601**, 66010V (2007)

K. Goede, M. Bachmann, W. Janke, M. Grundmann: *Specific Adhesion of Peptides on Semiconductor Surfaces in Experiment and Simulation*, AIP Conf. Proc. **893**, 611 (2007)

C. Junghans, M. Bachmann, W. Janke: *Thermodynamics of Peptide Aggregation Processes: An Analysis from Perspectives of Three Statistical Ensembles*, J. Chem. Phys. **128**, 085 103 (2008)

A. Kallias, M. Bachmann, W. Janke: *Thermodynamics and Kinetics of a Gō Proteinlike Heteropolymer Model with Two-State Folding Characteristics*, J. Chem. Phys. **128**, 055 102 (2008)

E. Lorenz, W. Janke: *Numerical Tests of Local Scale Invariance in Ageing q-State Potts Models*, Europhys. Lett. **77**, 10 003 (2007)

S. Mitternacht, S. Schnabel, M. Bachmann, W. Janke, A. Irbäck: *Differences in Solution Behavior Between Four Semiconductor-Binding Peptides*, J. Phys. Chem. B **111**, 4355 (2007)

A. Nußbaumer, E. Bittner, W. Janke: *Interface Tension of the Square Lattice Ising Model with Next-Nearest-Neighbour Interactions*, Europhys. Lett. **78**, 16 004 (2007)

A. Nußbaumer, E. Bittner, W. Janke: *Monte Carlo Study of the Droplet Formation-Dissolution Transition on Different Two-Dimensional Lattices*, Phys. Rev. E **77**, 041 109 (2008)

S. Schnabel, M. Bachmann, W. Janke: *Identification of Characteristic Protein Folding Channels in a Coarse-Grained Hydrophobic-Polar Peptide Model*, J. Chem. Phys. **126**, 105 102 (2007)

S. Schnabel, M. Bachmann, W. Janke: *Two-State Folding, Folding Through Intermediates, and Metastability in a Minimalistic Hydrophobic-Polar Model for Proteins*, Phys. Rev. Lett. **98**, 048 103 (2007)

T. Vogel, M. Bachmann, W. Janke: *Freezing and Collapse of Flexible Polymers on Regular Lattices in Three Dimensions*, Phys. Rev. E **76**, 061 803 (2007)

B. Wacław, L. Bogacz, Z. Burda, W. Janke: *Condensation in Zero-Range Processes on Inhomogeneous Networks*, Phys. Rev. E **76**, 046 114 (2007)

S. Wenzel, E. Bittner, W. Janke, A.M.J. Schakel: *Percolation of Vortices in the Abelian Lattice Higgs Model*, Nucl. Phys. B **793**, 344 (2008)

Books

M. Bachmann, W. Janke: *Thermodynamics of Protein Folding from Coarse-Grained Models' Perspectives*, in: *Rugged Free Energy Landscapes: Common Computational Approaches to Spin Glasses, Structural Glasses and Biological Macromolecules*, ed. by W. Janke, Lect. Notes Phys. **736** (Springer, Berlin 2008), p 203

E. Bittner, A. Nußbaumer, W. Janke: *Free-Energy Barriers of Spin Glasses*, in: *NIC Symposium 2008* , NIC Series, Vol. **39**, ed. by G. Münster, D. Wolf, M. Kremer (John von Neumann Institute for Computing, Jülich 2008), p 229

W. Janke: *Introduction to Simulation Techniques*, in: *Ageing and the Glass Transition*, ed. by M. Henkel, M. Pleimling, R. Sanctuary, Lect. Notes Phys. **716** (Springer, Berlin 2007) p 207

W. Janke: *Monte Carlo Methods in Classical Statistical Physics*, in: *Computational Many-Particle Physics*, ed. by H. Fehske, R. Schneider, A. Weiße, Lect. Notes Phys. **739** (Springer, Berlin 2008) p 79

W. Janke: *Rugged Free-Energy Landscapes – An Introduction*, in: *Rugged Free Energy Landscapes: Common Computational Approaches to Spin Glasses, Structural Glasses and Biological Macromolecules*, ed. by W. Janke, Lect. Notes Phys. **736** (Springer, Berlin 2008) p 1

W. Janke (Ed.): *Rugged Free Energy Landscapes: Common Computational Approaches to Spin Glasses, Structural Glasses and Biological Macromolecules*, Lect. Notes Phys. **736** (Springer, Berlin 2008)

W. Janke, A.M.J. Schakel: *Spacetime Approach to Phase Transitions*, in: *Order, Disorder and Criticality: Advanced Problems of Phase Transition Theory*, Vol. 2, ed. by Y. Holovatch (World Scientific, Singapore 2007) p 123

C. Junghans, M. Bachmann, W. Janke: *Phase Separation in Peptide Aggregation Processes – Multicanonical Study of a Mesoscopic Model*, in: *From Computational Biophysics to Systems Biology (CBSB07)*, NIC Series, Vol. **36**, ed. by U.H.E. Hansmann, J. Meinke, S. Mohanty, O. Zimmermann (John von Neumann Institute for Computing, Jülich 2007) p 169

in press

M. Bachmann, W. Janke: *Conformational Transitions in Molecular Systems*, in: Proc. Int. Conf. *Path Integrals – New Trends and Perspectives*, ed. by W. Janke, A. Pelster (World Scientific, Singapore 2008)

M. Bachmann, W. Janke: *Minimalistic Hybrid Models for the Adsorption of Polymers and Peptides to Substrates*, Phys. Part. Nuclei (2008)

B.A. Berg, W. Janke: *Multibondic Cluster Algorithm for Finite-Size Scaling Studies of Critical Phenomena*, Comp. Phys. Commun. (2008)

B.A. Berg, W. Janke: *Wang-Landau Multibondic Cluster Approach to Simulations of Second-Order Transitions*, in: *Computer Simulations in Condensed Matter Physics XX*, ed. by D.P. Landau, S.P. Lewis, H.-B. Schüttler (Springer, Heidelberg 2008)

R. Bischof, W. Janke: *Critical Exponents of Mixed Quantum Spin Chain*, in: Proc. Int. Conf. *Path Integrals – New Trends and Perspectives*, ed. by W. Janke, A. Pelster (World Scientific, Singapore 2008)

E. Bittner, W. Janke: *Vortex-Line Percolation in a Three-Dimensional Complex $|\psi|^4$ Theory*, in: Proc. Int. Conf. *Path Integrals – New Trends and Perspectives*, ed. by W. Janke, A. Pelster (World Scientific, Singapore 2008)

V. Blavatska, W. Janke: *Scaling Behavior of Self-Avoiding Walks on Percolation Clusters*, Europhys. Lett. (2008), arXiv:0804.2988 (cond-mat.dis-nn)

V. Blavatska, W. Janke: *Self-Avoiding Walks on Fractals: Scaling Laws*, in: Proc. Int. Conf. *Path Integrals – New Trends and Perspectives*, ed. by W. Janke, A. Pelster (World Scientific, Singapore 2008)

W. Janke, A. Pelster (Eds.): *Path Integrals – New Trends and Perspectives*, Proceedings of the International Conference, MPI PKS Dresden, 23.–28. September 2007 (World Scientific, Singapore 2008)

I. Juhász Junger, D. Ihle, L. Bogacz, W. Janke: *Thermodynamics of Heisenberg Ferromagnets with Arbitrary Spin in a Magnetic Field*, Phys. Rev. **B** (2008), arXiv:0802.3395

A. Nußbaumer, E. Bittner, W. Janke: *Evaporation/Condensation of Ising Droplets*, in: Proc. Int. Conf. *Path Integrals – New Trends and Perspectives*, ed. by W. Janke, A. Pelster (World Scientific, Singapore 2008)

A. Nußbaumer, E. Bittner, T. Neuhaus, W. Janke: *Universality of the Evaporation/ Condensation Transition*, in: *Computer Simulations in Condensed Matter Physics XX*, ed. by D.P. Landau, S.P. Lewis, H.-B. Schüttler (Springer, Heidelberg 2008)

J. Schluttig, M. Bachmann, W. Janke: *Comparative Molecular Dynamics and Monte Carlo Study of Statistical Properties for Coarse-Grained Heteropolymers*, J. Comp. Chem. (2008)

B. Wacław, L. Bogacz, Z. Burda, W. Janke: *Monte Carlo Methods for Generation of Random Graphs*, in: Proc. Int. Conf. *Path Integrals – New Trends and Perspectives*, ed. by W. Janke, A. Pelster (World Scientific, Singapore 2008)

B. Wacław, Z. Burda: *Counting Metastable States of Ising Spin Glasses on Arbitrary Graphs*, Phys. Rev. E (2008)

F.T. Winter, W. Janke, A.M.J. Schakel: *Geometric Properties of the Three-Dimensional Ising and XY Models*, Phys. Rev. E (2008)

Talks

M. Bachmann: *Intrinsic Structural Properties of Mesoscopic Models for Protein Folding and Aggregation*, 71st DPG Spring Meeting, Regensburg, 26. – 30. March 2007

M. Bachmann: *Specific Polymer and Peptide Adsorption to Attractive Solid Substrates*, CECAM Workshop "Modelling the Interaction of Biomolecules with Inorganic Surfaces", Lyon, France, 25. – 27. July 2007

M. Bachmann: *Specific Polymer and Peptide Adsorption to Attractive Solid Substrates*, Mini-Symposium "Adsorption Properties of Polymers and Proteins", Lund, Sweden, 07. March 2007

M. Bachmann: *Specific Polymer and Peptide Adsorption to Attractive Solid Substrates*, Seminar talk, Institut für Theoretische Physik, Martin-Luther-Universität Halle-Wittenberg, 24. January 2007

M. Bachmann: *Statistical Conformation Mechanics of Protein Folding, Aggregation, and Adsorption Transitions*, 9th Int. Conf. "Path Integrals – New Trends and Perspectives PI07", Dresden, 23. – 28. September 2007

E. Bittner: *Complex Eigenvalues of the Dirac Operator in Two-Color QCD with Chemical Potential*, "ENRAGE" Network School on Random Matrices and Random Geometry, Barcelona, Spain, 16. – 20. April 2007

E. Bittner: *Evaporation/Condensation Transition of Ising Droplets*, Seminar talk, Institut für Theoretische Physik (B), RWTH Aachen, 06. November 2007

E. Bittner: *Vortex-Line Percolation in a Three-Dimensional Complex $|\psi|^4$ Theory*, 9th Int. Conf. "Path Integrals – New Trends and Perspectives PI07", Dresden, 23. – 28. September 2007

M. Hasenbusch: *The Critical Behavior of 3D Ising Glass Models: Universality and Scaling Corrections*, 8th Int. NTZ-Workshop "New Developments in Computational Physics – CompPhys07", Universität Leipzig, 29. November – 01. December 2007

W. Janke: *Adsorption Phenomena at Hybrid Organic–Inorganic Interfaces*, invited talk, SFB 418 International Workshop *Soft meets Hard*, Lutherstadt Wittenberg, 13. – 15. September 2007

W. Janke: *Droplet Evaporation/Condensation Transition*, FOR 877 Workshop, Universität Leipzig, 27. November 2007

W. Janke: *Exploring Free-Energy Landscapes of Peptide Folding and Aggregation*, invited talk, Atelier Nancy *Statistical Physics and Low Dimensional Systems 2007*, Université Nancy, France, 23. – 25. May 2007

W. Janke: *Exploring Free-Energy Landscapes of Peptide Folding and Aggregation*, invited talk, EMBIO Workshop 2007, Interdisziplinäres Zentrum für Bioinformatik (IZBI), Universität Leipzig, 17. – 19. May 2007

W. Janke: *Finite-Size Adapted Wang-Landau/Multibondic Cluster Simulations for Second-Order Phase Transitions*, Symposium *Finite-Size Effects*, 71st DPG Spring Meeting, Regensburg, 26. – 30. March 2007

W. Janke: *Geometrical Picture of Criticality*, Physics Seminar, Complex Systems Division, Lund University, Sweden, 02. February 2007

W. Janke: *Geometrical Picture of Phase Transitions*, Physics Seminar, School of Engineering and Science, Jacobs University Bremen, 07. May 2007

W. Janke: *Microcanonical Analyses of Peptide Aggregation Processes*, CBSB Workshop 2007, NIC, Forschungszentrum Jülich, 02. – 04. May 2007

W. Janke: *Microcanonical Analyses of Peptide Aggregation Processes*, invited talk, CECAM Workshop *Modelling the Interaction of Biomolecules with Inorganic Surfaces*, ENS Lyon, France, 25. – 27. July 2007

W. Janke: *Modeling and Simulation of Biological Macromolecules*, Physikalisches Kolloquium, Technische Universität Chemnitz, 13. June 2007

W. Janke: *Modeling and Simulation of Biological Macromolecules*, Theorie-Kolloquium, Martin-Luther-Universität Halle-Wittenberg, 27. June 2007

W. Janke: *Multibondic Cluster Algorithm for Finite-Size Scaling Studies of Second-Order Phase Transitions*, CCP2007 – Conference on Computational Physics, Brussels, Belgium, 05. – 08. September 2007

W. Janke: *Nano-Structured Channels: Computer Simulations and Finite-Size Scaling*, Workshop, Universität Leipzig, 05. April 2007

W. Janke: *Spin Clusters and Loop Gases on Random Graphs*, ANet07 Conference, Jagellonian University, Krakow, Poland, 02. – 04. November 2007

W. Janke: *The LEIPZIG Team*, EU Network ENRAGE Midterm Review Meeting, Utrecht, The Netherlands, 06. September 2007

W. Janke: *Universal Aspects of Evaporation/Condensation Transition*, Physik-Kolloquium, Technische Universität Ilmenau, 03. July 2007

W. Janke: *Universality of Evaporation/Condensation Transition*, invited talk, 20th Ann. Workshop, University of Georgia, Athens, USA, 19. – 23. February 2007

A. Nußbaumer: *Football Fever: Goal Distributions in Football*, 71st DPG Spring Meeting, Regensburg, 26. – 30. March 2007

S. Schnabel: *Impact of Peptide Structure on Semiconductor Binding*, 71st DPG Spring Meeting, Regensburg, 26. – 30. March 2007

S. Schnabel: *Multicanonical Simulation of a Coarse Grained Heteropolymer Model*, Seminar talk, Deutsch-Französische Hochschule (Collège Doctoral), Université Henri Poincaré Nancy, France, 22. October 2007

S. Schnabel: *Multicanonical Simulation of a Coarse Grained Heteropolymer Model*, Seminar talk, Institut für Theoretische Physik, Universität Kassel, 11. July 2007

T. Vogel: *Freezing and Collapse of Flexible Polymers*, 8th Int. NTZ-Workshop "New Developments in Computational Physics – CompPhys07", Universität Leipzig, 29. November – 01. December 2007

B. Wacław: *Balls-in-Boxes Models on Networks*, ANet07 Conference, Jagellonian University, Krakow, Poland, 02. – 04. November

B. Wacław: *Multicanonical Simulations of Complex Networks*, 8th Int. NTZ-Workshop "New Developments in Computational Physics – CompPhys07", Universität Leipzig, 29. November – 01. December 2007

S. Wenzel: *Finite-Size Scaling of Quantum Phase Transitions in 2d Heisenberg Models*, Seminar talk, Deutsch-Französische Hochschule (Collège Doctoral), Université Henri Poincaré Nancy, France, 17. September 2007

S. Wenzel: *On the Phase Structure of 3D Abelian One-Higgs Model on the Lattice*, 8th Int. NTZ-Workshop "New Developments in Computational Physics – CompPhys07", Universität Leipzig, 29. November – 01. December 2007

Posters

M. Bachmann, C. Junghans, W. Janke: *Microcanonical Analysis of Polymer Aggregation*, Workshop on "Computer Simulations of Soft Matter and Biosystems", Heidelberg, 14. – 16. March 2007

E. Bittner, W. Janke: *Boundary Field Induced First-Order Transition in the 2D Ising Model: Numerical Study*, 71st DPG Spring Meeting, Regensburg, 26. – 30. March 2007

E. Bittner, A. Nußbaumer, W. Janke: *Replica-Exchange Cluster Algorithm*, 8th Int. NTZ-Workshop "New Developments in Computational Physics – CompPhys07", Universität Leipzig, 29. November – 01. December 2007

E. Bittner, A. Nußbaumer, W. Janke: *Replica-Exchange Cluster Algorithm*, CCP2007 – Conference on Computational Physics, Brussels, Belgium, 05. – 08. September 2007

E. Bittner, A. Nußbaumer, W. Janke: *The Evaporation/Condensation Transition of Ising Droplets*, XXIII Int. Conf. Statistical Physics of the Int. Union for Pure and Applied Physics (IUPAP) – Statphys 23, Genova, Italy, 09. – 13. July 2007

V. Blavatska, W. Janke: *Multifractal Properties of Self-Avoiding Walks Percolation Clusters*, 8th Int. NTZ-Workshop "New Developments in Computational Physics – CompPhys07", Universität Leipzig, 29. November – 01. December 2007

V. Blavatska, W. Janke: *Self-Avoiding Walks on Fractals: Scaling Laws*, 9th Int. Conf. "Path Integrals – New Trends and Perspectives PI07", Dresden, 23. – 28. September 2007

A. Nußbaumer, E. Bittner, W. Janke: *Evaporation/Condensation of Ising Droplets*, 8th Int. NTZ-Workshop "New Developments in Computational Physics – CompPhys07", Universität Leipzig, 29. November – 01. December 2007

A. Nußbaumer, E. Bittner, W. Janke: *Evaporation/Condensation of Ising Droplets*, 9th Int. Conf. "Path Integrals – New Trends and Perspectives PI07", Dresden, 23. – 28. September 2007

A. Nußbaumer, E. Bittner, W. Janke: *Evaporation/Condensation Transition on Different Ising Lattices*, CCP2007 – Conference on Computational Physics, Brussels, Belgium, 05. – 08. September 2007

S. Schnabel, S. Mitternacht, A. Irbäck, M. Bachmann, W. Janke: *Solution Behavior of Semiconductor-Binding Peptides*, 71st DPG Spring Meeting, Regensburg, 26. – 30. March 2007

T. Vogel, M. Bachmann, W. Janke: *Collapse and Freezing Transitions of Polymers on Regular Lattices*, 71st DPG Spring Meeting, Regensburg, 26. – 30. March 2007

T. Vogel, M. Bachmann, W. Janke: *Collapse and Freezing Transitions of Polymers on Regular Lattices*, CECAM Tutorial *Programming Parallel Computers*, Forschungszentrum Jülich, 22. – 26. January 2007

S. Wenzel, E. Bittner, A.M.J. Schakel, W. Janke: *Percolation of Vortex Networks in the $U(1)$ Lattice Higgs Model*, 71st DPG Spring Meeting, Regensburg, 26. – 30. March 2007

10.20 Guests

- Dr. Meik Hellmund
  Mathematisches Institut, Universität Leipzig, Germany
  26. April 2007

- Prof. Dr. Bernd Berg
  Florida State University, Tallahassee, USA
  14. – 16. June 2007
- Prof. Dr. Ramon Villanova
  Universitat Pompeu Fabra, Barcelona, Spain
  21. – 26. June 2007
- Prof. Dr. Rainer Klages
  School of Mathematical Sciences, Queen Mary, University of London, UK
  26. – 27. June 2007
- Prof. Dr. Bernhard Mehlig
  Göteborg University, Sweden
  28. – 29. June 2007
- Jean-Charles Walter
  Université Nancy, France
  October – December 2007
- Prof. Dr. Wolfgang Paul
  Institut für Physik, Universität Mainz, Germany
  07. – 09. November 2007
- Oleksandr Kapikranian
  Université Nancy, France
  October – November 2007
- Thierry Platini
  Université Nancy, France
  October – December 2007
- Prof. Dr. Joan Adler
  Technion, Haifa, Israel
  27. November – 02. December 2007
- Prof. Dr. Piotr Bialas
  Jagellonian University, Krakow, Poland
  09. – 15. December 2007

11

Molecular Dynamics / Computer Simulation

11.1 Introduction

Using methods of statistical physics and computer simulations we investigate classical many-particle systems interacting with interfaces. One aim of the research in our group is to built up a bridge between theoretical and experimental physics. By means of analytical theories of statistical physics and computer simulations (Molecular dynamics, Monte Carlo procedures, percolation theories) using modern workstations and supercomputers we examine subjects for which high interest exists in basic research and industry as well. The examinations involve transport properties (diffusion of guest molecules) in zeolites and the structural and phase behaviour of complex fluids on bulk conditions and in molecular confinements. Especially we are interested to understand

- the diffusion behaviour of guest molecules in zeolites in dependence on thermodynamic parameters, steric conditions, intermolecular potentials and the concentration of the guest molecules,
- structure and phase equilibria of complex (aqueous) fluids in interfacial systems (e.g. pores, thin films, model membranes) in dependence on geometric and thermodynamic conditions,
- and the migration of molecules in (random) porous media by the use of percolation theories

in microscopic detail and to compare the results with experimental data. The use of a network of PC's and workstations (Unix, Linux, Windows), the preparation and application of programs (Fortran, C, C^{++}), and the interesting objects (zeolites, membranes) give excellent possibilities for future careers of undergraduates, graduate students and postdocs. Our research is part of several national and international programs (DFG-Schwerpunktprogramm 1155, an International Research Graduate Training program (IRTG 1056), a joint research project DFG/TRF-Thailand, a joint research project DAAD/TRF-Thailand and joint research projects with UOIT Oshawa and SHARCNET, Canada) and includes a close collaboration with the Institute of Experimental Physics I (Physics of Interfaces and Biomembranes) of Leipzig University and many institutions in Germany and other countries. Details are given in the list of external cooperations.

Horst-Ludger Vörtler and Siegfried Fritzsche

11.2 Phase Equilibria of Fluids in Bulk Systems and in Micropores: Shift of the Critical Point

H.L. Vörtler, I. Nezbeda*, M. Kettler†

*Czech Academy of Sciences, Prague, Czech Republic
†Frankfurt

In this long-term research we study phase equilibria and critical data of several classes of fluids at interfaces and in micropores on the basis of hierarchic modelling of the intermolecular potential using both computer simulations and thermodynamic integration methods. Particularly, recent variants of test particle insertion methods (monomer/dimer insertion, gradual and scaled particle insertion) were implemented to efficiently simulate phase properties and critical data of dense aqueous phases. By combining these methods we were able to improve significantly the efficiency of phase equilibrium simulations of strongly associating water models [1] under both homogeneous and inhomogeneous conditions. In 2007 we estimated critical properties from the simulated phase equilibria for fluids with increasing geometrical restrictions starting with three-dimensional bulk fluids proceeding via a series of fluids confined into slits of decreasing width arriving at two-dimensional fluid monolayers. Particularly, we found a simple analytic expression (see Fig. 11.1) that describes with good accuracy the decrease of the critical temperature of swquare-well fluids with increasing geometrical restrictions [1]. These studies will be continued and extended to more complex systems. The long-term goals of this research are contributions to a statistical-mechanical theory of phase equilibria of inhomogeneous fluids with applications to nanoporous materials and biointerfaces. The research is performed in close collaboration with the group of Prof. Ivo Nezbeda (Prague/Usti).

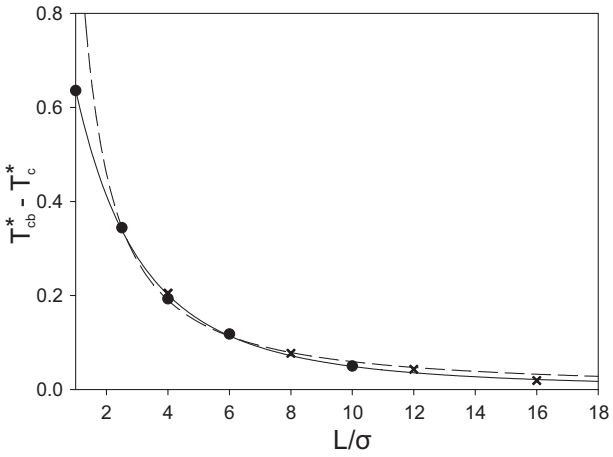

Figure 11.1: Shift of the critical temperature for the square-well fluid $\Delta T_c^* \equiv T_{cb}^* - T_c^*$ under the influence of confinement, modeling the transition from the 3D bulk fluid to a 2D monolayer via a series of hard slit-like pores with decreasing widths L. • – our results [2], × – results of [3] *dashed line* – scaling theory approximation, *solid line* – our analytic expression [2], describing accurately all existing data.

[1] H.L. Vörtler, M. Kettler: Mol. Phys. **104**, 233 (2006)

[2] H.L. Vörtler: *Simulation of Fluid Phase Equilibria in Square-Well Fluids: From three to two dimensions*, Collect. Czech. Chem. Comm., accepted (2008)
[3] J.K. Singh, S.K. Kwak: J. Chem. Phys. **126**, 024 702 (2007)

11.3 Simulation of Phase Equilibria in Two- and Three-Dimensional Fluids: Finite Size Effects

H.L. Vörtler, W.R. Smith*

*University of Ontario, Institute of Technology, Oshawa, Canada

An important aspect in molecular simulation studies of fluid phases under both homogeneous and inhomogeneous conditions is to estimate the expected size of of finite size effects due to the mapping of the infinite fluid system onto a relatively small simulation sample. In this project we study systematically the particle number dependence of the isotherms of the chemical potential and of phase equilibria obtained by Monte Carlo simulations with different number of particles in the subcritical vapour-liquid coexistence range. We perform canonical ensemble simulations and apply virtual (Widom-like) particle insertion and virtual volume variation steps. As a first approximation of a hierarchical modelling of the intermolecular potential of complex fluid phases we consider two- and three-dimensional square-well systems. The studies show [1–3] – in agreement with general theoretical considerations – a significant shrinking of the van der Waals-like loops of the chemical potential with increasing number of particles. Figure 11.2 shows that the loop for large particle numbers nearly disappears and a straight line, that represents the coexistence liquid–vapour chemical potential appears. In contrast to the large finite size effects on the chemical potential loops the influence of the system size on the phase equilibria data is only small. The results serve as reference data for a theoretical estimation of finite size effects of canonical simulations of phase equilibria of fluids under both homogeneous and inhomogeneous conditions.

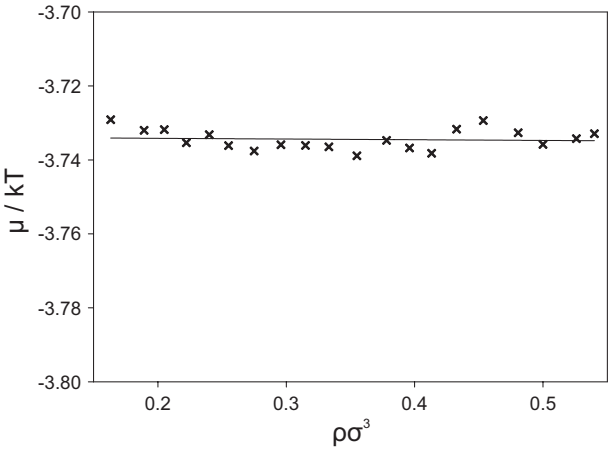

Figure 11.2: Estimation of the coexistence chemical potential of the 2D square well fluid for the largest system studied, with $N = 3200$ particles at $T^* = 0.55$, × – simulations, *solid line* – linear fit.

This research was supported by research fund of University of Ontario Institute of Technology (research stay of H.L. Vörtler in Oshawa) and by the facilities of SHARCNET computer network (Ontario, Canada).

[1] H.L. Vörtler et al.: *Finite-size effects on subcritical chemical potential isotherms in two- and three-dimensional square-well fluids*, 71th DPG Spring Meeting, Regensburg, 26. – 30. March 2007
[2] H.L. Vörtler et al.: *Finite-size effects on subcritical chemical potential isotherms in two- and three-dimensional square-well fluids*, Int. Conf. Thermodynamics 2007, Rueil-Malmaison, France, 26. – 28. September 2007
[3] H.L. Vörtler et al.: J. Phys. Chem. B **112**, 4656 (2008)

11.4 Analytical Treatment and Computer Simulations of the Influence of the Crystal Surface on the Exchange of Guest Molecules Between Zeolite Nanocrystals and the Surrounding Gas Phase

A. Schüring[*†], J. Gulín-González[*‡] S. Vasenkov[†§], S. Fritzsche[*]

[*]Institute for Theoretical Physics, Molecular Dynamics / Computer Simulation Workgroup
[†]Institute for Experimental Physics I, Physics of Interfaces Workgroup
[‡]University of Informatics Sciences, La Habana, Cuba
[§]University of Florida, Gainesville, USA

In continuation of the work done in the framework of the DFG priority program SPP 1155 over several years, now, a new analytical treatment of the surface effects influencing the dynamics of adsorption of guest molecules into porous crystals has been developped [1, 4–9]. Such effects are of high relevance for industrial purposes because e.g. in catalysis, relatively small crystals are used, to enhance efficiency and, furthermore, they also play an role in important rule in currently developed hierarchically ordered porous materials [2]. The analytical theory was tested by molecular dynamics simulations (MD) [1].

A new method for the evaluation of partition function ratios in Transition State Theory (TST) has been developped [3]. In this method the configuration space is explored at high temperature and the obtained histogram of potential energy values can be used to calculate the partition function ratios also at low temperatures. The method was tested and verified in [3] by MD simulations.

[1] A. Schüring: J. Phys. Chem. C, **111**, 11 285 (2007)
[2] Y. Tao, H. Kanoh: J. Am. Chem. Soc. **125**, 6044 (2003), doi:10.1021/ja0299405
[3] A. Schüring et al.: Chem. Phys. Lett. **450**, 164 (2007)
[4] A. Schüring: Diff. Fundam. **6**, 32.1 (2007)
[5] A. Schüring: Diff. Fundam. **6**, 33.1 (2007)
[6] A. Schüring et al.: *A New Type of Diffusional Boundary Effect at the Edges of Single-File Channels*, 15th Int. Zeolite Conf., Beijing, 12. – 17. August 2007

[7] A. Schüring et al.: *Which Boundary Condition is Suitable for Describing Adsorption of Guest Molecules from the Gas Phase into Zeolite Crystals?*, 15th Int. Zeolite Conf., Beijing, 12. – 17. August 2007
[8] A. Schüring et al.: *Transport through Zeolite Surfaces Studied by MD Simulations*, 19. Deutsche Zeolithtagung, 07. – 09. March 2007
[9] A. Schüring et al.: *Transport in the Transition Region Gas/Adsorbent Studied by Molecular Dynamics Simulations*, Diffusion Fundamentals II, L'Aquila, Italy, 26. – 26. August 2007

11.5 Diffusion of Water in the Zeolite Chabazite

S. Fritzsche, P. Biswas, A. Schüring, P.A. Bopp*, J. Kärger†

*Laboratoire de Physico-Chimie Moleculaire, University Bordeaux, France
†Institute for Experimental Physics I, Physics of Interfaces Workgroup

In continuation of earlier work [1] water in the zeolite chabazite has been investigated in a project in the framework of the International Research Training Group (IRTG) "Diffusion in Porous Materials". The nonmonotonic dependence of the self diffusion coefficient upon the concentration of water molecules could be verified and examined in more detail in MD simulations [2]. The reason for this effect is the presence of extra framwork cations forming strong adsorption sites. At higher concentrations of water these adsorption sites are saturated.

The calculations are extremely computer time consuming and could therefore, only be done at high temperatures. In the next period of the IRTG the self diffusion coefficient of water in this system at room temperature will be investigated by Transition State Theory.

[1] S. Jost: PhD Thesis, University of Leipzig (2004)
[2] S. Jost et al.: J. Phys. Chem. C **111**, 14 707 (2007)

11.6 How Do Guest Molecules Enter Zeolite Pores? Quantum Chemical Calculations and Classical MD Simulations

S. Fritzsche, R. Haberlandt, S. Hannongbua*, T. Remsungnen†, O. Saengsawang*, S. Thompho*

*Chulalongkorn University, Bangkok, Thailand
†Khon Khaen University, Khon Khaen, Thailand

In this common project of the German DFG and the NRCT (Thailand) effects connected with the silanol groups on the surface of zeolites with respect to diffusion are examined in quantum chemical calculations [1, 2] and nonequilibrium studies by Grand Canonical Molecular Dynamics for the system methane silicalite–1. The adsorption dynamics was

found to be influenced by the presence of the silanol groups. In the final equilibrium state the coverage of the surface by methane molecules depends upon the presence of silanol groups while the amount of adsorbed methane is not influenced.

[1] O. Saengsawang et al.: Stud. Surf. Sci. Catal. **158**, 947 (2005)
[2] O. Saengsawang et al.: J. Phys. Chem. B **109**, 5684 (2005)
[3] S. Thompho et al.: *Influence of the Silanol Groups on the External Surface of Silicalite–1 on the Adsorption Dynamics of Methane*, 20. Deutsche Zeolithtagung, Halle, 05. – 07. March 2008

11.7 Investigation of the Diffusion of Pentane in Silicalite-1

S. Fritzsche[*], A. Longsinruin[*†], A. Schüring[*], S. Hannongbua[†]

[*]Institute for Theoretical Physics, Molecular Dynamics / Computer Simulation Workgroup
[†]Chulalongkorn University, Bangkok, Thailand

This common project of the German DAAD and the TRF (Thailand Research Fund) was now finished by the Ph.D. thesis of A. Longsinruin [2]. In this work parameters obtained in earlier studies from quantum chemical calculations (Gaussian, MP2-level) [1] are used in classical MD simulations to investigate the structural distribution and the self diffusion of pentane in silicalite-1. The potential parameters were verifyed by calculation of the isosteric heat of adsorption and comparison with literature values. The achieved accuracy was compared with that of other papers in which also interaction parameters have been proposed.

[1] A. Loisruangsin et al.: Chem. Phys. Lett. **390**, 485 (2004)
[2] A. Loisruangsin: Dissertation, Chulalongkorn University, Bangkok, Thailand (2007)

11.8 Investigation of the Rotation and Diffusion of Pentane in the Zeolite ZK5

S. Fritzsche, O. Saengsawang, A. Schüring, P. Magusin[*], M.-O. Coppens[†], A. Dammers, D. Newsome

[*]Eindhoven University, The Netherlands
[†]Delft University, The Netherlands

In continuation of a project (project leader S. Fritzsche) in the International Research Training Group (IRTG) "Diffusion in Porous Materials" a Ph.D. thesis was submitted [3]. The rotation of ZK5 (γ-cage) was examined experimentally in [1]. Now, MD simulation could find agreement and explain many features of this phenomenon. But, some results in [1] could not be confirmed by the simulation. In cooperation with P. Magusin they

could be reinterpreted by showing that quantities which have been assumed to be temperature independant in [1] in reality depend upon the temperature.

The diffusion of pentane in ZK5 is to slow to be investigated by conventional MD simulations. Therefore, new challenging methods have been applied.

In cooperation with the group of Prof. M.-O. Coppens (A. Dammers, D. Newsome, Delft University) the challenging mew method of transition path sampling [2] was successfully applied to calculate one of the jump rates involved in this process. But, this method is not only very difficult to apply but, it is also very computer time demanding. Therefore, the newly developped method of HTCE [4] has been used and worked very efficiently. A dynamical correction (Bennett-Chandler) was computed additionally in order to take into account the recrossing events. The computed self diffusion coefficient was found within the range that has been obtained from the experiment [5].

[1] V.E. Zorine et al.: J. Phys. Chem. B **108**, 5600 (2004)
[2] C. Dellago et al.: Adv. Chem. Phys. **123**, 1 (2002)
[3] O. Saengsawang: PhD Thesis, submitted, University of Leipzig
[4] A. Schüring et al.: Chem. Phys. Lett. **450**, 164 (2007)
[5] P. C.M.M. Magusin et al.: Magn. Reson. Chem. **37**, 108 (1999)

11.9 Diffusion of Guest Molecules in Metal Organic Frameworks

S. Fritzsche, K. Seehamart, S. Hannongbua*, T. Remsungnen†

*Chulalongkorn University, Bangkok, Thailand
†Khon Khaen University, Khon Khaen, Thailand

A new class of nanoporous materials that is promising for industrial applications mainly because of the possibility of 'tayloring' and the huge surface/volume ratio is the class of Metal Organic Frameworks (MOF's) [1]. Already now, after few years, the number of different MOF's that have been synthesized is larger then the number of e.g. zeolite types. Many phenomina connected with adsorption and diffusion in these materials are not yet understood. The project was started to examine important open questions in that field. Cooperation with several experimental groups (Prof. Kärger, Leipzig; Prof. Caro, Hannover; Dr. Wiebcke, Hannover) is envisaged for 2008.

[1] B.F. Hoskins, R. Robson: J. Am. Chem. Soc. **112**, 1546 (1990)

11.10 Funding

Analytical Treatment and Computer Simulations of the influence of the crystal surface on the exchange of guest molecules between zeolite nanocrystals and the surrounding gas phase
S. Fritzsche, S. Vasenkov, A. Schüring
SPP1155, DFG FR1486/2-2

Diffusion of Water in the Zeolite Chabazite
S. Fritzsche, O. Saengsawang, P. Biswas, A. Schüring
DFG: IRTG 1056

Investigation of the rotation and diffusion of pentane in the zeolite ZK5
S. Fritzsche, O. Saengsawang, A. Schüring
DFG: IRTG 1056

How do guest molecules enter zeolite pores? Quantum Chemical calculations and classical MD simulations
S. Fritzsche, S. Thompho
DFG FR1486/1-4

Diffusion of Guest Molecules in Metal Organic Frameworks
K. Seehamart
funded by a stipend of the University of Technology Isan (RMUTI), Kon Khaen, Thailand

Simulation of phase equilibria in two- and three-dimensional Fluids
Research fund of University of Ontario Institute of Technology (research stay of H.L. Vörtler in Oshawa) and SHARCNET computer network (Ontario, Canada)

11.11 Organizational Duties

S. Fritzsche

- Project leader of one project in the International Research Training Group, IRTG 1056
- Project leader of one project in the SPP1155, DFG FR1486/2-2
- Project leader of a German/Thai research project, DFG FR1486/1-4
- Referee: Chem. Phys. Lett., Micropor. Mesopor., J. Mol. Graphics Model.

H.L. Vörtler

- Speaker of the MDC group
- Reviewer: Czech Science Foundation
- Referee: J.Chem. Phys, Chem. Phys. Lett, J. Molec. Liquids, Chem. Phys.

11.12 External Cooperations

Academic

- Chulalongkorn University, Bangkok, Thailand
  Prof. Dr. S. Hannongbua
- Indian Institute of Science, Bangalore, India
  Prof. Dr. S. Yashonath
- Khon Khaen University, Khon Khaen, Thailand
  Dr. T. Remsungnen

- University Bordeaux, France
  Prof. Dr. P. A. Bopp
- Eindhoven University, Eindhoven, The Netherlands
  Prof. Dr. P. Magusin
- Technical University, Delft, The Netherlands
  Prof. Dr. M.-O. Coppens, Dr. A. Dammers, Dr. D. Newsome
- University of California, Irvine, USA
  Prof. M. Wolfsberg
- Charles University and Czech Academy of Sciences, Prague, Czech Republic
  Prof. I. Nezbeda, Dr. M. Lisal
- University of Ontario, Institute of Technology, Oshawa, Canada
  Prof. W.R. Smith
- Universität Regensburg, Germany
  Prof. H. Krienke

11.13 Publications

Journals

S. Jost, P. Biswas, A. Schüring, J. Kärger, P.A. Bopp, R. Haberlandt, S. Fritzsche: *Structure and Self-Diffusion of Water Molecules in Chabazite: A Molecular Dynamics Study*, J. Phys. Chem. C **111**, 14 707 (2007)

O. Saengsawang, A. Schüring, T. Dammers, D. Newsome, S. Fritzsche: *Diffusion of n-Pentane in Zeolite ZK5*, Diff. Fundam. **6**, 31.1 (2007)

A. Schüring: *Analytical Estimate of the Entering Probability of Molecules into Crystalline Nanoporous Materials*, J. Phys. Chem. C **111**, 11 285 (2007)

A. Schüring: *The Probability that a Molecule Enters a Porous Crystal*, Diff. Fundam. **6**, 32.1 (2007)

A. Schüring, S.M. Auerbach, S. Fritzsche: *A simple method for sampling partition function ratios*, Chem. Phys. Lett. **450**, 164 (2007)

A. Schüring, J. Gulín-González, S. Fritzsche, J. Kärger, S. Vasenkov: *Transport in the Transition Region Gas/Adsorbent Studied by Molecular Dynamics Simulations*, Diff. Fundam. **6**, 33.1 (2007)

Talks

A. Schüring, J. Gulin-Gonzalez, S. Fritzsche, S. Vasenkov, J. Kärger: *Transport through Zeolite Surfaces Studied by MD Simulations*, 19. Deutsche Zeolithtagung, Leipzig, 07.–09. March 2007

S. Fritzsche: *Transition State Theory at Low Temperatures from Molecular Simulations at High Temperatures*, Chulalongkorn University, Bangkok, Thailand, 09. August 2007

H.L. Vörtler, K. Schäfer, W.R. Smith: *Finite-size effects on subcritical chemical potential isotherms in two- and three-dimensional square-well fluids*, 71th DPG Spring Meeting, Regensburg, 26. – 30. March 2007

H.L. Vörtler, K. Schäfer, W.R. Smith: *Finite-size effects on subcritical chemical potential isotherms in two- and three-dimensional square-well fluids*, Int. Conf. Thermodynamics 2007, Rueil-Malmaison, France, 26. – 28. September 2007

H.L. Vörtler, W.R. Smith, K. Schäfer: *System size effects at simulations of chemical potentials and fluid phase equilibria in two- and three-dimensional square-well fluids*, Int. Conf. Thermodynamics 2007, Rueil-Malmaison, France, 26. – 28. September 2007

Posters

S. Jost, P. Biswas, P.A. Bopp, A. Schüring, S. Fritzsche, J. Kärger: *Self Diffusion of Water Molecules in Chabazite Examined by Molecular Dynamics Simulations*, 19. Deutsche Zeolithtagung, Leipzig, 07. – 09. March 2007

O. Saengsawang, A. Schüring, T. Dammers, D. Newsome, M.-O. Coppens, S. Fritzsche: *Diffusion of n-Pentane in Zeolite ZK5*, Diffusion Fundamentals II, L'Aquila, Italy, 26. – 29. August 2007

O. Saengsawang, A. Schüring, T. Remsungnen, A. Loisruangsin, S. Hannongbu, P.C.M.M. Magusin, S. Fritzsche: *Rotational Motion of n-pentane in γ-cage of Zeolite H-ZK5*, 15th Int. Zeolite Conf., Beijing, China, 12. – 17. August 2007

O. Saengsawang, A. Schüring, T. Remsungnen, A. Loisruangsin, S. Hannongbua, P.C.M.M. Magusin, S. Fritzsche: *Rotational Relaxation Under the Confinement of Zeolite Cages Studied by NMR Experiments and MD Simulations*, 19th Deutsche Zeolithtagung, Leipzig, 07. – 09. March 2007

A. Schüring, S. Fritzsche, S. Vasenkov: *A New Type of Diffusional Boundary Effect at the Edges of Single-File Channels*, 15th Int. Zeolite Conf., Beijing, China, 12. – 17. August 2007

A. Schüring, J. Gulin-Gonzalez, S. Fritzsche, J. Kärger, S. Vasenkov: *Transport in the Transition Region Gas/Adsorbent Studied by Molecular Dynamics Simulations*, Diffusion Fundamentals II, L'Aquila, Italy, 26. – 29. August 2007

A. Schüring, J. Gulin-Gonzalez, S. Fritzsche, J. Kärger, S. Vasenkov: *Which Boundary Condition is Suitable for Describing Adsorption of Guest Molecules from the Gas Phase into Zeolite Crystals?*, 15th Int. Zeolite Conf., Beijing, China, 12. – 17. August 2007

11.14 Graduations

Doctorate

- Arthorn Loisruangsin
  Diffusion of Pentane Isomers in Silicalite-1 by Molecular Dynamics Simulation
  at the Chulalongkorn University, Bangkok, Thailand, under co-advisorship of S. Fritzsche in the framework of a DAAD/TRF joint project
  March 2007

11.15 Guests

- Dr. T. Remsungnen
  Khon Khaen University, Thailand
  01. August – 31. October 2007

12

Quantum Field Theory and Gravity

12.1 Geometry Dependence of the Casimir Force

M. Bordag

The vacuum of quantum fields shows a response to changes in external conditions with measurable consequences. The most prominent manifestation is the Casimir effect. It belongs to the few number of macroscopic quantum effects and it is of big importance in nanometer sizes systems. At present, the dependence of the Casimir forces on geometry is in the focus of actual research using a new representation in terms of a functional determinant. For the example of a cylinder in front of a plane the dependence of the force on the kind of boundary conditions was studied. Especially the weakening of the force when the surfaces become transparent was investigated, see [1].

[1] M. Bordag: Phys. Rev. D **76**, 065 011 (2007)

12.2 Higher Order Correlation Corrections to Color Ferromagnetic Vacuum State at Finite Temperature

M. Bordag, V. Skalozub*

*Physics Faculty, Dnepropetrovsk National University, Ukraine

Topic of the investigation is the stability of the ground state of QCD with temperature and color magnetic background field by means of the calculation of the polarization tensor of the gluon field. Special attention was payed to the investigation of the polarization tensor for the neutral gluons at finite temperature. A new technique for a parametric representation was found which allowed for an explicit separation of the Debye and the magnetic masses and, for instance, for an easy calculation of the Debye mass's field and temperature dependence, see [1].

[1] M. Bordag, V. Skalozub: International school-seminar "New physics and quantum chromodynamics at external conditions", Dnipropetrovsk, Ukraine, 03.–06. May 2007

12.3 Casimir Effect and Real Media

M. Bordag, B. Geyer, G.L. Klimchitskaya*, V.M. Mostepanenko†

*Physics Department, University of St. Petersburg, Russia
†University of Moscow, Russia

The vacuum of quantum fields shows a response to changes in external conditions with measurable consequences. The investigation of the electromagnetic vacuum in the presence of real media is of actual interest in view of current experiments as well as nanoscopic electro-mechanical devices. In recent experiments using atomic force microscopy the Casimir effect had been measured with high accuracy. This required a detailed investigation of the influence of real experimental structures on the corresponding force.

Since the year 2000, the behavior of the thermal correction to the Casimir force between real metals has been hotly debated. As was shown by several groups, the Lifshitz theory, which provides the theoretical foundation for calculations of both the van der Waals and Casimir forces, leads to different results depending on the model of metal conductivity used. To resolve these controversies, the theoretical considerations based on the principles of thermodynamics and new experimental tests were invoked. Additional, the study has to be extended to the case of dielectrics and semiconductors.

- In 2007 we have investigated the *van der Waals and Casimir forces between polar dielectrics*. It was shown that the substitution of their dielectric permittivity in the Lifshitz formula for the free energy results in a large correction that is linear in the temperature. The discovered thermal correction might play an important role in different phenomena. In a wider context it was shown that for all true dielectrics, i.e., for all materials possessing zero conductivity at zero temperature, the inclusion of their dc conductivity arising at nonzero temperature leads to a violation of Nernst's heat theorem in Lifshitz theory. This is relevant to insulators, intrinsic semiconductors, Mott-Hubbard dielectrics and doped semiconductors with the concentration of charge carriers below the critical one. Thus, for dielectrics described in the framework of the Lifshitz theory, dc conductivity should be discarded [1].

  On the same topic but in *application to conductors* important progress was achieved on the understanding of thermal Casimir force between real metals. After longllasting discussions in the literature, it was finally understood why the Drude dielectric function, when substituted into the Lifshitz formula, leads to contradictions with experimental data. The point is that for metal plates of finite area used in the experiments there would be an accumulation of charges on the opposite sides of the plate in the fields of low frequencies if the Drude model is used. This phenomenon is not taken into account in the Lifshitz theory which suppose that plates are neutral [2].

  As an alternative to the Drude dielectric function, we *applied the generalized plasma-like dielectric permittivity* to describe the thermal Casimir force between real metals. This permittivity disregards dissipation processes of conduction electrons, but takes into account the relaxation of core electrons. We have developed a perturbation theory in the relative skin depth and relative temperature

and proved that the Casimir entropy calculated using the generalized plasma-like permittivity satisfies the Nernst heat theorem. We have shown also that the generalized plasma-like permittivity combined with the Lifshitz formula is consistent with both short- and long-separation measurements of the Casimir force performed up to date. This makes the proposed approach most preferable among all approaches available in the literature [3].

- Furthermore, we have performed theoretical investigations for the needs of some *new experiments*.

  First, the experimental data on the modulation of the Casimir force between a gold-coated sphere and silicon plate illuminated with laser pulses have been analyzed on the basis of the Lifshitz theory for the cases of presence and of absence of laser light, i.e., at different charge carrier densities. The theoretical results were shown to be in excellent agreement with data if the dc conductivity of high-resistivity Si (i.e., in the absence of laser light) is not included in the model of dielectric response. The demonstrated new phenomenon on the modulation of the Casimir force with laser pulses permits to control the dispersion interaction in nanodevices [4].

  The second experiment that has been analyzed and compared with theory is the precise measurement of the Casimir force between gold-coated plates by means of a micromechanical torsional oscillator. Data were found to be in excellent agreement with the Lifshitz theory combined with the generalized plasma-like dielectric permittivity that takes into account the relaxation of core electrons. The measure of agreement between experiment and theory was used to set stronger *constraints on predictions of extra-dimensional physics* beyond the Standard Model. The known up to date constraints on the Yukawa-type hypothetical interaction were strengthened in several times over a wide interaction range [5].

  In collaboration with U. Mohideen a new experiment on precision measurement of the Casimir-Lifshitz force in a fluid by J.N. Munday and F. Capasso was analyzed. It was shown that this experiment is in error because the Casimir force was computed inaccurately with an error up to 25 % and the residual electrostatic force was underestimated by a factor of 590 [6].

- Finally, we have performed the investigation of *interaction between H atoms and singlewall carbon nanotubes*. For this purpose we have adapted the formalism elaborated in our group in 2006 and originally used for the configuration of H atoms near graphene. The generalization for the case of carbon nanotubes was achieved by using the proximity force approximation. The free energies and forces were computed for H atoms and molecules in close proximity to singlewall nanotubes. The obtained values were compared with those for nanotubes with several walls at different separations between a nanotube and an atom [7].

[1] G.L. Klimchitskaya, B. Geyer: *Problems in the theory of thermal Casimir force between dielectrics and semiconductors*, submitted to J. Phys. A Math. Gen.
[2] V.M. Mostepanenko, B. Geyer: *New approach to the thermal Casimir force between real metals*, submitted to J. Phys. A Math. Gen.
[3] B. Geyer et al.: J. Phys. A Math. Gen. **40**, 13 485 (2007)

[4] F. Chen et al.: Phys. Rev. B **76**, 035 338 (2007)
[5] R.S. Decca et al.: Eur. Phys. J. C **51**, 963 (2007)
[6] B. Geyer et al.: *Comment on "Precision measurement of the Casimir-Lifshitz force in a fluid"*, submitted to Phys. Rev. A
[7] E.V. Blagov et al.: Phys. Rev. B **75**, 235 413 (2007)

12.4 Quantum Field Theory of Light-Cone Dominated Hadronic Processes

B. Geyer, J. Blümlein*, D. Robaschik†, O. Witzel‡

*Institut für Hochenergiephysik, Zeuthen
†Institute for Theoretical Physics, Brandenburg Technical University, Cottbus
‡Institute for Physics, Humboldt-Universität Berlin

Light-cone dominated, polarized hadronic processes at large momentum transfer factorize into process-dependent hard scattering amplitudes and process-independent non-perturbative generalized distribution amplitudes. Growing experimental accuracy requires the entanglement of various twist as well as (target) mass contributions and radiative corrections. Their quantum field theoretic prescription is based on the nonlocal light-cone expansion [1] and the group theoretical procedure of decomposing *nonlocal, tensor-valued* QCD operators into tensorial harmonic operators with well-defined geometric twist (τ = dimension d − spin j) developed in our previous work [2, 3].

- First, extending former work about power resp. target mass corrections for virtual Compton scattering at twist–2 [2, 4, 5], we determined the complete target mass and finite (transverse) momentum corrections to *deeply inelastic diffractive scattering* [6] . The (imaginary part of the) corresponding amplitude, despite having a complicated structure, contained an integration over one internal variable, called ζ, which cannot be avoided. In addition, the dependence on that variable is not only complicated but remained partly implicit through the underlying GPD's $\Phi^{(i)}(\xi;\zeta)$. However, taking into account that this internal integration corresponds to an average over transverse degrees of freedom we can, in principle, introduce the nth ζ-moments $\Phi^{(i\,n)}(\xi)$ of these two-variable GPD's and expand all quantities with respect to ζ. The zeroth order corresponds to the prescription of diffractive deep inelastic scattering in terms of parton distributions with some corrections. The mass corrections, in the leading terms, follow the well-known pattern from DIS with the replacement $4M^2 \to 4M^2 - t$ and the substitution of the parton distributions by diffractive GPDs.

  While in absence of mass effects the two–particle problem could effectively be reduced to a single–particle description for the case $t \to 0$, this is no longer true for finite values of t and/or target masses. Here two–particle effects become relevant, which do not allow for a *direct* partonic description. The variables $t = (p_i - p_f)^2$ and $M^2 = p_i^2 = p_f^2$ are closely related and some simplification emerges if these scales vanish. In detail we

(a) proposed a possible approximation method which could be used for the parametrization of experimental data in the general case and

(b) discussed the limiting case to deep inelastic scattering as well as the relation to the massless case, i.e. the collinear limit, developed earlier [7].

- Second, the fundamental results [8] on the complete twist decomposition of generic non-local tensor operators for hadronic processes recently have been applied to *B-meson physics* [9]. Thereby, two- and three-particle distribution amplitudes of heavy pseudoscalar mesons of well-defined geometric twist were introduced. They are obtained from appropriately parametrized vacuum-to-meson matrix elements by applying those twist projectors which determine the enclosed light-cone operators of definite geometric twist and, in addition, observing the heavy quark constraint. Comparing these distribution amplitudes with the conventional ones of dynamical twist we derived relations between them, partially being of Wandzura–Wilczek type; also sum rules of Burkhardt–Cottingham type were derived.

  These results have been extended to derive the operator relations resulting from the quark equations of motion as well as from the relations between Dirac structures [10]. Under the constraints of HQET the equations of motion of heavy meson distribution amplitudes of definite geometric twist, using the knowledge of their off-cone structure, are reformulated as a set of algebraic equations. Together with equations due to the different Dirac structures various relations between the (sets of) independent two- and three particle distribution amplitudes of definite geometric twist are derived and presented using both the (double) Mellin moments and the re-summed non-local distribution amplitudes. Resolving these relations for the independent two-particle moments in terms of three-particle double moments we confirmed a representation which had been derived by Kawamura et al. [11] solving a (sub)set of differential equations resulting from the equations of motion.

[1] S.A. Anikin, O.I. Zavialov: Ann. Phys. N.Y. **116**, 135 (1978); D. Müller et al.: Fortschr. Phys. **42**, 101 (1994)
[2] B. Geyer et al.: Nucl. Phys. B **559**, 339 (1999); Nucl. Phys. B **618**, 99 (2001); B. Geyer, M. Lazar: Nucl. Phys. B **581**, 341 (2000), Phys. Rev. D **63**, 094 003 (2001); J. Eilers, B. Geyer: Phys. Lett. B **546**, 78 (2002)
[3] J. Eilers et al. Phys. Rev. D **69**, 034 015 (2004)
[4] B. Geyer et al.: Nucl. Phys. B **704**, 279 (2005)
[5] B. Geyer, D. Robaschik: Phys. Rev. D **71**, 054 018 (2005)
[6] J. Blümlein et al.: Nucl. Phys. B **755**, 112 (2006)
[7] J. Blümlein, D. Robaschik: Phys. Lett. B **517**, 222 (2001); Phys. Rev. D **65**, 096 002 (2002)
[8] J. Eilers: arXiv:hep-th/0608173
[9] B. Geyer, O. Witzel: Phys. Rev. D **72**, 034 023 (2005)
[10] B. Geyer, O. Witzel: Phys. Rev. D **76**, 074 022 (2007)
[11] H. Kawamura et al.: Phys. Lett. B **523**, 111 (2001); Phys. Lett. B **536**, 344E (2002); J. Mod. Phys. A **48**, 1433 (2003)

12.5 Structure of the Gauge Orbit Space and Study of Gauge Theoretical Models

G. Rudolph, S. Charzynski*, A. Hertsch, J. Huebschmann†, P. Jarvis‡, J. Kijowski‡, M. Schmidt

*Faculty of Physics, University of Warsaw, Poland
†Université des Sciences et Technologies de Lille, France
‡School of Physics, University of Tasmania, Hobart, Australia

The investigation of gauge theories in the Hamiltonian approach on finite lattices with emphasis on the role of nongeneric strata was continued, including

- singular Marsden-Weinstein reduction for concrete models [1, 2],
- stratified Kähler quantization for gauge groups SU(2) and SU(3) [3],
- physical effects of the stratification for gauge group SU(2).

The last two problems were studied in collaboration with J. Huebschmann.

Based on [4], the investigations of specific models of quantum lattice gauge theory in terms of gauge invariant quantities concerning the structure of the algebra of observables and its representations were continued, too.

A. Hertsch continued his worked on the classification of the orbit types of the action of the group of local gauge transformations on the space of connections for arbitrary compact gauge group.

[1] E. Fischer et al.: J. Geom. Phys. **57**, 1193 (2007)
[2] S. Charzyński et al.: arXiv:hep-th/0512129
[3] J. Huebschmann et al.: arXiv:hep-th/0702017
[4] J. Kijowski et al.: Ann. H. Poincaré **4**, 1137 (2003); J. Kijowski, G. Rudolph: J. Math. Phys. **46**, 032 303 (2005); Rep. Math. Phys. **55**, 199 (2005); P. Jarvis et al.: J. Phys. A **38**, 5359 (2005)

12.6 Noncommutative Geometry

G. Rudolph, P. Hajac*, R. Matthes*, W. Szymanski†

*Faculty of Physics, University of Warsaw, Poland
†Faculty of Science and Information Technology, University of Newcastle, UK

The study of quantum principal bundles was continued. In collaboration with U. Kraehmer (IMPAN Warsaw) and B. Zieliński (IMPAN Warsaw and Uni Lodz), the notion of a piecewise principal comodule algebra (generalizing the former notion of a locally trivial quantum principal bundle) has been introduced, and the relation to the global notion of principality has been investigated, see [1] and [2].

In collaboration with L. Dabrowski (Trieste) and T. Hadfield (London), noncommutative analogues of instanton bundles of arbitrary charge over a certain noncommutative 4-sphere have been constructed, using K-theoretic methods, see [3].

The investigation of observable algebras for lattice models of gauge theories [4] has been continued. Some work has been done on the question if these algebras can be obtained by C^*-algebraic quantization methods (strict deformation quantization).

[1] P.M. Hajac et al.: arXiv:arXiv:0707.1344
[2] R. Matthes: in *Proc. 7th Int. Workshop "Lie Theory and Its Applications in Physics"*, ed. by V.K. Dobrev et al. (Heron Press, Sofia 2008), in press
[3] L. Dabrowski et al.: arXiv:math.QA/0702001
[4] J. Kijowski, G. Rudolph: J. Math. Phys. **46**, 032 303 (2005); Rep. Math. Phys. **55**, 199 (2005)

12.7 Quantum Field Theory on Non-Commutative Geometries, Quantum Energy Inequalities, Generally Covariant Quantum Field Theory

R. Verch, P. Marecki, M. Borris, J. Schlemmer

One of the questions of recent interest is if there is a general framework for quantum field theory on non-commutative spacetimes. This question is analysed in collaboration with M. Paschke and M. Borris. On one hand, an approach to Lorentzian non-commutative geometry in the spirit of spectral geometry is being established. On the other hand, the quantization of such structures is shown to lead to simple examples of quantum field theories on non-commutative spacetimes for concrete non-commutative spacetime models. The research on these topics is in progress.

Another line of research is devoted to an extension of the framework of local general covariant quantum field theories to the case of a relation between quantum field theories on several, different dimensions. This connects to the question of how to distinguish theories of Kaluza-Klein type at the quantized level. The research work on these matters is carried out in collaboration with C.J. Fewster.

The definition and analysis of states which can be viewed as local thermal equilibrium states in quantum field theory will be extended to quantum fields in curved spacetime, with a view on application in cosmological situations. Current research work with J. Schlemmer points at a close connection between local thermal equilibrium states and quantum energy inequalities which is being further analyzed. Moreover, the validity of quantum energy inequlities in interacting quantum field models is being investigated in collaboration with C. Kopper.

A standing problem is the concept of quantum field theories on non-globally hyperbolic spacetimes. A special class of such spacetimes are certain types of rotating spacetimes. Several issues in setting up quantum field theories on such spacetimes are being studied by P. Marecki.

12.8 Funding

Structure of the gluon polarization tensor in a color magnetic field background at finite temperature
PD Dr. M. Bordag
DFG 436 UKR 17/25/06

Spectral Zeta Functions and Heat Kernel Technique in Quantum Field Theory with Nonstandard Boundary Condition
PD Dr. M. Bordag, Dr. D. Vassilevich
Heisenberg-Landau programme

Parallel nano assembling directed by short-range field forces
PD Dr. M. Bordag
PARNASS: Specific targeted research project within the 6th Framework Programme of EU, NMP4-CT-2005-017071

Improved study of the Casimir force between real metals and its application to constraints for testing extra-dimensional physics
B. Geyer
DFG 436 RUS 113/789/0-3

Quantum Theory of Lattice Gauge models
A. Hertsch
IMPRS fellowship

Local thermodynamic equilibrium in cosmological spacetimes
J. Schlemmer
IMPRS fellowship

12.9 Organizational Duties

M. Bordag
- Referee: J. Phys. A, Phys. Rev. D, J. Math. Phys.
- Organizer of the Workshop on Quantum Field Theory under the Influence of External Conditions (QFEXT07), Leipzig, Germany, 17. – 21. September 2007

B. Geyer
- Vertrauensdozent der Gesellschaft Deutscher Naturforscher und Ärzte (GDNÄ)
- Referee: DFG, DAAD, Humboldt Foundation

G. Rudolph
- Referee: Class. Quant. Grav., J. Math. Phys., J. Geom. Phys., J. Phys. A, Rep. Math. Phys.
- Director of the Institute for Theoretical Physics

M. Schmidt
- Referee: J. Phys. A, Int. J. Mod. Phys. A, Class. Quant. Grav., Gen. Relat. Gravit.

A. Uhlmann
- Board member: Rep. Math. Phys., Open Syst. Inf. Dyn.

R. Verch
- Associate Editor of J. Gen. Relat. Gravit.
- Chairman of the board for the Theoretical and Mathematical Physics Section, Deutsche Physikalische Gesellschaft (DPG)
- Referee: Commun. Math. Phys., J. Math. Phys., Rev. Math. Phys., Classical Quant. Grav., Eur. Phys. J. C, Springer Lecture Notes Physics, CEPJ,
- Reviewer for Mathematical Reviews

12.10 External Cooperations

Academic

- Institut für Physik / Computational Physics, Humboldt Universität zu Berlin, Germany
  Oliver Witzel
- DESY-Institute of High Energy Physics, Zeuthen, Germany
  Dr. Johannes Blümlein
- Institute of Theoretical Physics, Brandenburg Technical University, Cottbus, Germany
  Prof. Dr. Dieter Robaschik
- Mathematics Department, Universität Hamburg, Germany
  Dr. C. Fleischhack
- Institute for Mathematical Physics, Technical University Braunschweig, Germany
  Prof. Dr. R.F. Werner
- Department of Mathematics, University of Münster, Germany
  Dr. M. Paschke
- Polish Academy of Sciences, Center for Theoretical Physics, Warsaw, Poland
  Prof. Dr. J. Kijowski
- Polish Academy of Sciences, Mathematics Institute and University of Warsaw, Poland
  Prof. Dr. P. Hajac, Dr. R. Matthes
- St. Petersburg University, Russia
  Prof. Yu.V. Novozhilov
- Department of Physics, North-West Polytechnical University St. Petersburg, Russia
  Prof. Dr. Galina L. Klimchitskaya
- Noncommercial Partnership “Scientific Instruments” of Ministry of Industry, Sciences and Technologies, Moscow, Russia
  Prof. Dr. Vladimir M. Mostepanenko
- National University, Dnepropetrovsk, Ukraine
  Prof. V. Skalozub

- CPHT, Ecole Polytechnique, Palaiseau, France
  Prof. C. Kopper
- Université des Sciences et Technologies de Lille, France
  Prof. Dr. J. Huebschmann
- Dipartimento di Matematica, Universita di Trento, Italy
  Prof. Dr. V. Moretti
- Department of Mathematics, University of York, UK
  Dr. C.J. Fewster
- Department of Mathematics, University of Florida, Gainesville, USA
  Prof. Dr. S.J. Summers
- Department of Mathematics, Connecticut State University, New Britain, USA
  Prof. Dr. T. Roman
- Department of Physics, University of South Carolina, Columbia, USA
  Prof. Dr. P. Mazur
- Lawrence Livermore National Laboratory, Livermore, USA
  Dr. G.F. Chapline
- University of Tasmania, Hobart, Australia
  Prof. Dr. P. Jarvis
- University of Newcastle, Australia
  Prof. Dr. W. Szymanski

12.11 Publications

Journals

M. Bordag: *Generalized Lifshitz formula for a cylindrical plasma sheet in front of a plane beyond proximity force approximation*, Phys. Rev. D **75**, 065 003 (2007)

M. Bordag: *On the interaction of a charge with a thin plasma sheet*, Phys. Rev. D **76**, 065 011 (2007)

M. Bordag, A. Ribayrol, G. Conache, L.E. Fröberg, S. Gray, L. Samuelson, L. Montelius, H. Pettersson: *Shear stress measurements on InAs nanowires by AFM manipulation*, Small **3**, 1398 (2007)

C. D'Antoni, G. Morsella, R. Verch: *Scaling algebras for charge carrying quantum fields and superselection structure at short distances*, Contemp. Math. **437**, 31 (2007)

E. Fischer, G. Rudolph, M. Schmidt: *A Lattice Gauge Model of Singular Marsden-Weinstein Reduction. Part I. Kinematics*, J. Geom. Phys. **57**, 1193 (2007)

B. Geyer, G.L. Klimchitskaya, V.M. Mostepanenko: *Generalized plasma-like permittivity and thermal Casimir force between real metals*, J. Phys. A Math. Gen. **40**, 13 485 (2007)

B. Geyer, O. Witzel: *Heavy Meson Distribution Amplitudes of Definite Geometric Twist with Contribution of 3-Particle Distribution Amplitudes*, Phys. Rev. D **76**, 074 022 (2007)

Books

J. Blümlein, B. Geyer, D. Robaschik: *Target Mass Corrections in Diffractive Scattering*, in *Deep-Inelastic Scattering and Related Subjects*, ed. by G. Grindhammer, K. Sachs (DESY, Hamburg 2007), arXiv:0706.2478 [hep-ph]

in press

M. Bordag, V. Nikolaev: *Casimir force for a sphere in front of a plane beyond proximity force approximation*, J. Phys. A Math. Gen.

G.F. Chapline, P. Marecki: *Rotating De Sitter Space*, arXiv:0709.3479 [gr-qc]

B. Geyer, G.L. Klimchitskaya, V.M. Mostepanenko: *Analytic approach to the thermal Casimir force between metal and dielectric.*, Ann. Phys. **323**, 291–316 (2008)

G.L. Klimchitskaya, B. Geyer: *Problems in the theory of thermal Casimir force between dielectrics and semiconductors*, J. Phys. A

P. Marecki: *Balanced homodyne detectors in QFT*, arXiv:quant-ph/0703076

P. Marecki: *On the wave equation in spacetimes of Goedel type*, arXiv:gr-qc/0703018

V.M. Mostepanenko, B. Geyer: *New approach to the thermal Casimir force between real metals*, J. Phys. A

Talks

M. Bordag: *Beyond Proximity Force Approximation*, Seminar talk at the Consejo Superior de Investigaciones Cientificas, Instituto de Ciencias del Espacio (CSIC), Barcelona, Spain, 17. January 2007

M. Bordag: *Beyond Proximity Force Approximation in the Casimir effect*, 8th Workshop on Quantum Field Theory under the Influence of External Conditions (QFEXT07), Leipzig, Germany, 17. – 21. September 2007

M. Bordag: *On the interaction of a charge with a plasma sheet*, 8th Workshop on Quantum Field Theory under the Influence of External Conditions (QFEXT07), Leipzig, Germany, 17. – 21. September 2007

M. Bordag: *On the interaction of a charge with a plasma sheet*, Seminar Talk at the PTI of the Friedrich-Schiller-Universität Jena, 26. April 2007

M. Bordag: *On the interaction of a charge with a plasma sheet*, Seminar talk at the Laboratoire Kastler Brossel, Paris, France, 07. June 2007

M. Bordag: *Shear stress measurements on InAs Nanowires*, Seminar talk at the University of California, Riverside, USA, 22. June 2007

M. Bordag: *The one-loop polarization tensor of gluons in a magnetic background field at finite temperature*, Lecture on the International school-seminar "New Physics and Quantum Chromodynamics at External Conditions", Dnepropetrovsk National University, Dnepropetrovsk, Ukraine, 03. May 2007

B. Geyer, G.L. Klimchitskaya: *Problems in the theory of thermal Casimir force between dielectrics and semiconductors*, 8th Workshop on Quantum Field Theory under the Influence of External Conditions (QFEXT07), Leipzig, Germany, 17. – 21. September 2007

B. Geyer, V.M. Mostepanenko: *New approach to the thermal Casimir force between real metals*, 8th Workshop on Quantum Field Theory under the Influence of External Conditions (QFEXT07), Leipzig, Germany, 17. – 21. September 2007

P. Marecki: *Balanced homodyne detectors and Casimir energy densities*, 8th Workshop on Quantum Field Theory under the Influence of External Conditions (QFEXT07), Leipzig, Germany, 17. – 21. September 2007, arXiv:0711.1541

G. Rudolph: *Lattice gauge theory: singular reduction and quantization*, Université des Sciences et Technologies, Lille, France, 28. March 2007

G. Rudolph: *Singular Marsden-Weinstein reduction and quantization of lattice gauge models*, VIIth Workshop on Lie Theory and its Applications in Physics, Varna, Bulgaria, 18 – 24 June 2007

G. Rudolph: *Singuläre Reduktion und Quantisierung von Eichfeldmodellen*, University of Freiburg, Institute for Theoretical Physics, 06. July 2007

M. Schmidt: *Gauge theory and quantization on stratified spaces*, Université de Provence, Marseille, France, 16. February 2007

M. Schmidt: *Quantum Mechanics on a Space with Singularities*, VIIth Workshop on Lie Theory and its Applications in Physics, Varna, Bulgaria, 18. – 24. June 2007

M. Schmidt: *Quantum Mechanics on a Space with Singularities: Observables*, Mini-Workshop Fokoop Clausthal-Leipzig-Sofia, Technische University Clausthal, 10. – 12. November 2007

R. Verch: *Darker than vacuum*, Symposium Knowledge of the Early Universe, DPG Spring Meeting, Heidelberg, Germany, 05. – 09. March 2007

R. Verch: *Lorentzian non-commutative geometry and covariant quantum field theory*, DPG Spring Meeting, Heidelberg, Germany, 05. – 09. March 2007

12.12 Graduations

Diploma

- Sandra Stephan
  On the reduced phase space of lattice gauge theory
  April 2007

12.13 Guests

- J. Huebschmann
  Université des Sciences et Technologies de Lille, France
  29. October – 02. November 2007
- Prof. Dr. J. Kijowski
  Center for Theoretical Physics, Polish Academy of Sciences, Warsaw, Poland
  September 2007
- Prof. Dr. Galina L. Klimchitskaya
  Department of Physics, North-West Polytechnical University, St. Petersburg Russia
  20. June – 19. December 2007
- Dr. V. Marachevski
  State University St. Petersburg, Russia
  14. – 25. September 2007
- Prof. Dr. Vladimir M. Mostepanenko
  Noncommercial Partnership "Scientific Instruments" of Ministry of Industry, Sciences and Technologies, Moscow, Russia
  20. June – 19. December 2007
- Prof. V. Nesterenko
  JINR Dubna, Russia
  15. – 22. September 2007
- Prof. V. Skalozub
  Dnepropetrovsk National University, Ukraine
  11. – 16. September 2007, 22. – 28. September 2007

13

Statistical Physics

13.1 Introduction

The STP group works on the connections of statistical mechanics to quantum field theory, on the mathematical and physical aspects of renormalization group (RG) theory and on its applications to high-energy and condensed matter physics, and on quantum kinetic theory. Our methods range from mathematical proofs to computational techniques.

The RG method applied here is an exact functional transformation of the action of the system, which leads to an infinite hierarchy of equations for the Green functions. Truncations of this hierarchy are used in applications. In a number of nontrivial cases, this truncation can be justified rigorously, so that the method lends itself to mathematical studies. These mathematical aspects are also under investigation.

Another topic we study is the long-time dynamics of large quantum systems, with a view of understanding how dissipative dynamics on the macroscopic scale arises from the microscopically reversible dynamics in interesting scaling limits.

We have ongoing collaborations with the Max-Planck Institute for Solid State Research in Stuttgart, the University of British Columbia, Vancouver, the University of Munich, the University of Würzburg, the University of Mainz, and Harvard University.

The collaboration within Germany has now received funding through the DFG research group FOR723, "Functional Renormalization Group for Correlated Fermion Systems". The group, established in spring, 2007, is coordinated here in Leipzig. Its members are at the univerities of Aachen, Göttingen, Heidelberg, Leipzig, and Würzburg, and at the Max-Planck-Institut für Festkörperforschung, Stuttgart.

Manfred Salmhofer

13.2 Mathematical Theory of Singular Fermi Surfaces

J. Feldman*, M. Salmhofer

*Mathematics Department, University of British Columbia, Vancouver, Canada

We study the regularity properties of the fermionic self-energy for the case where the Fermi surface of the interacting system has singular points because the gradient of

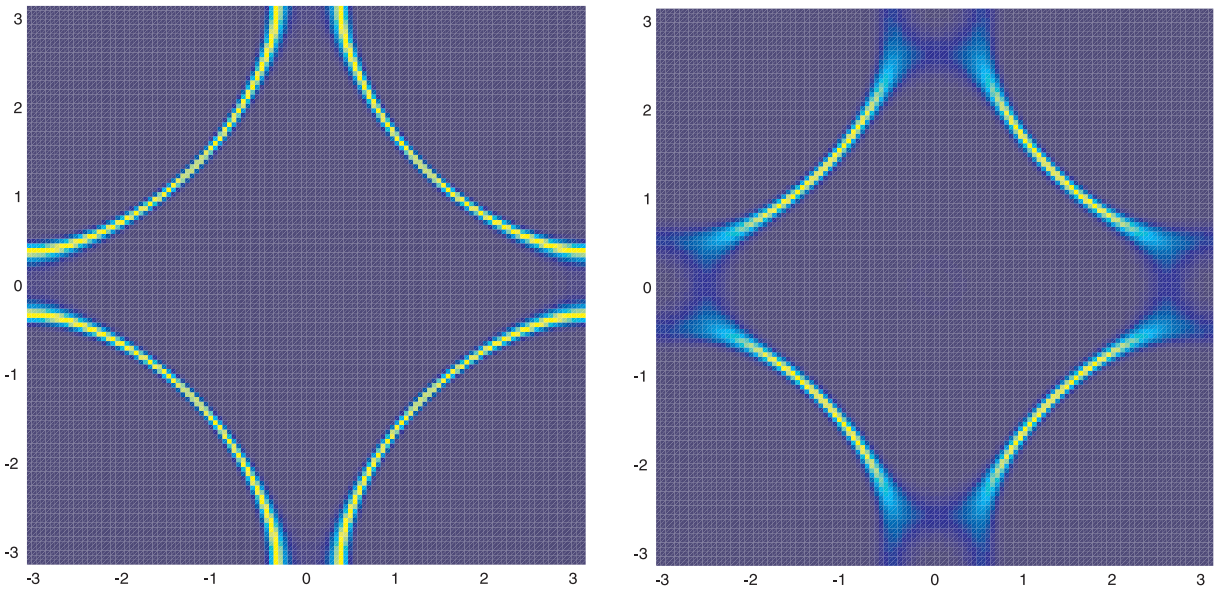

Figure 13.1: Fermi surface at positive temperature (defined via the derivative of the Fermi function), of two-dimensional fermions with nearest and next-to-nearest hopping near the Van Hove filling. *Left* – free fermions. *Right* – fermions with selfenergy from the interaction: the asymmetry between the frequency derivative and the spatial derivative of the fermionic selfenergy further suppresses the Fermi velocity near the Van Hove points, and thus broadens the Fermi function [3].

the dispersion relation vanishes (van Hove points). We prove regularity properties to all orders in perturbation theory using RG methods. We find a striking asymmetry in the derivatives of the self-energy, which gives a clear mathematical meaning to the "vanishing of the Fermi surface at the saddle points" (see Fig. 13.1), an effect that has been discussed in the context of normal state properties of high-T_c materials. Our results also indicate that the inversion theorem proven in [1] for regular Fermi surfaces is very unlikely to carry over to the case of singular Fermi surfaces, but that instead an extended van Hove singularity may appear [2, 3].

[1] J. Feldman et al.: Comm. Pure Appl. Math. **53**, 1350 (2000)
[2] J. Feldman, M. Salmhofer: *Singular Fermi Surfaces I. General power counting and higher-dimensional cases*, Rev. Math. Phys. (2008), in press
[3] J. Feldman, M. Salmhofer: *Singular Fermi Surfaces II. The Two-Dimensional Case*, Rev. Math. Phys. (2008), in press

13.3 Exchange Bosons in Fermionic Renormalization Group Flows

C. Husemann, M. Salmhofer

We have analyzed the leading weak coupling instabilities of the (t, t')-Hubbard model at van Hove filling within a new approximation of the one-loop renormalization group.

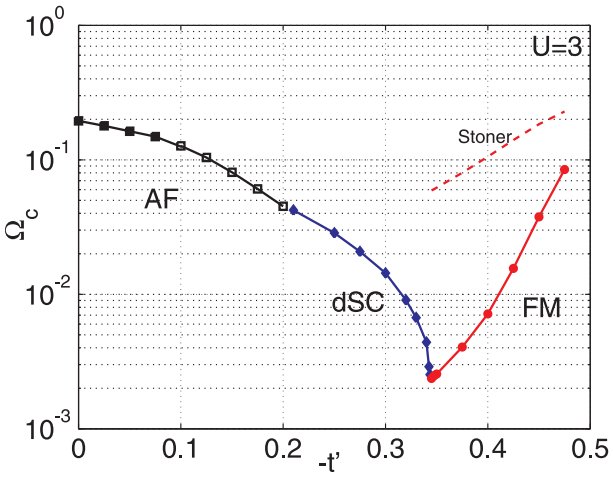

Figure 13.2: The critical scale Ω_c, indicating a breakdown of the Fermi liquid, is plotted over hopping $-t'$ at temperature zero. Corresponding to dominant terms in the renormalization group flow at Ω_c, antiferromagnetism (AF), $d_{x^2-y^2}$–superconductivity (dSC), and ferromagnetism (FM) are the leading instabilities of the (t, t')-Hubbard model.

The four-fermion interaction was expanded in terms of fermion bilinears interacting via an exchange boson. We argue that this expansion can be confined to a few terms and still preserve the qualitative structure of the full flow. That is, the method extracts important processes of the renormalization group flow, resulting in a reduction of computing cost. Moreover, the result can be used as a natural input for a Hubbard-Stratonovich transformation on a low energy scale. This avoids most of the ambiguities encountered in the Hubbard–Stratonovich decoupling of the initial interaction.

Using the Ω-scheme, a minimal regularization in the frequencies that does not artificially suppress small momentum particle–hole fluctuations, we were able to find the leading instabilities of the (t, t')-Hubbard model plotted in the Fig. 13.2. This result is qualitatively consistent with the temperature renormalization group [1]. However, we find weaker suppression of the strong coupling scale between ferromagnetism and superconductivity here [2].

[1] C. Honerkamp, M. Salmhofer: Phys. Rev. Lett. **64**, 184 516 (2001)
[2] C. Husemann: PhD Thesis, in preparation

13.4 The Ω-Scheme for RG Flows

M. Salmhofer, G. Schober

We investigate the mathematical properties of the Ω-scheme, a renormalization group scheme based on a minimal regularization in the Matsubara frequencies that does not artificially suppress small momentum particle–hole fluctuations, with the aim of extending the all-order and nonperturbative power counting, including improvements from overlapping loops [1], to the Ω-scheme (diploma work of G. Schober). This generalization involves some harmonic analysis, and the nonperturbative work on the scheme is based on the new determinant estimates proven in [2].

[1] J. Feldman et al.: J. Stat. Phys. **84**, 1209 (1996)
[2] W. Pedra, M. Salmhofer: *Determinant Bounds and the Matsubara UV Problem of Many-Fermion Systems*, to appear in Commun. Math. Phys. (2008)

13.5 Asymptotic Safety in Quantum Einstein Gravity: Nonperturbative Renormalizability and Fractal Spacetime Structure

O. Lauscher, M. Reuter*

*Institut für Physik, Universität Mainz

Quantized General Relativity, based upon the Einstein–Hilbert action, is well known to be perturbatively nonrenormalizable. Therefore, Einstein gravity was rather considered merely an effective theory whose range of applicability is limited to a phenomenological description of gravitational effects at distances much larger than the Planck length. However, recent investigations within the framework of the renormalization group and its effective average action approach indicate that four-dimensional Quantum Einstein Gravity (QEG) can be defined ("renormalized") nonperturbatively along the lines of Weinberg's asymptotic safety scenario. In the light of this evidence it seems quite possible to construct a quantum field theory of the spacetime metric which is not only an effective, but rather a fundamental one and which is predictive and mathematically consistent down to arbitrarily small length scales.

The average action approach has led to specific predictions for the spacetime structure in nonperturbative, asymptotically safe gravity. The general picture of the QEG spacetimes which emerged is as follows. At sub-Planckian distances spacetime is a fractal with an effective dimensionality $d_{\rm eff} = 2$. As one considers larger length scales where the RG running of the gravitational parameters comes to a halt, the "ripples" in the spacetime gradually disappear and the structure of a classical 4-dimensional manifold is recovered.

The original argument leading to $d_{\rm eff} = 2$ was based upon the anomalous dimension η of Newton's constant. In [1, 2] we show that also the spectral dimension $\mathcal{D}_s$ of asymptotically safe QEG (if it indeed exists) equals 2 microscopically, while it is equal to 4 on macroscopic scales. In fact, these results for $\mathcal{D}_s$ coincide with those which were recently obtained by Monte Carlo simulations of the causal dynamical triangulation model. This could be a first hint indicating that the discrete approach and QEG in the average action formulation might describe the same physics.

By studying the solution of the scale dependent counterpart of Einstein's equations it was also possible to gain some further insights into the fractal nature of QEG spacetime [2, 3]. The way in which this solution depends on the scale suggests that at sub-Planckian distances the QEG spacetime is a special kind of fractal with a self-similar structure.

[1] O. Lauscher, M. Reuter: J. High Energy Phys. **10**, 050 (2005); arXiv:hep-th/0508202

[2] O. Lauscher, M. Reuter: in *Quantum Gravity: Mathematical Models and Experimental Bounds*, ed. by B. Fauser et al. (Birkhäuser, Basel 2007) p 293, arXiv:hep-th/0511260
[3] O. Lauscher, M. Reuter: in *Approaches to Fundamental Physics*, Lect. Notes Phys. **721**, ed. by I.-O. Stamatescu, G. Seiler (Springer, Berlin 2007) p 265

13.6 Funding

Singular Fermi Surfaces
M. Salmhofer
DFG Einzelprojekt Sa 1362/2

Functional Renormalization Group for Correlated Fermion Systems
M. Salmhofer
DFG Forschergruppe FOR723

Andrejewski-Vorlesungen
M. Salmhofer
Andrejewski-Stiftung

13.7 Organizational Duties

M. Salmhofer

- Member of the advisory board of the *Andrejewski-Stiftung*.
  Organization of the Andrejewski lectures in Leipzig.
- Referee for Comm. Math. Phys., Phys. Rev. Lett., Phys. Rev. B, J. Stat. Phys., J. Phys. A, Foundations of Physics, J. Math. Phys. Eur. J. Phys.
- grant review for NSERC of Canada, DFG
- Associate editor J. Math. Phys.
- Organisation (joint with S. Adams) of the international workshop *Analysis and Stochastics in Quantum Many-Body Systems*, Max-Planck-Institut für Mathematik in den Naturwissenschaften, Leipzig, 17. – 19. May 2007;
  see www.mis.mpg.de/conferences/quantum07/
- Organisation (joint with C. Honerkamp) of the workshop of the research group FOR723 in Würzburg, 4. – 5. December 2007

13.8 External Cooperations

Academic

- Max-Planck-Institut für Festkörperforschung, Stuttgart, Germany
  W. Metzner
- Institut für Theoretische Physik und Astrophysik, Universität Würzburg, Germany
  C. Honerkamp

- Mathematics Department, University of British Columbia, Vancouver, Canada
  J. Feldman
- Mathematisches Institut, Universität München, Germany
  L. Erdös
- Mathematics Department, Harvard University, Cambridge, USA
  H–T. Yau
- Institut für Physik, Universität Mainz, Germany
  M. Reuter

13.9 Publications

Journals

L. Erdös, M. Salmhofer: *Decay of the Fourier Transform of Surfaces with Vanishing Curvature*, Math. Z. **257**, 261 (2007), arXiv:math-ph/0604039

L. Erdös, M. Salmhofer, H.-T. Yau: *Quantum diffusion for the Anderson model in the scaling limit*, Ann. H. Poincare **8**, 621 (2007), arXiv:math-ph/0502025

L. Erdös, M. Salmhofer, H.-T. Yau: *Quantum diffusion of the random Schrödinger evolution in the scaling limit II. The recollision diagrams*, Comm. Math. Phys. **271**, 1 (2007), arXiv:math-ph/0512015

M. Salmhofer: *Dynamical Adjustment of Propagators in Renormalization Group Flows*, Ann. Phys. (Leipzig) **16**, 171 (2007), arXiv:cond-mat/0607289

Books

O. Lauscher, M. Reuter: *Quantum Einstein gravity: Towards an asymptotically safe field theory of gravity*, in *Approaches to Fundamental Physics*, Lecture Notes in Physics **721**, ed. by I.-O. Stamatescu, G. Seiler (Springer, Berlin 2007) p 265

in press

L. Erdös, M. Salmhofer, H.-T. Yau: *Quantum diffusion of the random Schrödinger evolution in the scaling limit I. The non-recollision diagrams*, to appear in Acta Mathematica (2008), arXiv:math-ph/0512014

J. Feldman, M. Salmhofer: *Singular Fermi Surfaces I. General Power Counting and Higher-Dimensional Cases*, to appear in Rev. Math. Phys. (2008), arXiv:0706.1786v1 [math-ph]

J. Feldman, M. Salmhofer: *Singular Fermi Surfaces II. The Two-Dimensional Case*, to appear in Rev. Math. Phys. (2008), arXiv:0706.1788v1 [math-ph]

W. Pedra, M. Salmhofer: *Determinant Bounds and the Matsubara UV Problem of Many-Fermion Systems*, to appear in Comm. Math. Phys. (2008), arXiv:0707.2810v1 [math-ph]

Talks

C. Husemann: *Ferromagnetism and Superconductivity in the Hubbard Model*, Workshop der Forschergruppe FOR 723, Universität Würzburg, 5. December

O. Lauscher: *RG flows into phases with broken symmetry*, Universität Mainz, 5. October

M. Salmhofer: *A panorama of Wilson's renormalization group*, Workshop "Mathematical and physical aspects of perturbative approaches to quantum field theory", Internationales Erwin-Schrödinger-Institut für Mathematische Physik, Wien, Austria, 28. March

M. Salmhofer: *Many electrons: a (non-exhaustive) review*, Invited talk at the international conference "The electron is inexhaustible" on the occasion of Jürg Fröhlich's 61st birthday, ETH Zürich, Switzerland, 4. July

M. Salmhofer: *Mathematische Aspekte von Vielteilchensystemen*, Mathematisches Kolloquium, Universität Mainz, 18. January

13.10 Guests

- J. Yngvason
  Universität Wien, Austria
  21. – 27. January 2007

14

Theory of Condensed Matter

14.1 Introduction

Major research topics in our group include nonequilibrium phenomena and pattern formation in systems of various nature, e.g. in soft condensed matter and in biological systems. Modern analytic methods of statistical physics and computer simulations complement and stimulate each other. Cooperations with mathematicians, theoretical and experimental physicists, biologists and medical researchers e.g. in France, Germany, Italy, Ireland, UK, and USA are well established. Specifically we are interested in the following problems.

Noise induced phenomena (Behn). Noise induced non-equilibrium phase transitions are studied in coupled arrays of stochastically driven nonlinear systems. Furthermore, stability and statistical characteristics of stochastic nonlinear systems with time delay are investigated.

Mathematical modeling of the immune system (Behn). Using methods of nonlinear dynamics and statistical physics, we study the architecture and the random evolution of the idiotypic network of the B-cell subsystem and describe the regulation of balance of Th1/Th2-cell subsystems, its relation to allergy and the hyposensitization therapy (Cooperation with the Institute for Clinical Immunology).

Non-equilibrium dynamics in soft-condensed-matter systems (Kroy). The latter range from desert dunes spontaneously developing as a generic consequence of aeolian sand transport, through non-equilibrium gels of adhesive colloids and proteins, the viscoelastic mechanics of the cytoskeleton, to the non-equilibrium dynamics of single DNA molecules under strong external fields. (Related experimental work is currently in progress in the Soft Matter Physics and Molecular Physics groups at the Institute for Experimental Physics.) A common feature is the presence of strong fluctuations and stochastic dynamics on the micro-scale. The emergence of macroscopic structure and (non-linear) deterministic macroscopic dynamics is to be understood. The applied methods range from analytical studies of stochastic integro-differential equations through liquid-state theories, mode-coupling theory, effective hydrodynamic equations, phenomenological modeling, to numerical simulations.

Ulrich Behn, Klaus Kroy

14.2 Stochastic Phenomena in Systems with Many Degrees of Freedom

U. Behn, S. Gütter, P. Altrock, M. Krieger-Hauwede, L. Wetzel, M. Knorr

Arrays of spatially coupled nonlinear dynamical systems driven by multiplicative Gaussian white noise show close analogies to phase transitions in equilibrium [1]. Concepts developed to describe equilibrium phase transitions such as symmetry or ergodicity breaking, order parameter, critical behaviour, critical exponents etc. have been successfully transfered to noise induced nonequilibrium phase transitions. The structure of the theory will be generically of mean field type, if infinite globally coupled arrays are studied which allows for a number of analytical results [2].

Remarkably, due to the multiplicative nature of the noise, essential characteristics of phase transitions can already be found in finite arrays. We can introduce center of mass and relative coordinates and exploit that in the limit of strong coupling there is a clear separation of time scales. The relative coordinates relax very quickly to zero and the system behaves as a single entity described by the center of mass coordinate. The expectation value of the latter can be calculated analytically and exhibits a critical bahaviour. The results can be independently derived in the Fokker–Planck and in the Langevin approach and are corroborated by numerical simulations [3].

We also consider infinite arrays driven by independent additive and multiplicative noise in some limit cases which allow to determine analytically the critical values of the control parameter, the critical exponents of order parameter and susceptibility, and the ratio of susceptibility amplitudes (Gütter).

Stability and statistical properties of stochastic systems with delayed time argument driven by additive and multiplicative Gaussian white noise and by dichotomous Markov processes are studied analytically and by computer simulations (Wetzel [4], Krieger-Hauwede).

In collaboration with the Soft Matter Physics group (J. Käs, D. Koch) we developing a minimalistic model with the aim to characterize the stochastic dynamics of Lamellipodia for various cell types (Knorr).

[1] F. Sagués et al.: Rev. Mod. Phys. **79**, 829 (2007)
[2] T. Birner et al.: Phys. Rev. E **65**, 046 110 (2002)
[3] P. Altrock: Diplomarbeit, Universität Leipzig 2007; F. Senf et al.: in preparation
[4] L. Wetzel: Diplomarbeit, Universität Leipzig 2008

14.3 Mathematical Modeling of the Immune System

U. Behn, F. Groß, H. Schmidtchen, M. Thüne

In the last few years the paradigm of idiotypic networks which was developed about 30 years ago by Niels Jerne [1] experienced a renewed interest mainly from the side of system biology and from clinical research. For a recent review with focus also on modeling see [2].

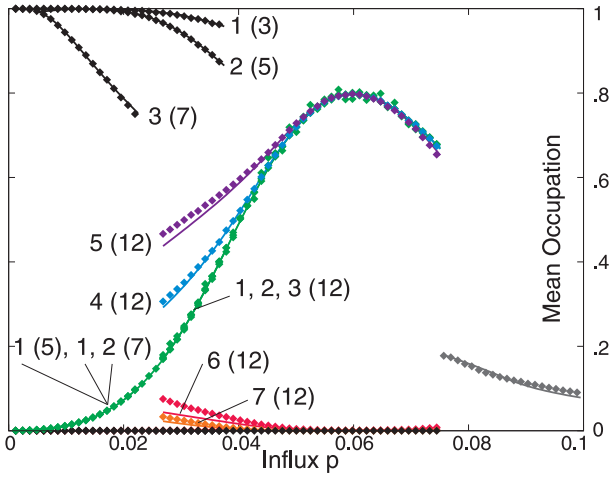

Figure 14.1: Mean occupation of groups vs. influx probability obtained by simulation (*symbols*) and in mean field theory (*lines*). The *lettering* indicates Group index (Number of groups in the pattern).

B-cells express on their membrane receptors (antibodies) of a given idiotype. Cross-linking these receptors by complementary structures (antigen or antibodies) stimulates the lymphocyte to proliferate. Thus a large functional network of interacting lymphocytes, the idiotypic network emerges. We developed a minimalistic model [3] where the idiotypes are represented by bitstrings. The dynamics of the idiotypic network is driven by the influx of new idiotypes randomly produced in the bone marrow and by the population dynamics of the lymphocytes themself. The random evolution of the network leads to a highly organized dynamical architecture where the nodes can be classified into groups with clearly distinct statistical characteristics. We found the building principles of this architecture allowing analytical computation of size and connectivity of the groups. Subsequently we developed a modular mean field theory. Mean occupation of the groups and mean life time of occupied nodes thus calculated are in good agreement with simulation results [4], cf. Fig. 14.1. Investigation of more sophisticated models is ongoing (Thüne).

T-helper lymphocytes have subtypes which differ in their spectrum of secreted cytokines. These cytokines have autocrine effects on the own subtype and cross-suppressive effects on the other subtype and regulate the type of immunoglobulines secreted by B-lymphocytes. The balance of Th1- and Th2-cells is perturbed in allergy: the response to allergen is Th2-dominated. In collaboration with a clinical immunologist (G. Metzner, Institute of Clinical Immunology) we have developed a mathematical model which provides a theoretical explanation of the switch from a Th2 dominated response to a Th1 dominated response to allergen in allergic individuals as a result of a hyposensitization therapy. Recently, a new type of T lymphocytes has been identified, the regulatory T-cells (Treg), which suppress other cells. Clinical studies show that during specific immunotherapy the concentration of Tregs is increasing [7, 8]. We therefore extended our previous model including Treg-cells. First results reveal a behaviour which is qualitatively similar to the experimental findings (Groß).

[1] N.K. Jerne: Ann. Inst. Pasteur Immunol. C **125**, 373 (1974)
[2] U. Behn: Immunol. Rev. **216**, 142 (2007)

[3] M. Brede, U. Behn: Phys. Rev. E **67**, 031 920 (2003)
[4] H. Schmidtchen, U. Behn: in *Mathematical Modeling of Biological Systems*, Vol. II, ed. by A. Deutsch et al. (Birkhäuser, Boston 2008) p 157; H. Schmidtchen, U. Behn: in preparation
[5] J. Richter et al.: J. Theor. Med. **4**, 119 (2002)
[6] R. Vogel, U. Behn: in *Mathematical Modeling of Biological Systems*, Vol. II, ed. by A. Deutsch et al. (Birkhäuser, Boston 2008) p 145
[7] M. Larché et al.: Nat. Rev. Immunol. **6**, 761 (2006)
[8] E. Mamessier et al.: Clin. Exp. Allergy **36**, 704 (2006)

14.4 Glassy Dynamics of Semiflexible Polymer Solutions

J. Glaser, C. Hubert, K. Kroy

We investigated the dynamical properties of solutions of semiflexible polymers. The starting point of our theoretical description is the wormlike chain (WLC), describing the dynamics of a semiflexible (weakly bending) polymer in solution. While this model is appropriate for isolated polymers, our approach was to modify the WLC in order to take into account cageing effects due to the surrounding polymer solution.

The key to the new description, called the "glassy wormlike chain" (GWLC) is an exponential stretching of the (long time) relaxation spectrum of an ordinary WLC. It is traced back to the activated relaxation of the transverse undulations over energy barriers, quantified by the stretching parameter $\mathcal{E}$ giving the height of the energy barriers [1] in units of k_BT. The predicted dynamic structure factor excellently fits experimental data, in particular the logarithmic tails observed in DLS [2]. The predictions for the (linear) shear moduli are also in very good agreement with microrheological data for live cells [3], cf. Fig. 14.2.

The theory also predicts a nonlinear shear modulus, which was found to resemble the differential modulus measured for F-actin solutions [2]. It will be the next step to classify the contributions of physiological parameters to the stretching parameter $\mathcal{E}$.

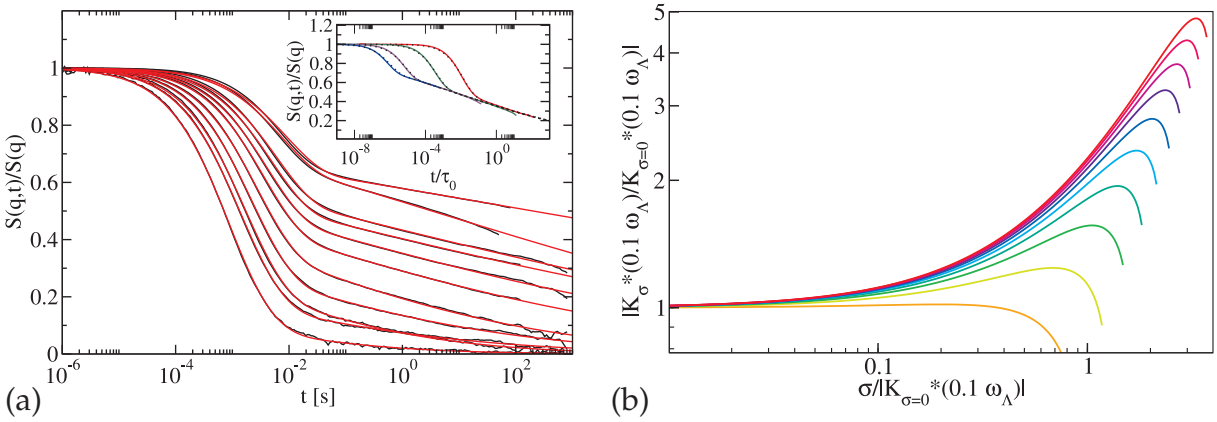

Figure 14.2: (**a**) Dynamic structure factor measured by DLS for several values of the scattering vector (*black lines*), *red lines* are theoretical fits. (**b**) Strain hardening and softening as predicted by the nonlinear modulus of the GWLC.

For instance, a temperature dependence of the shear modulus has been observed. On the other hand, it is known that metabolism rates in animals is temperature-dependent, too. A possible correspondence between these two phenomena is studied in terms of our theory. Extensions of the GWLC theory in several directions are possible, e.g. to semiflexible polymer bundles.

[1] K. Kroy, J. Glaser: New J. Phys. **9**, 416 (2007)
[2] C. Semmrich et al.: Proc. Natl. Acad. Sci. USA **104**, 20 199 (2007)
[3] B. Fabry et al.: Phys. Rev. Lett. **87**, 148 102 (2001)

14.5 A Microscopic Approach to the Nonlinear Rheology of Biopolymer Solutions

S. Grosser, P. Fernandez, K. Kroy

We consider a simple unit-cell approach to model the nonlinear response of semidilute solutions of semiflexible polymers (for example actin) to external shear stress. The model, which was created by Pablo Fernandez and Klaus Kroy, considers only freely slipping polymers. In this project, we want to overcome this restriction.

The unit-cell is one segment of a polymer for which the deformation resulting from shear is calculated for affine background deformations. This segment is taken as representative of the whole network, cf. Fig. 14.3. The exact solutions of nonlinear elastic bending are used. To the bending term we add a confinement energy term according to the tube model for semiflexible polymers. This is a simple method to take fluctuations and non-trivial correlations (entanglements) of the polymers approximately into account. The results of such an approach are considerably different from pure enthalpic bending rod models.

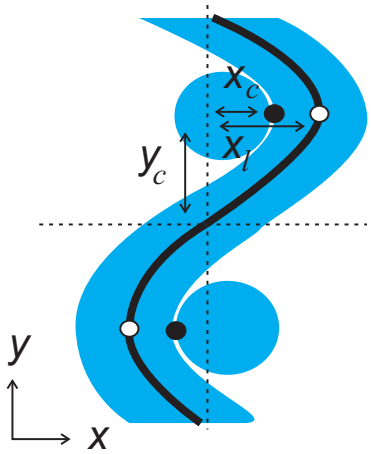

Figure 14.3: Under shear, a polymer (*black line*) and his thermal tube are distorted by the surrounding polymers.

14.6 Impact of Disorder on Flocculation and Semiflexible Polymer Conformations

S. Schöbl, A. Klopper, K. Kroy

Mechanical properties of cells are primarily determined by the cytoskeleton. The cytoskeleton is a polymer network containing mainly three kinds of filaments, microfilaments, intermediate filaments and microtubules. These filaments are semiflexible polymers. We perform Monte Carlo simulations to investigate the equilibrium behavior of a semiflexible polymer in various kinds of random potentials, which are supposed to mimic the interactions with the polymer network, cf. Fig. 14.4.

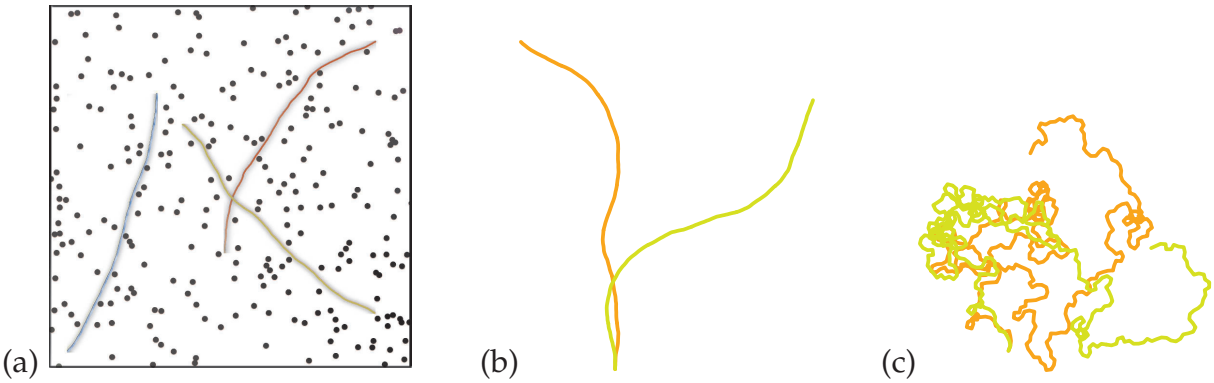

Figure 14.4: The illustrated conformations of semiflexible polymers found by Monte-Carlo simulations demonstrate the impact of disorder. (**a**) Semiflexible polymers in hard sphere background potential. (**b**) Free semiflexible polymer chain confirmations with $\xi = 2L$. (**c**) Polymer chain configurations in Gaussian white noise potential.

14.7 Colloidal Aggregation

D. Rings, S. Schöbl, K. Kroy

Aggregation of colloids has an impact on various technological as well as biological systems. In the framework of our toy model we study irreversible aggregation of a 2D colloidal suspension under shear.

We optimized our collision-driven algorithm based on hierarchical coarse-graining of cluster structures in space and the exact prediction of the hard disk trajectories. Thus, it allows a systematic investigation of the sol–gel transition for a broad range of particle concentrations, and especially different initial packing structures (on-lattice, fluid-like). We find a high sensitivity in the time to gelation and in structural properties of the largest clusters to initial conditions. In particular, for hard-disk fluid initial conditions, the system seems to escape the expected crossover of driven cluster aggregation to the percolation universality class, cf. Figs. 14.5 and 14.6.

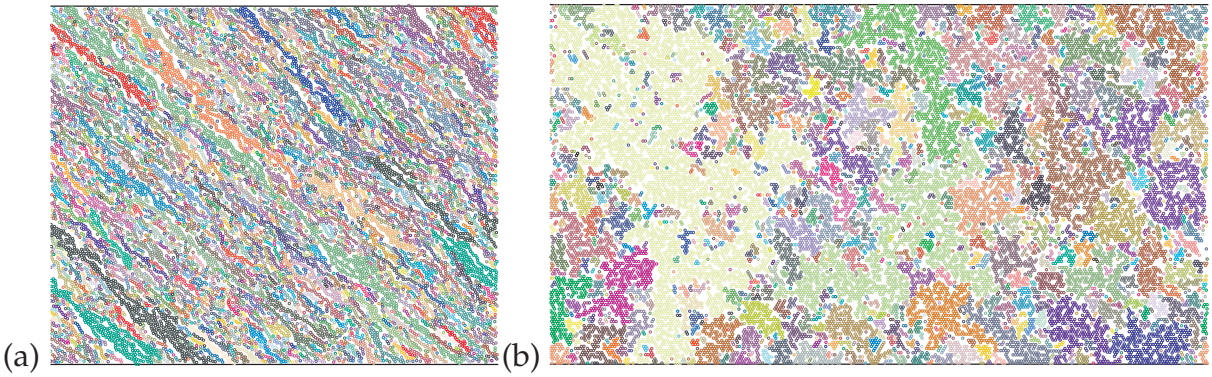

Figure 14.5: Snapshots of two systems at total occupied area fraction $\phi = 0.4$, but which have evolved from different initial configurations. (**a**) A hard disk fluid, when suddenly quenched to adhesive interactions, develops clusters under shear. At high densities, these take an essentially linear form and become oriented along the compression axis, and the longest span the whole system in the shear gradient direction. (**b**) Clusters grow quite isotropically and much more rapidly when a randomly occupied lattice is sheared. Spanning clusters have structural properties very similar to those of animal percolation clusters.

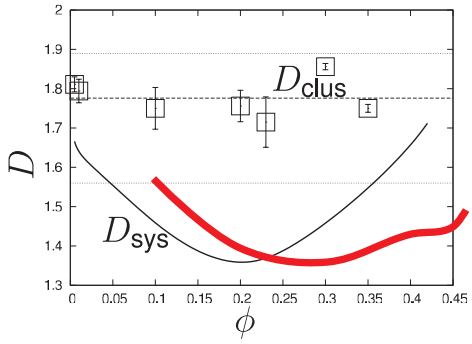

Figure 14.6: Starting from fluid structure, the "stringy" (low D) phase persists also at high densities (*red line*). This shows that the percolation universality class is broken in the absence of pre-formed clusters in shear driven flocculation.

14.8 Organizational Duties

U. Behn

- Speaker of the Condensed Matter Theory group
- Vertrauensdozent für die Nobelpreisträgertagungen in Lindau
- Referee: Phys. Rev. Lett., Phys. Rev. E, J. Theor. Biol., Physica D

K. Kroy

- Vice director of the ITP
- Member of the Graduiertenkommission of the University of Leipzig
- Referee: Phys. Rev. Lett., Phys. Rev. E, Nature, New J. Phys., Soft Matter

14.9 External Cooperations

Academic

- Universität Bayreuth, Germany
  Dr. P. Fernandez
- Technische Universität München, Germany
  Prof. Dr. A. Bausch, S. Fischer
- Edinburgh University, UK
  Prof. Dr. M.E. Cates
- Institut für Klinische Immunologie, Universität Leipzig, Germany
  Prof. Dr. G. Metzner
- University College Dublin, Department of Mathematical Physics, Ireland
  Prof. Dr. J. Pulé
- Joint Institute for Nuclear Research, Laboratory for Theoretical Physics, Dubna, Russia
  Prof. Dr. N.M. Plakida
- Center for Complex Systems Science, CSIRO, Canberra, Australia
  Dr. M. Brede
- Cyprus Institute of Neurology and Genetics, Nicosia, Cyprus
  Dr. J. Richter
- Harvard University, Program for Evolutionary Dynamics, Cambridge, USA
  Dr. A. Traulsen
- Centre de Physique Theorique, CNRS, Marseille, France
  Prof. Dr. V. Zagrebnov

14.10 Publications

Journals

W. Apel, U. Behn, D. Ihle, T. Butz: *Nachruf auf Wolfgang Weller*, Physik Journal **6**, 48 (2007)

U. Behn: *Idiotypic networks: toward a renaissance?*, Immunol. Rev. **216**, 142 (2007)

O. Hallatschek, E. Frey, K. Kroy: *Tension dynamics in semiflexible polymers I. Coarse-grained equations of motion*, Phys. Rev. E **75**, 031 905 (2007)

O. Hallatschek, E. Frey, K. Kroy: *Tension dynamics in semiflexible polymers II. Scaling solutions and applications*, Phys. Rev. E **75**, 031 906 (2007)

K. Kroy, J. Glaser: *The glassy wormlike chain*, New J. Phys. **9**, 416 (2007)

B. Obermayer, O. Hallatschek, E. Frey, K. Kroy: *Stretching dynamics of semiflexible polymers*, Eur. Phys. J. E **23**, 375 (2007)

C. Semmrich, T. Storz, J. Glaser, R. Merkel, A.R. Bausch, K. Kroy: *Glass Transition and Rheological Redundancy in F-Actin Solutions*, Proc. Natl. Acad. Sci. USA **104**, 20 199 (2007)

A.A. Vladimirov, D. Ihle, N.M. Plakida: *Static spin susceptibility in the t–J model*, Theor. Math. Phys. **152**, 1331 (2007)

Books

S. Fischer, K. Kroy: *Dynamics of Aeolian Sand Heaps and Dunes: The Influence of the Wind Strength*, in: *Traffic and Granular Flow '05*, ed. by A. Schadschneider, T. Pöschel, R. Kühne, M. Schreckenberg, D. Wolf (Springer, Heidelberg 2007)

in press

J. Glaser, K. Kroy: *Dynamic structure factor of a stiff polymer in a glassy solution*, under review at Eur. Phys. J. E

H. Schmidtchen, U. Behn: *Architecture of Randomly Evolving Idiotypic Networks*, in: *Mathematical Modeling of Biological Systems*, Vol. II, ed. by A. Deutsch, R. Bravo de la Parra, R. de Boer, O. Diekmann, P. Jagers, E. Kisdi, M. Kretzschmar, P. Lansky, H. Metz (Birkhäuser, Boston 2008) p 157

R. Vogel, U. Behn: *Th1–Th2 Regulation and Allergy: Bifurcation Analysis of the Non-autonomous System*, in: *Mathematical Modeling of Biological Systems*, Vol. II, ed. by A. Deutsch, R. Bravo de la Parra, R. de Boer, O. Diekmann, P. Jagers, E. Kisdi, M. Kretzschmar, P. Lansky, H. Metz (Birkhäuser, Boston 2008) p 145

Talks

U. Behn, H. Schmidtchen: *Randomly Evolving Idiotypic Networks*, Invited Talk, ANet07 – Applications of Networks: From fundamental physics to complex networks, Kraków, Poland, 2. November 2007

K. Kroy: *Dynamic Scaling of Desert Dunes*, DLR, Köln, 5. October 2007

K. Kroy: *The Glassy Wormlike Chain*, 71st DPG Spring Meeting, Regensburg, 26. – 30. March 2007

K. Kroy: *The Glassy Wormlike Chain*, Workshop "Soft Meets Hard", Wittenberg, 13. – 15. September 2007

K. Kroy: *Why is actin soft and why does this matter?*, International Research Training Group, Humboldt Universität, Berlin, 1. June 2007

K. Kroy: *Wormlike and Glassy Wormlike Chains*, Cavendish Laboratory, Cambridge, UK, 30. November 2007

K. Kroy: *Wormlike and Glassy Wormlike Chains*, Workshop "Macromolecular Systems for NanoScience - Chemistry, Physics and Engineering Aspects" des Elitenetzwerks Bayern, Irsee, 06. – 09. September 2007

K. Kroy: *Wormlike Chains in Disordered and Glassy Environments*, Workshop "Path Integrals", Dresden, 24. – 28. September 2007

D. Rings: *Jamming Transition in Two-Dimensional Shear-Driven Aggregation*, 71st DPG Spring Meeting, Regensburg, 26. – 30. March 2007

H. Schmidtchen, U. Behn: *Randomly Evolving Idiotypic Networks: A Mean Field Approach*, Eur. Conf. Complex Systems (ECCS 2007), Dresden, 3. October 2007

H. Schmidtchen, P. Altrock: *Deterministisches Chaos: Determinismus und Kausalität in der Physik*, Workshop, Promovendentreffen des Studienwerkes Villigst, Villigst, 30. November/1. December 2007

Posters

U. Behn, H. Schmidtchen: *Randomly Evolving Idiotypic Networks: Architecture and Mean Field Approach*, STATPHYS 23, Genova, Switzerland, 13. July 2007

U. Behn, R. Vogel, J. Richter, G. Metzner: *Th1–Th2 Regulation, Allergy and Hyposensitization Therapy: A Mathematical Model*, World Immune Regulation Meeting 2007, Davos, Switzerland, 12. April 2007

P. Fernandez: *Brave misfits – A microscopic approach to the nonlinear rheology of biopolymer solutions*, International Soft Matter Conference 2007, Aachen, 01. – 04. October 2007

P. Fernandez: *Living cell mechanics: stress stiffening and kinematic hardening*, International Soft Matter Conference 2007, Aachen, 01. – 04. October 2007

J. Glaser: *Dynamic light scattering of F-actin solutions*, 71st DPG Spring Meeting, Regensburg, 26. – 30. March 2007

J. Glaser: *Glass transition and rheological redundancy in F-actin solutions*, International Soft Matter Conference 2007, Aachen, 01. – 04. October 2007

A. Klopper: *Semiflexible chains in disordered media*, International Soft Matter Conference 2007, Aachen, 01. – 04. October 2007

D. Rings: *Influence of spatio-temporal correlations of random flows on inertial particle dynamics*, 396. Wilhelm and Else Heraeus-Seminar: Nonlinear Dynamics – From small scales to coherent structures, Bayreuth, 07. – 10. October 2007

D. Rings: *Influence of spatio-temporal correlations of random flows on inertial particle dynamics*, International Soft Matter Conference 2007, Aachen, 01. – 04. October 2007

H. Schmidtchen, U. Behn: *Randomly Evolving Idiotypic Networks: A Mean Field Approach*, CompPhys07, Leipzig, 29./30. November 2007

H. Schmidtchen, U. Behn: *Randomly Evolving Idiotypic Networks: A Mean Field Approach*, Eur. Conf. Complex Systems (ECCS 2007), Dresden, 2. October 2007

14.11 Graduations

Diploma

- Philipp Altrock
  Critical Properties of Coupled Systems Driven by Multiplicative Noise
  November 2007

14.12 Guests

- Dr. P. Benetatos
  Universität Göttingen, Germany
  31. January 2007
- Dr. Abigail Klopper
  Max-Planck-Institut für Physik komplexer Systeme, Dresden, Germany
  07. February 2007
- Dr. T. Slawig
  Technische Universität Berlin, Germany
  08. February 2007
- Dr. D. Masashi
  Forschungszentrum Jülich, Germany
  07. March 2007
- Dipl.-Math. B. Friedrich
  Max-Planck-Institut für Physik komplexer Systeme, Dresden, Germany
  03. May 2007
- Prof. Dr. Bernhard Mehlig
  Institutionen för Fysik, Göteborgs Universitet, Sweden
  28. June 2007
- Dr. Jörg Hackermüller
  Fraunhofer Institut für Zelltherapie und Immunologie Leipzig, Germany
  10. July 2007
- Dipl.-Phys. W. Michel
  Universität Bayreuth, Germany
  11. October 2007
- Prof. Christian Friedrich
  Universität Freiburg, Germany
  12. December 2007

15

Theory of Elementary Particles

15.1 Introduction

The Particle Physics Group performs basic research in the quantum field theoretic description of elementary particles and in phenomenology. Topics of current interest are conformal symmetry and its breaking in the context of supersymmetric theories, the formulation of models which realize noncommutative geometry, renormalization problems, electroweak matter at finite temperature, the lattice formulation of gauge theories, the derivation of Regge behaviour of scattering amplitudes from Quantum Chromodynamics and the related study of integrable models with and without supersymmetry. Perturbative and non-perturbative methods are applied to answer the respective questions. In perturbation theory the work is essentially analytic using computers only as a helpful tool. Lattice Monte Carlo calculations as one important non-perturbative approach however are based on computers as an indispensable instrument. Correspondingly the respective working groups are organized: in analytical work usually very few people collaborate, in the lattice community rather big collaborations are the rule. Our group is involved in many cooperations on the national and international level (DESY, Munich; France, Russia, Armenia, USA, Japan). Since elementary particles are very tiny (of the order of 10^{-15} m) and for the study of their interactions large accelerators producing enormously high energy are needed, it is clear that results in this direction of research do not have applications in daily life immediately. To clarify the structure of matter is first of all an aim in its own and is not pursued for other reasons. But particle theory has nevertheless a very noticeable impact on many other branches of physics by its power of providing new methodological insight. Similarly for the student specializing in this field the main benefit is her/his training in analysing complex situations and in applying tools which are appropriate for the respective problem. As a rule there will be no standard procedures which have to be learned and then followed, but the student has to develop her/his own skill according to the need that arises. This may be a mathematical topic or a tool in computer application. Jobs which plainly continue these studies are to be found at universities and research institutes only. But the basic knowledge which one acquires in pursuing such a subject opens the way to many fields where analytical thinking is to be combined with application of advanced mathematics. Nowadays this seems to be the case in banks, insurance companies and consulting business.

Klaus Sibold

15.2 Star Products in Quantum Field Theory

K. Sibold

At very short distances the structure of spacetime has to undergo presumably a drastic change. Qualitative arguments show that a horizon builds up which prohibits the interpretation of coordinates as on large distances. This points to a possible solution: consider the coordinates as selfadjoint operators on a Hilbert space and understand their eigenvalues as the replacement for the original coordinates. If these operators do not commute one has uncertainty relations which then permit to avoid the aforementioned clash. Implementing this idea in conventional field theories one possibility is the socalled Moyal product of field operators. The usual interactions become nonlocal and thus create all sorts of difficulties when deriving Feynman rules. Some of them have been overcome in earlier papers but the construction of higher orders is still a problem due to subtleties of the respective integrals. At present another notion of product is being developped. Related literatur is given in [1–6]. Work on this is in progress.

[1] S. Doplicher et al.: Commun. Math. Phys. **172**, 187 (1995)
[2] Y. Liao, K. Sibold: Eur. Phys. J. C **25**, 469 (2002)
[3] Y. Liao, K. Sibold: Eur. Phys. J. C **25**, 479 (2002)
[4] D. Bahns et al.: Phys. Lett. B **533**, 178 (2002)
[5] T. Reichenbach: Diploma Thesis, Leipzig University (2004)
[6] P. Heslop, K. Sibold: Eur. Phys. J. C **41**, 545 (2005)

15.3 The Lattice Gluon Propagator in Stochastic Perturbation Theory

E.-M. Ilgenfritz*, H. Perlt, A. Schiller

*Institut für Physik, Humboldt-Universität Berlin

To relate observables measured in lattice QCD to their physical counterpart in the continuum, renormalisation is needed. Besides non-perturbative renormalisation also perturbative approaches are useful. In addition, it is useful to know as precisely as possible perturbative contributions to lattice observables assumed to show confinement properties in order to separate non-perturbative effects (condensates etc.). The gluon and the ghost propagator belong to these observables.

It is well known that lattice perturbation theory (LPT) is much more involved compared to its continuum QCD counterpart. The complexity of diagrammatic approaches increases rapidly beyond the one-loop approximation. By now only a limited number of results up to two-loop accuracy have been obtained.

Applying the standard Langevin dynamics [1, 2] to the problem of weak coupling expansions for lattice QCD, a powerful numerical approach for higher loop calculations – called numerical stochastic perturbation theory (NSPT) – has been proposed in [3].

We started a programme [4] to calculate loop contributions up to four loops to the Landau gauge gluon propagator in numerical stochastic perturbation theory. For

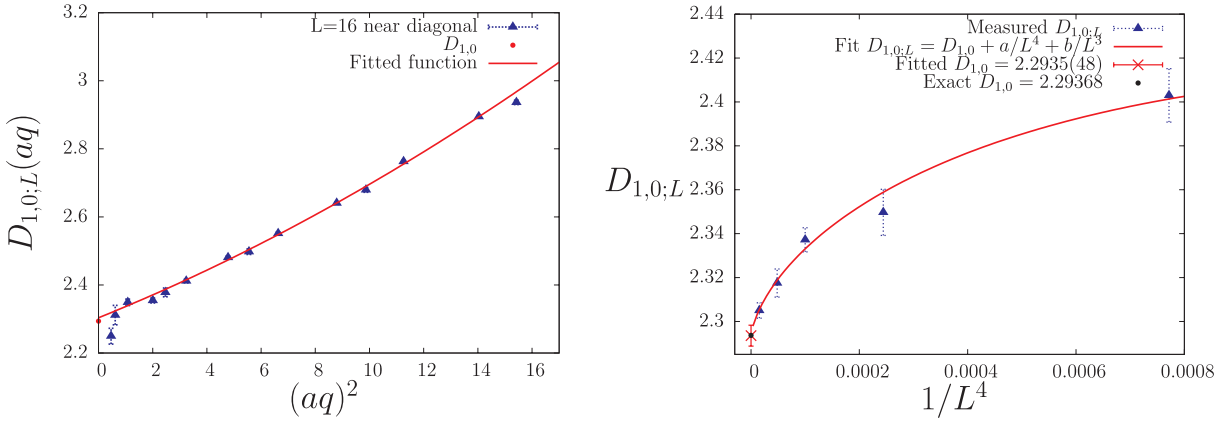

Figure 15.1: *Left*: Limit $a \to 0$: $D_{1,0;16} = 2.3050(35)$. *Right*: Limit $V \to \infty$: $D_{1,0;\infty} = 2.2935(48)$.

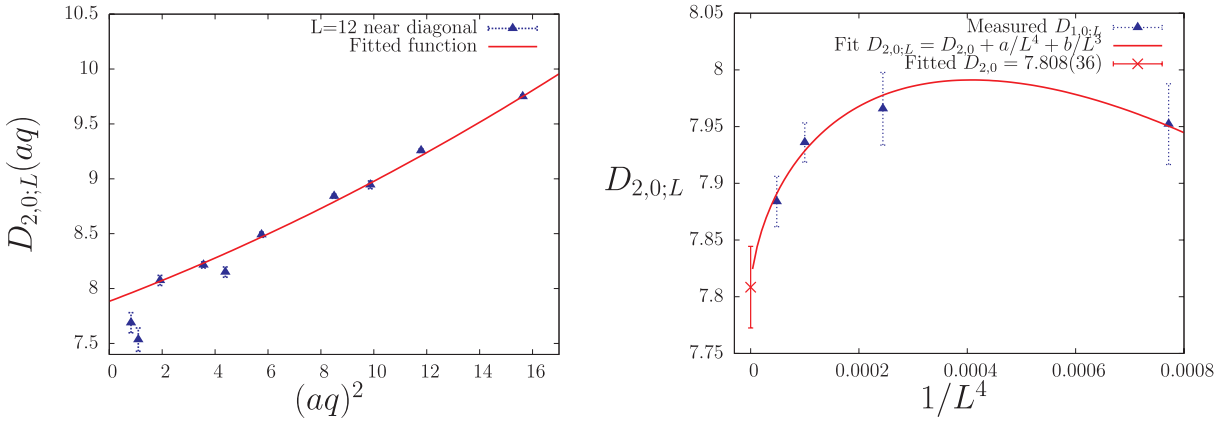

Figure 15.2: *Left*: Limit $a \to 0$: $D_{2,0;12} = 7.884(23)$. *Right*: Limit $V \to \infty$: $D_{2,0;\infty} = 7.808(36)$.

different lattice volumes we carefully have extrapolated the Euler time step to zero for the Langevin dynamics derived from the Wilson action.

As a very recent example we were able to check the finite one-loop contribution $D_{1,0}$ to the gluon wave function renormalization Z and gave a first prediction for the finite two-loop contribution $D_{2,0}$ in the RI′-MOM scheme not known so far by other methods:

$$Z^{2-\text{loop}}(a,q,\beta) = 1 + \frac{1}{\beta}\left(-0.24697\,\log(aq)^2 + D_{1,0}\right) + \frac{1}{\beta^2}\left(0.0821078\,\log^2(aq)^2 - 1.48445\,\log(aq)^2 + D_{2,0}\right) \tag{15.1}$$

As can be seen from Figs. 15.1 and 15.2, we could check the analytical calculation $D_{1,0} = 2.29368$ [5] and could predict $D_{2,0}$ [6].

[1] G. Parisi, Y.S. Wu: Sci. Sin. **24**, 483 (1981)
[2] G.G. Batrouni et al.: Phys. Rev. D **32**, 2736 (1985)
[3] F. Di Renzo et al.: Nucl. Phys. B **426**, 675 (1994), arXiv:hep-lat/9405019
[4] E.-M. Ilgenfritz et al.: PoS **LAT2007**, 250 (2007), arXiv:0710.0560 [hep-lat]
[5] H. Kawai et al.: Nucl. Phys. B **189**, 40 (1981)
[6] A. Schiller: Talk at CompPhys07, Leipzig, November 2007; F. Di Renzo et al.: in preparation

15.4 Integrable Quantum Systems and Gauge Field Theories

R. Kirschner

Integrable quantum systems are applied successfully to the study of the high-energy asymptotics and of the renormalization of composite operators in gauge theories [1–4]. These application stimulated the development of the methods of quantum systems.

We have developed appropriate methods of solving the Yang–Baxter relation and applied them to cases of one dimensional conformal symmetry and its supersymmetric extensions and algebraic deformations.

In particular we have noticed factorization properties of the Yang-Baxter operators which provide a powerful method of construction. We have treated the cases of the symmetry $sl(2)$ and the corresponding trigonomeric and elliptic deformations [5]. The application to higher symmetries, first of all $sl(3)$ with trigonometric deformation, has been worked out [6].

[1] L.N. Lipatov: Padova preprint DFPD-93-TH-70B; J. Exp. Theor. Phys. Lett. B **342**, 596 (1994)
[2] L.D. Faddeev, G.P. Korchemsky: Phys. Lett. B **342**, 311 (1995), arXiv:hep-th/9404173
[3] V.M. Braun et al.: Phys. Rev. Lett. **81**, 2020 (1998), arXiv:hep-ph/9805225
[4] N. Beisert: Phys. Rept. **407**, 1 (2004)
[5] S. Derkachov et al.: Nucl. Phys. B **785**, 263 (2007), arXiv:hep-th/0703076
[6] S.E. Derkachov et al.: Zapiski Nauchnych Sem. POMI **335**, 88 (2007) [in Russian]

15.5 Funding

The lattice gluon propagator in stochastic perturbation theory
Suppored by DFG through the DFG-Forschergruppe "Lattice Hadron Phenomenology" FOR465

Integrable quantum systems related to gauge field theories
Support of the visit of S.E. Derkachov (St. Petersburg) and D.R. Karakhanyan (Yerevan) by DFG, and NTZ

15.6 Organizational Duties

R. Kirschner

- Referee: Phys. Rev. D, Phys. Letters A and B
- Member of the PhD commission of the faculty

A. Schiller

- Referee: Phys. Rev. D

K. Sibold

- Associated member of the Graduiertenkolleg: "Analysis, Geometrie und die Naturwissenschaften"
- Coorganizer of the "Mitteldeutsche Physik-Combo"(joint graduate lecture courses with universities Jena and Halle)
- Member of the "Beirat" of the Fachverband "Mathematische und Theoretische Grundlagen der Physik" (German Physical Society)

15.7 External Cooperations

Academic

- Nuclear Physics Institute, St. Petersburg, Russia
  Prof. L.N. Lipatov
- St. Petersburg branch of Steklov Mathematical Institute, Russia
  Dr. S.E. Derkachov
- Yerevan Physics Institute, Theory Department, Armenia
  Prof. A. Sedrakyan
- Soltan Institut of Nuclear Studies, Warsaw, Poland
  Dr. L. Szymanowski
- Sobolev Institut of Mathematics, Novosibirsk, Russia
  Dr. D.Y. Ivanov
- Universität Hamburg, Institut für Theoretische Physik & DESY, Germany
  Prof. J. Bartels
- Universität Regensburg, Institut für Theoretische Physik, Germany
  Prof. A. Schäfer, Prof. V. Braun, Dr. M. Göckeler, Dr. C. Torrero
- Humboldt-Universität Berlin, Germany
  Dr. E.-M. Ilgenfritz, Prof. M. Müller-Preussker
- Adelaide University, Australia
  Dr. A. Sternbeck
- Ecole Polytechnique, Paris-Palaiseau, France
  Prof. B. Pire
- NIC, Zeuthen & DESY, Hamburg, Germany
  Prof. G. Schierholz
- Edinburgh University, UK
  Dr. R. Horsley
- Department of Mathematics, Liverpool University, UK
  Dr. P.E.L. Rakow
- Parma University, Italy
  Prof. F. Di Renzo

15.8 Publications

Journals

M. Bock, M.N. Chernodub, E.-M. Ilgenfritz, A. Schiller: *An Abelian two-Higgs model of strongly correlated electrons: phase structure, strengthening of phase transition and QCD at finite density*, Phys. Rev. B **76**, 184 502 (2007), arXiv:0705.1528 [cond-mat.str-el]

S.E. Derkachov, D. Karakhanyan, R. Kirschner: *Yang-Baxter R operators and parameter permutations*, Nucl. Phys. B **785**, 263 (2007), arXiv:hep-th/0703076

S.E. Derkachov, D. Karakhanyan, R. Kirschner, P. Valinevich: *Factorization of the R-matrix in the case of the quantum algebras* $sl_q(3)$, Zapiski Nauchnych Sem. POMI **335**, 88 (2007) [in Russian]

D. Galletly, M. Gürtler, R. Horsley, H. Perlt, P.E.L. Rakow, G. Schierholz, A. Schiller, T. Streuer: *Hadron spectrum, quark masses and decay constants from light overlap fermions on large lattices*, Phys. Rev. D **75**, 073 015 (2007), arXiv:hep-lat/0607024

E.-M. Ilgenfritz, M. Müller-Preussker, A. Sternbeck, A. Schiller, I.L. Bogolubsky: *Landau gauge gluon and ghost propagators from lattice QCD*, Braz. J. Phys. **37**, 193 (2007), arXiv:hep-lat/0609043

Talks

V.M. Braun, D. Brömmel, M. Göckeler, R. Horsley, Y. Nakamura, H. Perlt, D. Pleiter, P.E.L. Rakow, A. Schäfer, G. Schierholz, A. Schiller, W. Schroers, T. Streuer, H. Stüben, J.M. Zanotti: *Distribution Amplitudes of Vector Mesons*, PoS **LAT2007**, 144 (2007), arXiv:0711.2174 [hep-lat]

M. Göckeler, R. Horsley, Y. Nakamura, H. Perlt, D. Pleiter, P.E.L. Rakow, G. Schierholz, A. Schiller, T. Streuer, H. Stüben, J.M. Zanotti: *A status report of the QCDSF* $N_f = 2 + 1$ *Project*, PoS **LAT2007**, 041 (2007), arXiv:0712.3525 [hep-lat]

R. Horsley, H. Perlt, A. Schiller, P.E.L. Rakow, G. Schierholz: *Perturbative determination of* c_{SW} *with Symanzik improved gauge action and stout smearing*, PoS **LAT2007**, 250 (2007), arXiv:0710.0990 [hep-lat]

Posters

E.-M. Ilgenfritz, H. Perlt, A. Schiller: *The lattice gluon propagator in stochastic perturbation theory*, PoS **LAT2007**, 251 (2007), arXiv:0710.0560 [hep-lat]

15.9 Graduations

Master

- Martin Bock
  Monte-Carlo study of the phase structure of a three-dimensional abelian Higgs model on the lattice
  September 2007

Author Index

F

G

H

I

J

K

L

M

N

O

P

R

S

T

U

V

W

X

Y

Z

Stefano Brandani, Christian Chmelik, Jörg Kärger, Roberto Volpe (Eds.)

Diffusion Fundamentals II

L'Aquila 2007

$$\langle x^2(t)\rangle = 2Dt$$

$$\frac{\partial c}{\partial t} = D\,\frac{\partial^2 c}{\partial x^2}$$

complemented with

24 paintings of and around *L'Aquila* by **Taro Ito**

and an essay on "What might *Aquinas* have said"
by **Philip Kuchel** and **Marcel Sahade**

Leipziger Universitätsverlag

Wolfhard Janke
Editor

LECTURE NOTES IN PHYSICS 736

Rugged Free Energy Landscapes

Common Computational Approaches to Spin Glasses, Structural Glasses and Biological Macromolecules

Springer

ISBN 978-3-934178-94-6